The evaluation of a metabonomic approach to detect decomposition products in water and leachates using Liquid Chromatography-Mass Spectrometry.

Mared Fflur Williams

Thesis submitted for the degree of Doctor of Philosphy

June 2023

Keele University

Abstract

Statistics show that there was a 12% increase in missing persons' incidents in the UK between 2014 and 2019. Approximately 50% of these missing individuals are found within 24 hours, and on average a large number will be deceased. Land-based searches are relatively straight forward, however searches in aquatic environments can be significantly more complex and often require the deployment of significant manpower. As a result, there is a desire to use technology to increase the efficiency of these searches. The use of instrumentation to detect a 'chemical fingerprint' of decomposition in water would have significant potential to achieve this aim.

The focus of this work was on the chemical profile of water influenced by decomposition, and the effects different environmental factors have on this profile via metabonomic analysis. Liquid chromatography-mass spectrometry was combined with quality control measures, multivariate and statistical analysis to investigate these changes.

Initial studies focused on improving sample preparation, to allow maximum output from the instrument. It was discovered that pre-concentrating a 1 L sample of water exposed to decomposing remains using solid-phase extraction was the most effective way to capture and concentrate as many compounds as possible for this non-targeted research.

An investigation into species differentiation based on the chemical signature of water containing rabbit or duck remains was able to produce three positive identified markers (cadaverine, leucine and creatinine) that were significantly different between species. These significant differences are based on the change in abundance and behaviours of these markers over a series of time points, and whether these patterns are specific to a particular species or not. Furthermore, it was discovered that the nature of the water (moving and still water) influenced the speed in which these chemical processes occurred during

decomposition. It was also evident that the quantity of compounds in a sample taken from still water was much higher. The effects of temperature were investigated throughout this work. It was clear that although lower temperatures did affect the speed of decomposition and the amount of significantly different features in each sample compared to summer, it is important to note that chemical decomposition was still progressing, albeit slowly. These lab-based methods were also successfully implemented to analyse samples obtained from an experiment with human subjects.

These preliminary experiments have highlighted the potential of using metabonomic analysis to monitor non or semi volatile compounds leaching into the water as a result of decomposition. These initial developments could be applied further to assist the forensic science community.

Contents

List of Tables

List of Figures

Acknowledgements

I would like to take this opportunity to thank my supervisor, Dr Falko Drijfhout, for taking on this project with me and helping me grow my skills as a researcher. Your vast knowledge helped me understand the instrument inside out, now I am ready for anything!

I would also like to thank Dr Chrystelle Egger. Thank you for being someone I could look up to from science from my very first day at Keele. Your encouragement has filled me with confidence and helped me navigate my way through the last four years without getting too overwhelmed.

I was lucky to work in an office with such a supportive and encouraging environment. I would like to thank all of them personally and academically, for not only reading endless drafts, but for good conversations over coffee to calm the mind.

A special thank you to my wonderful family for keeping me motivated to work hard, to keep going, and believe in my abilities. I would not be where I am today without their encouragement and support. Diolch.

Finally, I would like to thank David Thompson. Thank you for igniting my excitement for research. Your unique scientific mind has not only made the last 4 years interesting, but also immensely fun. While your academic contribution is appreciated, your love and support helped me believe in myself whenever I was in doubt.

Chapter 1

Introduction

1.1 Decomposition

1.1.1 The decomposition process

The process of decomposition begins approximately 4 minutes after death [1]. In the first two days, autolysis begins. This is known as the fresh stage, where cellular material starts to break down due to the lack of oxygen. The carbon dioxide in the cells increase, the pH decreases, allowing accumulating waste to poison the cells. Simultaneously, cellular enzymes (lipases, proteases and amylases) digest the cells from the inside out, causing the cells to rupture [1]. Well known processes such as rigor mortis (stiffening of the muscles), livor mortis (pooling of the blood) and algor mortis (cooling of the body to ambient temperature) are observed [2]. Parallel to this, insect activity will establish itself in natural body openings and will speed up decomposition as the body is now exposed further [3]. Stage 2 is referred to as putrefaction. This occurs when enough cells have ruptured, assisting in the soft tissue breakdown. The catabolism of carbohydrates, proteins and lipids in soft tissue to small molecules of gases and liquids is happening due to microorganisms such as bacteria and fungi. Gases such as hydrogen sulphide are released due to a conversion of haemoglobin to sulfhaemoglobin [4]. Observations include bloating and

discolouration. This causes an increase in pressure, resulting in the eventual release of decomposition fluids through natural body openings and those created by insects [5]. Active decay begins once the skin is broken. The body deflates as various gases escape, and anaerobic and aerobic bacteria play an import part in the decline of soft tissue surrounding the body [6]. Amino acids produced from protein catabolism will decompose, forming volatile fatty acids and biogenic amines. The decay of lipids will also produce glycerol and phenolic compounds [7]. At this stage, all organs are exposed and therefore begin to decompose rapidly. Organs such as the intestines will decompose quickly. This continues until all soft tissue is removed by breakdown or feeding by insects and animals. This directly moves onto the dry stage, where only a skeleton remains [4]. The skin develops into a leather sheet that covers the bone, and will continue to decay until only the more resistant bone, teeth and cartilage are left [8].

1.1.2 The chemistry of decomposition

The body consists of approximately 64% water, 20% protein, 10% fat, 1% carbohydrate and 5% minerals [9]. During soft tissue decay, large biological macromolecules such as proteins, carbohydrates and lipids are broken down into gases (volatile compounds) and leachates (non-volatile compounds) by bacteria, fungi and protozoa [7]. The genetic makeup of a species will have an impact on the chemical composition of that particular species. The content and abundances of fatty acids, triglycerides, phospholipids and steroids also shows high variability between species [10, 11].

1.1.2.1 Decomposition of lipids

Lipids are most often found in the phospholipid membranes of animal cells. After death, intrinsic lipases hydrolyse the lipids, thus releasing them from their glycerol backbone forming a combination of saturated and unsaturated fatty acids, with some of the most common fatty acids being linoleic acid or arachidonic acid [9]. These fatty acids will either undergo oxidation, or further hydrolysis, depending on the type of environment they are in [12]. Oxidation occurs in open air (aerobic) environments, where the bacteria and fungi are able to convert these fatty acid into aldehydes, ketones, acids, esters, epoxides and hydrocarbons [13]. A buried body in an oxygen deficient environment will undergo further hydrolysis or hydrogenation by anaerobic microorganisms, magnified by the presence of moisture. In very precise conditions where moisture and enzyme activity are suitable, hydrolysis of tissue will proceed until all lipids have reduced to fatty acids, often resulting in the formation of adipocere, visible as a grey waxy substance [14].

1.1.2.2 Decomposition of carbohydrates

The breakdown of carbohydrates commonly occurs in the very early stages of decomposition. Microorganisms will break large polysaccharides such as glycogen down into sugar monomers such as glucose [14]. The majority of sugars are oxidised into carbon dioxide and water, while some are incompletely decomposed into alcohols and volatile fatty acids [12]. Pyruvate is an important molecule, a breakdown product of glucose from the Embden-Meyerhof-Parnas (EMP) and Entner-Doudoroff (ED) pathways. Fermentation of pyruvate from bacteria and yeasts yields ethanol, acetic acid, pyruvic acid, lactic acid, butanoic acid, propanoic acid, acetaldehyde, acetone, propan-1-ol and butan-1-ol. This can begin within 6-10 hours of death under warm conditions [14, 15]. The contribution of yeast in decay is much less than bacteria, however it is mostly found in the intestine, oral cavity,

sexual organs and between the fingers and toes of a vertebrate. The breakdown of carbohydrates instigated by both bacteria and yeast assist in forming the gaseous compounds that causing bloating, such as methane, hydrogen and hydrogen sulphide [13, 14].

1.1.2.3 Decomposition of proteins

Proteins are degraded via proteolysis, instigated by bacterial enzymes. Decay products include peptones, polypeptides and amino acids. Soft tissue proteins found in epithelial tissues are destroyed first, followed by proteins in the brain, liver and kidneys. Dissimilarly, muscle protein and the epidermis are more resistant to this process as they contain keratin (made from strong disulphide bonds). Keratin and collagen are often found intact on a skeleton [14].

Amino acids are known to be the major components of a variety of proteins in the body, such as muscle tissue, membrane proteins and additionally free proteins. Free amino acids are formed from the decay of peptones and polypeptides by microbial proteases and peptidases. Further degradation of these amino acids leads to the formation of volatile compounds [13]. Amino acids will subsequently follow three main breakdown paths, deamination, decarboxylation and desulfhydration [12]. The deamination of amino acids yields ammonia by the removal of the amine groups. This is done under anaerobic conditions, resulting in an increase of ammonia surrounding the grave environment. The carboxylation of amino acids removes the carboxyl groups, known to yield biogenic amines, in particular putrescine and cadaverine [12, 13]. Although well known for their contribution to decomposition, they have not yet been identified in volatile organic compound profiles of decomposition, therefore it is unclear what their significance is as degradation compounds [12, 16].

Amino acids that contain sulfur (cysteine and methionine) are broken down via anaerobic conditions to form sulfides, which can then convert to sulfuric acid, sulfur and sulfate under aerobic conditions. Decomposition gases containing the sulfhydryl group are known to be responsible for the bad odours of decomposition [14].

Table 1.1 gives detailed information of the metabolic pathways and products from the breakdown of amino acids, adapted from a table by Paczkowski & Schutz [13]

Table 1.1: Metabolic pathways and products for the degradation of each amino acid adapted from Paczkowski & Schutz [13].

Amino Acid	Metabolic Pathway	Metabolic Products
Arginine	Decarboxylation	Putrescine
Cysteine	Anaerobic	Sulphur, hydrogen sulphide, dimethyl sulphide, dimethyl trisulphide, dimethyltetrasulphide
	Desulfhydrase	Ammonia, hydrogen sulphide, pyruvate
Isoleucine	Ehrlich pathway, Anabolic biosynthetic pathway	1-Propanol, 2-methyl-1-propanol, 2-methyl-1-butanol,
	Yeasts	1-Propanol, 2-methyl-1-butanol, 1-pentanol
Leucine	Ehrlich pathway, Anabolic biosynthetic pathway	1-Propanol, 2-methyl-1-propanol, 2-methyl-1-butanol, 3-Methyl-1-butanol, 3-methylbutanal, 3-methylbutanoic acid
	Moraxella phenylpyruvica, *Staphylococcus xylosus*, *Staphylococcus starnosus transforme*	
	Yeasts	1-Propanol, 2-methyl-1-butanol, 1-pentanol
Lysine	Decarboxylation	Cadaverine
Methionine	Anaerobic	Hydrogen sulphide, dimethyl sulphide, dimethyl trisulphide, dimethyltetrasulphide, methanethiol
	Aerobic	Dimethylsulphide
Methionine (continued)	*H. alvei, E. agglomeran, S. liquefaciens, A. putrefaciens, A. hydrophila*	Dimethylsulphide, methanetiol
Threonine	Yeasts	1-Propanol, 2-methyl-1-butanol, 3-methyl-1-butanol, 1-pentanol
Tryptophan	*Bacteroides, Lactobacillus, Clostridium, Bifidobacterium, Peptostreptococcus*	Indole, Indonyl acetic acid, Indonyl propanoic acid
Tyrosine	*S. albus, B. fragilis, Fusobacterium sp., Bifidobacterium spp., C. paraputrificum, C. butricum, C. sporogenes, C. septicum*	4-Methylpehnol, propanoic acid phenyl ester
	E. coli, Proteus sp., E. faecalis, S. albus	Phenol
Valine	Ehrlich pathway, anabolic biosynthetic pathway	1-Propanol, 2-methyl-1-propanol, 2-methyl-1-butanol,

1.1.3 Decomposition in water

The process of decomposition will follow the five main stages regardless of whether the carcass is placed on land or in an aquatic environment. Be that as it may, the rate of decomposition occurring in these environments will differ greatly. Byard [17] summarises this up by stating "The degree of putrefaction of a body lying in the open after one week was the same as that of a body immersed in water for two weeks". This statement seems to suggest that a body will decompose twice as fast when out in the open, compared to being submerged. This highlights the delay in decomposition a body might experience when exposed to water. Aquatic environments are very diverse, consequently, the conditions in for example of part of a river may differ completely to another. It is important to consider these factors when looking at decomposition, as a body will not decompose at the same rate in every body of water.

When a body is deposited underwater, it will sink 95% of the time, and movement of the body underwater depends on factors such as current strength and drag forces. The buoyancy of the body increases when in the bloating stage, as the gases produced in the abdomen cause a decrease in body gravity. As a result, the body will float and resurface. It is difficult to determine the exact amount of time it takes for the body to bloat and float, as it is mostly dependent on the temperature of the water. Temperature changes in the water are just as important as temperature changes on land. Water temperatures are known to be cooler than air temperature, mostly due to the fact that the warmth of sun rays declines exponentially with depth. Other major influencers of temperature are depth of water, shading and the water flow. Higher water temperatures will accelerate decomposition, therefore causing the body to float earlier (due to the build-up of gases). Lower temperatures in deeper waters and higher pressure will prevent the body from floating, preserving it longer [18]. Exposing the body above water will accelerate decomposition as

animals and insects will feed on it. Subsequently, gases will slowly leak from the body via the ruptures in the skin, and the body will sink to the floor once more where it will continue to decompose.

The formation of adipocere also influences the process of decomposition in aquatic environments. It is identified as a waxy grey substance, formed a few hours after death if the body is located in specific conditions (pH 5-9 and temperatures of 22°C) [19]. Adipocere is made of fatty acids that are formed when triglycerides from fatty tissue undergoes hydrolysis. These will convert into saturated fatty acids by hydrogenation, which forms on the skin [20, 21]. This substance can continue forming for months, eventually forming a protective layer around the body, preventing further decomposition.

Research into the effects of different water environments on decomposition is not as popular as those that focus on land decomposition. Brief comparisons of the effects of marine and freshwater environments, as well as moving and still water, have been carried out in recent years [22-25]. These results are mostly based on physical observations of the carrion used, and highlights the difficulties in using physical indicators due to the varying conditions in aquatic environments.

1.2 Recovering human remains

1.2.1 Cadaver dogs

It is important to consider why it is necessary to conduct research into developing a new technique to assist in identifying human remains on land and in water, while other techniques are currently available worldwide. Cadaver dogs are used often during missing persons' investigations. As dogs mostly rely on olfactory information, they are a useful tool for many forensic applications such as searching for drugs, bombs, firearms and missing

people as their noses are a million times more sensitive compared to humans [26]. Human Remains Detection Dogs (HRD) are specifically trained to detect human remains, as they have the ability to track the scent as soon as decomposition begins, that being the case, dogs hold an advantage of working faster than humans. Although using dogs proves to be a relatively successful technique, it is still not known what compounds the dogs are identifying. Looking at statistics in the literature, strong contradictions appear on the success rate and behaviour of cadaver dogs, with the most influencing factor being temperature. Researchers such as Lasseter [27] discovered a 60% success rate in the dogs' ability in very hot conditions. Contradicting this, France [28] discovered a substantial decrease in the dogs' success rate in temperatures over 85^{o}F, the suggested cause being the degradation of bacteria in higher temperatures. Furthermore, Komar [29] found an 85% success rate in lower temperatures.

Other environmental factors are known to cause problems when using dogs, such as wind, humidity, terrain, and soil type. Frozen land can also cause issues for HRD dogs, as the ice may create a barrier which blocks any volatile compounds emerging from the ground [26]. Optimal conditions have been suggested, such as temperatures of 4-16^{o}C, 20% humidity and a wind speed of 8km h^{-1} [30]. Although overall, the dogs' success rate in identifying remains on land is relatively positive, more difficulties arise when remains are underwater. While it is possible to utilise cadaver dogs on the shoreline or by placing them on a boat, it is not a technique effective enough to allow them to identify scent particles from a specific location [31]. Bodies in aqueous environments may also move rapidly depending on what type of environment it is, as a result this may confuse the dog further and reduce its reliability. In recent years, more science-based techniques have been developed recently to try and work alongside cadaver dogs in detecting remains on land and in water.

1.2.2 Geophysics

Researchers Ruffell and Pringle [30] wrote a review of all current geoforensic techniques used to identify remains on land and in water, focusing on their advantages and disadvantages. Ground penetrating radar (GPR) has been frequently used to detect remains underground in criminal cases. Radar waves are pulsed from the antenna, which reflect off objects buried underground. The velocity of the radar waves changes depending on the physical and chemical characteristics of the ground. The travel times are measured and create a 3D data set, used to show a profile of the object that is identified. In recent years, GPR has been developed for use in water, now commonly known as water penetrating radar (WPR). So far, there are 3 conventional ways of using this equipment on water. The first is while driving along solid ice [32]. The second is the suspension of antennas over rivers and ponds, and the third way is to position it on a boat [33]. Although it is clear there are many different ways to use this technology, the literature is limited to only a few studies successfully implementing WPR [34]. WPR has a major advantage of being compact, fitting on small inflatable boats, however, the highest quality images can only be obtained in shallow depths. One major disadvantage to using WPR is that it is limited to freshwater environments, as radar signals are 'soaked up' by conductivity in saltwater. Regardless, publications are available on identifying objects underwater with WPR such as unexploded objects [35] and sunken motors [34], but none on the identification of human remains. This technology is able to identify that something might be present but cannot specify what it is.

The second most popular technique to identify objects in water is Sonar. The instrument releases pulses down to the sea floor across a wide angle. Sonar waves detect acoustic beams at right angles in the water and allow wide area searches, depending on the reflective wave strength [36]. A raised surface will return the signal. The target needs to be larger than the background to identify an object e.g. if a body is lying on sand. If a body is

wedged between rocks it would not be able to identify it [37]. Ruffell [38] highlights this issue in a paper explaining how Sonar was unable to produce clear images of the body of a suicide victim wedged 2m underwater between rocks. Regardless of these issues, its main advantages are speed of survey and clarity of images. This gives the ability to scan the area very quickly, usually in place ahead of dive teams in areas of low visibility [39]. It has also recently been developed as a handheld device to assist divers underwater [37]. Other techniques that are mentioned in this review, but not used as frequently are magnetometers and sesmic methods. Magnetometers are very similar to underwater metal detectors, but instead, detect local variations in magnetics fields caused by the submerged objects. They have an advantage of being able to detect objects from greater depth than military-grade metal detectors, however very little has been published regarding its use in forensic water searches [30]. Sesmic reflection methods have also been considered potentially useful in the detection of remains, as it is able to provide information about the sub-surface structure of the sea floor. Artificially generated acoustic waves are sent through the water, where different objects on the sea floor reflect the energy back according to their acoustic impendence and recorded by hydrophones [40]. 2D and 3D visual representations are created to profile the floor. A Chirp profiling system can be used for high resolution images in a shallow area [30]. Although this technique has been used in a variety of circumstances [41, 42] the literature has yet to show its effectiveness in detecting remains.

1.3 Volatile and Non-Volatile compounds

It is natural to associate the decomposition process to volatile compounds, due to the foul smell that is known to accompany any decomposing carcass. The chemistry of decomposition has been studied closely, heavily focused on what volatile compounds are released. The University of Tennessee's Anthropological Research Facility (ARF) developed

a Decomposition Odour Analysis Database (DOA) [43] . This was achieved by a group of researchers including Arpad Vass, by creating a chemical database of volatile compounds detected during human decomposition for a year and a half. Three human bodies were used for this research, buried in graves between 1.5-2.5ft deep. Triple Sorbent Traps were used to obtain volatile samples, and gas chromatography – mass spectrometry (GC-MS) was used in the laboratory for analysis. A total of 424 volatile compounds were detected during this study from eight separate classes. The most significant compounds detected are highlighted in Table 1.2. In addition to looking at which volatile compounds were present during the study, the time of year these compounds appeared was also investigated. This is shown in Table 1.3.

Table 1.2: Volatile compounds detected during human decomposition analysis over 1 year, taken from Vass et al [43].

Cyclic Hydrocarbons	**Non-Cyclic Hydrocarbons**	**Nitrogen Compounds**	**Sulfur Compounds**	**Acid/Ester Compounds**	**Oxygen Compounds**	**Halogen Compounds**
1,4 dimethyl benzene	Heptane	Methenamine	Sulfur Dioxide	Hexadecanoic acid, Methyl ester	Decanal	Trichloromono-fluoromethane
1,2 dimethyl benzene	2-methyl pentane	Benzonitrile	Carbon Disulfide	-	Benzene methanol, a,a dimethyl	Chloroform
Ethyl benzene	Undecane	-	Benzothiazole	-	1-hexanol, 2-ethyl benzaldehyde	Trichloroethene
Toluene	-	-	2,4-dimethylthiane, S,S-dioxide	-	Nonanal	Tetrachloroethene
Styrene	-	-	Dimethyl trisulfide	-	Benzene	Diochlorodiflu-romethane
1-methyl-2-ethyl benzene	-	-	Dimethyl trisulfide	-	2-propanone	Dichlorotetraflu-oroethane
C4-benzene	-	-	-	-	-	Trichloroethane
						Carbon tetrachloride

Table 1.3: Table showing the time of year each classes of compounds were detected at the soil surface over 1 year, taken from Vass et al [43].

	Approximate Range of Primary Production Summer Burial at Depth of 1.5ft	**Approximate Range of Primary Production Fall/Winter Burial at Depth of 2.5ft**
Compound Class	**Days Since Burial**	**Days Since Burial**
Cyclic Hydrocarbons	50-150	60-230
Noncyclic Hydrocarbons	30-150 250-400	90-230
Nitrogen Compounds	128-350	60-115
Oxygen Compounds	17-150	60-230
Acids/Esters	17-150	60-230
Halogen Compounds	75-150 200-350	25-185
Sulfur Compounds	17-150	90-230

In conjunction with identifying what volatile compounds are present during decomposition, an investigation into the time frame in which they are released gives insight into the potential of using this approach in the field. In the summer months, volatile compounds seem to be released quicker and of a higher concentration than from those buried in winter. This would suggest that decomposition proceeds at a slower pace during colder months. Temperature is widely known to have the most impact on the rate of decomposition [44], as "heat accelerates the process of autolysis by increasing the speed of catalytic enzymes within the body and consequently the increased rate of autolytic cell breakdown increases the rate of putrefaction" [20, 45]. During the warm summer months, animal and insect activity is much higher, leading to increased amount of feeding etc. [20].

Rosier [46] conducted many years of research into the study of volatile human specific markers. In 2015, 452 compounds were identified over 6 months using GC-MS, among them were eight apparent human and pig specific markers. The number of compounds were similar to those detected in research from Vass [43]. The specific markers were identified as ethyl propionate, propyl propionate, propyl butyrate, ethyl pentanoate,

pyridine, diethyl disulfide, methyl(methylthio)ethyl disulfide and 3-methylthio-1-propanol. These compounds were claimed to be able to separate pig and human sample from other animals, however they were unable to differentiate between the two. Further into study, 5 esters (3-methylbutyl pentanoate, 3-methylbutyl 3-methylbutyrate, 3-methylbutyl 2-methylbutyrate, butylpentanoate and propyl hexanoate) were predicted to be able to separate the pig remains from human remains [46]. In addition to results derived from this study, they were also compared to those from similar researchers. Table 1.4 shows a comparison of human-specific compounds between studies lifted from a paper by Rosier [46].

Table 1.4: A comparison of suggested human-specific markers derived from other literature [43, 46-48].

VOC	Research Study	Detected in human remains	Detected in animal remains
Phenylethene	Degreeff et al.	-	-
Methyl benzoate	Degreeff et al.	-	X
Propanoic acid	Cablk et al.	X	X
Pentanoic acid	Cablk et al.	X	X
Hexanoic acid	Cablk et al.	-	X
Butyl butyrate	Cablk et al.	X	X
Pentyl hexanoate	Cablk et al.	-	-
Hexyl hexanoate	Cablk et al.	-	-
2-hexenal	Cablk et al.	-	-
2-octen-3-ol	Cablk et al.	-	-
Tetrachloroethylene	Cablk et al.	-	X
Cyclohexanone	Cablk et al.	-	X
2-ethyl-1-hexanol	Cablk et al.	X	X
Pentane	Vass et al.	X	X
Decane	Vass et al.	X	X
Undecane	Vass et al.	X	X

Although similar compounds were identified, it is clear from the table presented that the compounds found in human samples were also identified from animal remains. When looking at all three studies, it is important to note that methods and samples vary greatly between them, which will inevitably lead to variable results. When comparing the compounds discovered by Rosier to other researchers in the same field [43, 49, 50] it is important to consider the variability in the methods, instruments and classes of compounds identified.

In 2017, after analysing a wider variety of human and animal remains, Rosier discovered that the compounds proposed in their previous discoveries were not correctly identified as human-specific markers [51]. Although frustrating, this strongly highlights the difficulties encountered in this field, and the need for further study and consistent methods. This is also emphasised in research from Cablk [47]. While close similarities were found in volatiles between pigs and humans, compounds from chicken samples were noted to share the most common compounds with human remains. This shows contradicting results to those obtained in other studies, such as Armstrong [52] and Dekeirsschieter [53] who use pigs during their research as they are scientifically advised to be most similar to humans.

Although the volatile compounds detected in these research studies were present during the process of decomposition, it is not confirmed that they are specific products of human decomposition. As a result, the data gathered here is useful in understanding what cadaver dogs could be identifying when searching for human remains, in addition to the effect of temperature on the rate of decomposition. However, the detection of human-specific decomposition markers would be difficult to obtain with so many environmental factors affecting the results. For chemical analysis of decomposition products, a more specific sampling method would be necessary to gain reliable results on human-specific markers.

1.4 Metabonomics

Metabonomics is the study of low molecular weight compounds (<1000Da) known as metabolites, which collectively form a metabolome. These include, but are not limited, to organic species such as fatty acids, carbohydrates, amino acids and lipids. Other 'omics' disciplines include genomics (the study of genes), transcriptomics (the study of RNA), and proteomics (the study of proteins) [54].Metabonomics is described as a "quantitative measurement of the dynamic multiparametric metabolic response of living systems to pathophysiological stimuli or genetic modification" [55]. It is commonly mistaken with the term metabolomics. Metabolomics is the study of the whole metabolome, while metabonomics is the study of how the metabolite profile changes as a direct result of modification or stimuli such as environmental influences [54, 56].

There are two main categories of metabonomic analysis, targeted and non-targeted [56]. Targeted methods are commonly used when looking for metabolites of interest that are already known to be affected by certain environmental factors, therefore the experimental workflow is tailored to that particular compound [57]. Non-targeted analysis is implemented when the content or effects of the biological sample is unknown. As a result, the workflow aims to profile as many metabolites as possible, to create a clear metabolite profile of the sample. Due to the vast number of metabolites present in most biological samples, untargeted analysis will produce large amounts of data. It is possible to narrow down the number of metabolites of interest using multivariate and statistical workflows to discover which compounds show significant differences or trends [57]. Although initial metabonomic studies focused on Nuclear Magnetic Resonance (NMR), there has been a significant increase in the use of mass spectrometry in the detection and monitoring of metabolites [58].

Metabonomics is such a broad concept that it can be applied to many areas of scientific and medical research, for example medicine [59], toxicology [60], food fraud [61] and disease detection [62].

1.5 Rationale and Aims

With calls to police force regarding missing people increasing every year, the need for specialised search teams to locate them are also increasing. Land-based searches are relatively straight forward, however searches in water environments can be significantly more complex; and often require the deployment of significant manpower. Unless clear physical evidence shows remains may be in a specific area, most lakes and rivers are left unsearched due to financial and time constraints. As the resources available to police forces are decreasing, it is clear that automation has a significant role to play in maximising those available resources without decreasing the scope of an investigation.

This work aims to gain a deeper understanding of the chemical changes happening during decomposition using non-volatile compounds. An untargeted small molecule profiling approach using LC-MS will facilitate a thorough analysis, allowing the identification of any biological markers that are present due to decomposition. This will give a well-rounded overview of the potential of using chemical analysis to monitor decomposition in water. The application of the workflows and techniques used in this research could also be implemented to help aid the development of modern instrumentation to assist what is already in place to search for missing individuals, encouraging the use of portable devices such as mass spectrometers, which could advance into the automation of these search processes.

The main aims of this research are outlined below:

- To develop an effective and robust workflow that is suitable for non-targeted metabonomic analysis.
- To investigate whether it is possible to create a chemical profile of water that has been directly influenced by a decomposing carcass, and if it can be monitored over time.
- To determine the metabolic differences between species decomposing in water, and whether they can be easily differentiated using metabonomic analysis.
- To analyse the effects of moving and still water on the chemical signature of the water containing a decomposing carcass, and if it influences the water chemistry.
- To determine the full effects of temperature on chemical decomposition and how it influences the chemical profile of the water.
- To incorporate the workflow developed during this preliminary work into a more realistic environment.

1.6 References

[1] A. Vass, Beyond the grave – understanding human decomposition, Microbiology Today 28 (2001) 190-192.

[2] A. Gunn, Essential Forensic Biology, John Wiley & Sons, Chichester, West Sussex, 2006.

[3] L. Li, Y. Wang, A comparative study of the decomposition of pig carcasses in a methyl methacrylate box and open air conditions, Journal of Forensic and Legal Medicine 42 (2016) 92-95.

[4] L. Goff, Early post-mortem changes and stages of decomposition in exposed cadavers, Experimental and Applied Acarology 49 (2009) 21-36.

[5] A. Vass, R. Smith, C. Thompson, Odor Analysis of Decomposition Buried Human Remains, Journal of Forensic Sciences 53(2) (2008).

[6] A. Vass, Beyond the grave – understanding

human decomposition, Microbiology Today 28 (2001) 190-192.

[7] A. Vass, S. Barshick, G. Sega, J. Caton, J. Skeen, J. Love, J. Synstelien, Decomposition Chemistry of Human Remains: A New Methodology for Determining the Postmortem Interval, Journal of Forensic Sciences 47(3) (2002) 542-553.

[8] L. Swann, S. Forbes, S. Lewis, Analytical separations of mammalian decomposition products for forensic science: A Review, Analtyica Chimica Acta 682 (2010) 9-22.

[9] B. Dent, S. Forbes, Review of human decomposition processes in soil, Environmental Geology 45(4) (2004) 576-585.

[10] M. Gurr, Lipid metabolism in man, Proceedings of the Nutrition Society 47 (1988) 277-285.

[11] M. Esteves, D. Morcuende, S. Ventanas, R. Cava, Analysis of volatiles in meat from Iberian pigs and lean pigs after refrigeration and cooking by using SPME-GC-MS., Journal of Agricultural and Food Chemistry 51 (2003) 3429-3435.

[12] S. Forbes, Decomposition Chemistry in a Burial Enviornment, Soil Analysis in Forensic Taphonomy, CRC Press, New York, 2008, pp. 203-223.

[13] S. Paczkowski, S. Schutz, Post-mortem volatiles of vertebrate tissue, Applied Microbiology and Biotechnology 91(4) (2011) 917-935.

[14] R. Janaway, S. Percival, A. Wilson, Microbiology and Aging, 2009, pp. 313-334.

[15] V. Boumba, K. Ziavrou, Vougiouklakis, Biochemical pathways generating post-mortem volatile compounds co-detected during forensic ethanol analyse, Forensic Science International 174 (2008) 133-151.

[16] J. Dekeirsschieter, F. Verheggen, Cadaveric volatile organic compounds released by decaying pig carcasses (Sus domesticus L.) in different biotopes, Forensic Science International 189(1-3) (2009) 46-53.

[17] R. Byard, E. Farrel, E. Simposon, Diagnostic yield and characteristic features in a series of decomposed bodies subject to coronal autopsy, Forensic Science, Medicine, and Pathology 4 (2008) 9-14.

[18] T. Simmons, V. Heaton, Postmortem Interval: Submerged Bodies, Wiley Encyclopedia of Forensic Science, John Wiley & Sons, New Jersey, 2013.

[19] S. Forbes, B. Stuart, B. Dent, The effect of the burial environment on adipocere formation, Forensic Science International 154 (2005) 24-34.

[20] M. Sorg, W. Haglund, Forensic Taphonomy: The Postmortem Fate of Human Remains, 1st Edition ed., CRC Press, Florida, 1996.

[21] J. Caruso, Decomposition Changes in Bodies Recovered from Water, Academic Forensic Pathology International 6(1) (2016) 19-27.

[22] N. Hobischak, G. Anderson, Time of Submergence Using Aquatic Invertebrate Succession and Decompositional Changes, Journal of Forensic Sciences 47(1) (2002) 142-151.

[23] N. Hobischak, G. Anderson, Freshwater-Related Death Investigations in British Columbia in 1995-1996. A Review of Coroners Cases, Canadian Society of Forensic Science Journal 32(2-3) (1999) 97-106.

[24] M. Petrik, N. Hobischak, G. Anderson, Examination of Factors Surrounding Human Decomposition in Freshwater: A Review of Body Recoveries and Coroner Cases In British Columbia, Canadian Society of Forensic Science Journal 37(1) (2004) 9-17.

[25] G. Anderson, N. Hobischak, Decomposition of carrion in the marine environment in British Columbia, Canada, International Journal of Legal Medicine 118 (2003) 206-209.

[26] M. Sorg, D. Edward, Forensic Osteology: Advances in the Identification of Human Remains, Charles C. Thompson Publisher, Illinois, 1998.

[27] A. Lasseter, K. Jacobi, Cadaver dog and handler team capabilities in the recovery of buried human remains in the southern United States, Forensic Science Journal 48(3) (2003) 617-621.

[28] D. France, T. Griffin, Forensic Taphonomy: The Postmortem Fate of Human Remains, CRC Press, Florida, 1997.

[29] D. Komar, The use of cadaver dogs in locating scattered remains: Preliminary field test results, Journal of Forensic Science 44(2) (1999) 405-408.

[30] A. Ruffel, J. Pringle, J. Cassella, R. Morgan, The use of geoscience methods for aquatic forensic searches, Earth-Science Reviews 171 (2017) 323-337.

[31] A. Snovak, Guide to Search and Rescue Dogs, Barron's Educational Series, New York, 2004.

[32] A. Annan, J. Davis, Impulse radar and time-domain reflectometry experiments in permafrost terrain during 1976, In: Section 12, Report of Activities, Part B; Geological Survey of Canada Paper 77-1B (1977) 67.

[33] P. Sellmann, A. Delaney, S. Arcone, Sub-bottom surveying in lakes with ground-penetrating radar, In: U.S. Army Corps of Engineers Cold Regions (1992).

[34] A. Ruffell, Under-water scene investigation using ground-penetrating radar (GPR) in the search for a sunken jetski, Northern Ireland, Science & Justice 46 (2006) 150-159.

[35] J. Pope, R. Lewis, T. Welp, Beach and Underwater occurrences of ordnance at a former defense site, Erie Army Deport, Ohio, Army Corps of Engineers CERC Report 96-1, (1996).

[36] R. Parker, A. Ruffell, D. Hughes, J. Pringle, Geophysics and the search of freshwater bodies: a review, Science & Justice 50 (2010) 141-149.

[37] C. Healy, J. Schultz, K. Parker, B. Lowers, Detecting submerged bodies: controlled research using side-scan sonar to detect submerged proxy cadavers, Journal of Forensic Science 60 (2015) 743-752.

[38] A. Ruffell, Lacustrine flow (divers, side scan sonar, hydrogeology, water penetrating radar) used to understand the location of a drowned person, Journal of Hydrology 513 (2014) 164-168.

[39] O. McGrane, A. Cronin, D. Hile, Use of handheld sonar to locate a missing diver, Wilderness & Environmental Medicine 24 (2013) 28-31.

[40] A. Micallef, Developments in Earth Surfaces: Geomorphological Mapping, Elseiver, Oxford, 2011.

[41] J. Reynolds, The role of environmental geophysics in the investigation of an acid tar lagoon, Llwyneinion, North Wales, UK, First Break 20(10) (2002) 630-636.

[42] K. Koper, T. Wallace, S. Taylor, H. Hartse, Forensic seismology and the sinking of the Kursk, Eos 82(4) (2001) 37-52.

[43] A. Vass, R. Smith, C. Thompson, Decompositional odor analysis database, Journal of Forensic Sciences 49(4) (2004) 760-769.

[44] R. Mann, W. Bass, L. Meadows, Time Since Death and Decomposition of the Human Body: Variables and Observations in Case and Experimental Field Studies, Journal of Forensic Sciences 35(1) (1990) 103-111.

[45] M. Sorg, W. Haglund, Postmortem Changes in Soft Tissues, Foresnic Taphonomy: The Postmortem Fate of Human Remains, CRC Press, Florida, 1996, pp. 151-164.

[46] E. Rosier, S. Loix, W. Develter, The Search for a Volatile Human Specific Marker in the Decomposition Process, PLos One 10(9) (2015) 1-15.

[47] M. Cablk, E. Szelagowski, Characterization of the volatile organic compounds present in the headspace of decomposing animal remains, and compared with human remains, Forensic Science International 220(1-3) (2012) 118-125.

[48] L. DeGreeff, K. Furton, Collection and identification of human remains volatiles by non-contact, dynamic airflow sampling and SPME-GC/MS using various sorbent materials, Anal Bioanal Chem 401(4) (2011) 1295-1307.

[49] M. Statheropolous, A. Agapiou, Combined chemical and optical methods for monitoring the early decay stages of surrogate human models, Forensic Science International 210(1-3) (2011) 154-163.

[50] E. Hoffman, A. Curran, Characterization of the volatile organic compounds present in the headspace of decomposing human remains, Forensic Science International 186(3) (2009) 6-13.

[51] E. Rosier, S. Loiz, W. Develter, Differentiation between decomposed remains of human origin and bigger mammals, Journal of Forensic and Legal Medicine 50 (2017) 28-35.

[52] P. Armstrong, Establishing the volatile profile of pig carcasses as analogues for human decomposition during the early postmortem period, Heliyon 2(2) (2016).

[53] J. Dekeirsschieter, F. Verheggen, Cadaveric volatile organic compounds released by decaying pig carcasses (Sus domesticus L.) in different biotopes, Forensic Science International 189(1-3) (2009) 46-53.

[54] J. Nicholson, J. Lindon, Metabonomics, Nature 455 (2008) 1054-1056.

[55] J. Nicholson, Global Systems Biology, personalized medicine and molecular epidemology, Molecular Systems Biology 2 52 (2006).

[56] B. Zhou, J. Xiao, L. Tuli, H. Ressom, LC-MS-based metabolomics, Molecular Biosystems 8 (2012) 470-481.

[57] H. Gika, G. Theodoridis, R. Plumb, I. Wilson, Current practice of liquid chromatography mass spectrometry in metabolomics and metabonomics, Journal of Pharmaceutical and Biomedical Analysis 87 (2014) 12-25.

[58] G. Theodoridis, H. Gika, I. Wilson, LC-MS based methodology for global metabolite profiling in metabonomics/metabolomics, Trends in Analytical Chemistry 27(3) (2008) 251-260.

[59] J. Lindon, E. Holmes, J. Nicholson, Metabonomics Techniques and Applications to Pharmaceutical Research & Development, Pharmaceutical Research 23 (2006) 1075-1088.

[60] D. Robertson, Metabonomics in Toxicology: A Review, Toxicological Sciences 85(2) (2005) 809-822.

[61] K. Sidwick, A. Johnson, C. Adam, L. Pereira, D. Thompson, Use of Liquid Chromatogrphy Quadrupole Time-of-Flight Mass Spectrometry and Metabolic Profiling to Differentiate between Normally Slaughtered and Dad on Arrival Poultry Meat, Analytical Chemistry 89(22) (2017) 12131-12136.

[62] J. Brindle, H. Antti, E. Holmes, G. Tranter, J. Nicholson, H. Bethell, S. Clarke, P. Schofield, E. McKilligin, D. Mosedale, D. Grainger, Rapid and noninvasive diagnosis of the presence and severity of coronary heart disease using ^{1}H-NMR-based metabonomics, Nature Medicine 8 (2002) 1439-1445.

Chapter 2

Analytical techniques and instrumentation

2.1 Chromatography

Chromatography is a technique that allows separation, identification, and purification of compounds in a complex mixture between the mobile phase and the stationary phase. The stationary phase contains a porous small particle surface active material, or a liquid coated column wall. The mobile phase consists of a gas or liquid, depending on the type of chromatography used [1]. The complex mixture is suspended in the mobile phase, traveling through a column packed with the stationary phase. Compounds that prefer the stationary phase are retained longer on the column than those that have affinity to the mobile phase, resulting in separation [2].

2.1.1 Solid-phase extraction

Solid phase extraction (SPE) is a popular sample preparation method put in place prior to chromatographic analysis [3]. It is used to concentrate and purify analytes from a solution. The goal of SPE is to remove the analyte in question from the solution and recover it in a small volume of organic solvent [4]. Its high recovery level, low solvent use, and quick process are only a few of the advantages of SPE as a sample preparation technique. Similar

to chromatography, SPE is based on the partition of an analyte between the sorbent (solid phase) and the solvent (liquid phase). The analyte in question retains on the sorbent, and can only be eluted by providing a more physiochemically desirable environment (e.g. for a reversed phase SPE organic solvent) [5]. Figure 2.1 illustrates the four step process of solid-phase extraction. The organic solvent of choice is passed through the cartridge to wet the packing material and solvate the functional groups to activate the column. It is important to ensure the packing material does not go dry, as recovery will be poor. The sample is then loaded onto the column where the analyte will retain on the packing material [4]. The column is then rinsed to eliminate any interferences, followed by the elution step. The appropriate organic solvent is chosen to elute the analyte from the column, disrupting the analyte-sorbent interaction.

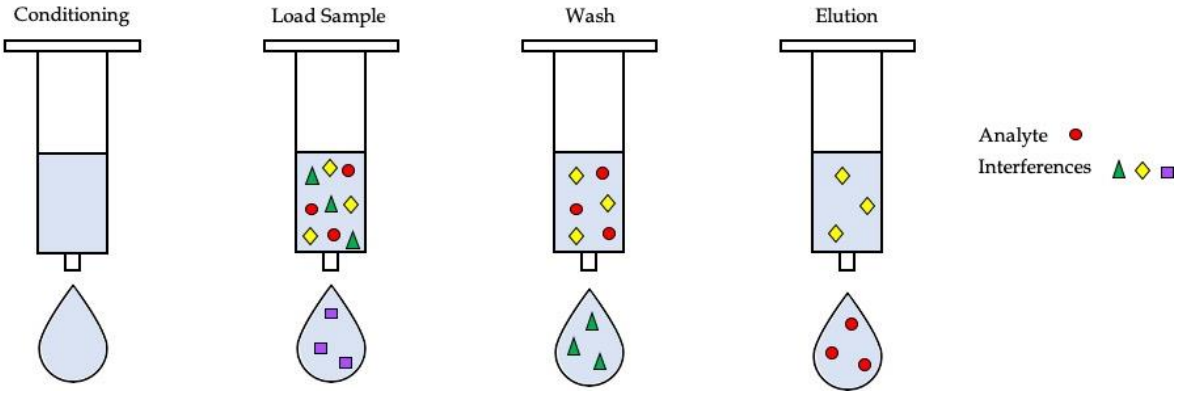

Figure 2.1. Diagram showing the solid-phase extraction workflow. The interference ■ eluting when loading the sample does not retain on the stationary phase. The interference ▲ will elute during the wash with a weaker solvent. The interference ◆ does not elute with the target analyte and retains on the stationary phase.

2.1.2 High performance liquid chromatography (HPLC)

Liquid chromatography separates compounds in a complex liquid mixture. The solvent is forced through the column under high pressure, which increases the speed of separation, leading to the name 'high performance' or 'high pressure' liquid chromatography. HPLC allows smaller particles in the column packing that creates a larger surface area in the stationary phase, allowing more interaction.

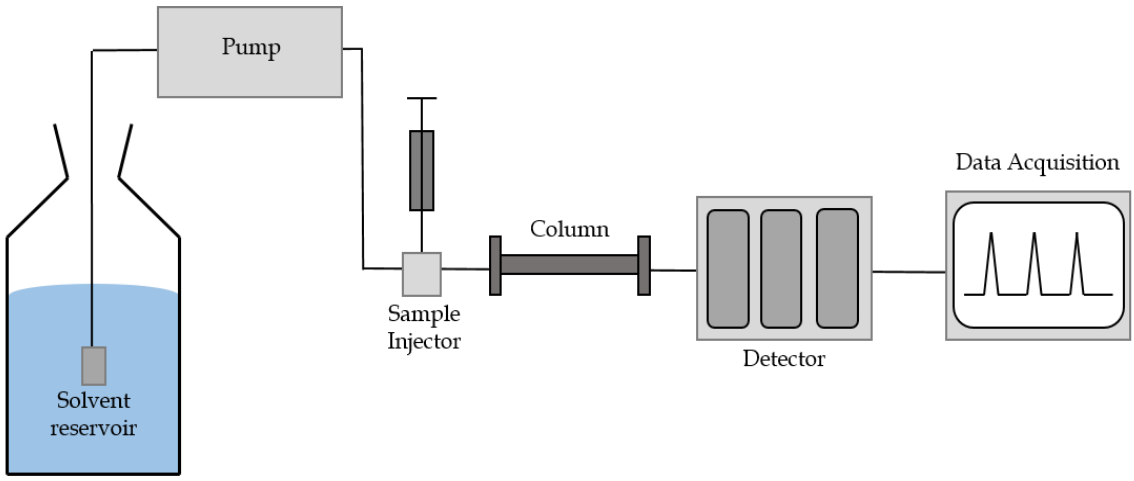

Figure 2.2: Schematic diagram of a HPLC system. Adapted from Meyer [1].

The instrument may vary from different manufacturers, however they all include a basic setup. These components are a solvent reservoir, pump, injector port, column, detector and data acquisition system [6]. This is shown in Figure 2.2. The solvent reservoir contains the mobile phase, which routinely consists of an organic solvent, and water. The mobile phase is used to transfer the sample through the instrument, and aids separation in the column. The pump is used to push the mobile phase through at a high pressure. The sample injector must inject a precise volume of sample as fast as possible to minimise disturbance to the mobile phase flow. The rotary valve system used has two positions. In the load position, the sample is injected into the loop while the mobile phase is flowing to the column, while

in the inject position the mobile phase flows through the loop and carries the sample to the column [7].

The column contains a stationary phase, and combined with the mobile phase, enables separation of the sample mixture depending on each compound's affinity to the stationary phase. Silica gel beads and alumina are among the most popular adsorbents used within a stationary phase. Each compound detected on the instrument will have a retention time (RT). The retention time reflects the amount of time a compound is retained on the column (From when the sample is injected, to when it reaches the detector). If a compound has a higher affinity for the stationary phase it will retain on the column, and as a result have a longer retention time. Those compounds with high affinity to the mobile phase will travel through the column quickly, having a short retention time. Each compound's retention time will create a peak in a chromatogram obtained during data acquisition. Those with a high affinity to the mobile phase will appear first on the chromatogram, followed by those that are retained on the stationary phase longer. This is shown in Figure 2.3.

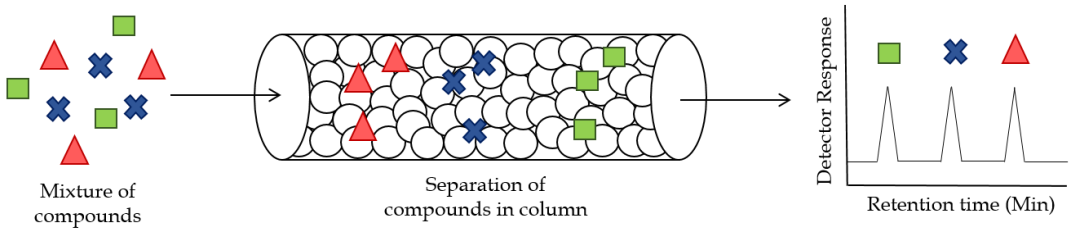

Figure 2.3: Separation of compounds in Reverse Phase Liquid Chromatography. Adapted from Meyer [1].

The packing of the stationary phase strongly depends on what type of chromatography is used. The two most prominent types used around the world are normal phase and reverse phase chromatography. Normal phase chromatography utilises a stationary phase that is

more polar than the mobile phase. As a result, polar (hydrophilic) analytes will retain on the column much longer than non-polar ones. This type is particularly useful for neutral and ionisable compounds [8].

Reverse phase chromatography however is one of the most popular techniques, as it is able to separate a wider variety of compounds. This phase uses alkyl chains that covalently bond to the stationary phase particles to create a hydrophobic stationary phase. The longer the carbon chain (C1, C4, C8, C12, C18), the less polar the phase. Contradicting the normal phase, this stationary phase has a high affinity for less polar compounds, inverting the polarity between the stationary and mobile phase. As a result, non-polar compounds will retain on the column and elute slower than more polar compounds [9].

The mobile phase includes an aqueous solvent and organic solvent (which holds a stronger eluting power). Methanol and acetonitrile are the most common organic solvents used in HPLC. Holding the organic and aqueous solvent constant throughout the analysis is known as an isocratic elution. This is useful when you know when your compound may elute. However, when analysing an unknown mix of compounds, a gradient separation is more suitable. A reverse-phase gradient elution usually begins at a low % of organic solvent, gradually increasing to 100% organic. Increasing the organic solvent will decrease the polarity in the column, therefore the non-polar compounds retained on the column will elute quicker. Additionally, the speed in which the organic solvent increases will affect separation. Changing the elution steepness can affect the relative elution times, which could help eliminate the issue of co-elution [1]. This allows an initial assessment of where and when each compound will elute. It is then possible to develop a method based on this information, to achieve the best separation while increasing efficiency. Once separation has occurred through chromatography, the individual compounds will travel to a detector. One of the most common detectors coupled to a HPLC instrument is a mass spectrometer.

2.2 Mass spectrometry

Mass spectrometry (MS) is an analytical technique that measures the *mass-to-charge* (*m/z*) ratio of an ion, which is used to calculate the exact molecular weight of each compound [10]. Is it a popular technique to analyse a variety of substances, for example gases, pharmaceuticals, drugs, environmental pollutants, explosives, proteins and cancers [11]. This technique has the ability to quantify known compounds and identify unknown compounds, while also able to elucidate the structure of these compounds. When a sample is introduced into a mass spectrometer, it undergoes ionisation, mass separation and lastly detection (As shown in Figure 2.4).

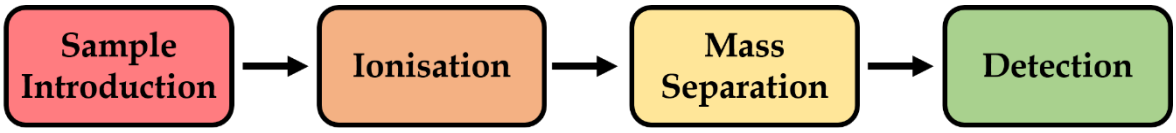

Figure 2.4: A basic 4-step sequence in a mass spectrometer.

When using liquid chromatography-mass spectrometry (LC-MS), the sample is introduced into the mass spectrometer after separation by liquid-chromatography. In the ionisation step, the analytes are vaporised and converted to gaseous ions in the ion source. Mass separation occurs in the mass analyser where the ions are separated based on their *m/z*. These ions then strike the detector which neutralises the charge, generating an electrical current. The current represents the abundance of the ion. The mass spectrum shows the *m/z* of each ion and its relative abundance.

2.2.1 Electrospray Ionisation

A variety of ion sources are used in mass spectrometry. In this particular work, an electrospray ionisation (ESI) method was utilised. ESI is a soft ionisation technique that uses electrical potential to atomize the liquid flowing out of the capillary into small charged droplets [12, 13]. The solution travels through the capillary tube at high voltage creating a solution of only one charge, as ions of the opposite charge are repelled from the electrical potential [11]. This allows the instrument to operate in positive and/or negative mode. The charged solution is passed through a stream of inert gas (Nitrogen) that nebulises the sample into charged droplets, followed by a secondary flow of heated drying gas.

Electrospray ionisation can be used via two different models. Low molecular weight analytes follow the ion evaporation model, whilst the charged residue model is used with larger species. A schematic diagram of both models is seen in Figure 2.5 [14].

The ion evaporation model explains that the charged droplets are continuously reduced in size by evaporation of the solvent assisted by the drying gas. This leads to an increase in surface charge density, and a decrease in droplet radius [15]. When the Coulomb force exceeds the surface tension of the charged droplet, it reaches a critical point at which it is energetically possible for the ions at the surface of the droplets to be ejected into the gas phase [16]. This is shown schematically in Figure 2.5. The ions are then accelerated into a mass analyser for subsequent analysis.

The charged residue model is used to describe the ionisation of large molecules such as proteins. This model suggests that the ionisation process generates droplets that contains one analytical ion. By successive scissions via a taylor cone mechanism, the droplet dimension is reduced until one analytical ion remains.

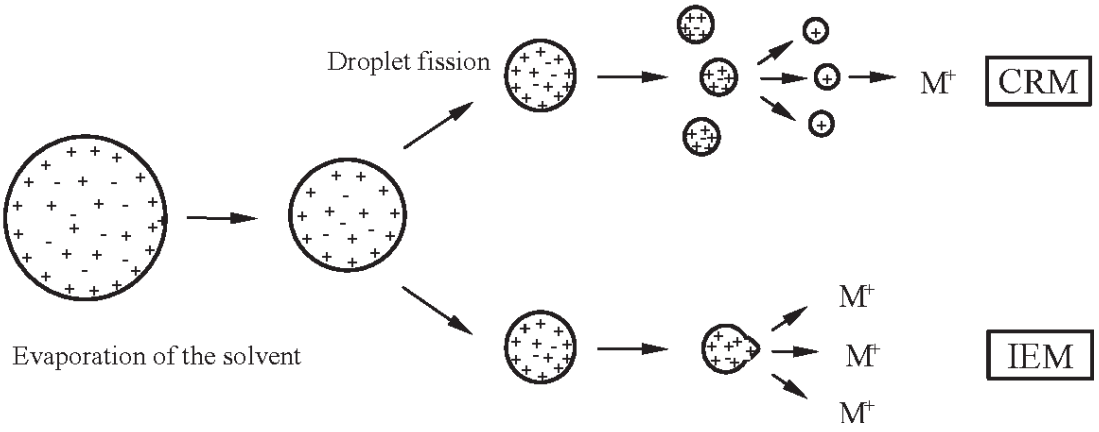

Figure 2.5: Schematic representation of the electrospray ionisation process following the ion evaporation model and charged residue model, taken from Crotti et al [14].

2.2.2 Mass analysers

Now that the gas phase ions have been produced, they travel through to the mass analyser where ions are separated based on their *mass-to-charge (m/z)* ratio. A variety of mass analysers have been developed, differentiated by how the different fields such as magnetic, static and dynamic are used to achieve separation [1]. When considering which mass analyser to use, there are five main characteristics to consider. The performance of a mass analyser is based on mass range limit, analysis speed, transmission, mass accuracy, and resolution. This is shown in more detail below in Table 2.1. The mass analysers discussed in this chapter are ones that were used within this research project, based on their unique properties.

Table 2.1: A brief definition of the five characteristics that affect the performance of a mass analyser.

Mass Range	The range in which the instrument can measure the *m/z* of an ion.
Analysis Speed	Also known as scan speed, is the rate the mass analyser can measure over a specific mass range in units per second (u s^{-1}).
Transmission	The ratio of the number of ions entering the mass analyser, and the number of ions reaching the detector (Loss of ions).
Mass Accuracy	The accuracy of the *m/z* provided.
Resolution	The ability of the instrument to differentiate between two ions with very similar *m/z's*.

2.2.2.1 Quadrupole

A quadrupole mass analyser consists of four metal rods, placed parallel to each other around a central void. The perfect alignment of these rods is crucial to obtain the ideal electrical field to separate ions of different *m/z*. All four rods have an electric potential, the rods opposite each other having the same charge, while the adjacent rod will have a different charge. A positive ion entering the quadrupole will initially be pulled towards the negative rod. If the electric potential switches to positive at the correct time, the ion will change direction, continuing through the quadrupole [11]. This is known as a stable trajectory, and can only happen when an ion with a specific *m/z* (Chosen by the analyst) is travelling through the quadrupole. An ion of any other *m/z* will quickly collide with the rod, also known as having an unstable trajectory [17]. These ions are immediately removed from the sample stream (See Figure 2.6). This mass analyser is most suitable for targeted analysis, looking for a specific compound in a sample mixture.

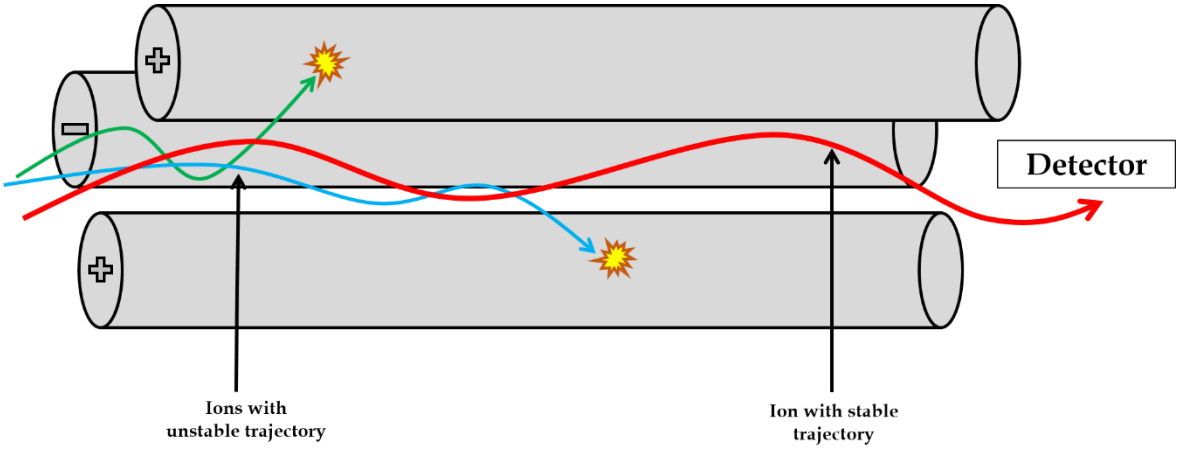

Figure 2.6: A diagram showing the stable trajectory of an ion through the quadrupole that reaches the detector (red) and two unstable trajectories (blue and green). The fourth pole has been removed to visualise the inside of the quadrupole.

2.2.2.2 Time-of-flight

Another type of mass analyser is a time-of-flight (TOF) analyser. It can separate ions based on their velocity in a flight tube [10]. When ions leave the ionisation source, they pass through a series of ion optics to focus the flow of ions. Upton entering the flight tube, an ion pulser produces a high voltage that accelerates the ions through the flight tube and to the detector. As there is a very short pause before the next pulse, therefore some ions are removed from the analysis as the continuous stream flows past the ion pulser at this short time. This reduces the sensitivity of the technique, however, having an exact start time on the pulser enables greater mass accuracy and selectivity [11]. Each ion entering the flight tube will have a different mass-to-charge ratio and will travel through the tube at different velocities. Lighter ions will have more kinetic energy, reaching the detector first. The larger ions have low kinetic energy, taking more time to reach the detector [18]. A mass spectrum is then created with each peak representing an ion. There are two main types of TOF mass analysers, linear and reflectron. A representation of a linear type is shown in Figure 2.7.

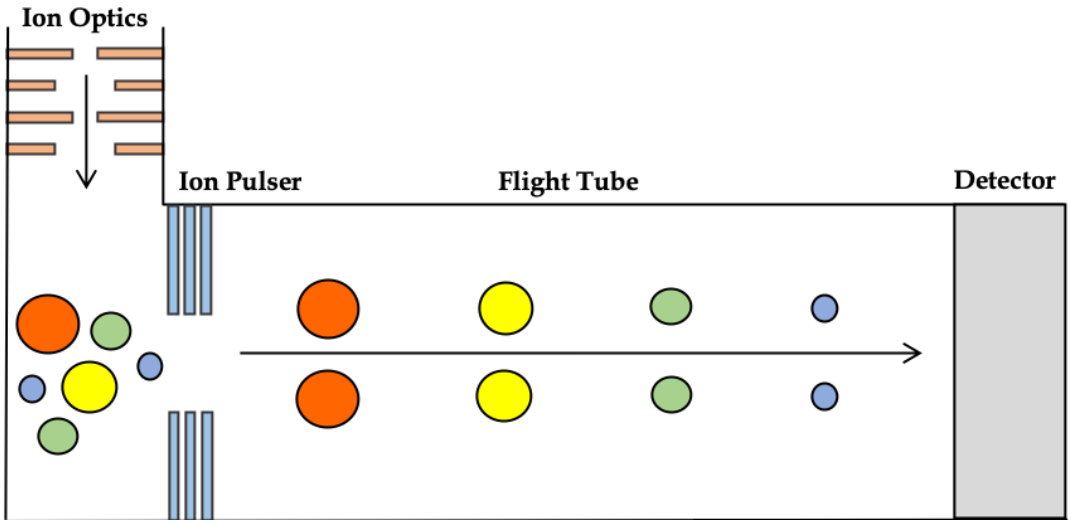

Figure 2.7: Representation of a linear TOF mass analyser. The blue ions are small with high kinetic energy, while the red ions are heavier with low kinetic energy.

In order to improve resolving power, a reflectron TOF instrument is used. The reflectron acts like an ion mirror, when hit, the ions are deflected back down the flight tube to the detector. Using a reflectron accounts for minor differences in the velocity of those ions with the same *m/z*, therefore correcting the kinetic energy dispersion of the ions. Ions with higher kinetic energy penetrate deeper and spend more time in the reflectron than those with lower kinetic energy, as their velocity is higher. As a result, ions with the same *m/z* but different kinetic energies will reach the detector at the same time [10] (Shown in Figure 2.8). The reflectron TOF instrument has achieved an increase in the flight path of the ions, without having to increase the size of the mass spectrometer.

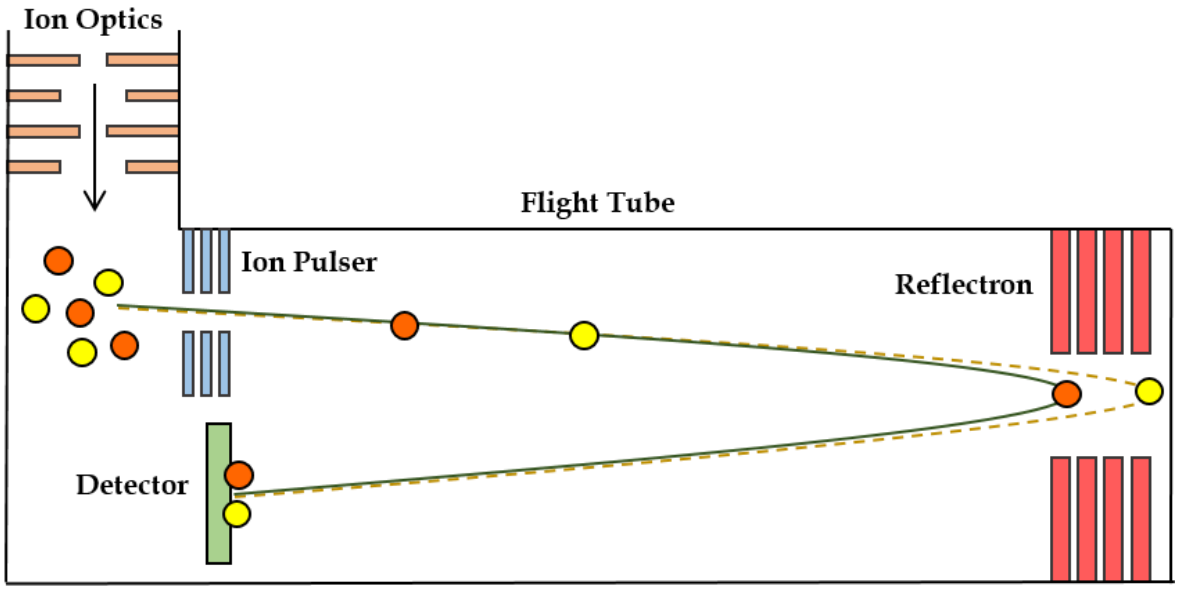

Figure 2.8: Representation of a TOF mass analyser with a reflectron. The orange and yellow ions both have the same mass-to-charge ratio, but different kinetic energy.

2.2.2.3 Orbitrap

The Orbitrap is an ion trap, of which moving ions are trapped in an electrostatic field. The analyser consists of two outer electrodes and a central electrode, which enables it to be an analyser and a detector. The ions are injected into the Orbitrap through 'electrodynamic squeezing' and start oscillating around the central electrode. These ions are separated based on the frequency of their oscillation. Fourier transform is used to obtain oscillation frequencies of ions with different masses. This allows an accurate reading of their *m/z* [19].

The Orbitrap can generate very high resolution measurements, and can deliver sub 1 ppm mass accuracy. This technique can be used as a quantitative and qualitative analysis on a single platform, and as a result is increasingly used for a wide range of challenging analyses such as non-targeted identifications [19].

2.2.3 Hybrid mass analysers

2.2.3.1 Quadrupole time-of-flight

Hybrid mass analysers consist of two or more mass separation devices, combining the advantages of both to give better performance [10]. During this research project, a quadrupole time-of-flight (Q-TOF) instrument was used. This particular instrument can be used in MS and MS/MS mode. For untargeted analysis, single MS mode allows all ions through the quadrupole, acting like an ion guide to the TOF mass analyser. In targeted analysis MS/MS mode allows the first quadrupole to act as a mass filter based on the *m/z* of the ion (As described in Section 2.2.2.1). The second quadrupole is a collision cell where fragmentation occurs as the ions collide at elevated potential with neutral collision gas molecules [20]. These fragmented ions then pass through the ion optics, focused into a beam to the TOF mass analyser (See Figure 2.9) [10].

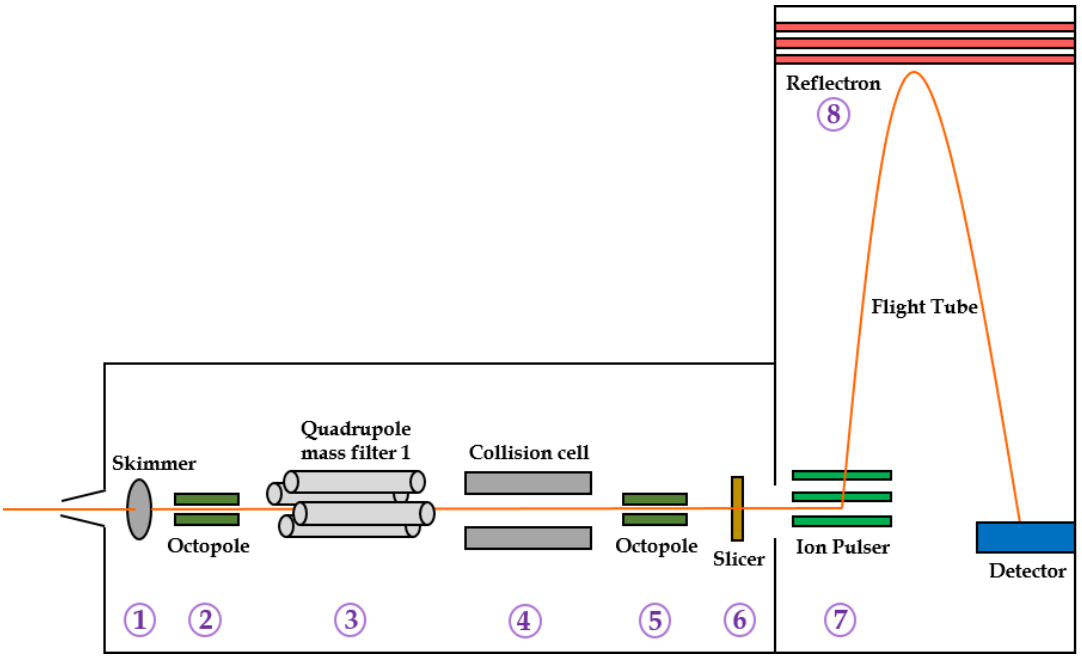

1) **Skimmer** – Maximises ion transmission and reduces transmission of neutral gas molecules.
2) **First Octopole** – Focus the ions into the mass filter.
3) **Quadrupole Mass Filter** - Separates ions based on the stability of their flight trajectories through an oscillating electric field in the quadrupole.
4) **Collision Cell** – The ion undergoes repeated collisions with the collision gas, fragmenting into precursor ions.
5) **Second Octopole** - Keeps ions together allowing collision gas to be pumped away.
6) **Slicer** - Reduced variation in momentum of ions.
7) **Ion Pulser** – High voltage pulse is applied to the back of the stack of plates, accelerating the ions through the flight tube.
8) **Reflectron** – An ion mirror to reverse the trajectory of the ion back down the flight tube. This minimizes the spread of kinetic energy of ions with the same *m/z*.

Figure 2.9: Diagram showing a quadrupole time-of-flight mass spectrometer.

2.2.3.2 MS/MS

MS/MS, or otherwise known as tandem mass spectrometry is an instrument that uses two or more mass analysers coupled together to break down selected ions (precursor ions) into fragments (product ions). This technique can provide detailed information about specific ions of interest, therefore often implemented in targeted analysis [21].

Looking back at Figure 2.9, when the sample is ionised, the precursor ions of a specific *m/z* are selected in quadrupole 1, then fragmented in the collision cell by collision–induced dissociation. The second quadrupole will separate these fragments by their *m/z* and send them to the detector [10]. Tandem MS can be used in space or in time. Instruments such as the triple quadrupole, QTOF and hybrid are most often used in-space, which contain two mass analysers in series. Tandem-in-time MS/MS is where different MS/MS stages are carried out successively in the same space but separately in time with instruments such as ion trap and FT-ICR MS. MS/MS has been applied to a many research areas such as protein identification, trace analysis of biological tissue, identifying food contaminants and drug testing [22].

2.3 Considerations in metabonomic analysis

2.3.1 Sample randomisation

Any changes in instrument sensitivity during an analytical run is most likely due to ion source contamination, the extent depending on the type of sample analysed [23]. Running the sample in a random order will eliminate the extent in which an issue with the instrument affects a particular sample group. Additionally, if for any reason the analytical run was unable to complete, randomisation will allow a partial data set to be obtained.

2.3.2 Quality control samples

Quality control (QC) samples are employed to monitor the system performance. Metabonomic analysis is well known for large sample batches as they often look for differences between a variety of sample groups. Instrumental drift often occurs in long analytical runs [24]. Instrumental drift has the potential to significantly affect the retention time of compounds, and if this is the case, questions the reliability of the analysis. QC samples have been developed to resolve this issue by pooling an equal aliquot of each sample within the analytical run as an overall representation of each compound [25]. The QC sample is analysed at the beginning, scattered randomly in the middle and at the end of the analytical run. It is also used to assess the condition of the column at the very beginning with multiple injections to assess the time it takes for the instrument to stabilise [23, 25, 26]. The number of injections used for stability significantly depends on the type of sample, the column and the system used.

A pre-analysis of QC injections will show how many injections are necessary to stabilise the chromatogram. QC samples can be used in a variety of ways to assess the stability of the instrument and quality of the data. Looking at the chromatograms will give an initial indication as to whether there is an immediate issue with retention time drift or deviations in the baseline. If the QC samples are visually stable, a multivariate statistics approach can be taken to look deeper into the data and assess the quality.

Multivariate analyses such as Principal Component Analysis (PCA) (See **Section 2.4.3**) can be used to assess instrument stability. Samples of a similar composition are expected to cluster close together on a PCA plot, showing no time-related trends [25]. As a result, the QC samples are expected to tightly cluster on the plot, if the instrument is demonstrating accuracy and stability. This suggest that the difference in multiple injections is less than the biological differences between sample groups [27]. This is shown in Figure 2.10. Additional

in-depth investigations can also be carried out on specific peaks on the QC sample chromatogram, to assess the variability of peak area and retention time from one sample to the next. Any outlier QC sample highlights instrument variation during that particular section of the analytical sequence. Variation observed within a specific QC sample brings awareness that instrument variation could be affecting experimental samples surrounding that particular QC sample in the sequence.

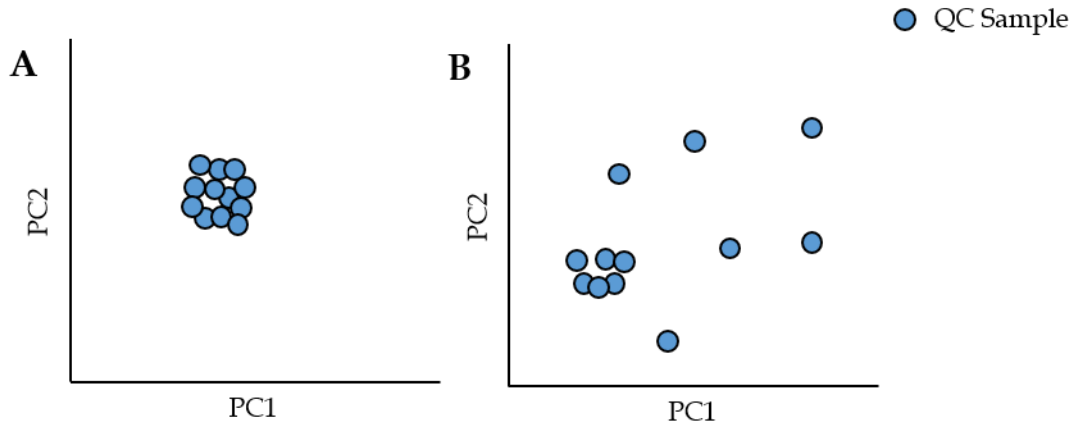

Figure 2.10: Two PCA scores plots, one with an instrument showing the result of a stable instrument (A) and an unstable instrument (B).

2.3.3 Reference ions

A reference mass solution of purine (*m/z* 121.0509) and hexakis (1H, 1H, 3H-tetrauoropropoxy) phosphazine (*m/z* 922.0098) was continuously infused throughout the analysis. These molecular ions are used as internal reference masses to ensure mass accuracy during the analytical run, assisting in mass correction [28].

2.4 Statistical analysis

Figure 2.11 is a flow chart that highlights a brief overview of the statistical workflow used for this particular metabonomic analysis, showing the software and parameters used at each step.

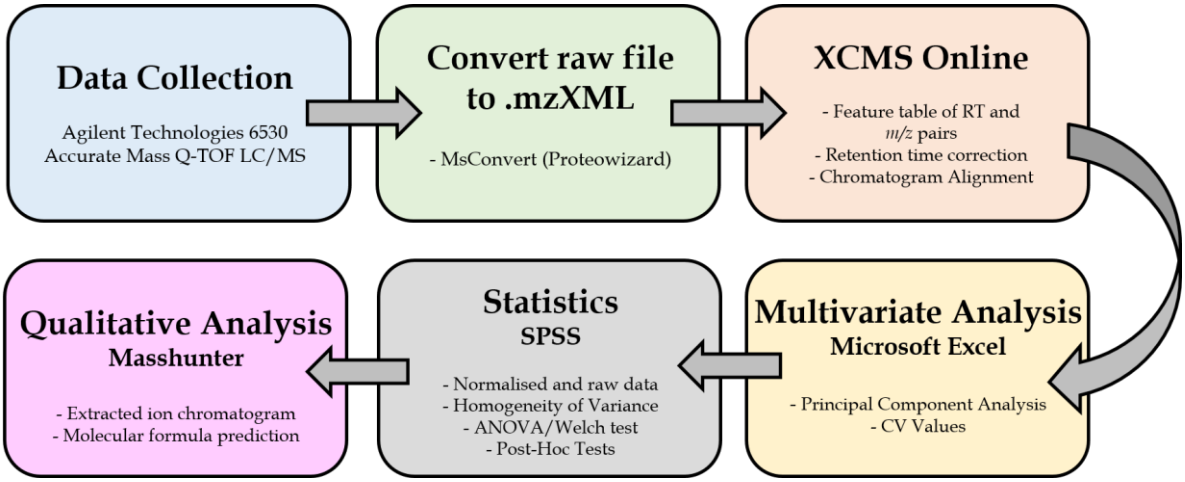

Figure 2.11: An overview of the data processing workflow used with various software.

2.4.1 Data pre-processing

The data used in this research project was pre-processed using *XCMS Online*, followed by statistical analysis on *Microsoft Excel* and *SPSS Statistics* software. *XCMS Online* is a free online platform that can perform feature detection, retention time correction, and alignment of chromatograms [29]. To upload data files onto *XCMS Online*, each file is converted from a .d file to a .mzXML file via *MSConvert* from Proteowizard, a set of open-source tools for proteomics data analysis. Once uploaded, the predefined parameters available on *XCMS Online* can be adapted depending on the nature of the analysis. The result can be viewed online, or downloaded in a results folder. This folder includes all the information available

online and a feature table in *Microsoft Excel* including *m/z* pairs, retention times and peak area for each feature detected in the sample. This file can be used for further statistical analysis on the data. *Microsoft Excel* was used to carry out statistical analysis from the data processed on *XCMS Online*.

Principal component analyses were carried out using a Multivariate Analysis add-in, followed by additional statistical analysis on *SPSS* such as homogeneity of variance,

Welch test and ANOVA. These analyses were carried out on raw data (Peak areas obtained from *MassHunter Qualitative Analysis*) and normalised data (Peak areas on *XCMS Online*).

2.4.2 Coefficient of variation

The coefficient of variation (CV), also known as relative standard deviation (RSD), is often used in analytical chemistry as an expression of precision and reliability of the data in question. Is it defined as the ratio of the standard deviation to the mean for a particular data set. The CV value is expressed as a percentage (%), reflecting the spread of results as a proportion of the mean value. This is crucial as it allows direct comparison in datasets where large differences may be present between the means [30]. The CV is calculated using the following equation:

$$CV\% = \frac{Standard\ deviation}{Mean} \times 100$$

The CV value does not represent the percentage of error in the data, rather the precision measured as a percentage. It is calculated using the peak areas of each feature detected in the quality control samples. Using the quality control samples will help predict the stability of the instrument, and precision in the data [30]. According to the literature, a CV value of 30% or less is deemed acceptable, taking into account the untargeted nature of metabonomic analyses and biomarker discovery [23, 27]. Any markers with a CV value above 30% are seen as unreliable, therefore removed from any further statistical analysis.

2.4.3 Multivariate statistics

Untargeted metabonomic analyses produce overwhelmingly large data sets, and therefore rely on chemometric methods to help visualise the data. Multivariate statistics are designed to analyse multiple variables. Examining the contribution of each one is essential when looking at pattern recognition [31, 32].

The most widespread multivariate statistical technique used for this purpose is Principal Component Analysis (PCA). PCA is able to reduce the amount of data given, focusing on a smaller data set containing specific features, called principal components. [33]. These are essentially a linear combination of the original variables. An eigenvalue is given to each principal component, accounting for the variance between the data sets.

The first principal component will have the largest amount of variance, and the second has the next highest, and so on [34]. 'Loadings' are another value given in PCA, which exist between all principal components in the data. A high loading value indicates that particular feature is responsible for most of the variation in that particular principal component [35].

The values for each principal component are known as scores. Plotting the scores from one principal component against another to produces a score plot. This plot visualises the data,

revealing where any differences lie [35]. Figure 2.12 represents a PCA plot showing results from three sample sets.

The quality control (QC) samples are clustered together as expected as they are repeat injections of the same sample. If these QC samples were to drift apart (as shown previously in Figure 2.10), it is a sign of instrumental drift. Minimal differences between the QC samples are deemed acceptable, shown by the arrow on the plot, as there is always a small chance that instrumental drift occurs during an analytical run.

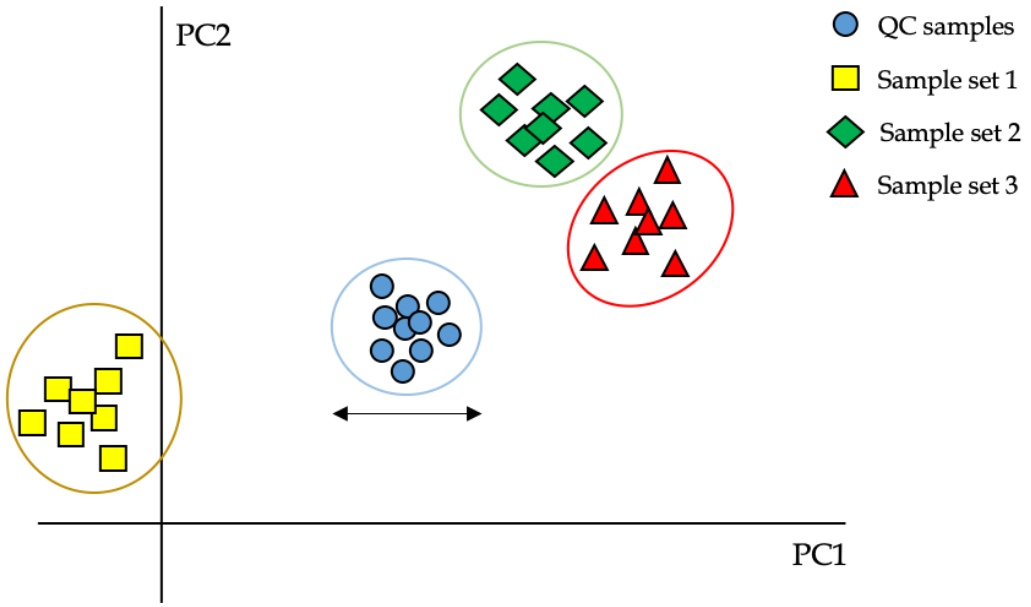

Figure 2.12: Simple representation of a PCA plot showing the main features.

Sample set 1 is at the bottom left corner of the plot, clearly separated visually from sample set 2 and 3. The spread of the QC samples is smaller than the distance between sample set 1 and the other sample sets, confirming that they are separated only by chemical differences. Although sample sets 2 and 3 can be grouped separately on the plot, the spread of the QC's is larger than the distance between these sample groups, therefore they cannot be distinguished from one another based on chemical composition alone. The principle

component showing the most separation on the plot is utilised to find the specific features that cause the separations on the plot, in this case it is PC1. Although this is a very effective way of isolating important features within the data, PCA does not always successfully separate sample groups on the plot. This could be due to differences that are very small and discreet. Other statistical tests can be used alongside PCA to acquire as much information as possible from each sample.

2.4.4 Univariate statistics

Univariate statistics focus on the analysis of one variable within the data set. Unlike Multivariate analysis, it does not look at causes and relationships, instead it aims to describe the patterns found in the data. There are to take into consideration when carrying out univariate analysis, such as normality and the variance within the data.

2.4.4.1 Normal distribution

Also known as the Gaussian distribution, the normal distribution depends on two main factors, the mean and the standard deviation [30]. The mean of the distribution determines the location of the centre of the graph, while the standard deviation determines the height and width of the graph [36]. A normal distribution will always have a symmetric, bell-shaped curve, as shown in Figure 2.13.

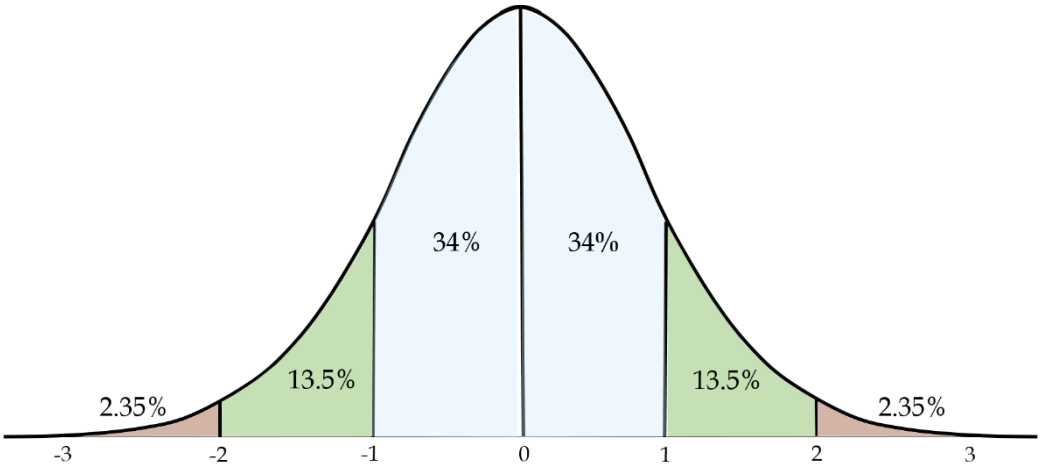

Figure 2.13: A normal distribution curve

Every normal curve conforms to a set of rules known as the 'empirical rule'. The first is about 68% of the area under the curve falls within one standard deviation of the mean. Consequently, 95% of the area under the curve falls within two standard deviations of the mean, and 99.7% within three standard deviations of the mean [36]. Normality of the data can be assumed when only one independent variable is changed during the experiment, and the rest are controlled. Parametric statistical tests are used when a data set follows a normal distribution, while non-parametric tests are used for data that is not normally distributed. In this work, normality of the data was assumed, and parametric tests were used. The remaining variables were controlled using quality control samples.

2.4.4.2 Homogeneity of variance

Homogeneity of variance must be calculated prior to a variety of statistical tests, to ensure the correct one is utilised. Homogeneity of variance is simply defined as having equal variation between samples in a specific data set [37]. This assumption is focused on the distribution of all the values within a sample group around the mean of that sample group.

If the sample sets vary in size, the variance will be unequal. The *F*-Test or the Levene's test is carried out in order to determine whether the variance is equal or unequal.

The *F*-test is used to compare the variance between only two sample sets. This test focuses on the variation between sample means, and the variation within the sample. A *p*-value is given to show the probability of observing an *F* value being greater than the observed *F* value if the null hypothesis is true (Equal variance) [37]. A *p*-value of $P<0.05$ indicates that the sample has equal variances, while a *p*-value over $P>0.05$ will have unequal variances.

If the data has two or more sample sets, a Levene's test is used to determine the homogeneity of variance [37]. The absolute deviations of each mean value from the sample set is used in a one-way analysis of variance (ANOVA). This test will again determine whether there is a significant difference in variance between each sample set, and therefore if the variance is equal or unequal [37]. If the data shows equal variance, an ANOVA is used, and a Welch's test if the data has unequal variances.

2.4.4.3 Student's t-test

The student's t-test is used to look at the differences between the population mean of two sample groups to determine whether the null hypothesis is true (No significant difference between the two groups) [37]. The equation for the null hypothesis showing that two means are equal is $H_0 : \mu_1 = \mu_2$ and the alternative hypothesis is $H_1 : \mu_1 \neq \mu_2$, stating the two means are not equal. There are two types of student's t-test considered in this work. A one-tailed test is used if the mean of a single sample is different to the expected value, while a two-tailed test is used to look at the difference between two independent sets of measurements [38]. A two-tailed test was used in this work, as the data sets were always independent to each other.

2.4.4.4 Analysis of variance and Welch's test

Analysis of Variance (ANOVA) is a statistical test used to compare the means between sample sets to identify if there are any significant differences between them when the variance is equal [33]. Unlike t-tests, ANOVA look into the variability of the data instead of the mean itself. A one-way ANOVA is carried out when only a single variable is compared between data sets [39]. ANOVA is used to compare the ratio of the between-group variability, and within-group variability, using the F-test [38]. Within-group variability looks at how the data varies within each group, while between-group variability looks at the difference between means from each group, then compares that to the overall mean. If the variance is unequal, a Welch's test is implemented instead of ANOVA due to its ability to correct the heterogeneity of variances by modifying the F-statistic [40, 41]. The software will report a *p*-value, which is the probability of observing an F-value equal to or greater than the observed F value, if the null hypothesis was true [37].

2.4.4.5 Post-hoc tests

A post-hoc test is carried out to provide a pairwise comparison of all the sample sets used in that particular analysis to determine exactly where the significant differences lie between them [42]. The Tukey test is utilised for a pairwise comparison for equal variances, while the Games-Howell is used for data sets with unequal variances. Both follow similar procedures to the two-tailed t-test [43] .

2.5 Summary

The metabonomic workflow consists of many stages, and although time consuming, each one is equally important to derive the maximum amount of information possible from each sample. Having a detailed experimental design allows high quality and accurate data collection during LC-MS analysis. Pre-processing the data and using a variety of statistical tests gives wide range of results, looking at the data from different angles. This allows a clear interpretation of any biological markers identified.

2.6 References

[1] V. Meyer, Practical High Performance Liquid Chromatography, 5th ed., Wiley, Sussex, 2010.

[2] R. Scott, Principles and Practice of Chromatography, Reese-Scott Partnership, LLC, 2002.

[3] M. Hennion, Solid-phase extraction: method development, sorbent, and coupling with liquid chromatography, Journal of Chromatography A 856 (1999) 3-54.

[4] E. Thurman, M. Mills, Solid-Phase Extraction: Principles and Practice, John Wiley & Son, Canada, 1998.

[5] S. Otles, C. Kartal, Solid-Phase Extraction (SPE): Principles and Applications in Food Samples, Acta Scientiarum Polonorum 15(1) (2016) 5-15.

[6] O. Coskun, Separation techniques: Chromatography, Northern Clinics of Istanbul 3(2) (2016) 156-160.

[7] F. Rouessac, A. Rouessac, Chemical Analysis: Modern Instrumentation Methods and Techniques, 2nd ed., John Wiley & Sons Ltd., West Sussex, 2007.

[8] D. Watson, The Theory of HPLC - Normal Phase Chromatography, CHROMacademy LCGC (2014) 6-8.

[9] Y. Kazakevich, R. Lobrutto, HPLC For Pharmaceutical Scientists, John Wiley & Sons, New Jersey, 2007.

[10] E. Hoffman, V. Stroobant, Mass Spectrometry, 3rd ed., Wiley, England, 2007.

[11] J. Greaves, J. Roboz, Mass Spectrometry for the Novice, CRC Press, Florida, 2014.

[12] M. Wilm, Principles of Electrospray Ionization, Molecular & Cellular Proteomics 10(7) (2011) 1-8.

[13] S. Banerjee, S. Mazumdar, Electrospray Ionization Mass Spectrometry: A Technique to Access the Information beyond the Molecular Weight of the Analyte, International Journal of Analytical Chemistry 2012 (2011) 2-39.

[14] S. Crotti, R. Seraglia, P. Traldi, Some thoughts on electrospray ionization techniques, European Journal of Mass Spectrometry 17 (2011) 85-100.

[15] C. Ho, C. Lam, M. Chan, R. Cheung, L. Law, L. Lit, K. Ng, M. Suen, H. Tai, Electrospray Ionisation Mass Spectrometry: Principles and Clinical Applications, The Clinical Biochemist Reviews 24 (2003) 3-12.

[16] T. Rohner, N. Lion, H. Girault, Electrochemical and theoretical aspects of electrospray ionisation, Physical Chemistry Chemical Physics 6 (2004) 3056-3068.

[17] W. Niessen, Liquid Chromatography-Mass Spectrometry, 3rd ed., CRC Press, Florida, 2006.

[18] A. Saitman, Introduction to Mass Analyzers: Quadrupole vs. Time-of-flight (TOF), PhD, Center for Advanced Laboratory Medicine, University of California San Diego (2015) 1-3.

[19] R. Zubarev, A. Makarov, Orbitrap Mass Spectrometry, Analytical Chemistry 85(11) (2013) 5288-5296.

[20] D. Allen, B. McWhinney, Quadrupole Time-of-Flight Mass Spectrometry: A Paradigm Shift in Toxicology Screening Applications, The Clinical Biochemist Reviews 40(3) (2019) 135-146.

[21] A. Klupczynska, M. Misiura , W. Miltyk, I. Oscilowska, J. Palka, Z. Kokot, J. Matysiak, Development of an LC-MS Targeted Metabolomics Methodology to Study Proline Metabolism in Mammalian Cell Cultures, Molecules 20 (2020) 4639.

[22] S. Kotretsou, A. Koutsodimou, Overview of the Applications of Tandem Mass Spectrometry (MS/MS) in Food Analysis of Nutritionally Harmful Compounds, Food Reviews International 22 (2006) 125-172.

[23] E. Want, P. Masson, F. Michopoulos, I. Wilson, G. Theodoridis, R. Plumb, J. Shockor, N. Loftus, E. Holmes, J. Nicholson, Global metabolite profiling of animal and human tissues via UPLC-MS, Nature Protocols 8(1) (2012) 17-32.

[24] E. Zelena, W. Dunn, D. Broadhurst, S. McIntyre, K. Carroll, P. Begley, S. O'Hagan, J. Knowles, A. Halsall, I. Wilson, D. Kell, Development of a Robust and Repeatable UPLC-MS Method for the Long-Term Metabolomic Study of Human Serum, Analytical Chemistry 81 (2009) 1357-1364.

[25] T. Sangster, H. Major, R. Plumb, A.J. Wilson, I.D. Wilson, A pragmatic and readily implemented quality control strategy for HPLC-MS and GC-MS-based metabonomic analysis, Analyst 131(10) (2006) 1075-1078.

[26] L. Lai, F. Michopoulos, H. Gika, G. Theodoridis, R. Wilkinson, R. Odedra, J. Wingate, R. Bonner, S. Tate, I. Wilson, Methodological considerations in the development of HPLC-MS methods for the analysis of rodent plasma for metabonomic studies, Molecular Biosystems 6 (2010) 108-120.

[27] G. Theodoridis, H. Gika, E. Want, I. Wilson, Liquid chromatography-mass spectrometry based global metabolite profiling: A review, Analytica Chimica Acta 711 (2012) 7-16.

[28] J. Olsen, L. Godoy, G. Li, B. Macek, P. Mortensen, R. Pesch, A. Makarov, O. Lange, S. Horning, M. Mann, Part per Million Mass Accuracy on an Orbitrap Mass Spectrometer via Lock Mass Injection into a C-Trap, Molecular & Cellular Proteomics 4(12) (2005) 2010-2021.

[29] R. Tautenham, G. Patti, D. Rinehart, G. Siuzdak, XCMS Online: A Web-Based Platform to Process Untargeted Metabolomic Data, Analytical Chemistry 84 (2012) 5035-5039.

[30] C. Adam, Essential Mathematics and Statistics for Forensic Science, John Wiley & Sons Ltd., West Sussex, 2010.

[31] R. Brereton, Applied Chemometrics for Scientists, John Wiley & Sons Ltd., New York, 2007.

[32] G. Theodoridis, H. Gika, I. Wilson, LC-MS based methodology for global metabolite profiling in metabonomics/metabolomics, Trends in Analytical Chemistry 27(3) (2008) 251-260.

[33] J. Miller, J. Miller, Statistics and Chemometrics for Analytical Chemistry, 6 ed., Pearson Education Ltd., Essex, 2010.

[34] H. Abdi, L. Williams, Principal component analysis, Computational Statistics 2 (2010) 433-459.

[35] R. Bro, A. Smilde, Principal component analysis, Analytical Methods 6 (2014) 2812-2831.

[36] D. Lucy, Introduction to Statistics for Forensic Scientists, Wiley, West Sussex, 2005.

[37] S. Ellison, V. Barwick, T. Farrant, Practical Statistics for the Analytical Scientist: A Bench Guide, 2nd ed., Royal Society of Chemistry, Cambridge, 2009.

[38] R. Ennos, M. Johnson, Statistical And Data Handling Skills In Biology, 3rd ed., Pearson Education Limited, Harlow, England, 2018.

[39] J. McDonald, Handbook of Biological Statistics, Sparky House Publishing, Baltimore, 2015.

[40] J. S-L, G. Shieh, Sample size determinations for Welch's test in one-way heteroscedastic ANOVA, British Journal of Mathematical and Statistical Psychology 67 (2014) 72-93.

[41] A. Lee, Optimal sample sizes determined by two-sample welch's t test, Communications in Statistics - Simulation and Computation 21(3) (1992) 689-696.

[42] H. Kim, Analysis of variance (ANOVA) comparing means of more than two groups, Restorative Dentistry & Endontics 20(3) (2000) 235-241.

[43] M. Shingala, A. Rajyaguru, Comparison of Post Hoc Tests for Unequal Variances, International Journal of New Technologies in Science and Engineering 2(5) (2015) 22-33.

Chapter 3

Method Development

The aim of this chapter was to determine whether it was possible to identify a chemical signature of decomposition in water containing decomposing remains, using non-targeted metabonomic profiling. Developing an appropriate workflow for this purpose consisted of two main goals. The first goal was to identify the most effective sample preparation method, to ensure that a wide range of compounds were captured for analysis. The second goal was to investigate how the sample interacts with a variety of column chemistries, to determine which column would achieve maximum output suitable for non-targeted analysis.

3.1 Introduction to HPLC method development

The most important aim of any high-performance liquid chromatography (HPLC) method is to achieve optimum resolution, in the minimum amount of time. This helps to obtain high quality data, whilst keeping costs and running times low. The purpose of any method development process is to create a suitable method for the specific analytes of interest. There are a wide range of choices available to method developers such as equipment, columns, eluent and instrumental parameters. While it seems complex, they are essential to create a reproducible and robust method. There are a variety of separation techniques and principles to keep in mind when developing a new method.

3.1.1 Separation techniques and principles

Chromatographic mode

The chromatographic system is defined as the type of interaction occurring between the stationary phase and the desired analyte. The classic mode of chromatography is known as the Normal phase. The stationary phase is more polar than the mobile phase, and separation is highly based on the polarity of the compounds. Less polar solutes will elute first, while polar compounds spend more time adsorbed onto the stationary phase as a result of hydrogen bonding and van der Waals forces. As a result, more polar compounds are retained on the column longer. The mobile phase used for normal phase separation is typically 100% organic with no aqueous component. One of the main advantages of normal phase chromatography is that polarity differences between compounds can be as discreet as a result of the addition/loss of a functional group or even their location within the molecule [1].

Reverse-phase chromatography uses a non-polar stationary phase, where separation is largely based on hydrophobicity, not just polarity. With the use of an aqueous component alongside an organic solvent, it facilitates a hydrophobic interaction between the non-polar stationary phase and the analytes. Due to its reproducibility and broad range of applications, reverse-phase chromatography (RPC) is now used for around 75% of all HPLC analyses. C18 bonded silica is currently the most popular packing material for reverse-phase chromatography. RPC is popular for peptides, proteins and many other molecules [2].

Column

Being one of the most important experimental factors within the technology, there are many factors to consider when choosing a column. The packing material, length, particle size, carbon loading and diameter of a column will influence efficiency, selectivity, and quality of the separation. The most common packing material (stationary phase) used is silica. Silica can be modified depending on the nature of the solute, making it a desirable and popular phase. Recent developments have introduced other packing materials such as cross-linked organic polymers and zironica. A short column (20-50mm) will allow shorter analysis times and low backpressure, while a longer column (250-300mm) will produce higher resolution at the expense of longer analysis times and increased back pressure.

Plate Theory

The efficiency of the column can be defined by the number of plates (N) it has. The plate theory suggests that a chromatographic column has a number of separate 'layers' called plates. These plates provide a theoretical basis for the assessment of column efficiency [3]. A high number of plates suggests greater column efficiency. Another way to utilise plates is by using the plate height (Height Equivalent to a Theoretical Plate - HETP) [4]. The theory behind column efficiency can be described by the Van Deemter equation (*Eq 1*), where A is eddy diffusion, B is longitudinal diffusion, C is resistance to mass transfer and u is average mobile phase velocity. The lower the value of HETP, the higher the column efficiency [3].

$$\mathbf{HETP = A + (B / u) + Cu} \qquad \textit{(Eq 1)}$$

The graph below in Figure 3.1 visualises each component of the equation, giving the location of the optimum efficiency of the column based on each value. Each factor in the equation has a unique effect on the column's efficiency.

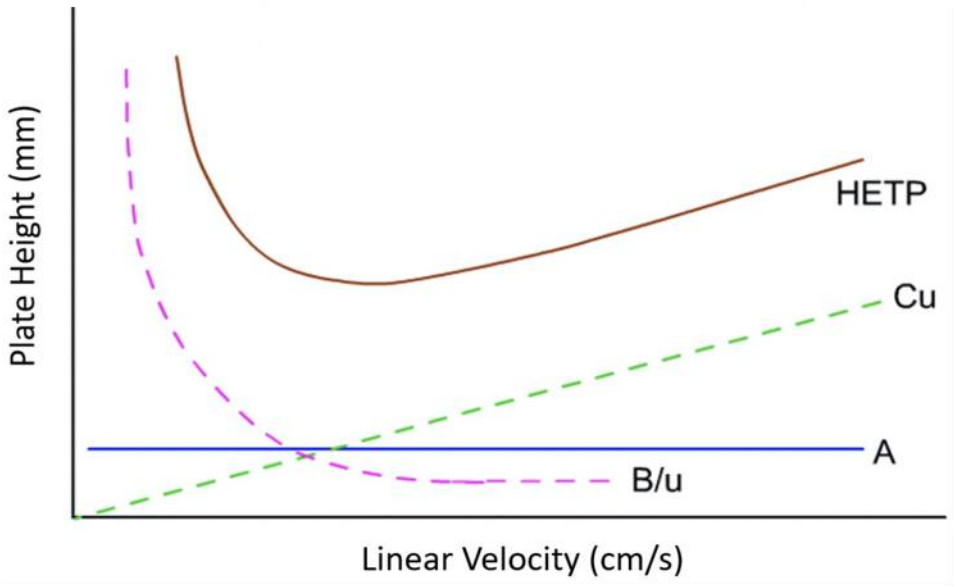

HETP - Height equivalent to a theoretical plate
A - Eddy diffusion
B - Longitudinal diffusion
C - Resistance to mass transfer
u - Average mobile phase velocity

Figure 3.1: Graph showing each individual component of the Van Deemter equation (Eq 1) [5].

All molecules, even those that are the same size can take an infinite number of 'paths' when traveling through the column due to the packing of the stationary phase. This leads to the diffusion of the molecules through the column, known as eddy diffusion [4]. An example is shown in Figure 3.2.

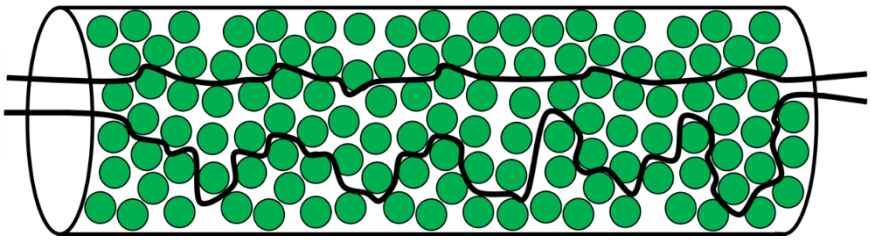

Figure 3.2: Diagram showing how two molecules of the same size can travel by two different paths through the column.

As a result, a smaller particle size can increase the efficiency of the column, as it allows the molecules to travel through easier. A graph below in Figure 3.3 [6] highlights the effects of particle size on plate height. It is clear that the smaller particle size yields higher column efficiency.

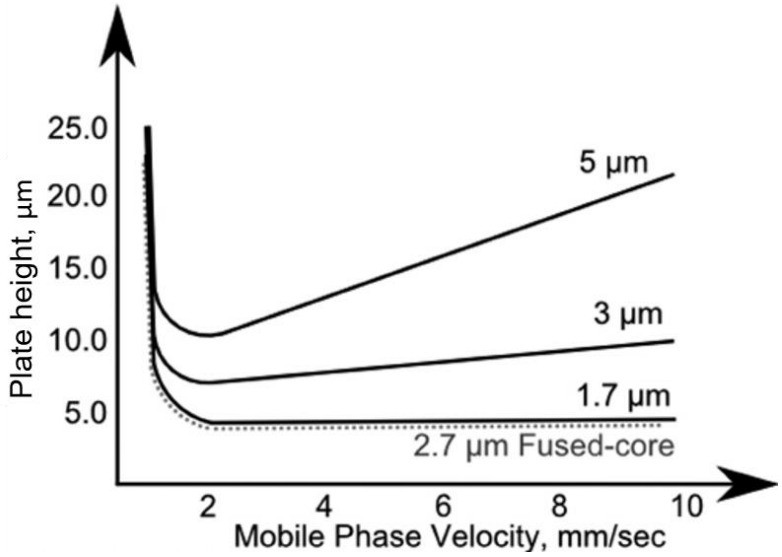

Figure 3.3: Graph showing the effect of the particle size of the stationary phase on the efficiency of the column [7].

When a band of molecules travel through the column, its highest concentration will be at the centre. The more time these molecules spend in the column, the more they will start to diffuse towards the edges. This is called longitudinal diffusion, which can also result in band broadening [4]. The higher the velocity of the mobile phase, the faster the molecules will travel through the column, reducing the effects of longitudinal diffusion [3].

Resistance to mass transfer refers to the molecule's interaction with the stationary phase pores. Whilst some molecules will penetrate the stationary phase, others may not due to their size, speed and direction of flow (Shown in Figure 3.4). As a result, the ones that have penetrated will take longer to re-enter the mobile phase, which can again cause band broadening [4]. A slower flow rate allows less lag between the compounds that interacted with the stationary phase, and those flowing directly through the column. It is important to consider a balance between both B and C, as they are improved by opposite changes. Calculating its location on the Van Deemter curve can help determine whether the flow rate needs to increase or decrease.

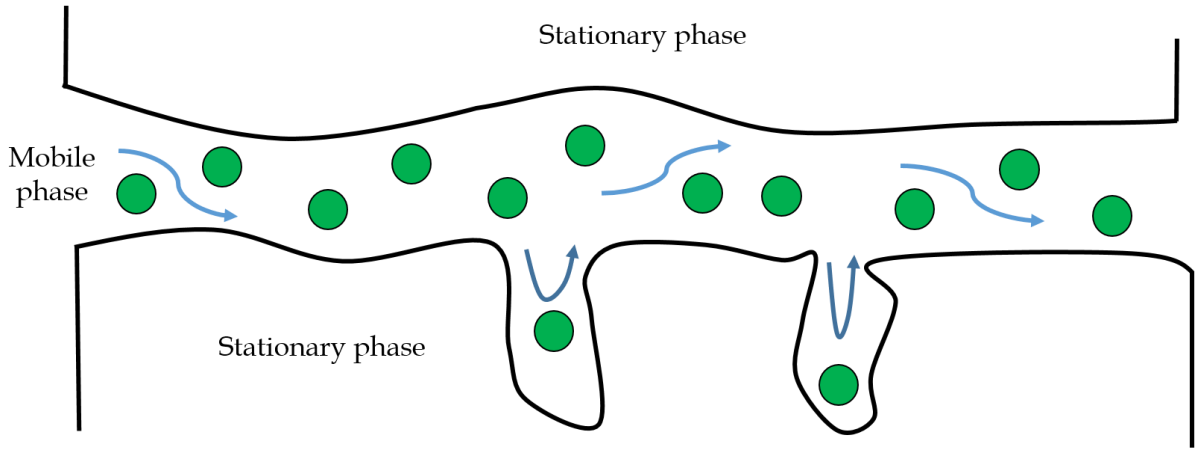

Figure 3.4: Diagram showing the molecule's interaction with the stationary phase, with those that penetrate the phase and those who flow straight through. Adapted from Meyer [4].

Mobile phase

The nature of the mobile phase has a strong influence on the separating power of the chromatographic system. The solvent used is strongly dependent on how it will react with the solute, as their chemical properties will affect the interaction between the silica surface and target compounds. The most common organic modifiers to accompany water are methanol (MeOH) or acetonitrile (ACN). Both are miscible with water and compatible with popular mobile phase additives and buffers [8]. The advantages and disadvantages of each solvent depends on their interaction with the analytes in question. The low viscosity of ACN mixed with water generates lower backpressure. Low backpressure creates opportunities to increase flow rates and reduce analysis time. ACN is also known to have higher elution strength. Whilst this could also help to shorten the analysis time, it could cause co-elution if solute contains multiple compounds eluting close together. As a result, the optimum choice of solvent is application driven. Investigating the use of both solvents is advised during method development.

Isocratic or gradient elution

An isocratic elution means that the mixture of the mobile phase is consistent throughout the entire analysis time. A gradient elution is when the mobile phase mixture is changed from a low to high elutropic strength. An isocratic method is simpler, however using a gradient elution will help resolve and separate peaks quicker [9]. Although gradient elutions are preferred, issues arise such as ghost peaks, peak asymmetry and baseline drift, whilst an isocratic elution can produce peaks with a more uniform width due to the elimination of errors due to a changing gradient. Similar to most aspects of method development, the type of elution is largely dependent on the behaviour of the analytes.

Temperature

The effect of temperature is slightly underrated in LC-MS, as it is assumed to be more relevant in Gas Chromatography (GC). High temperatures in an LC system can cause a decrease in retention due to the increase in chromatographic separation. Recent developments have produced columns that can withstand higher temperatures (for example Hypercarb). Being able to operate at higher temperature can decrease solvent viscosity, resulting in lower backpressure. That allows use of higher flow rate without sacrificing efficiency, therefore optimising the resolution. More research is required in this field to fully understand the effects of temperature [10].

Buffer

The buffer is used to control the pH of the mobile phase. Small changes in pH can have a large effect on retention and peak spacing if the mobile phase pH is near the compounds pKa. A general starting point for method development suggests a mobile phase with a pH of 2-3. At this pH, there will be no ionization of any silanol groups (to prevent interaction with the free silanols on the stationary phase) or ionization of any organic acids [11]. A buffer can maintain the pH of the solvent by adding a small amount of acid or base. The most commonly used buffers for LC-MS are ammonium acetate and formic acid for low pH [12].

3.1.2 Solid-phase extraction

Solid phase extraction (SPE) is a sample preparation technique that separates compounds in a liquid mixture based on their physical and chemical properties. It has been demonstrated to be a reliable and cost-effective technique for the selective isolation and concentration of a wide range of analytes and sample matrices. The most popular applications for SPE are environmental tracing of organic pollutants, extraction of pesticides, purification of peptides and drug analysis in clinical applications [13, 14]. A detailed description of the four-step process in shown in Chapter 2, Section 2.1.1.

An SPE cartridge is made of a plastic or glass container filled with an adsorptive phase with different characteristics depending on the characteristics of the analyte itself [15]. The success of an SPE experiment is determined by the type of sorbent used. Due to the increase in research and popularity of SPE, there are a wide variety of sorbents available, that can be changed depending on the type of interaction happening between analyte and sorbent. The most frequently used sorbents are chemically modified silica gel, polymer sorbents and graphitized or porous carbon [15]. Silica is the most popular material used in SPE. To increase its applicability, the silica surface can be modified with a variety of functional groups on the surface to change its functionality e.g. non polar (C18), polar (NH_2) or ionic/mixed mode (C8, cation exchange) [15]. For many years, C18 modified silica contain a high surface area of 500 to 600 m^2/g, guaranteeing the maximum amount of octadecyl chains at the silica surface [14].

Activated charcoal

Research has shown that activated carbon is an adsorbent phase that can be used efficiently for removal of a broad spectrum of pollutants/compounds from air, soil and liquids [16]. Charcoal itself provides poor absorbability, with a small surface area as the pores are filled with resins and products of incomplete combustion which occurs during its production [17]. Activated charcoal is created from carbon-rich materials burned at high temperatures. Carbon-rich materials such as wood, coconut shells or coal, are burned at a high temperature (between 600°C and 900°C) to carbonise them, thus creating a charcoal powder [16]. The powder is then granulated using tar or pitch binder, and then activated with steam or flue gas at 800-1000°C. The activation process eliminates the residual tar and resin which increases the porosity of the charcoal, and significantly increases the surface area from 2-4 m^2/g to more than 1000 m^2/g [18]. The applications of activated charcoal in recent years are very broad. The most prominent include decreasing environmental pollution, such as gases and vapours in the industrial environment, heavy metal ions such as mercury, lead and cadmium in drinking water, and the removal of taste, colour, odours and other objectionable impurities from liquids, water supplies and vegetable and animal oils [16] [19, 20]. More recently, it has also been applied to treat poisonings, drug overdoses, and various diseases by adsorbing the toxins from the stomach [21, 22]. The ability of activated charcoal to adsorb a wide range of compounds is potentially beneficial in non-targeted analysis.

Due to the untargeted nature of this work, activated charcoal was chosen as the stationary phase for SPE analysis due to its ability to adsorb a wide range of compounds spanning a polarity range, unlike many traditional SPE sorbents. This will allow the SPE to capture a wider variety of compounds from the sample.

3.2 A preliminary experiment to investigate the potential of identifying the chemical signature of decomposition in a beaker of water containing decomposing tissue.

3.2.1 Aims

The purpose of this preliminary work was to create a very basic lab-controlled experiment to monitor decomposition in water to determine whether non-targeted metabonomic profiling is an effective way to monitor the influence of decomposition on the water chemistry. If successful, a robust workflow could be designed and incorporated into a more realistic field experiment.

A lab-based environment ensures full control of the temperature, volume of water, weight of decomposing tissue and definitive sampling schedules. Sampling was carried out at a number of time intervals with two different sample preparation methods for comparison. This would give a clear indication of first whether it is possible to identify the chemical signature of decomposition in the water, and second, the best way to extract the maximum amount of information from each sample. Looking at how this sample interacts with a variety of column chemistries will also assist in achieving the most effective and robust method for the workflow.

3.2.2 Experimental method

3.2.2.1 Materials

Methanol (HPLC grade), formic acid, activated charcoal, all columns and a reference mass solution consisting of purine (*m/z* 121.0509) and hexakis (1*H*, 1*H*, 3*H*-tetrafluropropoxy)phosphazine (*m/z* 922.0098) were purchased from Fisher Scientific (Loughborough UK) and ultra-pure water (18.2 MΩ) was purified using a Purelab Option-Q system by Veolia Water (Saint Maurice, France). Pig liver was purchased from Tesco (Meir, UK).

3.2.2.2 Experimental setup

The experiment consisted of five beakers filled with 1.1 L of water, covered with cling film. All beakers were placed in a fume hood in a temperature controlled lab (23°C). Two of the beakers only contained water (control samples), while the remaining three beakers each contained 120 g of pig liver. The beakers containing liver were sampled after one day, four days and seven days, while the control beaker was sampled after one day and seven days. At each time point, two samples were taken. A 1 ml sample was pipetted into a LC vial, and a 1 L sample was taken for SPE extraction.

3.2.2.3 Sample preparation and storage

Each 1 ml sample was evaporated under nitrogen and reconstituted with 50:50 methanol and ultrapure water. The vials were vortexed for 20 s to ensure full recovery of sample. Each 1 L sample was filtered through an SPE cartridge containing an activated charcoal

phase. The SPE cartridge was designed and made in-house using glass wool (1 cm) and activated charcoal (0.2 g) in a plastic syringe (Figure 3.5). The steps for the procedure are shown in Table 3.1 All samples were placed in a 1.5 ml Eppendorf tube and centrifuged for 10 minutes at 16100 rcf to remove any particulates, then stored in a freezer at -25°C prior to analysis.

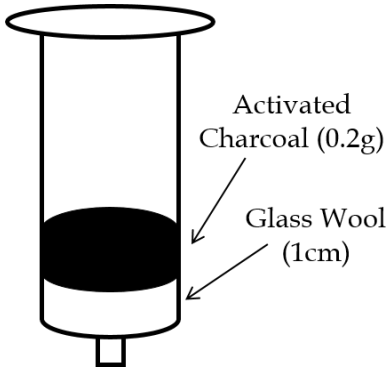

Figure 3.5 Diagram of SPE cartridge design.

Table 3.1: The 5 step procedure used for solid phase extraction.

Step	Procedure
1	1 ml Methanol into cartridge *(Out to waste)*
2	1 ml Ultrapure water into cartridge *(Out to waste)*
3	Sample into cartridge *(Out to waste)*
4	1 ml Ultrapure water into cartridge *(Out to waste)*
5	Elute with 1ml Methanol into LC vial

3.2.3 Instrumental setup

3.2.3.1 Quality control

Due to the non-targeted nature of the analysis, quality control (QC) samples were used to monitor the stability of the instrument and the quality of the data produced. The QC samples were produced by pooling an equal aliquot of each sample within the analytical sequence. A QC sample was analysed at the start of the analysis, then every five samples during the sequence to monitor the reproducibility of the analysis using a previously accepted approach [23]. The Coefficient of Variance percentage (CV%) of each identified marker (*m/z*-retention time pair) was calculated using peak areas derived from the QC samples. The column was equilibrated for 30 minutes (10 column volumes) before starting the analysis.

3.2.3.2 Chromatographic parameters

The chromatographic separation was carried out using an Agilent Technologies 1260 Infinity Binary HPLC system. Three columns were used during analysis. The development of each gradient began with a steady increase of the organic solvent (for reverse-phase, aqueous solvent for HILIC) over a 90 minute gradient, allowing a clear view of the interaction of the sample with the stationary phase. The solvent compositions and gradient were then adapted based on the initial chromatogram observed. The three columns described below were chosen as they provide three completely difference column chemistries which will give a clear insight to how the sample interacts with each one.

C18 Column. Thermo Fisher C18 Hypersil Gold (100 mm x 2.1 mm, 1.9 µm particle size). The column temperature was maintained at 40ºC, and the injection volume was 5 µl. The mobile phase consisted of (A) Water with 0.1% formic acid and (B) Methanol with 0.1% formic acid. The flow rate was 0.2 ml min^{-1}. The solvent gradient is shown in Table 3.2.

Table 3.2: Solvent gradient used for the analysis of liver decomposing in beaker of water, using a C18 column.

Time (minutes)	Solvent A (%)	Solvent B (%)
0	95	5
11	82	18
16	10	90
20	10	90
21	0	100
33	0	100
35	95	5

Hypercarb Column. Hypercarb Porous Graphitic Carbon HPLC Column (100mm x 2.1mm). The column temperature was maintained at 40ºC, and the injection volume was 7µl. The mobile phase consisted of (A) Water with 0.1% formic acid and (B) Methanol with 0.1% formic acid. The flow rate was 0.5 ml min^{-1}. The solvent gradient used is shown in Table 3.3.

Table 3.3: Solvent gradient used for the analysis of liver decomposing in beaker of water, using a Hypercarb column.

Time (minutes)	Solvent A (%)	Solvent B (%)
0	97	3
46	30	70
47	0	100
57	0	100
58	97	3

HILIC Column. HILIC Accucore HPLC Column (100 mm x 2.1 mm, 2.6 µm particle size). The column temperature was maintained at 40°C, and the injection volume was 5 µl. The mobile phase consisted of (A) Water with 0.1% formic acid and (B) Methanol with 0.1% formic acid. The solvent gradient used is shown in Table 3.4.

Table 3.4: Solvent gradient used for the analysis of liver decomposing in beaker of water, using a HILIC column.

Time (minutes)	Solvent A (%)	Solvent B (%)
0	3	97
80	97	3
90	97	3
91	3	97

3.2.3.3 Mass spectrometry parameters

Samples were analysed using an Agilent Technologies 6530 Accurate-Mass Quadrupole-Time-of-Flight mass spectrometer. This was operated in positive ionisation mode, with an electrospray ionisation source. The instrumental parameters used are those suggested by the instrument software, shown in Table 3.5 1. The parameters remained consistent for each column. A reference mass solution consisting of purine (*m/z* 121.0509) and hexakis (1*H*, 1*H*, 3*H*- tetrafluropropoxy)phosphazine (*m/z* 922.0098*)* was analysed simultaneously to ensure mass accuracy.

Table 3.5: Mass spectrometer parameters for the Agilent Technologies 6530 Accurate-Mass Quadrupole-Time-of-Flight mass spectrometer.

Capillary voltage	4000 V
Drying gas temperature	320°C
Drying gas flow rate	7.5 L min^{-1}
Nebulizer pressure	40 psig
Fragmentor voltage	125 V
Skimmer voltage	65 V

3.2.4 Data pre-processing

Data was extracted for processing and visualisation using *XCMS online.* This software enables a combination of data pre-processing and data analysis. However, for this research, this software was used as a pre-processing tool that produced a marker table on

Microsoft Excel 2016 that includes each compound represented by their *m/z* and retention times [24]. The parameters are set for each individual instrument, followed by the customisation of the signal/noise threshold, mass tolerance, methods for feature detection, retention time correction, alignment and annotations.

3.2.5 Data analysis and statistical analysis

All features that had a coefficient of variance (CV) value of 30% or more were removed, due to 30% being the accepted level of variance in non-targeted analysis [25]. A principal component analysis was carried out on the remaining features using a Multivariate Analysis add-in on *Microsoft Excel 2016*, and a scores plot produced to visualise any separation between sample groups. The first six principal components were plotted to determine which would best represent the separation.

A manual t-test was carried out on each feature in *Microsoft Excel.* Any features with a *p-value* more than 0.05 were removed. The top 100 significantly different markers were analysed in *SPSS* with an ANOVA/Welch test to further confirm their significance. This was carried out at a 95% confidence level. A p-value of <0.05 indicated a statistical difference between the means of the sample groups analysed.

3.2.6 Results and discussion using a C18 column.

3.2.6.1 QC Analysis

Figure 3.6 shows the overlaid chromatograms for each QC sample throughout the analytical sequence. The QC samples appear to be extremely stable, with no visible baseline drift or retention time drift. QC's 1-5 were analysed at the beginning to allow adequate conditioning of the column. Although this chromatogram shows excellent stability, five QC samples were analysed at the beginning of each sequence as a precaution, as it does not increase the analysis time a substantial amount. To investigate further into the stability of the instrument, six peaks were chosen from the chromatogram and their retention time and peak area were recorded in each QC sample.

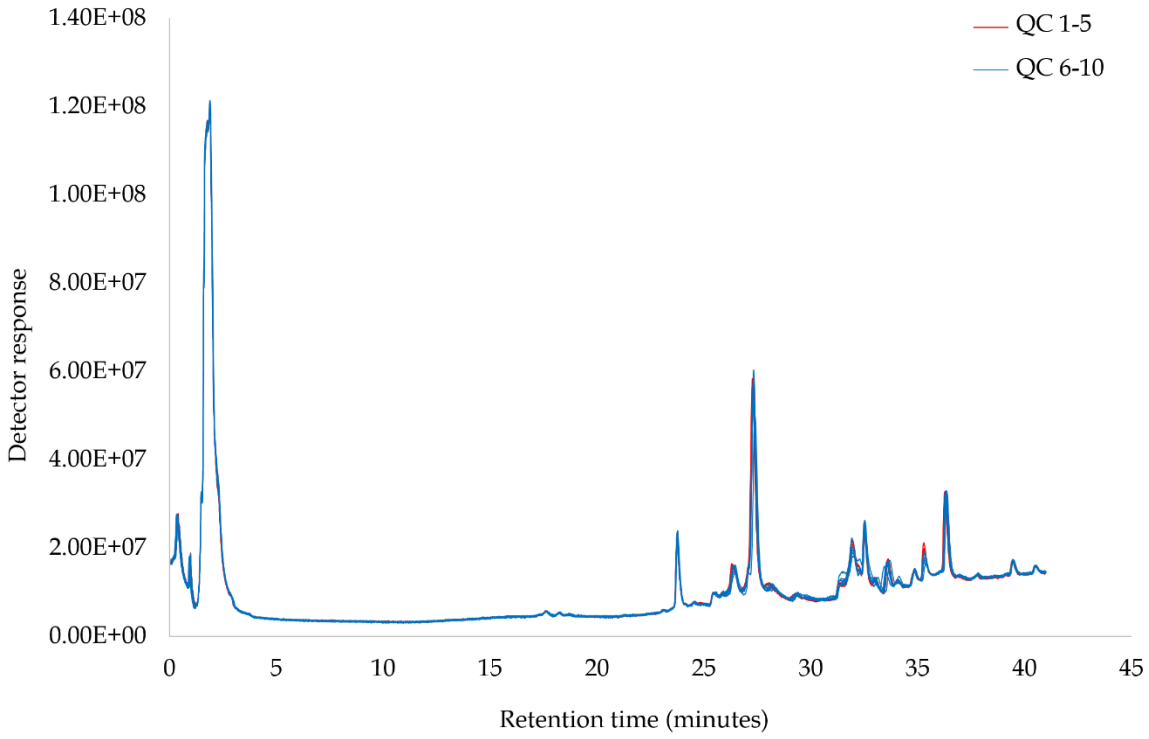

Figure 3.6: Total ion chromatograms of QC samples from liver decomposing in a beaker of water over 7 days, using a C18 column.

Table 3.6: Variability of peak area (A) and retention time (B) from 6 selected peaks in the QC samples during the analytical sequence for the liver decomposing in a beaker of water over 7 days using a C18 column.

A

Peak	QC5	QC6	QC7	QC8	QC9	QC10	Average	St. Dev	CV%
1	11217140	11612743	14022564	12072377	13420828	11136989	**12247107**	**1204659**	**10%**
2	22819172	22310668	21864636	23499784	22781080	21893450	**22528132**	**629783**	**3%**
3	15193504	14575530	13466038	15677312	14296447	16125197	**14889005**	**971241**	**7%**
4	22302984	19789560	18632346	19109512	20219720	18104078	**19693033**	**1489221**	**8%**
5	24522756	24060332	23785728	25492478	24858048	26265310	**24830775**	**924886**	**4%**
6	32517432	32975740	31211880	30703884	32207844	30894156	**31751823**	**939935**	**3%**

B

RT	QC5	QC6	QC7	QC8	QC9	QC10	Average	St. Dev	CV%
1	0.88	0.89	0.90	0.89	0.89	0.89	**0.89**	**0.0046**	**0.51%**
2	23.74	23.75	23.75	23.74	23.75	23.75	**23.75**	**0.0046**	**0.02%**
3	26.37	26.38	26.39	26.38	26.38	26.38	**26.38**	**0.0046**	**0.02%**
4	31.92	31.93	31.94	31.93	31.94	31.93	**31.93**	**0.0046**	**0.01%**
5	32.52	32.52	32.53	32.53	32.53	32.53	**32.53**	**0.0047**	**0.01%**
6	36.32	36.33	36.33	36.32	36.33	36.33	**36.32**	**0.0046**	**0.01%**

Table 3.6 presents the CV values for both peak area (A) and retention time (B) of six peaks in the QC samples. With the peak area obtaining a highest CV value of 10%, and retention time obtaining a highest CV value of 0.51%, it is clear that the instrument was stable throughout the analytical sequence as each value was far under the accepted CV value of 30%[25].

3.2.6.2 Metabolic profiling

The chromatograms in Figure 3.7 present the first insight into the chemical profile of water containing decomposing meat at day 1, 4 and 7 of the experiment from a 1 ml sample analysed with a C18 column.

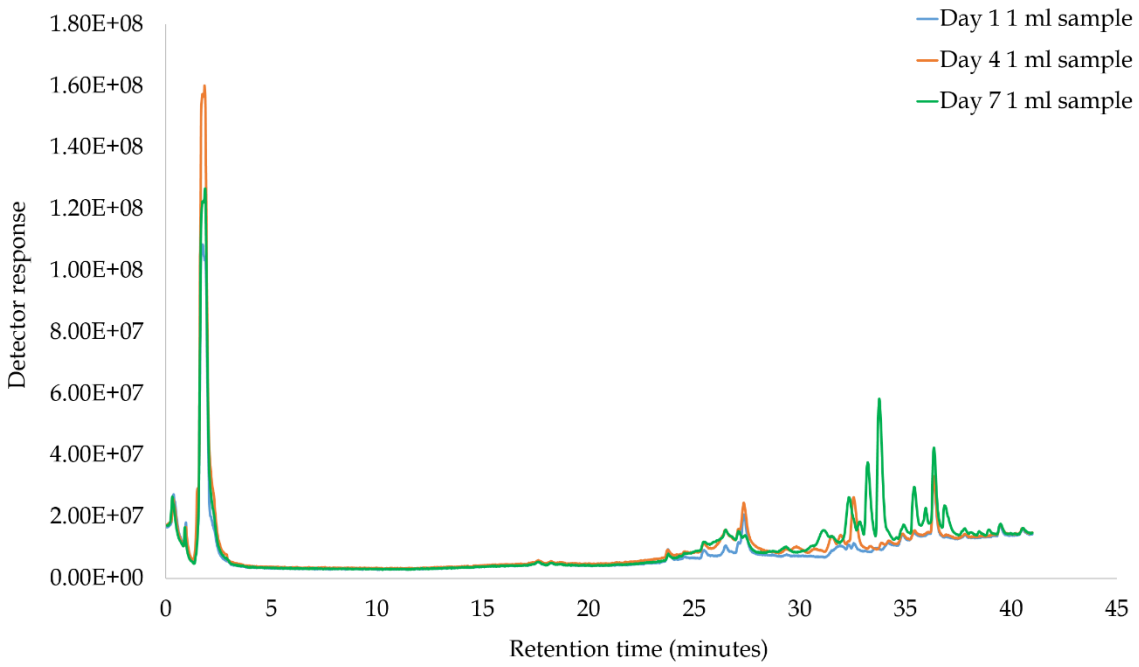

Figure 3.7: Total ion chromatogram (TIC) of 1 ml samples taken on day 1, 4 and 7 of liver decomposing in a beaker of water, using a C18 column.

The chromatograms show some development over time in the chemical profile of the water. There is an increase in the number of peaks and their intensities over time between 25-40 minutes of the analysis, however they are minimal with relatively poor peak shape. The chromatograms in Figure 3.8 present the 1 L samples taken at day 1, 4 and 7 of the experiment, analysed with a C18 column.

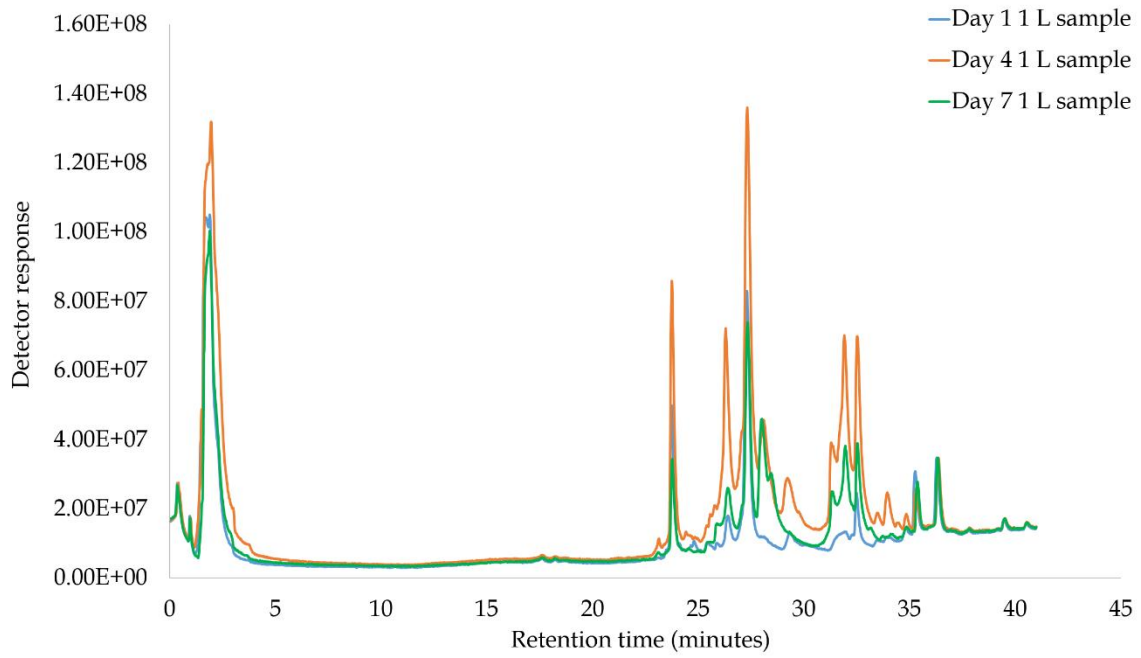

Figure 3.8: Total ion chromatogram (TIC) of 1 L samples concentrated using SPE taken on day 1, 4 and 7 of liver decomposing in a beaker of water, using a C18 column.

It is evident that there are clear differences between the chromatograms of the 1 L samples and 1 ml samples. The peaks have a much higher peak intensities and better overall quality in the 1 L sample chromatogram. Although the sample seems to retain on the column until 20 minutes into the analysis, there are more distinct differences in the chemical profile of the samples over time in the 1 L sample compared to the 1 ml sample.

It is clear that there is progression over time in the chemical signature of the water exposed to meat decomposition with the 1 ml sample and 1 L pre-concentrated sample. Further analysis focused on each individual time interval, to investigate what compounds were causing these differences.

Figure 3.9 presents the TIC's for the control sample and a 1 ml and 1 L sample taken from a beaker containing decomposing meat for 1 day. There are clear differences between the peak intensities of all three chromatograms. The chromatogram for the 1 ml sample shows only a small number of peaks, and those are of low resolution. In comparison, the chromatogram for the 1 L sample presents peaks of a higher intensities and better resolution. The peaks of interest observed in both samples are not present in the control sample.

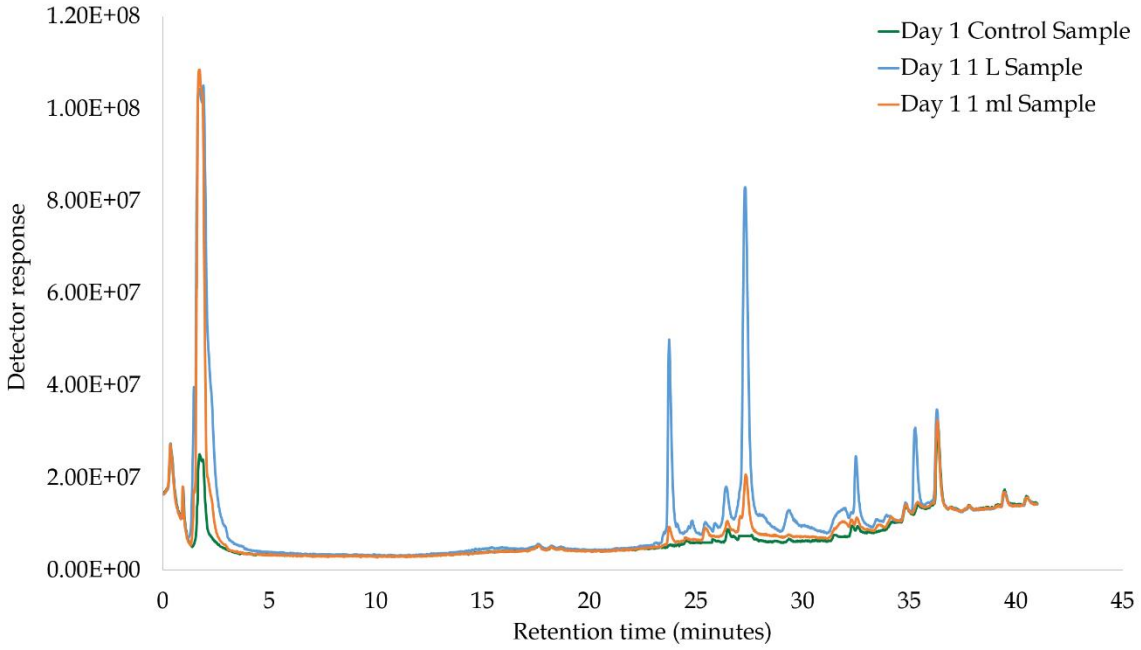

Figure 3.9: Total ion chromatogram (TIC) of a 1 ml sample, and a 1 L sample concentrated using SPE following one day of liver decomposing in a beaker of water, using a C18 column.

Figure 3.10 shows the chromatograms of a 1 L and 1 ml sample taken following 4 days of decomposition in water. Only very small chromatographic changes are observed in the 1 ml sample from day 1. The 1 L sample chromatogram shows that the peak intensities are much higher, accompanied by additional peaks that are not present in the 1 ml sample. This highlights that not only is the chromatographic resolution improved with the use of a pre-concentration step, but that you can also see an increase in the pool of compounds in the water over time as a result of decomposition.

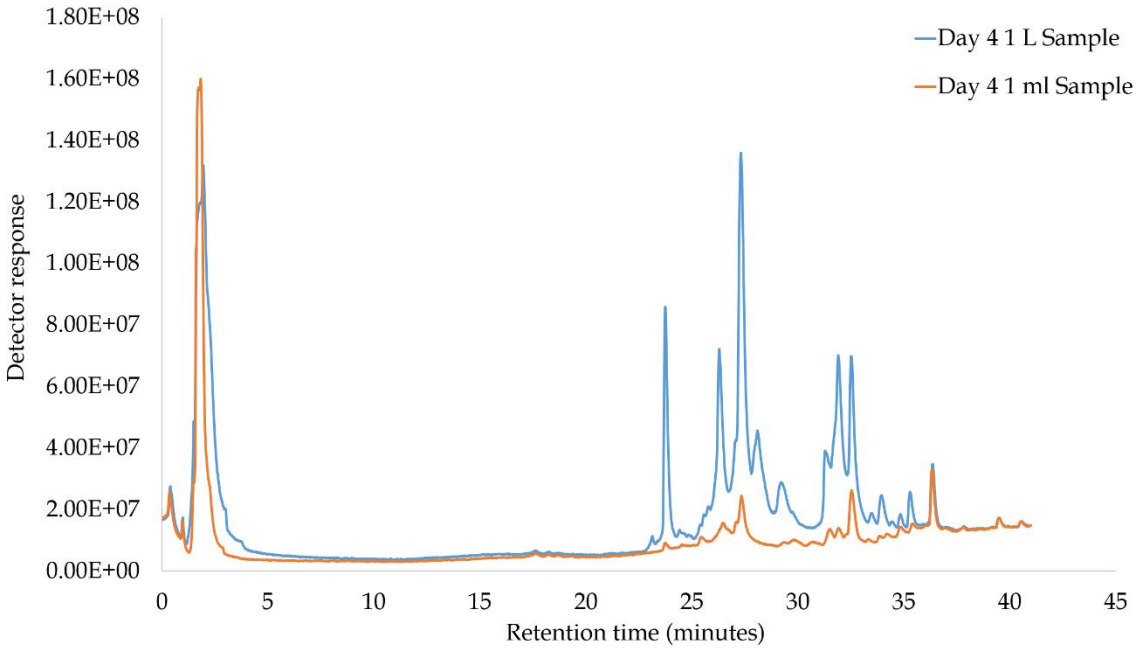

Figure 3.10: Total ion chromatogram (TIC) of a 1 ml sample, and a 1 L sample concentrated using SPE following four days of liver decomposing in a beaker of water, using a C18 column.

Figure 3.11 presents the chromatograms of a control sample, and a 1 ml and 1 L sample taken following 7 days of decomposition in water. The peak intensities in the 1 L sample chromatogram have decreased from day 4, however are still much higher than those in the 1 ml sample chromatogram. It is important to note that in the 1 ml sample chromatogram, additional peaks have appeared between 32-35 minutes that are not present in the 1 L sample.

It was assumed that peak intensities would increase throughout the experiment, however, there is a possibility that certain compounds may have broken down into smaller ones, suggesting that decomposition could have reached its peak at day 4 in these particular conditions. It is also possible that these smaller compounds could have a *m/z* smaller than the detection limit. The exact cause at this stage is unknown.

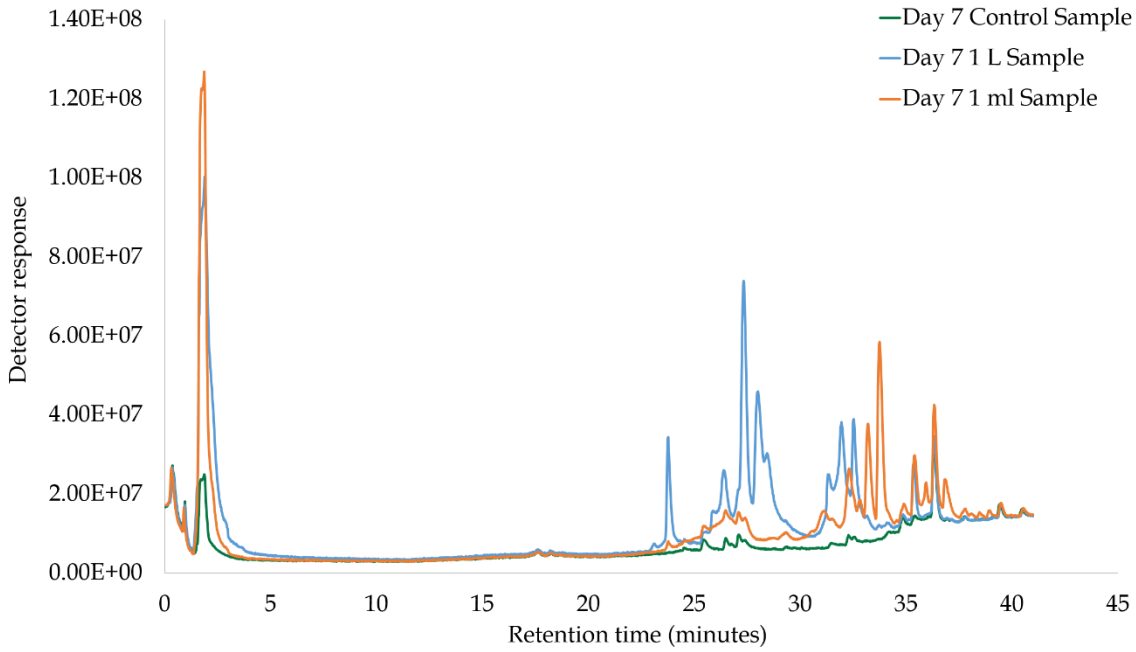

Figure 3.11: Total ion chromatogram (TIC) of a 1 ml sample, and a 1 L sample concentrated using SPE following seven days of liver decomposing in a beaker of water, using a C18 column.

3.2.6.3 Multivariate analysis

Multivariate analysis was used to look further into the data for specific patterns, similarities, and differences between each sample. Figure 3.12 shows the PCA scores plot of the 1 ml sample and 1 L sample over the three time intervals, accompanied by control samples and QC samples.

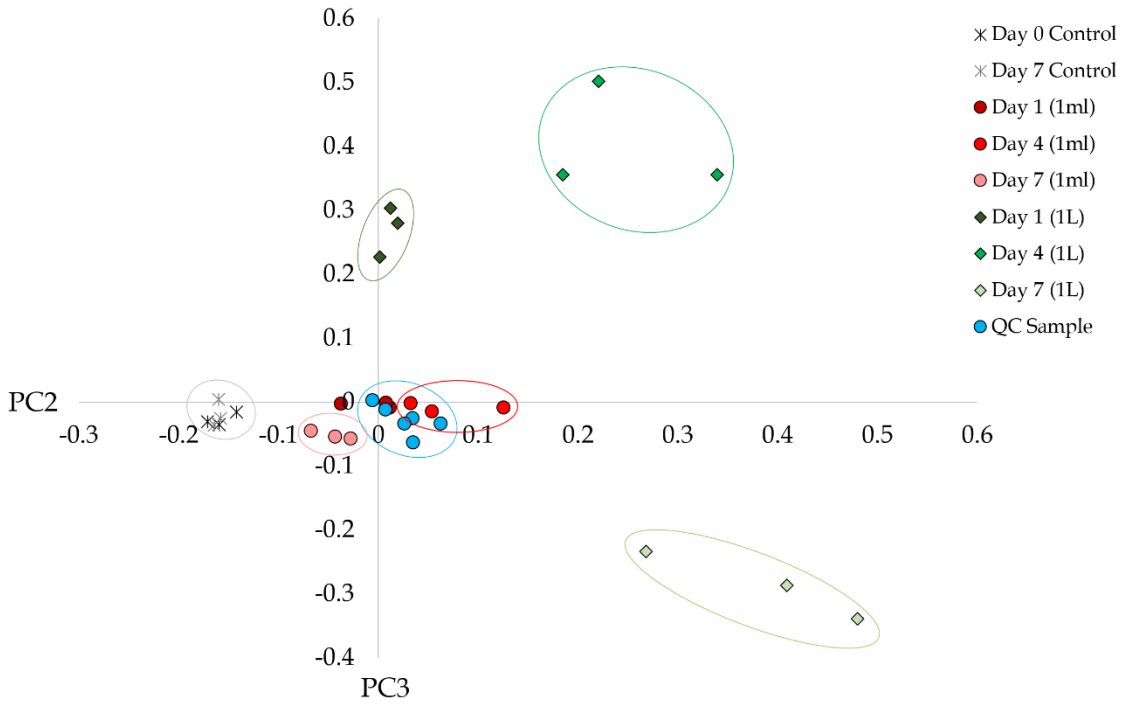

Figure 3.12: PCA score plot of PC2 (7.81%) and PC3 (3.29%) for liver decomposing in water over seven days sampled as 1 ml and 1 L concentrated using SPE, using a C18 column.

The QC samples are tightly clustered in the centre of the plot, indicating minimal instrumental drift during the analysis. The control samples from day 0 and day 7 are clustered together on the left side of the plot away from the experimental samples. This supports the fact that the changes to the chemical profile of the water is a direct result of decomposition, not due to the natural stagnation of the water. The most obvious

differences between the 1 ml and 1 L sample is the separation between each time interval. When looking at the 1 ml sample, all three time intervals are clustered close together in the centre of the plot. There is enough separation to be able to organise them into discreet groups, however, the distance between each sample group is smaller than the spread of the QC samples, therefore they do not show any reliable differences. On the other hand, the 1 L samples show each time interval clearly separated from the next, and are clearly separated from the control samples even after one day of decomposition in water. The distance between each sample group is further apart than the spread of the QC samples, implying that these differences are not at risk of being due to instrumental effects. Once more, the results seen here support the use of solid phase extraction as a sample preparation method to enhance the differences observed and robustness of the results.

3.2.6.4 Statistical analysis

The number of features detected in this analysis via *XCMS Online* was 4417. All features with a CV value of less than 30% were removed, with 2119 remaining. Statistical analysis was performed on both 1 L and 1 ml samples separately. The number of compounds showing significant differences between time points when analysing a 1 ml sample of water was 330, and 369 with the 1 L sample. There seems to be a similar number of significantly different compounds appearing in both samples, with only an additional 39 compounds showing significant differences in the 1 L sample. Although not a large difference, non-targeted analysis relies on the detection of as many compounds as possible in the sample. Table 3.7 shows the top 20 compounds showing significant differences between the three time points from a 1 ml sample.

Table 3.7: Summary of the top 20 compounds that show significant differences between all three time points with a 1 ml sample, analysed using a C18 column.

1 ml sample							
Significant differences between day 1 and day 4				Significant differences between day 4 and day 7			
m/z	Retention time (min)	CV	p-value	m/z	Retention time (min)	CV	p-value
106.9473	1.65	18%	<0.001	130.6023	1.79	22%	0.003
123.0629	1.98	29%	0.004	176.0641	1.94	25%	<0.001
220.0312	1.94	28%	<0.001	205.1414	2.17	24%	<0.001
244.1917	2.07	29%	<0.001	219.1039	1.97	27%	<0.001
275.1667	1.52	12%	<0.001	237.0713	2.13	28%	0.002
291.9712	1.89	28%	<0.001	244.2221	2.38	15%	0.003
333.2345	33.7	17%	<0.001	286.0945	2.19	11%	<0.001
345.2361	32.7	16%	0.004	294.1751	1.83	25%	<0.001
401.2776	1.85	25%	<0.001	314.1946	2.05	16%	<0.001
516.2125	1.96	24%	<0.001	336.4583	34.08	19%	<0.001
590.2978	26.41	28%	<0.001	359.2562	1.8	21%	<0.001
630.481	23.81	13%	0.002	365.1889	2.01	26%	<0.001
682.7791	23.8	26%	<0.001	477.2669	2.01	14%	<0.001
744.4025	2.01	8%	<0.001	508.3145	2.2	11%	0.003
792.6011	25.03	16%	<0.001	524.2683	33.71	16%	<0.001
819.1354	23.8	22%	<0.001	551.3059	1.98	23%	<0.001
910.0393	23.8	9%	<0.001	566.3168	34.6	9%	0.003
929.2252	27.25	10%	<0.001	598.3157	1.8	23%	<0.001
940.7525	33.68	8%	0.001	600.3288	1.79	24%	<0.001
946.2478	25.8	28%	<0.001	634.3027	34.22	13%	<0.001

The table above highlights that these compounds are highly statistically significant based on their *p-values*. The compounds in dark blue are those found to show significant differences between both sets of time points.

Table 3.8 shows the top 20 compounds showing significant differences between the three time points from a 1 L sample pre-concentrated using SPE. While only one compound showed significant differences over both sets of time intervals in the 1 ml sample, four were identified in the 1 L sample.

Table 3.8: Summary of the top 20 compounds that show significant differences between all three time points with a 1 L sample, analysed using a C18 column.

1 L sample							
Significant differences between day 1 and day 4				Significant differences between day 4 and day 7			
m/z	Retention time (min)	CV	p-value	m/z	Retention time (min)	CV	p-value
106.9473	1.65	18%	<0.001	131.5746	1.55	14%	<0.001
136.1078	1.95	21%	<0.001	133.0329	1.48	24%	<0.001
113.5853	1.71	16%	0.006	137.5976	1.73	26%	<0.001
123.0629	1.98	29%	0.008	152.5819	1.55	23%	0.001
147.1113	1.98	26%	0.001	176.0641	1.94	25%	<0.001
152.5819	1.55	23%	<0.001	194.6481	1.53	18%	<0.001
176.0641	1.94	25%	<0.001	205.1414	2.17	24%	<0.001
194.6481	1.53	18%	0.001	223.1052	1.97	28%	<0.001
223.0551	2.07	29%	0.002	319.2972	33.67	23%	0.001
239.1508	1.9	27%	<0.001	321.237	33.11	8%	<0.001
240.1199	1.97	19%	<0.001	325.2557	33.66	20%	<0.001
258.4221	2.01	22%	0.007	345.2361	32.7	16%	0.001
275.1787	1.78	27%	<0.001	357.2677	30.64	29%	0.006
316.2799	33.11	12%	0.008	359.2482	34.18	16%	<0.001
343.2139	33.1	11%	0.001	413.2203	33.69	18%	<0.001
367.2161	32.71	23%	0.001	504.2998	35.85	27%	<0.001
405.2742	1.82	27%	0.002	609.1471	33.13	11%	<0.001
520.3336	34.31	17%	0.001	623.5042	33.68	14%	0.003
542.3141	34.3	11%	0.001	639.4788	33.67	12%	<0.001
744.541	35.35	11%	0.001	643.4803	33.68	24%	<0.001

Table 3.9 presents the *m/z* of the compounds that have shown significant differences between time points. A similar pattern is shown for both the 1 ml and 1 L samples, where the percentage of smaller compounds (*m/z* 0-300) increase over time, and the percentage of larger compounds (*m/z* 600-900) decrease over time. This supports the expected pattern of large compounds such as proteins and carbohydrates breaking down into smaller products as decomposition progresses.

Table 3.9: Table showing the size of the compounds that produced significant differences between time points, expressed as a percentage.

	1ml sample		**1L sample**	
	Significant differences between :			
m/z	**Day 1 and day 4**	**Day 4 and day 7**	**Day 1 and day 4**	**Day 4 and day 7**
0-300	24%	38%	32%	57%
300-600	25%	40%	32%	29%
600-900	51%	22%	36%	28%

As both the 1 ml sample and 1 L sample produced similar results, it is safe to assume that a very similar collection of compounds is present even after pre-concentration using SPE. Figure 3.13 and Figure 3.14 present a bar chart showing the progression of the peak area of two ions *m/z* 244.1917 and *m/z* 223.0551 respectively. These two ions were chosen as they were showing significant differences at both sets of time points in the 1 ml or 1 L sample.

It was assumed that the peak area of the compounds would increase over time with continuous leaching into a contained body of water, however both Figures 3.13 and Figure 3.14 show that the peak area reaches its highest point at day 4, and significantly decreases

by day 7. This suggests that they are no longer produced, and could have evaporated. This emphasises the complexity of metabolic processes in decomposition. It is important to note that both bar charts show that the peak areas are significantly higher for the 1 L pre-concentrated sample compared to the 1 ml sample.

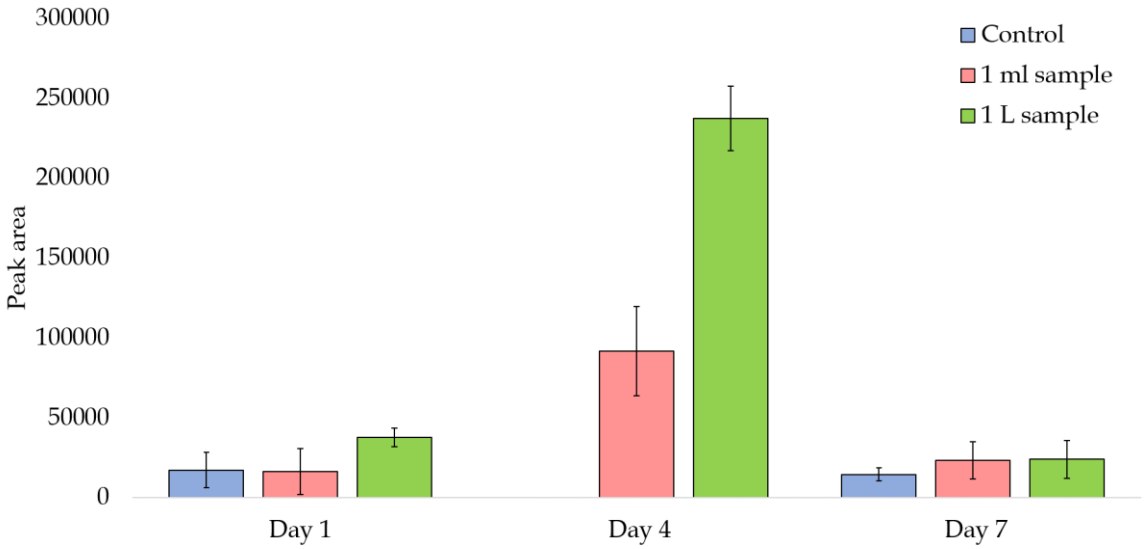

Figure 3.13: Bar chart showing the change in peak area over three time points of m/z 244.1917, analysed using a C18 column, with error bars ±1 standard deviation.

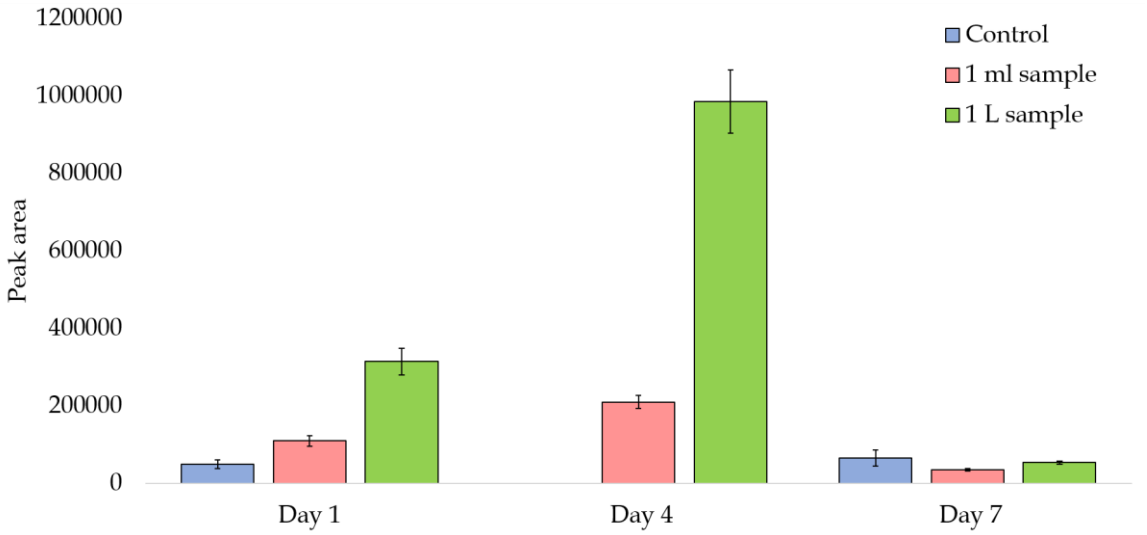

Figure 3.14: Bar chart showing the change in peak area over three time points of m/z 223.0551 analysed using a C18 column with error bars ±1 standard deviation.

3.2.7 Results and discussion using a Hypercarb column

3.2.7.1 QC analysis

Figure 3.15 shows the chromatograms of the 10 QC samples from this analytical sequence. A small amount of retention time drift is seen in a conditioning QC sample (red) between 0-10 minutes. There are also some inconsistencies between 30-40 minutes of the analysis between the conditioning QC samples and the ones analysed between samples. Although it is minor, there was no sign of any retention time drift when using a C18 column. To ensure the instrument was stable enough to collect reliable data, six peaks were chosen from the above chromatograms and their retention time and peak area were recorded.

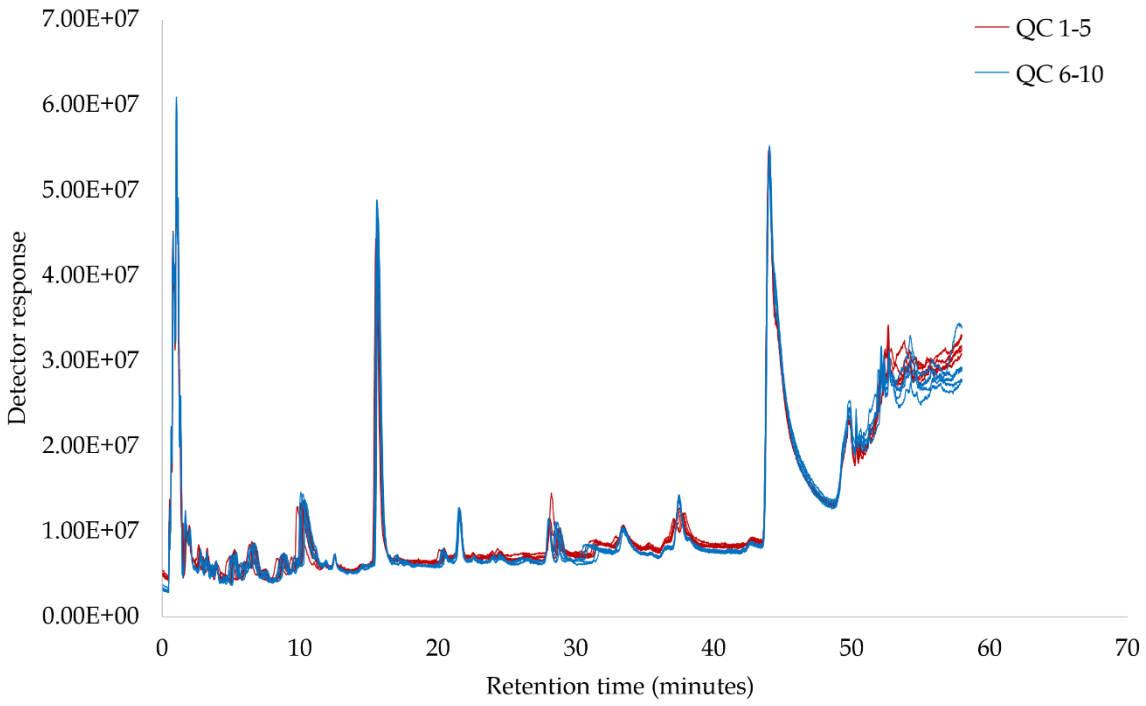

Figure 3.15: Total ion chromatograms of QC samples from liver decomposing in a beaker of water over 7 days, using a Hypercarb column.

The accepted level of variance was assessed in Table 3.10. The variability in the retention time (B) and the peak area (A) is very minimal when comparing six QC samples. The highest CV value for the peak area is 15%, and 0.16% for the retention time. This confirms that the instrument was stable throughout the analytical sequence, as each value was far under the accepted CV value of 30% [25]. These figures are very similar to those obtained on a C18 column, suggesting that the instrument was able to produce reliable data on both columns.

Table 3.10: Variability of peak areas (A) and retention time (B) from 6 selected peaks in the QC samples during the analytical sequence for the liver decomposing in a beaker of water over 7 days using a Hypercarb column.

A

Peak	QC5	QC6	QC7	QC8	QC9	QC10	Average	St. Dev	CV%
1	10377934	10324695	10018477	10138854	9773393	9821361	**10075786**	**251668**	**2%**
2	8577528	8216587	8587671	7029661	6282252	6270541	**7494040**	**1102096**	**15%**
3	6863404	6279285	6728527	6257618	5817882	6205057	**6358629**	**380555**	**6%**
4	44204004	43837904	45977812	46480168	44303324	43105108	**44651387**	**1302143**	**3%**
5	10716616	10656951	10962855	11217108	11111464	10936883	**10933646**	**217483**	**2%**
6	23013144	23491076	24559300	24504724	25235824	24147666	**24158622**	**799818**	**3%**

B

RT	QC5	QC6	QC7	QC8	QC9	QC10	Average	St. Dev	CV%
1	2.03	2.03	2.03	2.03	2.03	2.03	**2.03**	**0.003**	**0.16%**
2	6.70	6.71	6.70	6.71	6.71	6.70	**6.70**	**0.003**	**0.05%**
3	9.85	9.85	9.85	9.85	9.85	9.85	**9.85**	**0.003**	**0.03%**
4	15.66	15.67	15.66	15.67	15.67	15.67	**15.67**	**0.003**	**0.02%**
5	28.09	28.09	28.09	28.09	28.09	28.09	**28.09**	**0.003**	**0.01%**
6	49.86	49.86	49.86	49.86	49.86	49.86	**49.86**	**0.003**	**0.01%**

3.2.7.2 Metabolic profiling

The chromatograms in Figure 3.16 show the chemical profile of the 1 ml sample taken at day 1, 4 and 7 of the experiment, analysed with a Hypercarb column.

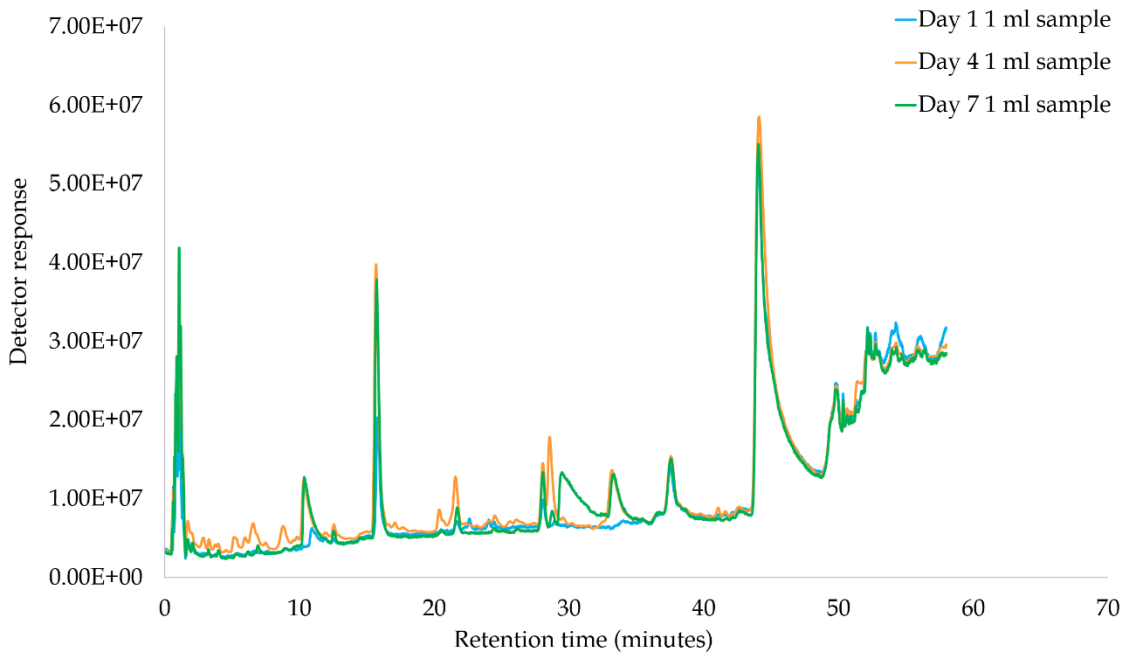

Figure 3.16: Total ion chromatogram (TIC) of 1 ml samples concentrated using SPE taken on day 1, 4 and 7 of liver decomposing in a beaker of water, using a Hypercarb column.

It is possible to see slight changes to the chemical profile of each chromatogram over time, even with a 1 ml sample. There is a slight increase in peak intensities over time with some additional peaks observed at day 4 that are not present in any other chromatogram. Analysis with the Hypercarb column has produced peaks throughout the chromatogram, in comparison to analysis with the C18 column where peaks only appeared between 25-40 minutes.

The chromatograms in Figure 3.17 present the 1 L samples taken at day 1, 4 and 7 of the experiment, analysed with a Hypercarb column. There is a drastic increase in peak intensities in the day 4 chromatogram between 0-40 minutes. The chromatographic patterns of the sample taken at day 7 is similar to that of day 1, showing a significant decrease in the quantity of the compounds detected compared to day 4.

It is clear that the C18 column is able to produce more distinct chromatographic differences between the two sample preparation techniques, compared to the Hypercarb column. Apart from the 1 L sample taken on day 4, there are no significant chromatographic differences between both sample preparation techniques as would be expected

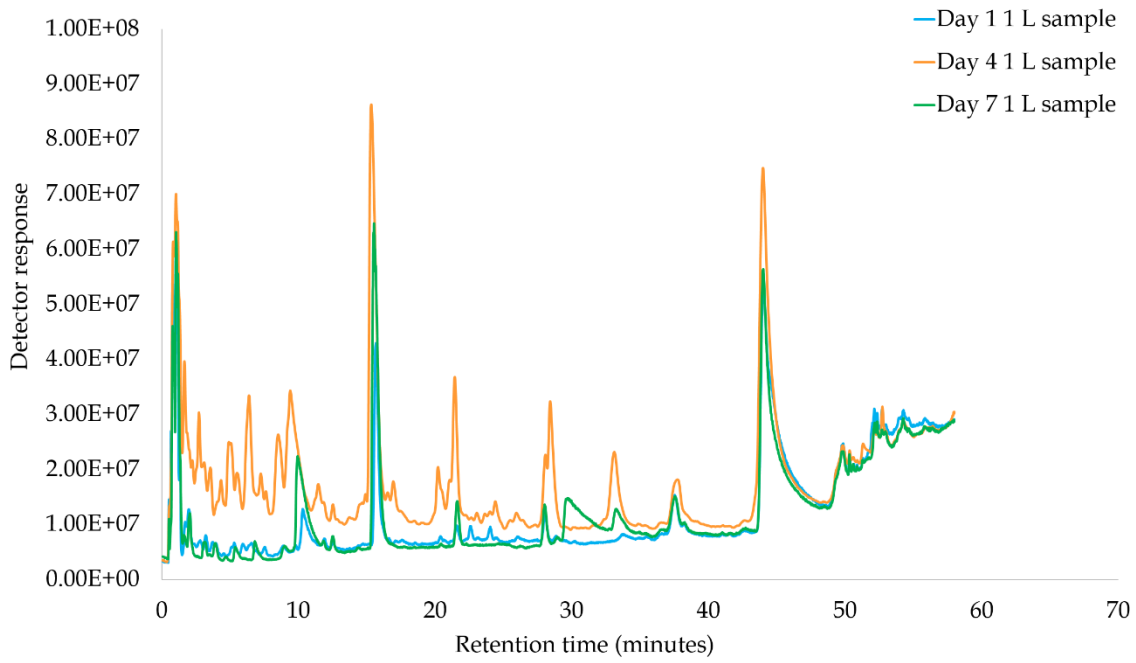

Figure 3.17: Total ion chromatogram (TIC) of 1 L samples concentrated using SPE taken on day 1, 4 and 7 of liver decomposing in a beaker of water, using a Hypercarb column.

To investigate further, each time point was analysed in detail to find any significant differences between the 1 ml and 1 L samples. Figure 3.18 shows the total ion chromatograms (TIC's) for the 1 ml sample and 1 L sample taken from the beaker after one day, analysed with a Hypercarb column.

As observed when using a C18 column, the sample concentrated with SPE shows peaks of higher intensities and overall better peak shape and resolution. When looking at the first 10 minutes of the 1 L sample chromatogram, the peaks seem to be clustered together. Any further method development would address this to avoid the possibility of co-elution. These peaks are not visible in the 1 ml sample chromatogram. In the first 30 minutes of the analysis, none of the peaks observed in the 1 ml or 1 L sample chromatograms are present in the control sample.

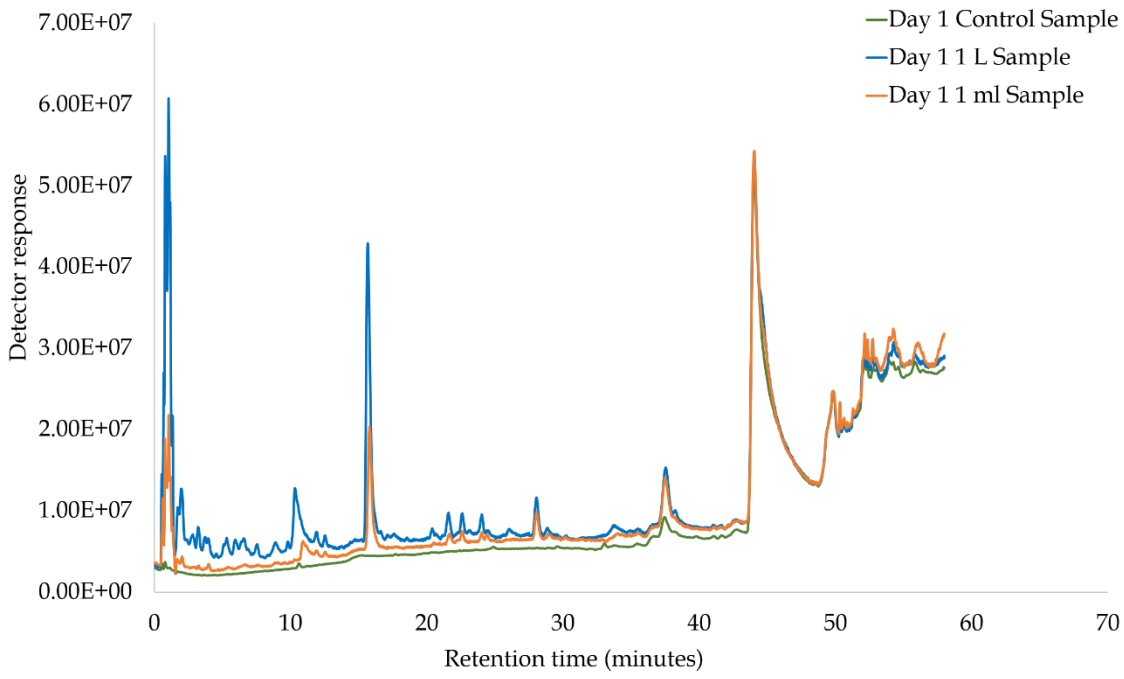

Figure 3.18: Total ion chromatogram (TIC) of a 1 ml sample, and a 1 L sample concentrated using SPE following one day of liver decomposing in a beaker of water, using a Hypercarb column.

Figure 3.19 shows the chromatograms of the 1 ml and 1 L water samples taken following four days of decomposition. It is clear that the peak intensities are higher throughout the 1 L sample chromatogram, compared to the 1 ml sample. There are now peaks present in the first 10 minutes of the analysis in the 1 ml sample chromatogram, however these are of poor resolution.

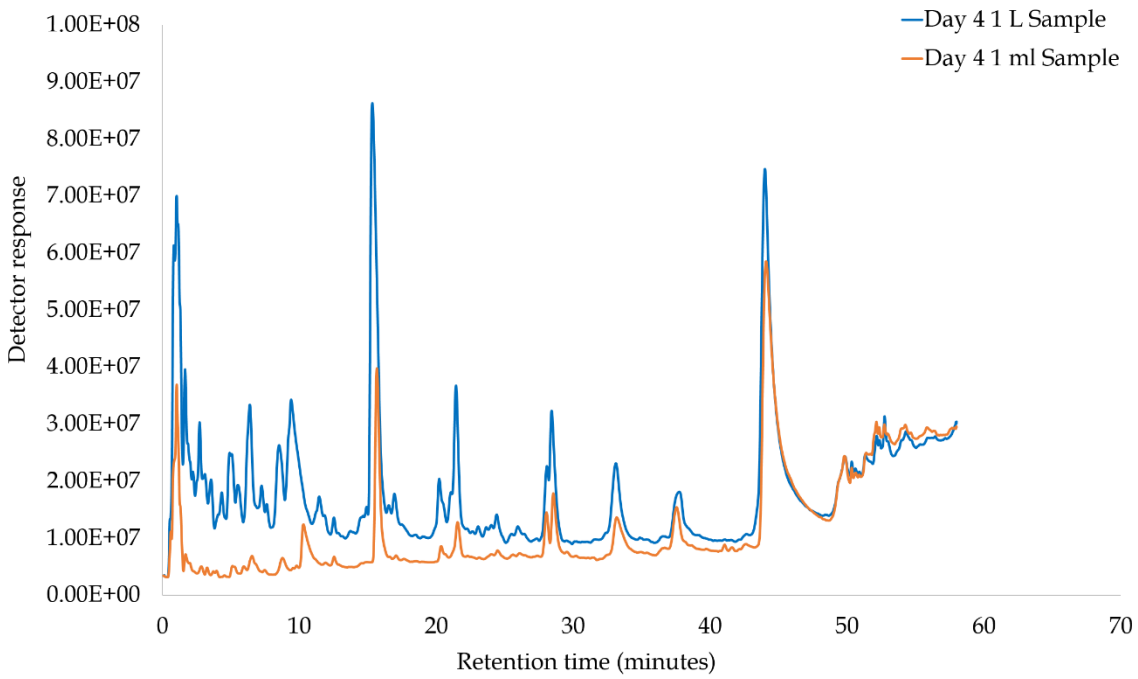

Figure 3.19: Total ion chromatogram (TIC) of a 1 ml sample, and a 1 L sample concentrated using SPE following four days of liver decomposing in a beaker of water, using a Hypercarb column.

Figure 3.20 moves on to show the chromatograms of the control sample, 1 ml and 1 L sample taken on the 7th day of decomposition. Very similar to the results obtained from the C18 column, there is a decrease in the number of peaks, and peak height on day 7. It is also important to note that this chromatographic result followed the expected pattern that the previous chromatograms have shown, that the pre-concentration step produces better peak resolution and peak height.

Although both the C18 and Hypercarb columns show very similar results in terms of patterns and trends during this experiment, the C18 column seems to demonstrate better quality chromatograms in terms of peak resolution and peak shape.

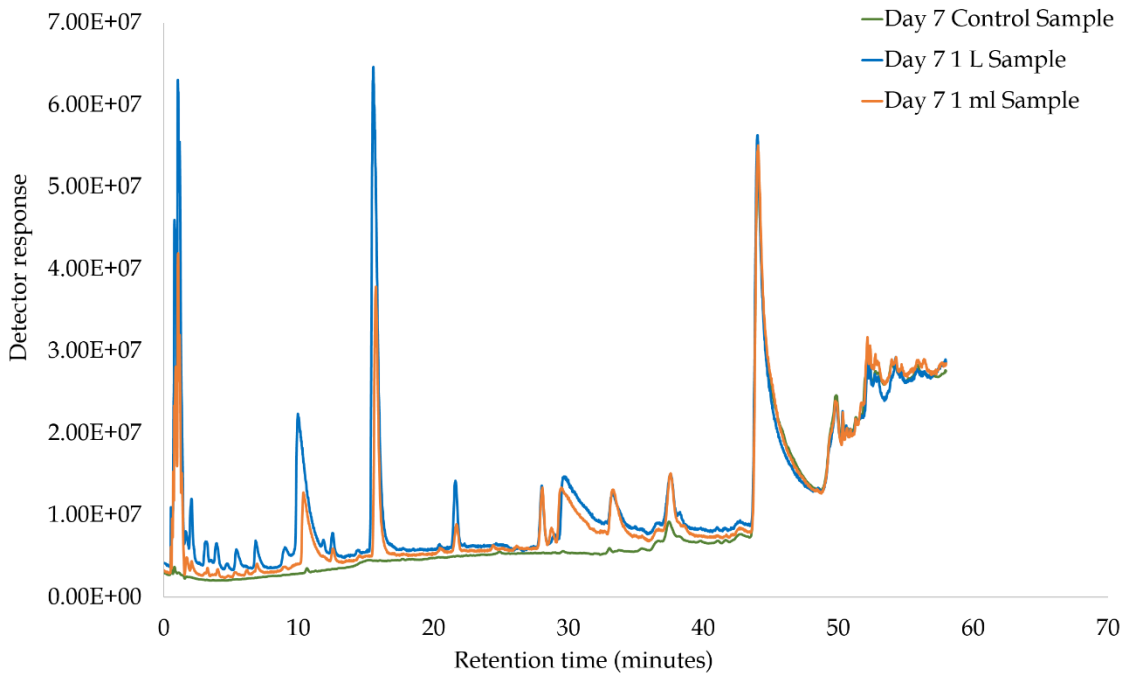

Figure 3.20: Total ion chromatogram (TIC) of a 1 ml sample, and a 1 L sample concentrated using SPE following seven days of liver decomposing in a beaker of water, using a Hypercarb column.

3.2.7.3 Multivariate analysis

Figure 3.21 shows the PCA scores plot of the 1 ml sample and 1 L sample filtered with SPE over three time intervals, accompanied by a control sample. The QC samples are reasonably clustered together, however do overlap some sample groups. This may suggest that the data obtained in this analysis may not be as robust as those obtained using a C18 column, where the QC samples are seen tightly clustered in the middle of the plot.

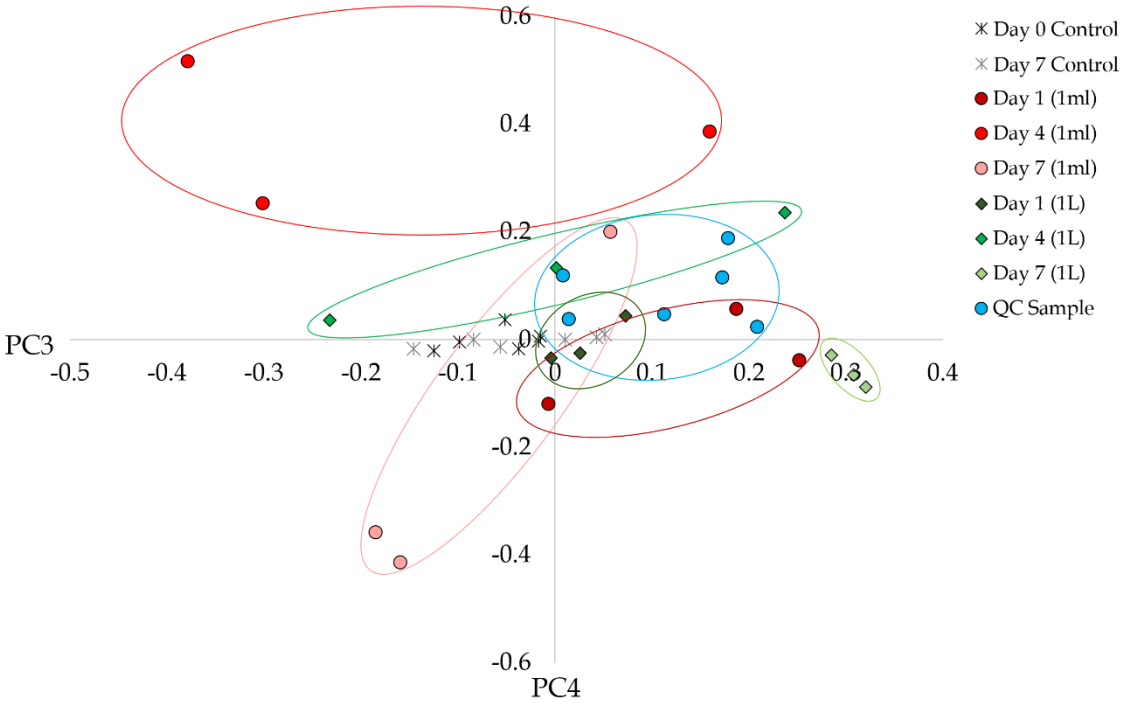

Figure 3.21: PCA score plot of PC3 (1.66%) and PC4 (0.65%) for liver decomposing in water over seven days sampled as 1 ml and 1 L concentrated using SPE, using a Hypercarb column.

While it is possible to clearly define each sample group on the plot, there is considerable amount of overlap between sample groups. The control samples are surrounded by the experimental sample groups, whilst the results from the C18 column showed the control samples clustered away on the left side of the plot.

There is also significant overlap between the 1 L samples and the 1 ml samples on the plot, with the only sample group clearly separated from the others being the 1 ml sample taken on day 4. When analysing these samples with a C18 column, there is a clear difference in the ability to separate the 1 L and 1 ml sample groups over time. It is also important to note that the plot created from the analysis using a C18 column was able to produce better separation power using lower PC's compared to the Hypercarb column. The inability of the Hypercarb column to distinguish the differences between the direct and pre-concentrated samples suggests that the Hypercarb was not able to detect the compounds that facilitated these differences.

3.2.7.4 Statistical analysis

The number of features detected in this analysis via *XCMS Online* was 5117. All features with a CV value of less than 30% were removed, with 3352 remaining. Statistical analysis was performed on both 1 L and 1 ml samples separately. The number of compounds showing significant differences between time points when analysing a 1 ml sample was 214, and 329 with the 1 L sample. The considerable difference of 115 additional markers in the 1 L sample again highlights the importance of pre-concentrating the sample for non-targeted analysis. Table 3.11 looks at the top 20 compounds showing significant differences between time points from a 1 ml sample.

Table 3.11: Summary of the top 20 compounds that show significant differences between all three time points with a 1 ml sample, analysed using a Hypercarb column.

1 ml sample							
Significant differences between day 1 and day 4				Significant differences between day 4 and day 7			
m/z	Retention time (min)	CV	p-value	m/z	Retention time (min)	CV	p-value
105.0513	1.67	24%	0.004	156.584	6.95	28%	0.001
112.0863	1.01	3%	<0.001	189.117	1.21	19%	<0.001
121.0474	26.02	26%	0.008	190.121	2.86	17%	<0.001
156.5837	6.95	28%	0.001	194.641	9.11	16%	0.002
175.1066	2.14	14%	<0.001	223.106	16.82	6%	<0.001
190.1208	2.86	17%	<0.001	246.185	9.46	19%	<0.001
194.6406	9.11	16%	<0.001	249.066	2.36	28%	<0.001
223.1057	16.82	6%	<0.001	251.099	5.43	18%	<0.001
229.6478	8.41	24%	<0.001	261.142	6.06	9%	0.002
232.1244	1.79	20%	<0.001	263.116	28.8	29%	<0.001
270.118	2.55	26%	<0.001	270.118	2.55	26%	<0.001
286.1718	8.59	17%	<0.001	286.172	8.59	17%	0.001
302.1491	51.73	17%	0.006	288.201	15.07	17%	0.003
332.2123	16.05	18%	<0.001	332.212	13.53	9%	<0.001
377.2363	1.54	27%	<0.001	346.192	16.12	27%	<0.001
405.2641	2.67	14%	<0.001	373.204	5.94	15%	<0.001
416.2838	9.16	10%	<0.001	405.264	2.67	14%	<0.001
463.2449	1.42	25%	0.003	505.32	9.27	22%	<0.001
521.2745	9.16	18%	<0.001	522.28	9.19	7%	<0.001
659.3964	44.05	14%	<0.001	659.396	44.05	14%	<0.001

The table shows that these compounds are highly significant, with low *p-values*. This table shows an increase in the number of compounds (8) showing significant differences for both sets of time points compared to using a C18 column. Table 3.12 shows the top 20 compounds showing significant differences between the three time points from a 1 L sample.

Table 3.12: Summary of the top 20 compounds that show significant differences between all three time points with a 1 L sample, analysed using a Hypercarb column.

1 L sample							
Significant differences between day 1 and day 4				Significant differences between day 4 and day 7			
m/z	Retention time (min)	CV	p-value	m/z	Retention time (min)	CV	p-value
121.0474	26.02	26%	<0.001	121.0474	26.02	26%	<0.001
221.0879	7.1	21%	<0.001	123.0505	15.43	28%	0.001
229.6478	8.41	24%	0.001	221.0879	7.1	21%	<0.001
232.1681	5.61	27%	0.001	232.1681	5.61	27%	0.001
234.1479	4.33	23%	0.001	234.1479	4.33	23%	0.005
237.0708	24.46	25%	0.004	237.0708	24.46	25%	<0.001
240.1023	24.46	19%	0.001	240.1023	24.46	19%	0.001
245.0885	20.17	29%	<0.001	245.0885	20.17	29%	<0.001
248.1291	6.13	23%	<0.001	248.1291	6.13	23%	<0.001
263.4555	28.53	28%	<0.001	259.0877	5.86	24%	<0.001
272.1574	7.28	15%	<0.001	263.5959	28.69	27%	<0.001
302.1491	51.73	17%	0.004	272.1574	7.28	15%	0.008
332.2123	16.05	18%	0.008	276.1171	4.22	22%	0.001
345.2094	10.28	13%	0.001	280.1286	16.94	14%	<0.001
383.223	18.19	19%	0.001	283.115	21.99	10%	0.003
415.2159	19.92	13%	<0.001	303.1584	5.69	25%	<0.001
550.1523	15.38	13%	<0.001	308.0124	1.68	27%	<0.001
560.1468	15.37	12%	<0.001	332.2123	13.53	9%	<0.001
712.2335	15.39	17%	0.004	346.1934	15.66	26%	<0.001
716.2324	15.37	14%	<0.001	415.2159	19.92	13%	<0.001

These samples also present very low *p-values*, showing high significance in the data. There are 11 compounds present in both columns of the table, compared to only four when using a C18 column.

Table 3.13 presents the *m/z* of the compounds that have shown significant differences between time points. A similar pattern is presented for both the 1 ml and 1 L samples. The percentage of smaller compounds (*m/z* 0-300) increased over time, and the larger

compounds (*m/z* 600-900) decreased over time. This suggests that although the number of compounds and their quantities in the 1L sample might be higher, it is of a similar chemical composition to the 1 ml sample. This confirms that there is not a large loss of important compounds when using SPE. The results are similar when using both C18 and Hypercarb columns.

Table 3.13: Table showing the size of the compounds that produced significant differences between time points, expressed as a percentage.

	1ml sample		**1L sample**	
	Significant differences between:			
m/z	**Day 1 and day 4**	**Day 4 and day 7**	**Day 1 and day 4**	**Day 4 and day 7**
0-300	38%	63%	67%	79%
300-600	51%	35%	27%	21%
600-900	12%	2%	6%	0%

The two bar charts presented in Figure 3.22 and Figure 3.23 follow the changes in peak area of two ions at three time points, *m/z* 223.1057 and *m/z* 121.0474. These were chosen as they produced significant differences between the two sets of time points in the 1 ml and 1 L samples respectively. The ion *m/z* 223.1057 shows a similar pattern to the bar charts presented from analysis using a C18 column where the peak area is highest at day 4, followed by a decrease by day 7. The ion *m/z* 121.0474 behaves differently. The peak area is increasing at each time point in both the 1 ml and 1 L sample, while the control sample is consistently low. Having identified two ions showing completely different patterns over time highlights the complexity of the metabonomic processes occurring during decomposition, and how quickly the quantity of certain ions can increase or decrease.

It is clear in both figures that the 1 L pre-concentrated sample has a higher peak area than the 1 ml sample. It is important to note that although the 1 L sample should be 1000 times more concentrated compared to the 1 ml sample, this is not reflected entirely in these bar charts. This could have occurred for a variety of reasons, for example saturation of the phase, the sampling area, and the execution of the pre-concentration step.

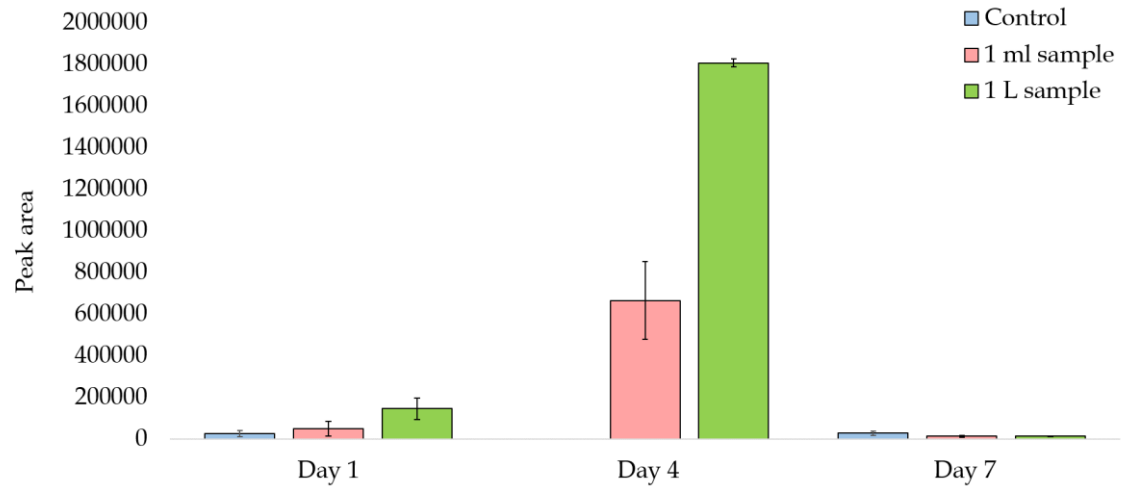

Figure 3.22: Bar chart showing the change in peak area over three time points of m/z 223.1057, analysed using a Hypercarb column with error bars ±1 standard deviation.

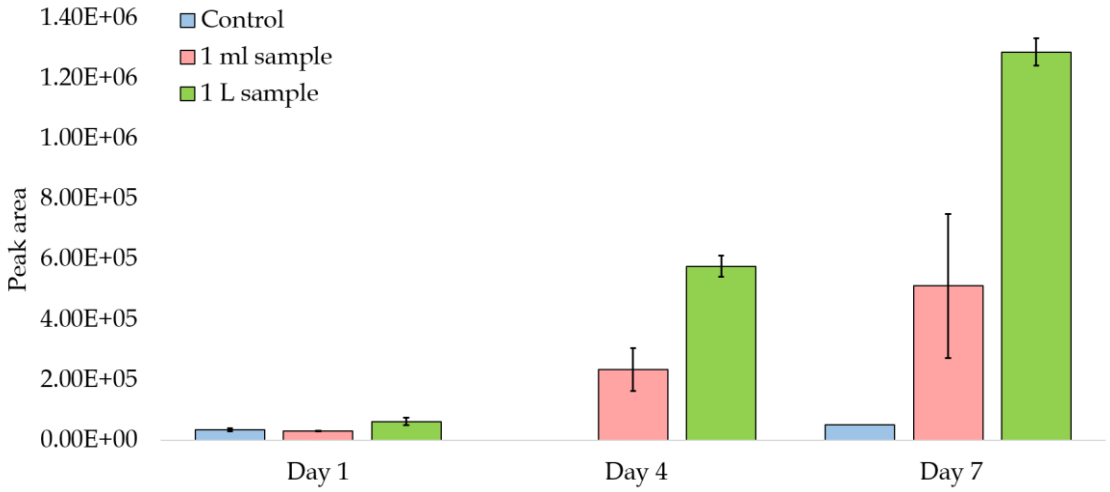

Figure 3.23: Bar chart showing the change in peak area over three time points of m/z 121.0474, analysed using a Hypercarb column with error bars ±1 standard deviation.

3.2.8 Results and Discussion using a HILIC column

3.2.8.1 Early method development

Initial attempts to develop a suitable method using a HILIC column proved to be difficult. Figure 3.24 shows a chromatogram from a 90-minute analysis using a shallow gradient elution. Only two peaks are seen on the chromatogram, and those appear at the very beginning, suggesting a lack of interaction between the compounds and the stationary phase. A variety of factors were adjusted to try and improve the quality of the analysis, such as flow rate, solvent, gradient, and sample preparation. These developments seemed to show no effect on the retention times, and overall success of the method. As a result, it was decided it was not viable to continue with method development for a HILIC column.

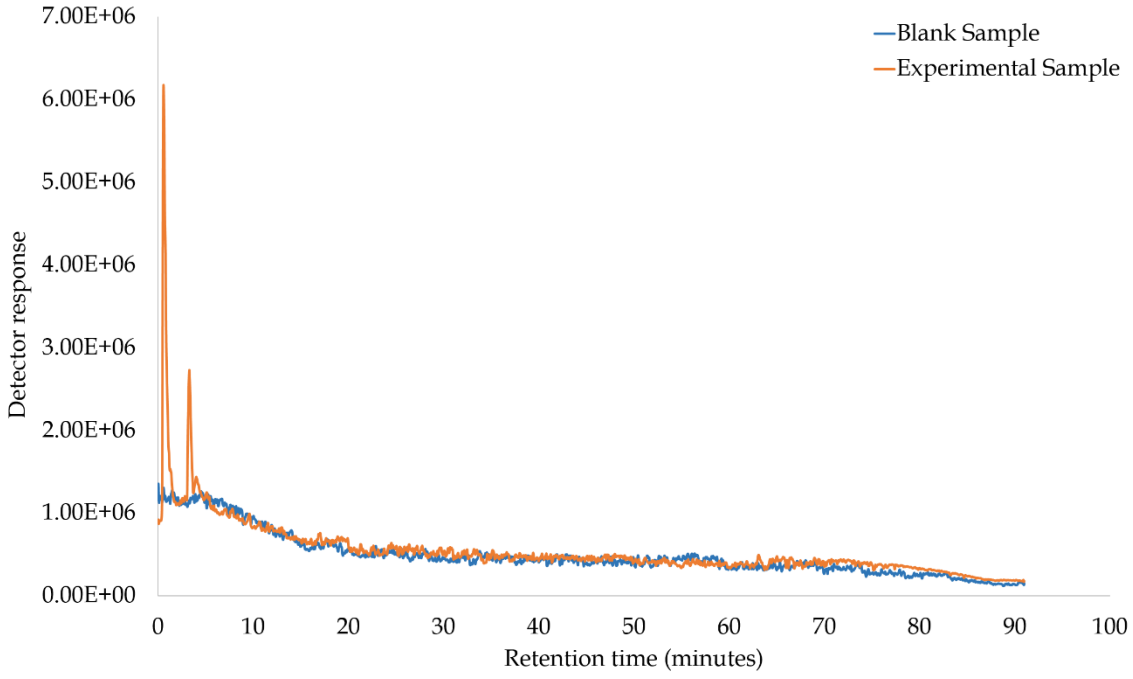

Figure 3.24: Two chromatograms showing a blank sample and an experimental sample using a HILIC column during method development.

3.2.9 Conclusion

This preliminary experiment showed that it is possible to identify a chemical signature of decomposition in the water using non-targeted metabonomic profiling. Pre-concentrating the water using SPE was the most effective sample preparation technique for a variety of reasons. The higher number of peaks and peak intensities, accompanied by better peak shape highlighted the improved quality of the chromatograms. Better separation between sample groups was presented on the PCA plot, along with a more robust dataset available for statistical analysis, resulting in clear patterns between different ions over time.

It was also unveiled that the C18 column would provide the most appropriate stationary phase for the sample matrix. It was clear that the quality of the chromatograms, increased separation on the PCA plot followed by a more accurate depiction of what we expected based on our prior knowledge of decomposition chemistry, lead to the decision to use this column for further analysis. The workflow created from the preliminary experiment will be challenged further in a field-based experiment, faced with a number of confounding variables.

3.3 An experiment to challenge the lab-based workflow in a field-based decomposition experiment in water using whole animal carcasses.

3.3.1 Aims

The purpose of this second experiment is to incorporate the workflow created in **3.2** to a more realistic field experiment. The chosen sample preparation method, followed by the most appropriate column chemistry was used moving forward. A number of factors will still inevitably be controlled such as the type of animal carcass, size of the container, the type of water used and strict sampling intervals. The temperature of the air and water, weather, insect activity and debris will be from the surrounding environment. This will determine whether the workflow can compete with the confounding variables of the harsh environment outside.

3.3.2 Materials

Heavy duty 60 litre storage boxes were purchased from Key Manutan Group Industrial Commercial Equipment, (Dorset, UK). HPLC grade methanol, formic acid, activated charcoal and a reference mass solution consisting of purine (*m/z* 121.0509) and hexakis (1*H*, 1*H*, 3*H*- tetrafluropropoxy)phosphazine (*m/z* 922.0098*)* was purchased from Fisher Scientific (Loughborough, UK). Ultrapure water (18.2 MΩ) was purified using a Purelab Option-Q system by Veolia Water (Saint Maurice, France). Intact rabbits carcasses were purchased from Livefood UK Ltd (Somerset UK).

3.3.3 Experimental method

A total of three rabbit carcasses were placed in separate 60 L boxes along with three control boxes. Two holes were drilled into the lids of each box to allow airflow and insect activity. Each box was filled with 40 L of water from a single source and placed outside. Temperature probes were used to monitor the temperature of the water and the air every 15 minutes. The experiment ran for nine weeks from July to September. Each week, a total of six samples were taken: 3 control water samples and 3 water samples from a box containing a rabbit carcass. Samples from the beginning, middle and end of the experiment were used to demonstrate proof of concept. From each box, 1 ml and 1 L samples were taken to compare two different sample preparation methods. It was decided that 1 L of water was taken as it provides a large amount of sample for concentration, and would not adversely affect the data as there was a total of 40 L of water in each box. In total 48 samples were analysed (2 conditions, 2 sample preparation methods, 3 replicates, 4 time intervals).

3.3.4 Sample preparation and storage

This work was carried out exactly as described in **Section 3.2.2.3**.

3.3.5 Instrumental setup

3.3.5.1 Quality control

This work was carried out exactly as described in **Section 3.2.3.1**.

3.3.5.2 Chromatographic parameters

The chromatographic separation was carried out using an Agilent Technologies 1260 Infinity Binary HPLC system. A Thermo Fisher C18 Hypersil Gold (100mm x 2.1mm, 1.9µm particle size) column was used. The column temperature was maintained at 40^{o}C, and the injection volume was 5µl. The mobile phase consisted of (A) Water with 0.1% formic acid and (B) Methanol with 0.1% formic acid. The flow rate was 0.2 ml min^{-1}. The solvent gradient is shown in Table 3.14. Due to the increase in number of peaks present on the chromatogram compared to the preliminary analysis in **Section 3.2.3.2**, the solvent gradient was modified to accommodate these changes.

Table 3.14: Solvent gradient used for the analysis of water containing a decomposing carcass in the summer season.

Time (minutes)	Solvent A (%)	Solvent B (%)
0	95	5
3	65	35
13	65	35
14	25	75
24	25	75
25	0	100
35	0	100
36	95	5
40	95	5

3.3.5.3 Mass spectrometry parameters

This work was carried out exactly as described in **Section 3.2.3.3**.

3.3.6 Data pre-processing

This work was carried out exactly as described in **Section 3.2.4**.

3.3.7 Data analysis and statistical analysis

This work was carried out exactly as described in **Section 3.2.5**.

3.3.8 Results and discussion

3.3.8.1 QC analysis

The QC samples in this analysis (Figure 3.25) produced reproducible chromatograms, showing no variability in retention time. There is a slight difference in peak intensity in peaks between 30 to 35 min, where the first two samples have a higher peak intensity, however this stabilises following additional injections.

To further investigate the stability of the instrument, Table 3.15 shows the variability of peak area (A) and retention time (B) from six peaks selected from the QC sample chromatograms.

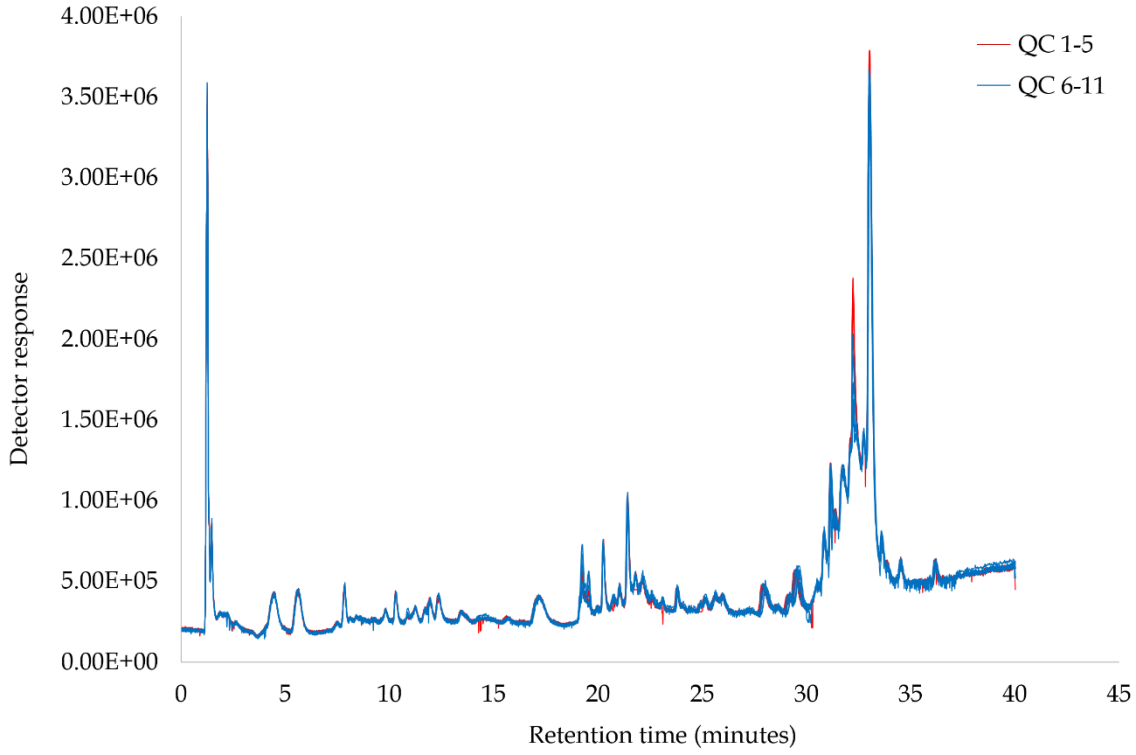

Figure 3.25: Total ion chromatograms of QC samples of water containing decomposing carcass over 9 weeks, showing initial conditioning of the column.

The retention time is stable in each peak, and only slight variation is seen in the peak areas. Comparing the CV values obtained here to the accepted value of variance facilitated further confirmation that the instrument was stable. The maximum variance was 7% for peak area, and 0.12% for retention time, demonstrating that the instrument was stable throughout the analytical sequence [25].

Table 3.15: Variability of peak area (A) and retention time (B) from 6 selected peaks in the QC samples during the analytical sequence for the analysis of water containing a decomposing carcass in the summer season.

A

Peak	QC6	QC7	QC8	QC9	QC10	QC11	Average	St. Dev	CV%
1	412698	414641.	40728	412079	428496	428029	**417205**	**8901**	**2%**
2	463367	464055	458825	464040	475255	438173	**460619**	**12266**	**2%**
3	412317	422420	400483	400999	423109	436798	**416021**	**14168**	**3%**
4	707900	708566	700353	752011	739443	759466	**727957**	**25469**	**3%**
5	994798	944391	92760	1023177	1020838	1022647	**988910**	**42676**	**4%**
6	393076	397082	460763	458540	428519	456334	**432386**	**31206**	**7%**

B

RT	QC6	QC7	QC8	QC9	QC10	QC11	Average	St. Dev	CV%
1	4.45	4.44	4.43	4.44	4.45	4.44	**4.44**	**0.0053**	**0.12%**
2	7.85	7.84	7.83	7.84	7.85	7.84	**7.84**	**0.0057**	**0.07%**
3	10.28	10.28	10.27	10.27	10.29	10.28	**10.28**	**0.0053**	**0.05%**
4	20.25	20.25	20.24	20.24	20.26	20.25	**20.25**	**0.0053**	**0.03%**
5	21.42	21.41	21.40	21.41	21.42	21.41	**21.41**	**0.0056**	**0.03%**
6	28.12	28.12	28.11	28.11	28.12	28.12	**28.11**	**0.0053**	**0.02%**

3.3.8.2 Metabolic profiling

Figure 3.26 presents the overlaid chromatograms of the 1 ml water samples taken at week 1, 2, 6 and 9 of the experiment. This figure focuses on how the chemical profile of the water changes over time from direct sampling from the box. The chromatograms for week 1 and week 2 are fairly similar, showing only a very limited number of peaks of low intensities. At week 6 there is an increase in both the number of peaks and their intensities, and the majority of these peaks show a further increase at week 9.

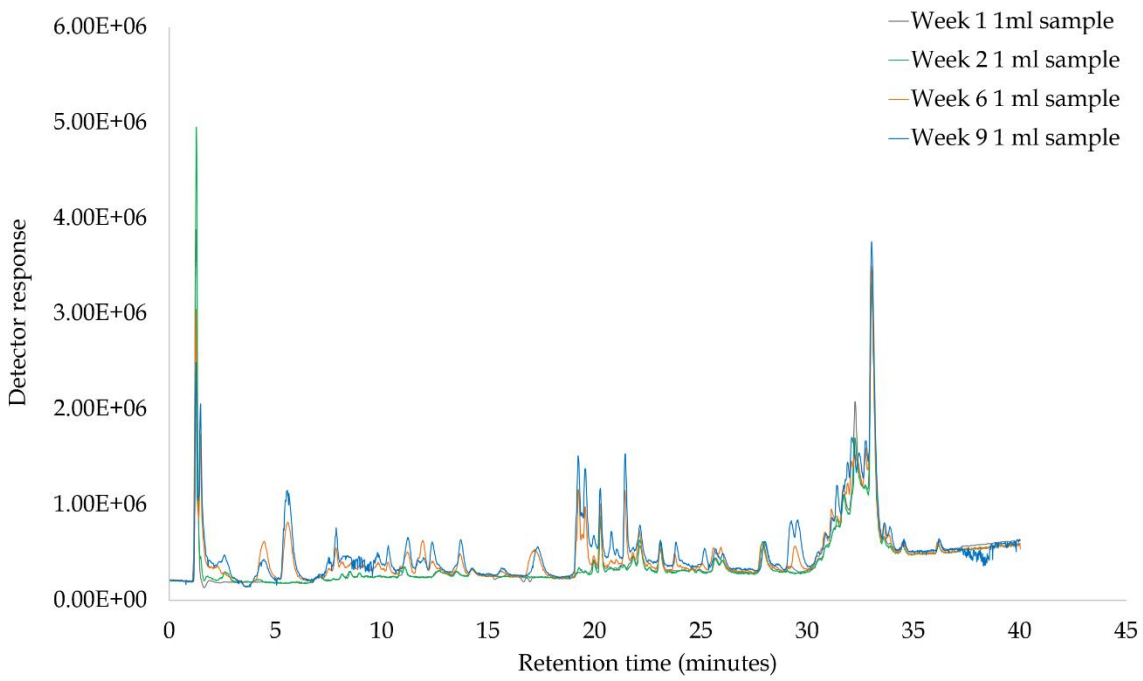

Figure 3.26: Example total ion chromatogram (TIC) of 1 ml water samples taken from a box containing decomposing remains in water at week 1, 2, 6 and 9 of the experiment.

The overlaid chromatograms in Figure 3.27 show the 1 L samples taken at week 1, 2, 6 and 9 of the experiment. These chromatograms effectively highlight how the chemical signature of the water exposed to decomposition changes over time. It is was expected that the peak intensities would increase over time, however, few peaks across the chromatograms show higher intensities at week 6. This suggests that the chemical profile of the water is not just influenced by the increasing number of compounds in the water, but also the fluctuation in the quantity of these compounds. For example, a peak with its highest intensity at week 6 could include compounds that have broken down into their smaller counterparts by week 9, evaporated from the sample, or even overshadowed by other compounds in larger quantities.

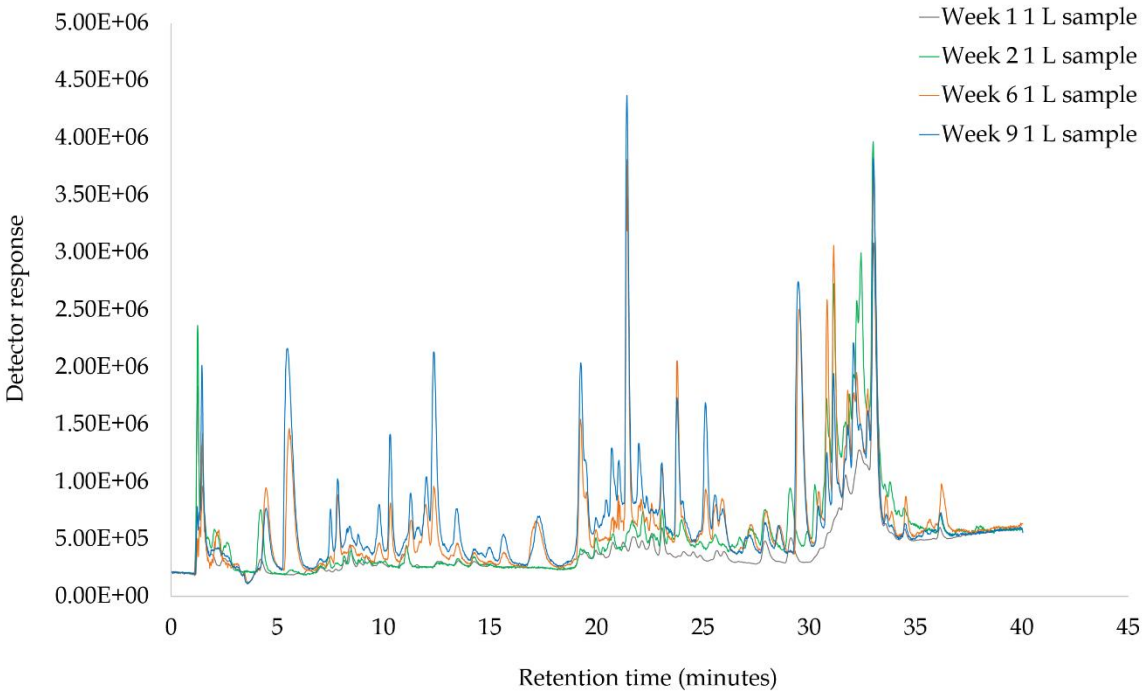

Figure 3.27: Example total ion chromatogram (TIC) of 1 L water samples taken from a box containing decomposing remains in water at week 1, 2, 6 and 9 of the experiment.

Instantly it is obvious that there is a distinct difference between the chromatograms of the 1 ml samples and 1 L pre-concentrated samples over time. The overall peak patterns seem similar, where week 1 and week 2 show limited peak numbers and low peak intensities, and week 6 and week 9 showing more changes to the chemical signature of the sample. It is evident that the 1 L pre-concentrated sample produced chromatograms that presented valuable information about the progression of chemical decomposition over time, and how it influences the water chemistry.

To investigate the differences between the sample preparation methods in detail, comparisons have been made at each time point throughout the analysis. Figure 3.28 presents the chromatograms of a 1 ml sample and 1 L sample taken after 1 week of decomposition in water.

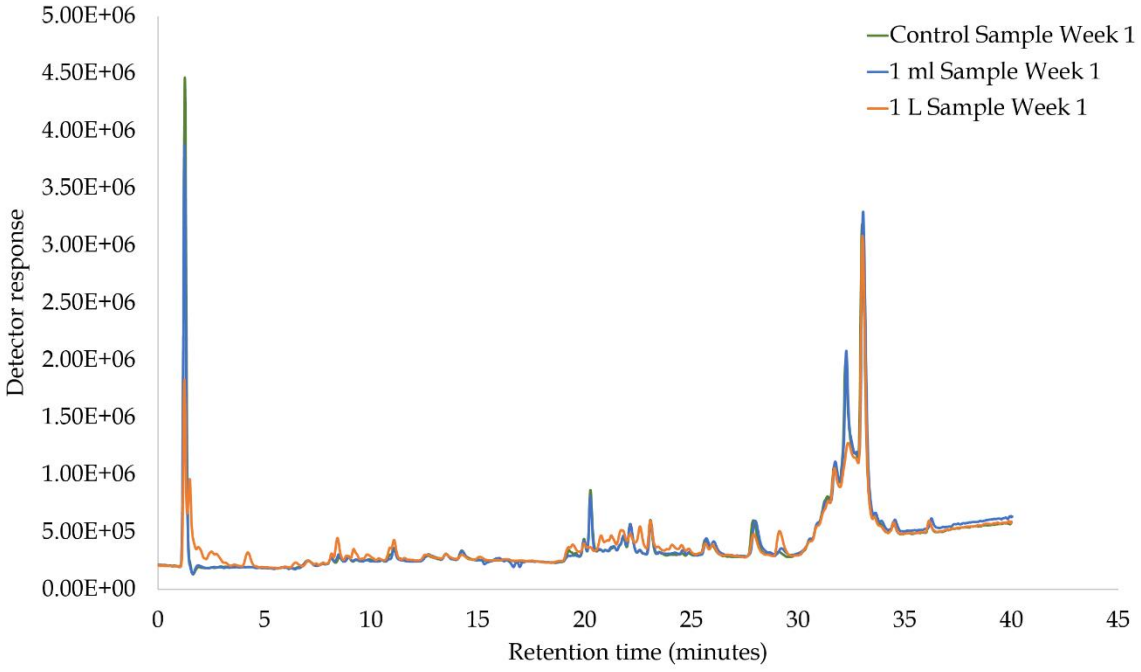

Figure 3.28: Total ion chromatogram (TIC) of a control sample, 1 ml sample and a 1 L sample, filtered through SPE following 1 week of decomposition in water.

The chromatograms representing week 1 reflect what was expected during the early stages of decomposition. Whilst it is clear that the water has already been influenced by the decomposing remains, the peaks observed are of low intensity. It is possible to see small differences between the 1 ml and 1 L samples, however what is surprising is that two peaks at around 20 and 32 minutes are present in the 1 ml sample, and showing high peak intensities. The cause is unclear at this stage, however there is a possibility that the compounds in this peak were not retained well on the SPE cartridge.

The chromatograms in Figure 3.29 show that after two weeks of remains decomposing in water, a clear chemical signature is seen. The chromatogram showing the control sample seems to be very similar to the chromatogram for the 1 ml sample, suggesting that it is still difficult to identify leaching compounds from such a small sample after 2 weeks. The 1 L sample filtered through an SPE cartridge shows a higher number of peaks, and greater peak height in comparison to the 1 ml sample.

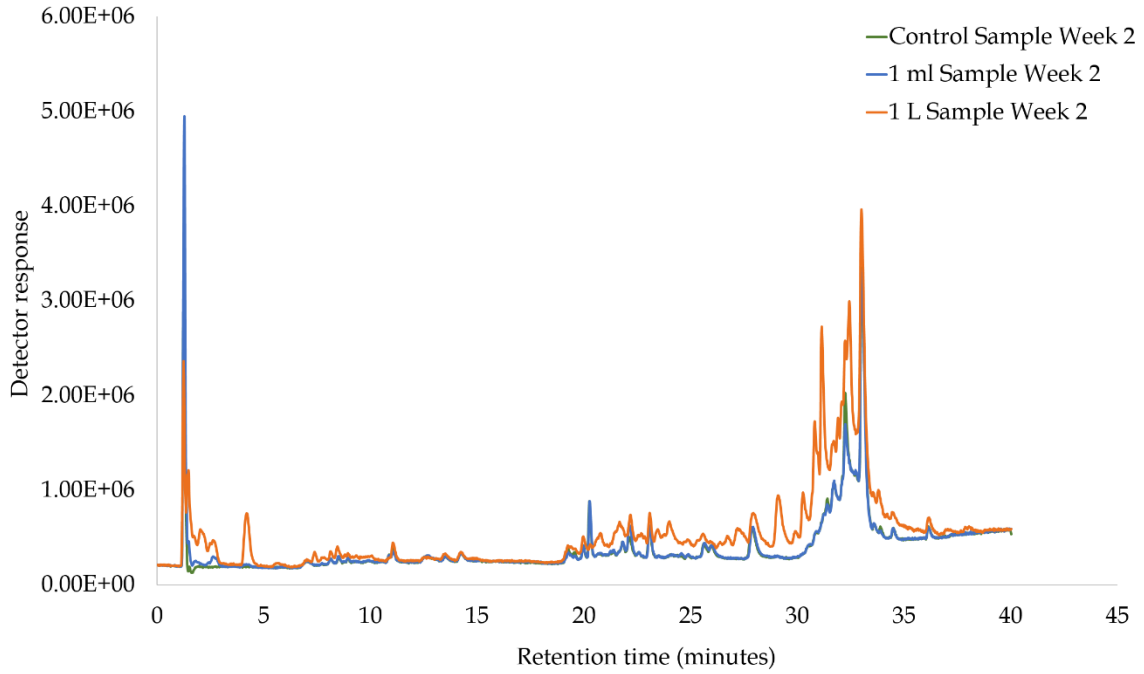

Figure 3.29: Total ion chromatogram (TIC) of a control sample, 1 ml sample and a 1 L sample, filtered through SPE following 2 weeks of decomposition in water.

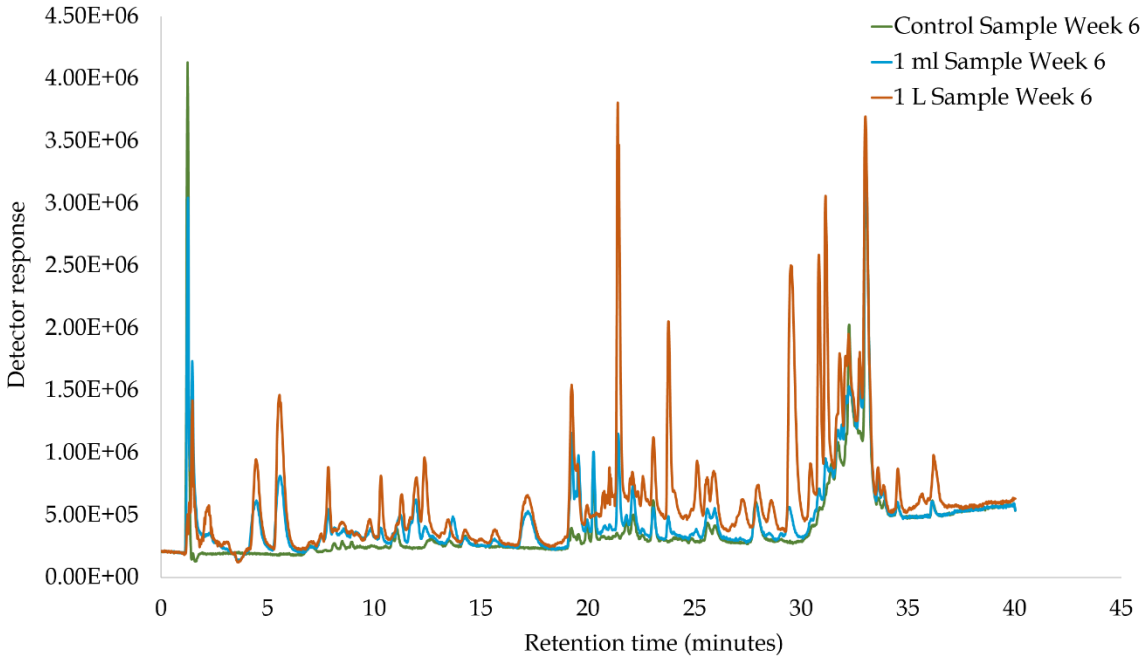

Figure 3.30: Total ion chromatogram (TIC) of a control sample, 1 ml sample and a 1 L sample filtered through SPE following 6 weeks of decomposition in water.

Figure 3.30 shows a chromatogram for each sample after six weeks of decomposition in water. Here, we see a dramatic change in the chemical signature of the water. The number of peaks has increased in both the 1 ml sample and 1 L sample, and it is clear that these additional peaks are not present in the control water chromatogram. The majority of the peaks in the 1 L sample chromatogram show higher peak intensities compared to the 1 ml sample chromatogram.

Figure 3.31 presents the chromatogram of each sample taken at week 9 of the experiment. The 1 L sample chromatogram shows a further increase in peak intensities, specifically between 5-15 min of the analysis. These changes are not reflected as much in the 1 ml sample chromatogram.

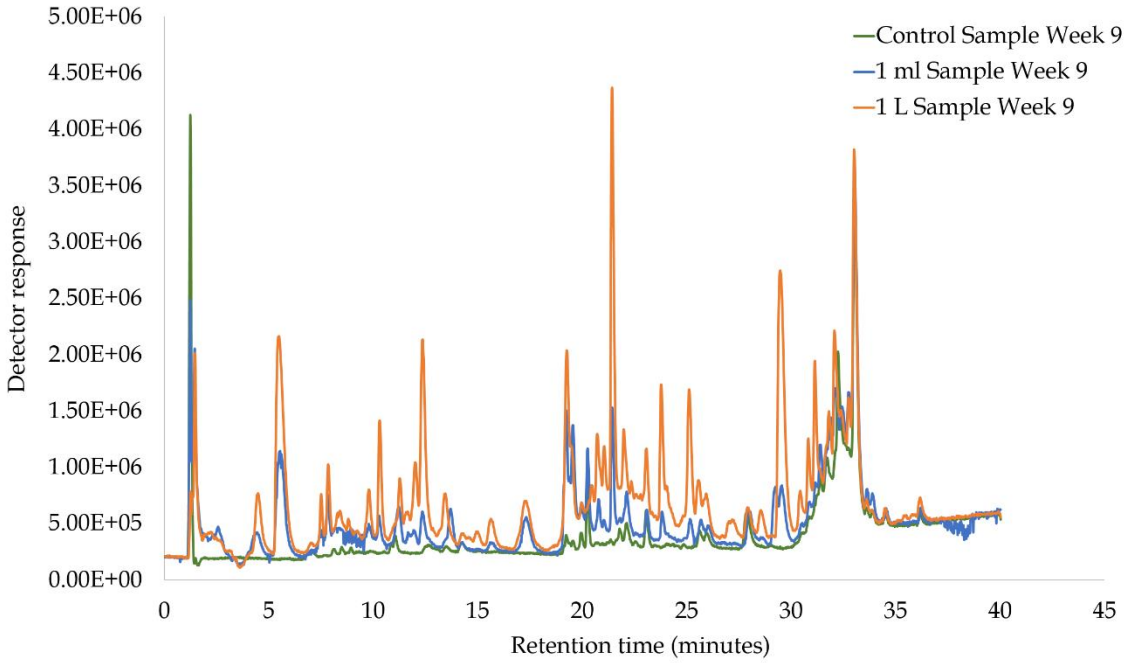

Figure 3.31: Total ion chromatogram (TIC) of a 1 ml sample, and a 1 L sample filtered through SPE following 9 weeks of decomposition in water.

These chromatographic results clearly show the benefit of including the pre-concentration step during sample preparation. The lab-based workflow was successfully used in a more realistic experimental setting and produced similar results. As a result, these methods were not only able to detect the chemical profile of decomposition in water, but can also monitor the changes over time visually on the chromatogram. It is important to consider if it is possible to link these chromatographic patterns changing over time to the process of chemical decomposition.

It is clear that the chromatogram from the analysis of week 2 shows a limited number of peaks, and those present are between 20-35 minutes on the chromatogram. When using a C18 column, the pore size will affect the speed compounds of certain weight travel through the stationary phase. This may suggest that the larger compounds from the early

stages of decomposition are seen in this chromatogram, as they take longer to elute from the column. As the chemical signature of the water changes over nine weeks, the peaks appearing at the beginning of the chromatograms could indicate the further breakdown of decomposition products. Previous research states that soft tissue is broken down by endogenous enzymes and micro-organisms such as bacteria and fungi into gases (volatiles) and liquids (leachate) [26]. Carbohydrates break down into their monomers, and further to carbon dioxide, water and fatty acids [27, 28]. Proteins are broken down into peptones, polypeptides, and ultimately into smaller amino acids [27]. Additionally, lipids can be broken down into a mixture of fatty acids which can further undergo hydrolysis and oxidation in the correct conditions [29].

The lipophilicity of a compound is represented as a distribution coefficient (LogD) [30]. As compounds break down during decomposition to their smaller counterparts, their chain length decreases. As a result, the LogD decreases as the molecules are less lipophilic. Therefore, they will interact less with the stationary phase, resulting in these compounds eluting much sooner from the column compared to the parent compound.

This could explain the increase in the number of peaks and peak height appearing at the beginning of the chromatogram as the experiment progresses. Although this is observed in both the 1 ml and 1 L pre-concentrated sample, it is noticeably more prominent in the 1 L samples, particularly between weeks six and nine.

3.3.8.3 Multivariate analysis

The PCA scores plot in Figure 3.32 shows the 1 ml samples taken at weeks 1 ,2, 6 and 9 of the experiment, accompanied by control samples. The QC samples are tightly clustered on the plot, reflecting high precision in the data. The control samples from week 1, 2, 6 and 9 are all clustered to the left of the plot. This implies that any changes to the chemical signature of the water is not due to the stagnation of the water itself over time but rather the compounds leaching from the decomposing carcass.

It is important to note that samples from week 1 are clustered with the control samples, suggesting that their chemical profile is similar. The plot shows enough separation between each time interval to be able to group them, however, samples from weeks 1 and 2 overlap, as do weeks 6 and 9.

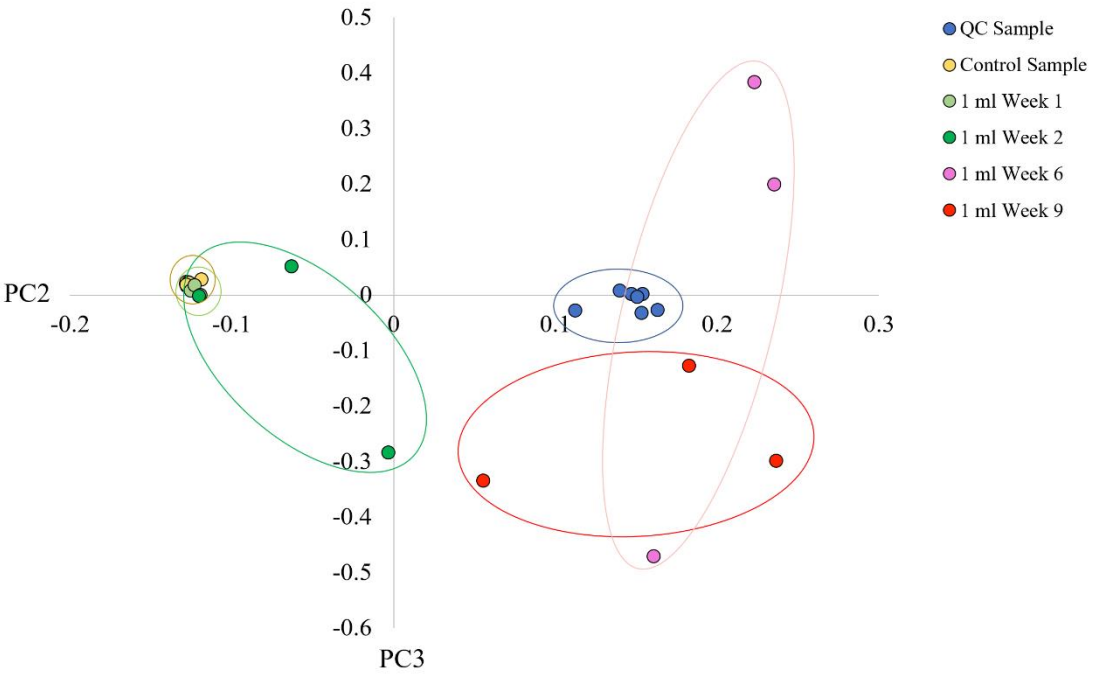

Figure 3.32: PCA score plot of PC2 (18.16%) and PC3 (4.20%) showing 1 ml water samples containing decomposing carcass sampled over 9 weeks, and a control.

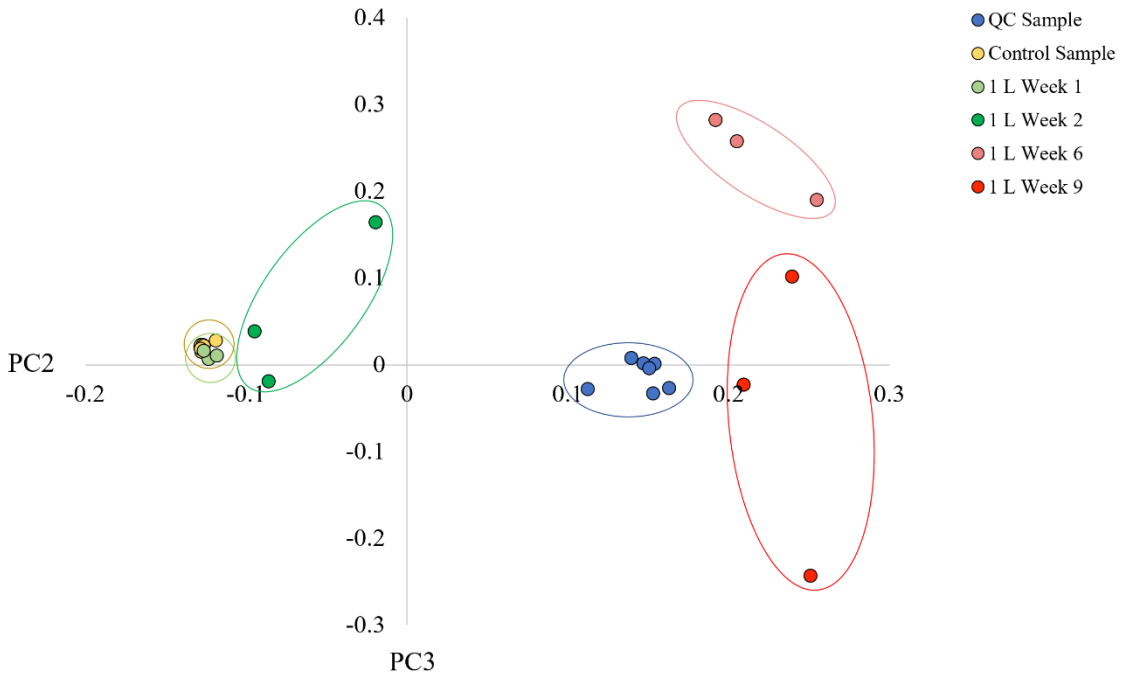

Figure 3.33: PCA score plot of PC2 (18.16%) and PC3 (4.20%) showing 1 L concentrated water samples containing decomposing carcass sampled over 9 weeks, and a control.

Figure 3.33 shows the PCA plot for the 1 L samples. The QC samples are clustered towards the middle of the plot, and the control samples from all four time intervals are also clustered to the left of the plot, similar to the plot for the 1 ml sample in Figure 3.32. The biggest difference between the 1 ml and 1 L samples is shown in the separation between time intervals. When looking at the 1 L samples, each time interval can be clearly distinguished from the next, with no overlap between groups. It is clear that using SPE as a sample preparation method has been successful. This also demonstrates that multivariate analysis is a useful tool to visualise the change in the chemical signature of water containing a decomposing carcass, and to show the differences between different sample preparation techniques. It allows the potential to identify which compounds are responsible for the separation observed on the PCA scores plot.

3.3.8.4 Statistical analysis and significant markers

The number of features detected in this analysis via *XCMS Online* was 7504. All features with a CV value of less than 30% were removed, with 5891 remaining. Statistical analysis was performed on both 1 L and 1 ml samples separately. The number of compounds showing significant differences between all time points when a 1 ml sample of water was 5, and 59 with the 1 L sample. Further breakdown of the statistical analysis is shown in Table 3.16, where the number of features showing significant differences between each time point is presented following analysis with the 1 L pre-concentrated sample, and the 1 ml sample. It is clear from the table that there is a much higher number of features showing significant differences between each time point following analysis with a 1 L pre-concentrated sample. It is also noted that the number of features seem to increase towards the middle of the experiment, followed by a sharp decrease toward the end.

Table 3.16: Presenting the number of features showing significant differences from statistical analysis carried out between each time point, following analysis with a 1 L and 1 ml sample.

Sample type	**1 ml sample**			**1 L sample**		
	Compounds showing significant differences between :					
Time points	**Week 1 and 2**	**Week 2 and 6**	**Week 6 and 9**	**Week 1 and 2**	**Week 2 and 6**	**Week 6 and 9**
No. features	275	607	280	1204	1348	588

Table 3.17 presents the size of these features that have shown significant differences between time points, expressed as a percentage.

Table 3.17: Table showing the size of the compounds that produced significant differences between time points, expressed as a percentage.

	1 ml sample			1 L sample		
	Compounds showing significant differences between :					
m/z	**Week 1 and 2**	**Week 2 and 6**	**Week 6 and 9**	**Week 1 and 2**	**Week 2 and 6**	**Week 6 and 9**
0-300	38%	59%	6%	38%	44%	56%
300-600	58%	39%	28%	45%	44%	27%
600-900	4%	2%	67%	17%	12%	17%

When looking at the 1 L pre-concentrated sample in Table 3.17, the results show the expected pattern of an increase in the percentage of smaller compounds (*m/z* 0-300) over time, and a decrease in the amount of larger compounds (*m/z* 300-600, *m/z* 600-900) over time. The 1 ml sample shows the opposite effect between week 6 and 9, with a sharp increase in the larger compounds instead. This does not follow the expected trends of decomposition. Table 3.18 and Table 3.19 show the top 20 compounds showing significant differences between each time interval in the 1 ml and 1 L samples respectively.

Table 3.18: Summary of the top 20 compounds that show significant differences between all four time points, following the analysis of a 1 ml sample.

1 ml sample											
Compounds showing significant differences between :											
Week 1 and week 2				Week 2 and week 6				Week 6 and week 9			
m/z	Retention time (min)	CV	p-value	m/z	Retention time (min)	CV	p-value	m/z	Retention time (min)	CV	p-value
126.0610	2.09	23%	0.003	59.0480	6.08	6%	0.001	102.0885	7.85	17%	0.006
169.0439	38.45	27%	0.004	93.5075	10.09	17%	0.001	114.0651	1.48	7%	<0.001
210.1777	1.6	11%	<0.001	111.0406	6.65	4%	<0.001	186.1075	1.6	21%	0.006
219.0519	6.06	4%	0.001	115.9594	1.52	12%	0.001	219.0519	6.06	4%	0.006
242.1442	3.23	26%	0.004	123.5186	10.09	8%	0.001	425.2832	34.14	27%	0.006
283.1612	7.71	16%	0.002	129.0541	6.63	9%	<0.001	437.1919	24.32	18%	0.003
288.2508	21.33	16%	0.004	135.0992	7.19	8%	0.001	572.4558	31.96	21%	<0.001
335.0594	1.54	13%	<0.001	205.0064	10.09	8%	0.001	579.2854	25.92	3%	0.004
347.1317	8.35	25%	<0.001	215.1205	10.17	4%	0.002	588.4060	33.67	5%	0.005
355.0934	10.09	6%	0.001	231.1095	11.49	15%	0.002	610.4080	33.82	9%	0.004
360.8438	1.32	17%	0.003	256.9559	10.09	20%	<0.001	644.7967	34.1	9%	0.006
421.1325	7.21	13%	<0.001	258.0064	21.98	24%	0.002	664.4773	34.23	12%	0.006
466.1582	8.51	16%	0.001	265.0070	10.11	24%	0.002	666.7977	34.23	15%	0.004
527.1541	1.52	10%	0.002	303.0139	17.53	15%	<0.001	668.4725	32.63	7%	0.004
559.1108	10.1	10%	0.001	311.2078	28.21	4%	0.001	685.1453	34.37	5%	0.003
573.8264	1.3	8%	0.002	351.9882	22.33	21%	<0.001	698.9721	32.75	7%	0.003
579.2854	25.92	3%	0.004	372.0627	22.36	6%	<0.001	703.1731	34.51	13%	0.005
580.2916	25.92	4%	0.001	413.2663	34.63	3%	0.001	750.5359	32.61	27%	<0.001
589.8092	1.33	5%	0.004	455.3330	23.27	7%	0.001	757.0153	33.05	7%	0.002
734.7415	1.35	6%	0.003	457.3356	23.27	8%	0.002	873.5962	33.67	4%	0.003

Table 3.19: Summary of the top 20 compounds that show significant differences between all four time points, following the analysis of a 1 L sample.

1 L sample											
Compounds showing significant differences between :											
Week 1 and week 2				Week 2 and week 6				Week 6 and week 9			
m/z	Retention time (min)	CV	p-value	m/z	Retention time (min)	CV	p-value	m/z	Retention time (min)	CV	p-value
105.0665	5.86	14%	<0.001	81.0701	26.16	25%	<0.001	62.06041	1.49	20%	0.002
122.0928	5.85	6%	<0.001	159.0605	7.89	23%	<0.001	102.0885	7.85	17%	0.001
132.9451	2.72	21%	<0.001	171.0943	9.56	15%	<0.001	147.0853	9.81	10%	<0.001
203.0210	2.13	14%	<0.001	212.6376	26.17	11%	<0.001	159.0605	7.89	23%	0.002
206.1535	20.73	27%	<0.001	278.6990	26.15	14%	<0.001	162.0920	12.2	12%	0.001
214.1211	23.35	15%	<0.001	364.9598	22.33	10%	<0.001	227.0880	9.16	27%	0.002
266.8388	1.41	10%	<0.001	383.2439	26.16	5%	<0.001	301.2302	30.51	26%	0.002
290.9399	22.34	29%	<0.001	387.1703	22.01	5%	<0.001	310.2282	19.62	7%	<0.001
364.9598	22.33	10%	<0.001	399.2902	26.16	13%	<0.001	332.2070	19.63	6%	<0.001
369.1174	23.3	9%	<0.001	400.2964	26.17	14%	<0.001	388.1754	22.02	7%	0.002
372.0627	22.36	6%	<0.001	409.1573	22	4%	<0.001	400.2964	26.17	14%	0.001
374.0586	22.36	20%	<0.001	440.2439	26.16	10%	<0.001	405.2043	22.02	10%	<0.001
394.9781	22.35	10%	<0.001	461.2681	25.78	8%	<0.001	409.1573	22	4%	<0.001
409.1573	22	4%	<0.001	499.2734	22.01	7%	<0.001	425.1267	22.01	10%	<0.001
418.9705	22.34	9%	<0.001	539.4130	26.15	6%	<0.001	476.3218	8.61	20%	0.002
455.1855	1.59	14%	<0.001	571.3577	26.15	4%	<0.001	505.1104	10.06	13%	0.002
480.9393	22.35	7%	<0.001	599.3515	26.15	4%	<0.001	687.2425	21.98	9%	0.001
678.9792	22.33	3%	<0.001	638.2049	21.65	11%	<0.001	712.5101	34.88	23%	0.001
682.9730	22.35	5%	<0.001	687.2425	21.98	9%	<0.001	790.5850	28.81	6%	0.001
796.3342	22.01	4%	<0.001	795.3314	22.01	4%	<0.001	797.3363	22.05	8%	<0.001

Table 3.18 shows the top 20 features from the 1 ml sample that show significant differences between weeks 1-2, weeks 2-6 and weeks 6-9. The features *m/z* 219.0519 and *m/z* 579.2854 appear to be the only compounds that are showing significant differences between more than two time points.

Table 3.19 shows the top 20 features from the 1 L sample that show significant differences between weeks 1-2, weeks 2-6 and weeks 6-9. Looking in detail, *m/z* 409.1573 shows significant differences throughout, while *m/z* 364.9598, *m/z* 400.2964, *m/z* 159.0605 and *m/z* 687.2425 show significant differences between at least two time points. With only two features showing significant differences in more than one column of the table in the 1 ml sample, compared to 5 for the 1 L sample, again suggests that a pre-concentrating the sample does influence the sample matrix. It allows greater insight into the compounds that create drastic changes in the chemical signature of the water.

The ability to track a single feature (*m/z* 409.1573) through all time points in the 1 L sample suggests that the pre-concentration methods are consistently capturing the same type of compounds throughout the experiment, as well as new emerging compounds. Pre-concentrating the sample also allows the instrument to detect compounds of low concentration that might be inundated with new emerging compounds in the 1 ml sample. This creates an opportunity to monitor compounds that fluctuate dramatically over time, rather than those dominating the sample at any one time. This increases confidence in the ability of the method to accurately detect the changes in the chemical signature of the water influenced by decomposition.

Figure 3.34 presents a bar chart monitoring the changes in peak area over four time intervals for *m/z* 409.1573.

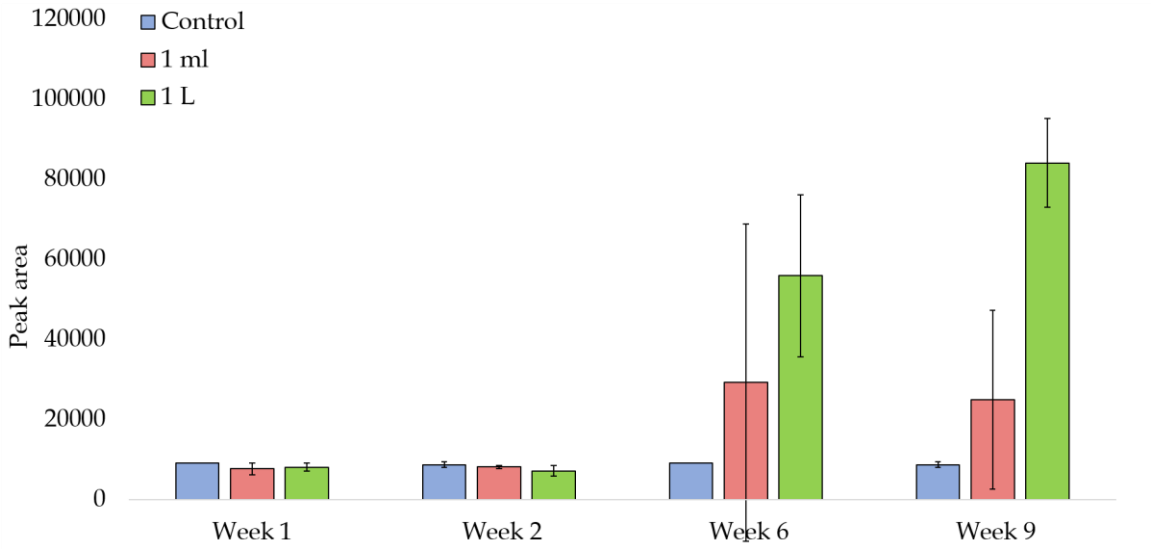

Figure 3.34: Bar chart showing the change in peak area over four time points of m/z 409.1573 *in a control sample, 1 ml sample and 1 L sample with error bars ±1 standard deviation.*

This marker shows that although the peak area seems low at the first two time points, there is a clear increase in the peak area further into the experiment. The peak area for the 1 ml sample seems to only increase slightly, with no distinct changes between the last two time points when comparing to the 1 L sample. The error bars for the 1 ml sample also highlights the error due to the vast differences in the range of peak area for each sample. This suggests the data is not as reliable and robust as that obtained from the 1 L sample.

Figure 3.35 and Figure 3.36 show the changes in peak area over time for ions *m/z* 159.0605 and *m/z* 364.9598 respectively. The peak area for *m/z* 159.0605 seems to increase slowly over time, with a dramatic spike in peak area at week 9. The marker *m/z* 364.9598 only shows a change in peak area at week 6, followed by a sudden decrease. The behaviour of these two example markers demonstrate how the chemical signature of the water is influenced by a variety of different metabonomic processes, as ions can appear and disappear over time.

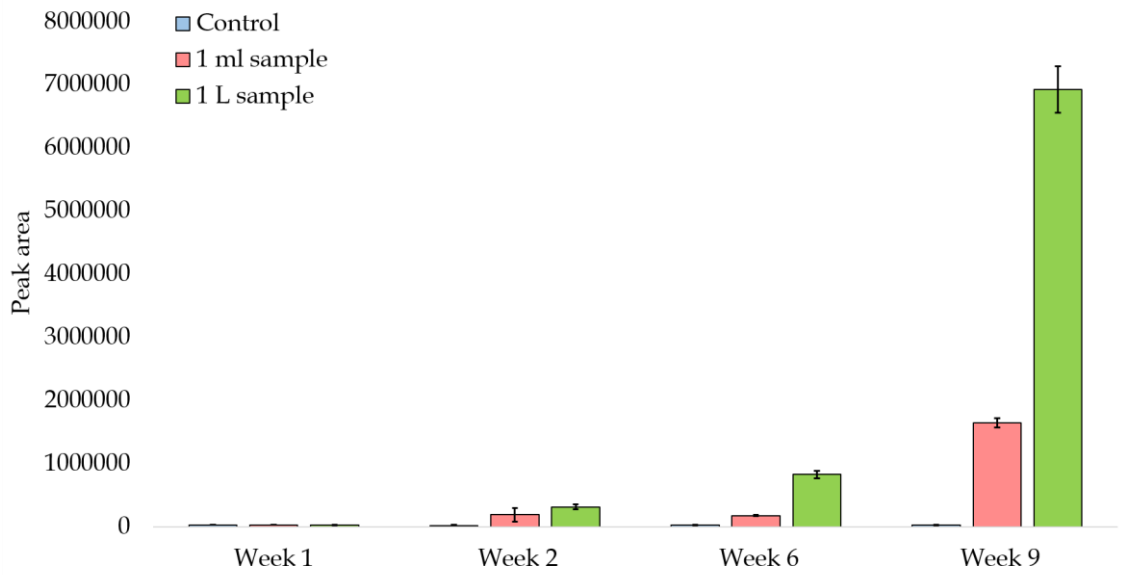

Figure 3.35: Bar chart showing the change in peak area over four time points of m/z 159.0605 in a control sample, 1 ml sample and 1 L sample with error bars ±1 standard deviation.

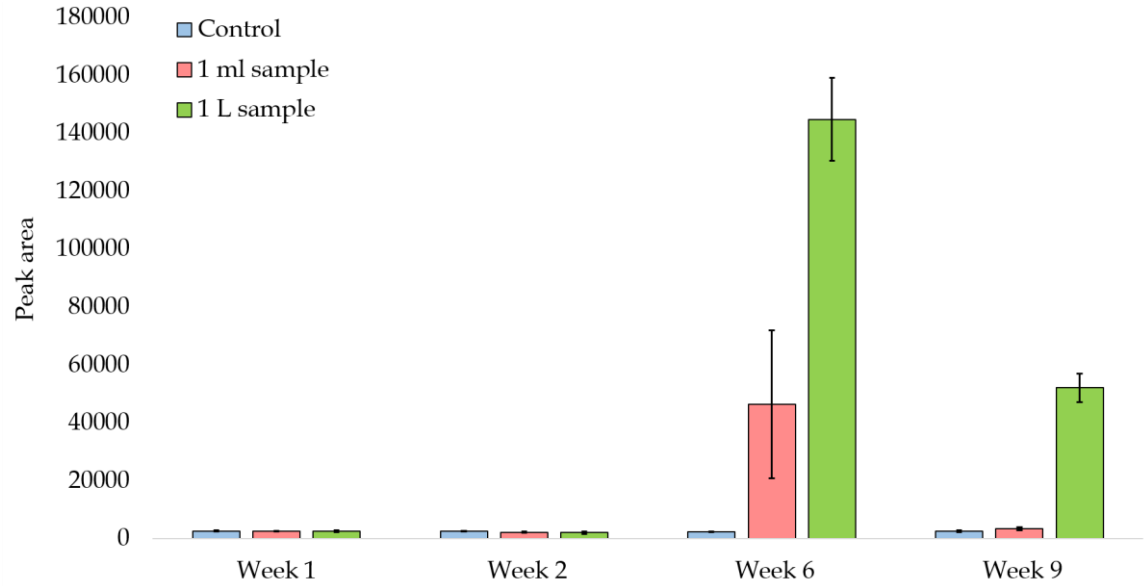

Figure 3.36: Bar chart showing the change in peak area over four time points of m/z 364.9598 in a control sample, 1 ml sample and 1 L sample with error bars ±1 standard deviation.

3.4 Conclusion

This preliminary work has shown that metabonomic profiling methods can detect a chemical signature of decomposition in water containing animal remains. This approach has also shown that it is possible to conduct statistical analysis on large datasets to identify and track specific biological markers that leach into the water during decomposition. The analytical technique of liquid chromatography-mass spectrometry has shown to produce reliable and robust data using a variety of methods, with very limited retention time and peak area variability. As a result, it was possible to use a variety of method development techniques to produce an effective and robust workflow for further analysis of these samples in a real-life environment. The two most important factors considered during this method development were sample preparation, and column chemistry.

A small preliminary lab-based experiment with meat decomposing in a beaker of water created an initial view of how the sample may interact during preparation, and with a variety of stationary phases before conducting a large experiment. A HILIC, C18 and Hypercarb column were used, with each looking at the difference in results between a 1 ml sample and a 1 L pre-concentrated sample. Their success was based on retention, stability, quality of data and run times.

It is clear from the results that a small 1 ml direct sample from the water containing a decomposing carcass produced limited data due to the low concentration of the compounds. Using solid-phase extraction as a sample preparation technique to pre-concentrate a 1 L sample yielded the best result. With a higher number of peaks, increased peak height, more valuable information when using multivariate analysis, and notably more stable biological markers that could be monitored, it was concluded that solid phase

extraction using an activated charcoal phase would be the most effective way to prepare these samples.

Due to the poor chromatographic resolution obtained from the HILIC column and the lack of improvement to the method following extensive efforts, it was decided that a HILIC column was not suitable for this particular type of analysis. A detailed comparison between the C18 and Hypercarb column was conducted to determine the most appropriate column for future analysis. Stability throughout the analysis appears to be more consistent when using a C18 column, with no retention time drift and very limited variance in the peak area of the quality control samples. Both columns produced CV values under the accepted value of 30% for variance.

Both the Hypercarb and C18 column also produced statistically significant data and a variety of markers that could be visualised, however, the lack of separation on the PCA plot using the Hypercarb suggests that a C18 column may be better suited for this particular analysis. The PCA plot produced following analysis on a C18 column showed each sample set grouped well together, with no overlapping between the time intervals. As a result, it was decided that a C18 column would be utilized for future experiments.

A second experiment focused on applying the techniques developed from the first experiment, into a large scale experiment in a more realistic setting. Although aspects of this second experiment were still heavily controlled, using whole carcasses in a larger body of water outside gave a better indication of the type of chemical profile expected, based on more interferences in natural conditions. The results from this experiment also concluded that using a 1 L sample concentrated with SPE was a very effective sample preparation technique to obtain the highest quality and quantity of data. The fact that

analysis of the 1 ml sample only offered five markers that showed significant differences over time, compared to 71 markers in 1 L samples highlights that low concentrations of compounds in the water make it very difficult to detect them. It concludes that pre-concentration of the sample is necessary to gain in-depth information about the chemical signature of water containing a decomposing carcass.

Overall, the method development carried out using these analytical techniques has been successful, and future work in this field will include looking at a variety of conditions such as moving and still water, differences between species, the monitoring of specific markers over time, and identifying these markers. The ability to do this could provide an opportunity to apply these methods into realistic circumstances.

3.5 References

[1] S. Parida, S. Dash, S. Patel, B. Mishra, Adsorption of organic molecules on silica surface, Advances in Colloid and Interface Science 121(1-3) (2006) 77-110.

[2] D.A. Wellings, A Preparative Handbook of HPLC, Elseiver, Oxford, UK, 2006.

[3] F. Gritti, G. Guiochon, The van deemter equation: Assumptions, limitations, and adjustments to modern high performance liquid chromatography, Journal of Chromatography A 1302 (2013) 1-13.

[4] V. Meyer, Practical High Performance Liquid Chromatography, 5th ed., Wiley, Sussex, 2010.

[5] Crawford Scientific, Van Deemter equation - The Lockdown guide. From HPLC Practice. <https://www.crawfordscientific.com/chromatography-blog/post/van-deemter-equation-the-lockdown-guide>, 2020 (accessed 17th Nov 2021.).

[6] D. Ibrahim, A. Ghanem, Sub 2-µm Silica Particles in Chiral Separation, New Uses of Micro and Nanomaterials (2018) 55-72.

[7] A. Jakimska, A. Kot-Wasik, J. Namiesnik, The Current State-Of-The-Art in the Determination of Pharmaceutical Residues in Environmental Matrices Using Hyphenated Techniques, Critical Reviews in Analytical Chemistry 44 (2014) 227-298.

[8] B. Boyes, M. Dong, Modern Trends and Best Practices in Mobile-Phase Selection in Reversed-Phase Chromatography, LCGC North America 36(10) (2018) 752-768.

[9] A.P. Schellinger, P.W. Carr, Isocratic and gradient elution chromatography: A comparison in terms of speed, retention reproducibility and quantitation, Journal of Chromatography A 1109 (2006) 253-266.

[10] J.L. Anderson, A. Berthod, V.P. Estevez, A. Stalcup, Chapter 2 Basic LC Method Development and Optimization, Analytical Separation Science, Wiley, West Sussex, UK, 2015.

[11] R. Scott, Principles and Practice of Chromatography, Reese-Scott Partnership, LLC, 2002.

[12] J. Dolan, A Guide to HPLC and LC-MS Buffer Selection, ACE HPLC Columns2011.

[13] C. Poole, New trends in solid-phase extraction, Trends in Analytical Chemistry 22(6) (2003) 362-373.

[14] M. Hennion, Solid-phase extraction: method development, sorbent, and coupling with liquid chromatography, Journal of Chromatography A 856 (1999) 3-54.

[15] A. Zwir-Ferenc, M. Biziuk, Solid Phase Extraction Technique - Trends, Opportunities and Applications, Polish Journal of Environmental Studies 15(5) (2006) 677-690.

[16] A. Mohammad-Khah, R. Ansari, Activated Charcoal : Preparation, Characterization and Applications : A review article, International Journal of ChemTech Research 1(4) (2009) 859-864.

[17] H. Marsh, F. Rodriguez-Reinoso, Activated Carbon, Elseiver Ltd, Oxford UK, 2006.

[18] J. Value, How useful is activated charcoal?, British Medical Journal 306 (1993) 78-79.

[19] B. Eftekhar, M. Skini, M. Shamohammadi, J. Ghaffaripour, F. Nilchian, The Effectiveness of Home Water Purification Systems on the Amount of Fluoride in Drinking Water, Journal of Dentistry 16(3) (2015) 278-281.

[20] S. Wang, T. Lin, C. W, Removal of tryptophan in drinking water using biological activated carbon filter, Water Supply 18(4) (2017) 1420-1427.

[21] T.P. Zellner, D, E. Faber, Hoffmann-Walbeck, D. Genser, F. Eyer, The Use of Activated Charcoal to Treat Intoxications, Dtsch Arztebl Int. 116(18) (2019) 311-317.

[22] A. Alkhatib, K. Zailaey, Medical and Environmental Applications of Activated Charcoal:Review Article, European Scientific Journal 11(3) (2015) 50-56.

[23] T. Sangster, H. Major, R. Plumb, A.J. Wilson, I.D. Wilson, A pragmatic and readily implemented quality control strategy for HPLC-MS and GC-MS-based metabonomic analysis, Analyst 131(10) (2006) 1075-1078.

[24] R. Tautenham, G. Patti, D. Rinehart, G. Siuzdak, XCMS Online: A Web-Based Platform to Process Untargeted Metabolomic Data, Analytical Chemistry 84 (2012) 5035-5039.

[25] G. Theodoridis, H. Gika, E. Want, I. Wilson, Liquid chromatography-mass spectrometry based global metabolite profiling: A review, Analytica Chimica Acta 711 (2012) 7-16.

[26] A. Vass, S. Barshick, G. Sega, J. Caton, J. Skeen, J. Love, J. Synstelien, Decomposition Chemistry of Human Remains: A New Methodology for Determining the Postmortem Interval, Journal of Forensic Sciences 47(3) (2002) 542-553.

[27] B. Dent, S. Forbes, Review of human decomposition processes in soil, Environmental Geology 45(4) (2004) 576-585.

[28] S. Paczkowski, S. Schutz, Post-mortem volatiles of vertebrate tissue, Applied Microbiology and Biotechnology 91(4) (2011) 917-935.

[29] S. Forbes, Decomposition Chemistry in a Burial Enviornment, Soil Analysis in Forensic Taphonomy, CRC Press, New York, 2008, pp. 203-223.

[30] Cambridge MedChem Consulting, Lead Optimization, Physiochem, Lipophilicity, Drug Discovery Resources (2019).

Chapter 4

The use of metabonomic profiling to differentiate between species decomposing in water during summer and winter.

The main focus of this experiment was to investigate whether it is possible to use metabonomic profiling methods to differentiate between species decomposing in the water, using a workflow that identifies the chemical signature of the water. The first aim was to determine if there were any markers that showed significant differences between species, and whether these markers could be monitored over time. The second aim was to explore how the temperature of the environment affected this outcome. Conducting the experiment in UK summer and winter temperatures gave an opportunity to see whether lower temperatures would affect the method's ability to detect species specific markers and monitor their behaviour over time. An attempt to identify these preliminary markers would provide helpful insight into the type of compounds that are causing the differences between species, and whether this could be applied in the future to more specific research into species differentiation.

4.1 Introduction

The ability to differentiate between species, specifically in meat products has dominated the research world in recent years. Fraudulent behaviour such as mislabelling and hidden substitutions has led to the demand of safe and reliable meat products [1]. The development of technology to differentiate between species began with enzyme-linked immunosorbent assay (ELISA) and polymerase chain reaction (PCR) techniques. ELISA is commonly used to measure antibodies, antigens, proteins and glycoproteins in a variety of biological samples. It is known to be the most commonly used immunoassay for biomarker detection [2]. PCR is used to amplify small segments of DNA quickly and accurately making it a highly sensitive method, though limited to the detection of DNA and RNA. In 1992, a technique called the immuno-PCR was developed, combining the power of PCR and versatility of ELISA [3]. In the early 2000's, a significant amount of research into species differentiation was conducted using ELISA [4, 5] and PCR [6-8].

A sudden influx of proteomics introduced the potential of using mass spectrometry for species differentiation by the separation of complex protein mixtures [9-11]. Following the recent food fraud scandals in 2013 where food products advertised as beef were found to contain undeclared horse meat, Montowska [12-14] introduced a proteomic method that could differentiate between species of meat in both raw and processed foods. Following this, an abundance of studies were carried out to identify unique markers that could be used as species specific markers [15-18].

In recent years, the ever-increasing interest in non-targeted metabonomic analyses has led to a spike in the use of these methods for species differentiation. Whilst food fraud is still a rapidly growing field, researchers have branched out to investigate species differentiation in other areas such as plants [19-21], bacteria [22], lipids [23] and fish [24,

25]. The most recent study by Man [26] in 2021 utilised non-targeted metabonomic analysis to identify the geographical location of beef samples due to growing concerns of fraud based on the provenance and production methods. The chemical profile of beef contained 24 metabolites that could differentiate between beef samples from different origins (USA, Australia, and Hong Kong), and 7 metabolites that could differentiate samples taken from organic farms as opposed to other farms in Australia. Their ability to do this reflects how successful metabonomic analyses are at creating chemical profiles that can be differentiated, even when the differences are incredibly small.

The use of targeted and non-targeted metabonomic analyses has also grown in popularity due to the rise in concern about the contamination of ground water and natural bodies of water. The majority of research into the contamination of our waters is focused on targeted methods; using routine analysis methods for monitoring and screening known compounds. These include pesticides, pharmaceuticals, microorganisms, organometallic species, arsenic, and tin [27-29]. Concerns lie in the pharmaceutical industry, where large quantities of antibiotics are suspected to be contaminating the water supply. Targeted LC-MS is routinely used to detect these known compounds, quantify and assess the level of risk [30-32]. This is also a concern in the farming industry, as the effects of using antibiotics in dairy and meat farming are being exposed [33, 34] .

While routine targeted analyses are still carried out, a new focus on non-targeted analysis is emerging due to the alarming rise in new contaminants not previously identified [35, 36]. Examples of these include hormones, perfluroinated compounds, flame retardants, plasticisers, personal care products, impurities from commercial formulations, surfactants, drugs of abuse and leachate from remains [37]. One relevant example for the work carried out in this chapter is the investigation on the effects of animal burial sites on

the groundwater quality. There are strict rules that need to be followed for the disposal of animals. The majority of animal producers believe that the easiest way for them to dispose of their animals is on-farm burial to limit the costs [38]. This work began as targeted analysis in the 1990's primarily on poultry, looking at compounds that may contaminate the ground water such as ammonia, nitrate, chlorate, and faecal pathogens [39-41]. Recently, the development of technology and increased knowledge of the decomposition process has allowed more detailed investigations into the effects of carcass leachates on the groundwater quality [42-45].

In 2016, Lim [46] used GC-MS to investigate the possibility of using fatty acid profiles of decomposing carcasses to identify any contamination in the surrounding groundwater. Arachidonic acid was named as a potential marker for the contamination of groundwater from decomposing carcasses. Similarly, in 2013 Choi [47] used LC-MS to investigate the behaviour of a selection of amino acids between livestock wastewater and carcass leachates. They discovered that the average amino acid concentration in carcass leachates was 300 times higher than in livestock wastewater. The combination of both studies strongly suggests the potential of using leachates from a decomposing carcass to provide a chemical signature of decomposition.

The literature discussed highlights the need for further research into the analysis of non-volatile compounds associated with decomposition. This work aims to investigate whether a preliminary metabonomic approach can yield biomarkers that differentiate between species decomposing in water, and if they can be monitored over time.

4.2 Methods and materials

4.2.1 Experimental method

4.2.1.1 Materials

Methanol (HPLC grade), formic acid, activated charcoal, C18 Hypersil Gold column and a reference mass solution consisting of purine (*m/z* 121.0509) and hexakis (1*H*, 1*H*, 3*H*-tetrafluropropoxy)phosphazine (*m/z* 922.0098) were purchased from Fisher Scientific (Loughborough UK) and ultra-pure water (18.2 MΩ) was purified using a Purelab Option-Q system by Veolia Water (Saint Maurice, France). 60 L heavy duty storage boxes were purchased from Key Manutan Group Industrial Commercial Equipment (Dorset, UK). Intact rabbit carcasses were purchased from Livefood UK Ltd (Somerset UK), and intact duck carcasses purchased from Glasfryn (Wales, UK).

4.2.1.2. Experimental setup

A total of three rabbit and three duck carcasses were placed in separate 60 L boxes along with three control boxes. Two holes were drilled into the lids of each box to allow airflow and insect activity. Each box was filled with 40 L of water from a single source and placed outside. Temperature probes were used to monitor the temperature of the water and the air every 15 minutes.

Experiment 1 ran for eight weeks from July to September, while Experiment 2 ran for eight weeks from January to March. Each week, a total of 9 samples were taken: 3 control water samples, 3 samples from the boxes containing rabbit remains and 3 samples from the boxes containing duck remains. In this particular experiment, only samples from week

0[1], 3 and 7 were analysed to limit analysis time in order to minimise the risk of instrumental drift. As the aim of the experiment was to investigate whether it is possible to detect chemical changes over time in the water, a sample from the beginning, middle and end of the experiment was sufficient to achieve proof of concept. In total 54 samples (3 treatments at 3 time intervals with 3 replicates each in summer and winter conditions) were analysed.

4.2.1.3 Sample collection and preparation

At weeks 0[1], 3 and 7, 1 L of water was removed from each box into a Duran bottle, and filtered through an SPE cartridge with an activated charcoal phase on the same day. 1 ml of methanol was used to elute the sample, followed by the addition of 1 ml of ultrapure water to create a 50:50 MeOH:H_2O solution. All samples were placed in an Eppendorf tube and centrifuged for 10 minutes at 16100 rcf to remove any particulates, then stored in a freezer at -25^{o}C prior to analysis.

4.2.1.4 Solid phase extraction (SPE)

Solid phase extraction was carried out exactly as described in **Chapter 3, Section 3.2.2.3**.

[1]*The sample labelled at week 0 was taken two days into the experiment. This sample will be referred to as 'Week 0' for the duration of the experiment.*

4.2.2 Instrumental setup

4.2.2.1 Quality control

This work was carried out exactly as described in **Chapter 3, Section 3.2.3.1**.

4.2.2.2 Chromatographic parameters

This work was carried out exactly as described in **Chapter 3, Section 3.3.5.2.**

4.2.2.3 Mass spectrometry parameters

This work was carried out exactly as described in **Chapter 3, Section 3.2.3.3**.

4.2.3 Data pre-processing

This work was carried out exactly as described in **Chapter 3, Section 3.2.4.**

4.2.4 Data analysis and statistical analysis

This work was carried out exactly as described in **Chapter 3, Section 3.2.5.**

The data analysis workflow for this experiment is shown in Figure 4.1.

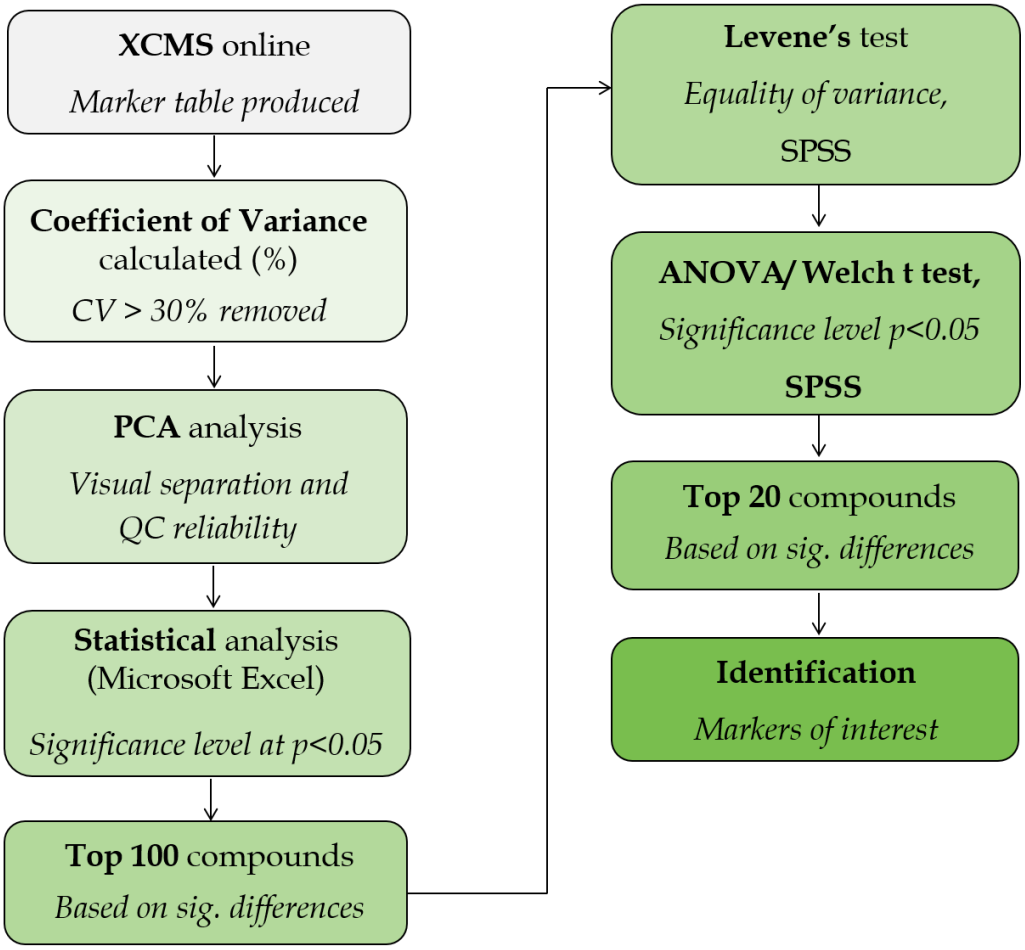

Figure 4.1: Diagram showing the data analysis workflow used in this non-targeted analysis.

4.2.5 Identification of markers

Agilent Technologies' Masshunter Qualitative Analysis software was used for identification of features. It produced a predicted molecular formula for each compound based on the monoisotopic mass, abundances and peak spacing within the mass spectra. It also produced a probability score for each compound, based on how close the isotope abundance ratios in the sample mass spectrum match those expected from the predicted formula given [48]. The compounds that were assigned a predicted formula were searched on METLIN. The mass spectra of the sample and the mass spectra of the suspected compound available on the METLIN database were compared. A full identification was confirmed using a chemical standard analysed in MS/MS mode along with the original sample. The targeted analysis was set to the *m/z* of the chemical standard along with the retention time of the tentatively identified marker. A mass range of *m/z* 100-1000 was used. The chromatogram produced would only show if that particular ion was present at the specified retention time. A collision energy of 10 V, 20 V and 40 V was used. The MS spectra for the sample and the standard were compared to confirm the identity of the marker.

4.3 Results and discussion

4.3.1 Temperature

An important focus of this experiment was to investigate the effects of temperature on a decomposing carcass in water, and its influence on the chemical signature of the water. The temperature was monitored continuously during the summer and winter experiments. Figure 4.2 shows the average temperature fluctuation including the highest and lowest temperature each week. This graph represents the typical trends expected for this climate, specifically the significant drop in temperature during the winter months. It is important to note that fluctuation between the highest and lowest temperatures each week is high during the summer experiment. This suggests that there are more erratic changes in temperatures during the summer months.

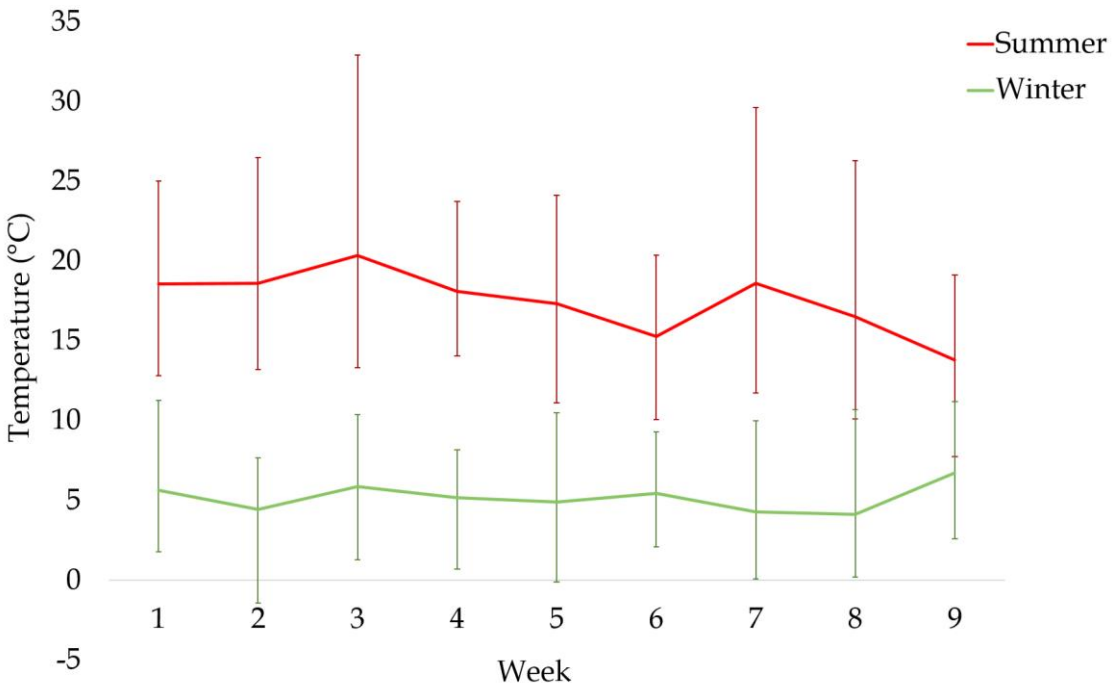

Figure 4.2: Graph showing the average change in temperature over a 9-week period during the summer and winter experiments. The bars represent the highest and lowest temperature each week.

4.3.2 Differences in the metabolite profiles of two species decomposing in water during the summer months.

4.3.2.1 The physical changes visible during the decomposition of two species in water during the summer months.

It was important to record observations of the physical changes as a result of decomposition during the experiment, allowing a comparison to the chemical changes that influence the water chemistry. Identifying a specific group of compounds leaching into the water at certain 'stages' of decomposition could lead to valuable insight on the use of non-volatile compounds leaching into the water to differentiate between species. Figure 4.3 presents the images of both rabbit and duck carcasses following 0 days of decomposition in water.

Figure 4.3: Images of 3 rabbit and 3 duck carcasses in water following 0 days of decomposition in summer conditions.

Each carcass had floated to the surface of the water on the first day of submersion. No insect activity or other visual signs of decomposition were showing. Insect activity began on day 2, quickly increasing each day. There seemed to be more insects surrounding the rabbit boxes. On the sixth day, all rabbits showed bloating on the abdomen along with slight skin slippage. The water had turned a pale yellow colour, and insect activity was prevalent in every box.

A week after submersion (Figure 4.4), eggs laid by the flies were hatching and colonising all three rabbit carcasses and two of the ducks. The water began to turn a brown-yellow colour, with a strong odour when standing above them.

Figure 4.4: Images of 3 rabbit and 3 duck carcasses in water following 1 week of decomposition in summer conditions.

On the ninth day of the experiment (Figure 4.5), maggots had colonised all decomposing carrion. Insect activity was rapidly increasing, resulting in a layer of foam surrounding the maggots on day 9. The rabbit carcass' internal organs were now visible.

(A) **(B)**

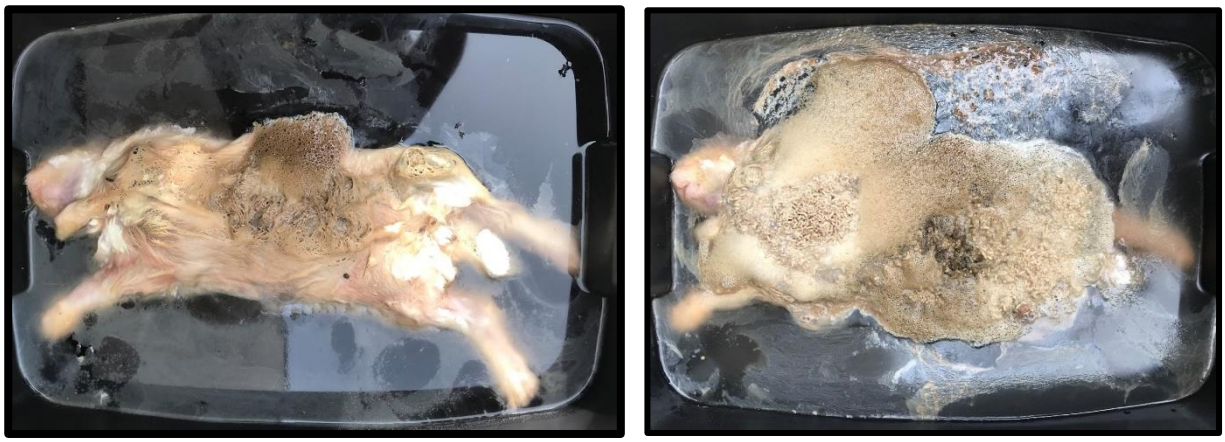

Figure 4.5: Images showing the foam increasing around the maggots on a rabbit sample in box 7 on day 8 (A) and day 9 (B) in summer conditions.

Figure 4.6 shows the images following exactly two weeks of decomposition in water. Insect activity had ceased, resulting in a large number of deceased maggots floating in the water. Some skeletisation was visible on both duck and rabbit carcasses. The water was still a brown-yellow colour, and a strong odour was present even when standing 5 m away from the boxes.

Figure 4.6: Images of 3 rabbit and 3 duck carcasses in water following 2 weeks of decomposition in summer conditions.

Following 3 weeks of decomposition in water, Figure 4.7 shows that the rabbit carcasses were beginning to sink to the bottom of the box, while the duck carcasses were still exposed at the surface. A thin coating of film formed on the surface of the water from boxes containing rabbit.

Figure 4.7: Images of 3 rabbit and 3 duck carcasses in water following 3 weeks of decomposition in summer conditions.

After 4 weeks of decomposing in water, Figure 4.8 shows the rabbit carcasses had sunk to the bottom of the box. Two of the duck carcasses were beginning to sink, while the third had already sunk. By day 30, all carcasses had sunk to the bottom of the box, with a thick film coating the surface of the water. The water stayed a yellow-brown colour accompanied by a pungent smell until the experiment came to an end. There were no further visible changes observed.

Figure 4.8: Images of 3 rabbit and duck carcasses in water following 4 weeks of decomposition in summer conditions.

4.3.2.2 QC analysis

The chromatograms in Figure 4.9 show QC samples 1-11. QC samples 1-5 show a slightly higher baseline while conditioning the column, however the QC samples remain stable throughout the rest of the analysis. QC7 is labelled green on the chromatogram due to an anomaly between 23-30 minutes. Minor variation in retention time is also seen after the first 20 minutes of the analysis.

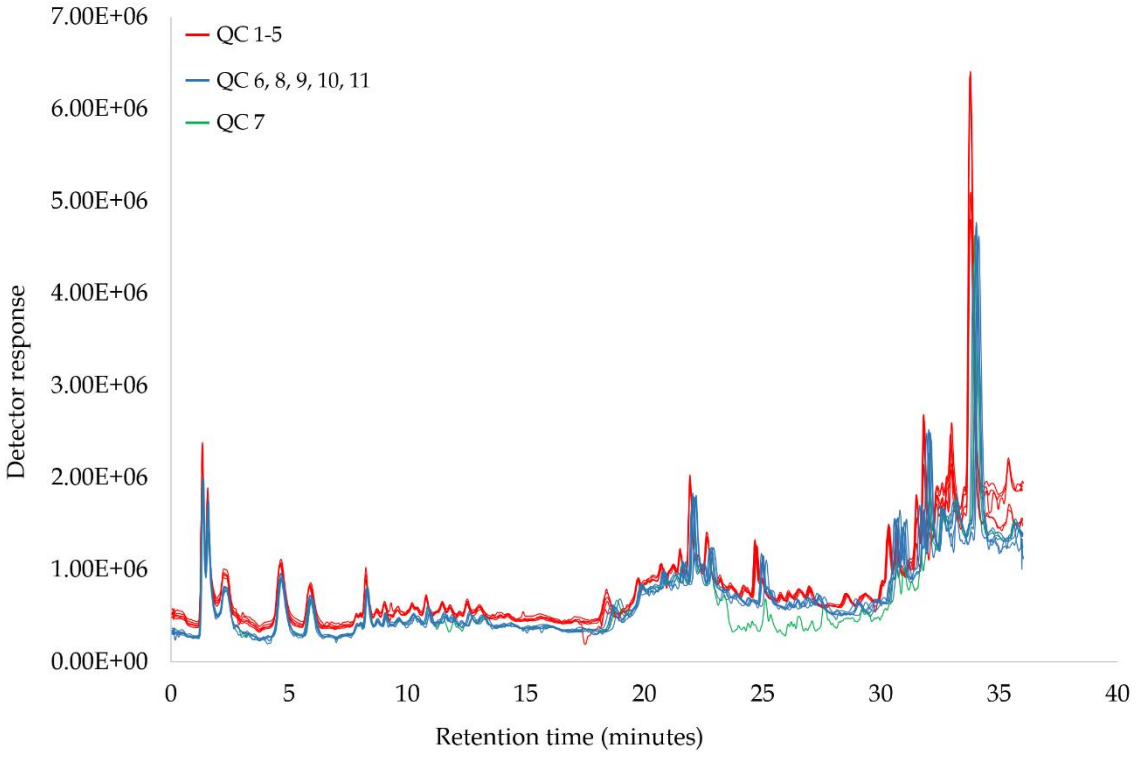

Figure 4.9: Total ion chromatograms of 11 QC samples throughout the analytical run for water samples taken from both summer and winter experiments.

Due to the slight variability identified within the QC samples, Table 4.1 looks specifically at the amount of variance in the peak area and retention times, and whether they fall within the accepted limit for non-targeted analysis.

Table 4.1: Variability of peak area (A) and retention time (B) from 6 selected peaks in the QC samples during the analytical sequence for water samples taken from both summer and winter experiments.

A

Peak	QC6	QC7	QC8	QC9	QC10	QC11	Average	St. Dev	CV%
1	1684541	1733832	1631403	1729683	1684400	1515419	**1663213**	**81442**	**5%**
2	765057	781369	816440	797901	770374	808649	**789965**	**20934**	**3%**
3	878434	883690	946243	932841	859162	888245	**898102**	**33860**	**4%**
4	773223	667216	678458	701772	695611	665089	**696895**	**40209**	**6%**
5	845158	740013	744681	756347	747735	647630	**746927**	**62692**	**8%**
6	522765	560720	606723	563685	598781	447764	**550073**	**58469**	**11%**

B

RT	QC6	QC7	QC8	QC9	QC10	QC11	Average	St. Dev	CV%
1	1.32	1.33	1.32	1.31	1.33	1.33	**1.32**	**0.0062**	**0.47%**
2	2.33	2.32	2.31	2.32	2.32	2.32	**2.32**	**0.0055**	**0.24%**
3	4.65	4.64	4.63	4.65	4.65	4.64	**4.64**	**0.0055**	**0.12%**
4	5.92	5.93	5.92	5.91	5.93	5.92	**5.92**	**0.0062**	**0.10%**
5	8.26	8.27	8.26	8.25	8.27	8.26	**8.26**	**0.0059**	**0.07%**
6	18.75	18.76	18.75	18.74	18.76	18.76	**18.75**	**0.0062**	**0.03%**

Table 4.1 presents the coefficient of variance (CV) value for six peaks selected from the chromatograms. The highest CV value for the peak area is 11%, and 0.47% for the retention time. These values are well under the accepted value for variance in non-targeted analyses, which is 30%. This confirms that this analytical sequence has provided reliable and robust data for further analysis.

4.3.3.3 Metabolic profiling

The chromatograms in Figure 4.10 look at the chemical changes happening in water containing decomposing rabbit at week 0, 3 and 7 of the experiment. A dramatic change in the metabolic profile of the water over time gives an initial insight into the numerous chemical processes happening here. The peak intensities and overall number of peaks are very low in samples taken after 0 weeks of decomposition in water, however, this was expected in the very early stages of decomposition. At week 3, the chromatogram shows an increase in the number of peaks, those specifically with higher peak intensities between 30–40 minutes. This was also the case for samples taken at week 7, with an increase in peak intensities throughout and additional peaks appearing for the first time between 10-15 minutes.

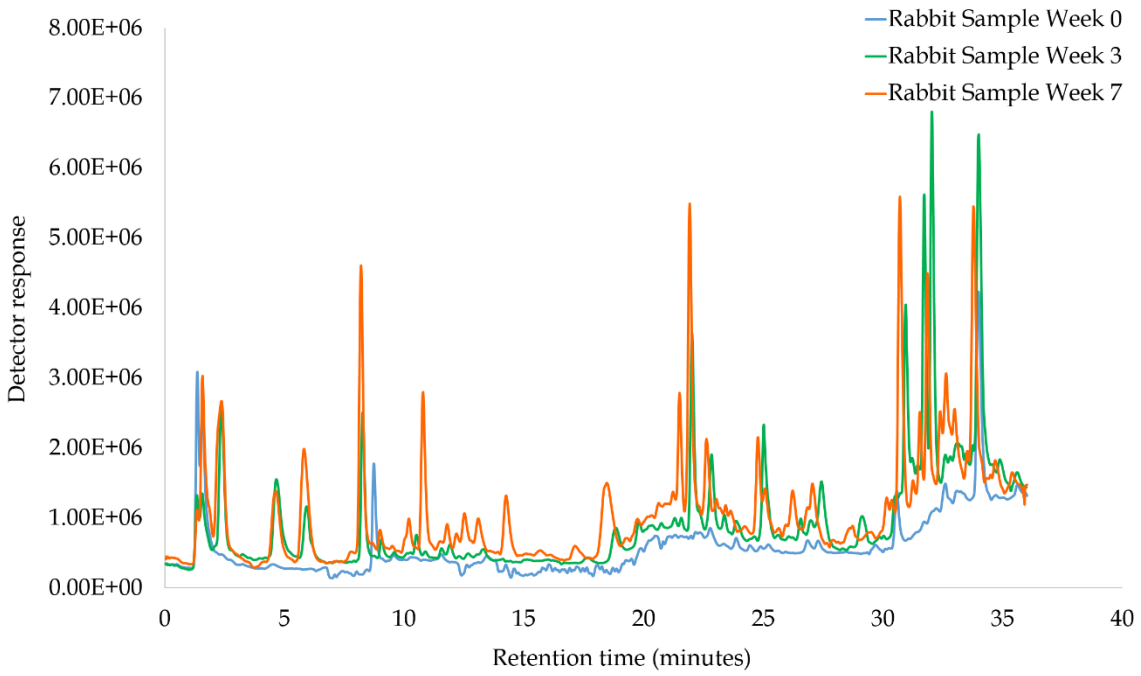

Figure 4.10: Example total ion chromatogram (TIC) of water samples containing a decomposing rabbit carcass at week 0, 3 and 7 of the summer experiment.

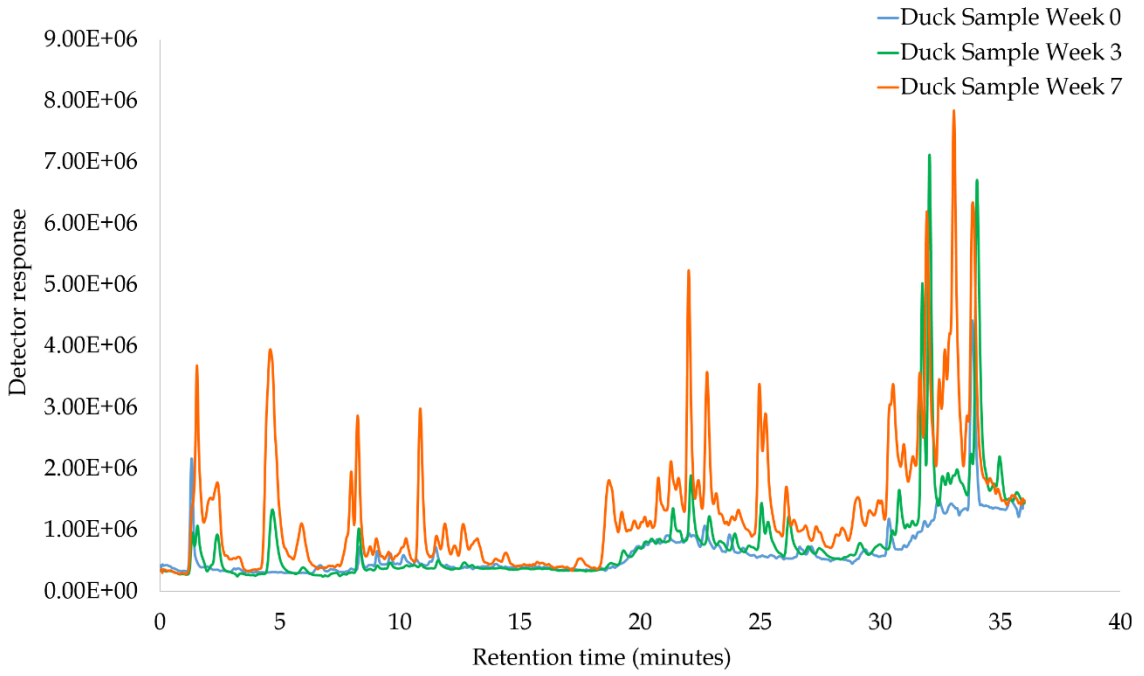

Figure 4.11: Example total ion chromatogram (TIC) of water samples containing a decomposing duck carcass at week 0, 3 and 7 of the summer experiment.

Figure 4.11 presents the chromatograms of water samples taken at week 0,3 and 7 from boxes containing duck. The chromatograms show a very small number of peaks at week 0, followed by a dramatic increase in the number of peaks and their intensities after 3 weeks and furthermore after 7 weeks of decomposition. This pattern is similar to what was found in the boxes containing rabbit.

The chromatograms for both rabbit and duck carcasses decomposing in water over time show very similar peak patterns, suggesting that a similar class of compounds are produced and leaching into the water. However, there are also individual characteristics to each species that indicate the potential of being able to differentiate between mammals and birds.

4.3.3.4 Multivariate analysis

The PCA scores plot in Figure 4.12 shows the separation between water samples from boxes containing rabbit at week 0, 3 and 7, accompanied by a control sample. The QC samples are tightly clustered in the centre of the plot, indicating minimal instrumental effects. The control samples and samples at week 0 are clustered together and overlapping, suggesting similarities in their chemical profiles. The samples from weeks 3 and 7 are separated well across the plot. The distance between each of the three time points is further apart than the spread of the QC samples, highlighting that these differences are likely to be genuine, and not from any instrumental influences.

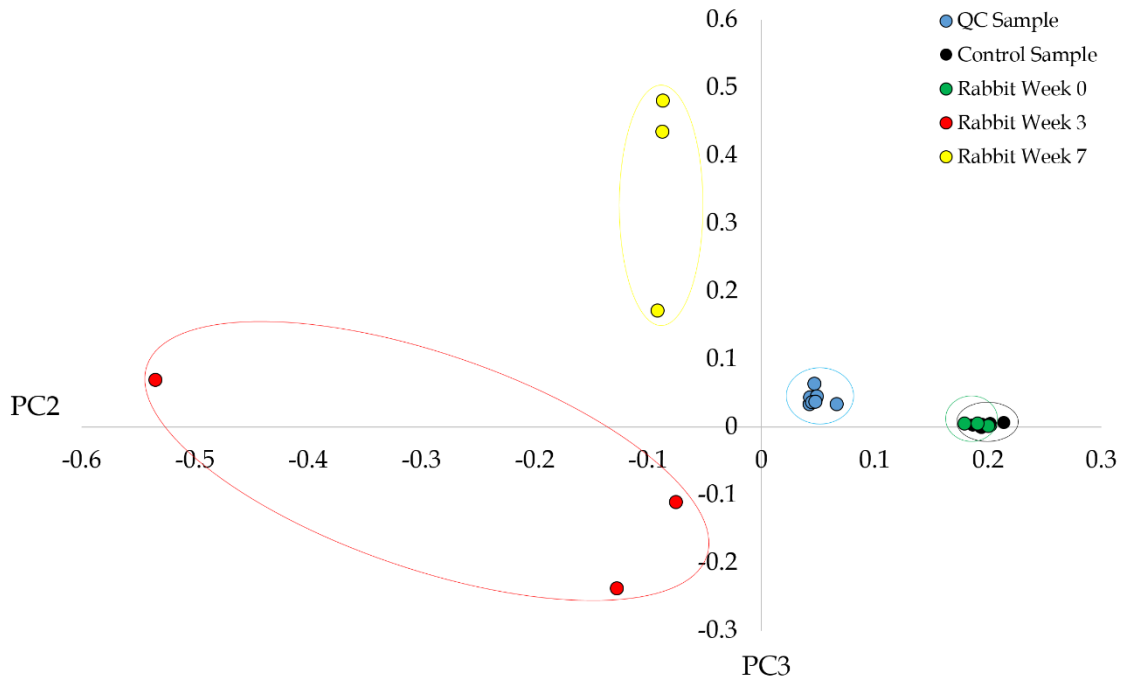

Figure 4.12: PCA scores plot of PC2 (19.92%) and PC3 (7.90%) for water samples containing a decomposing rabbit carcass at week 0, 3 and 7 of the summer experiment.

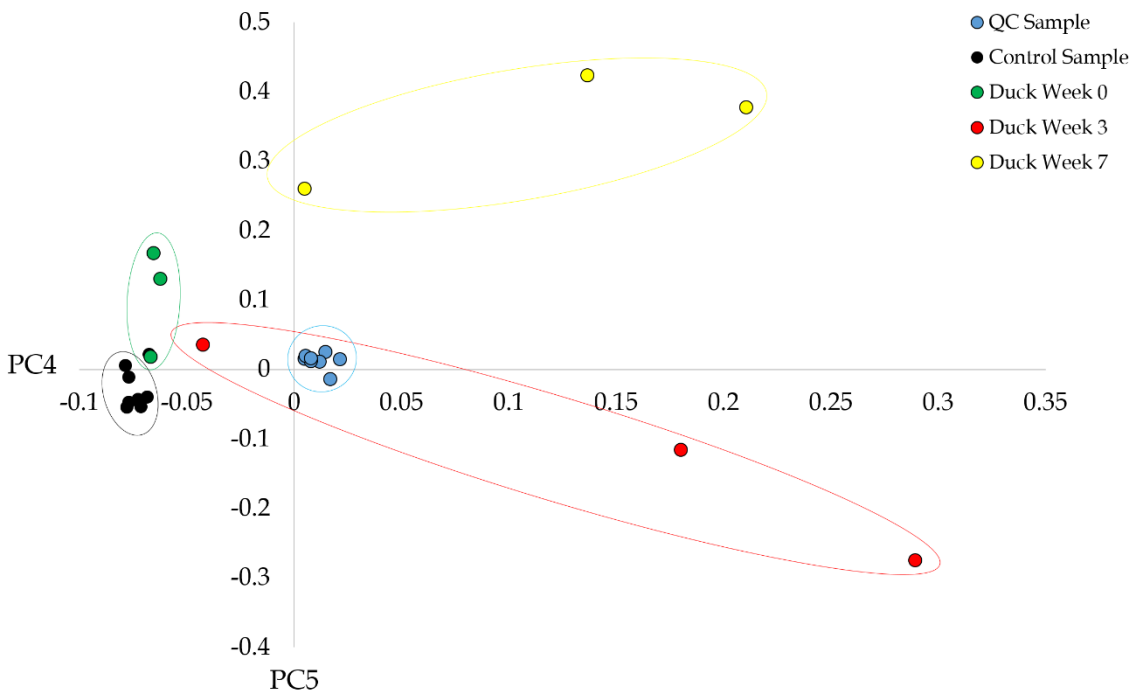

Figure 4.13: PCA scores plot of PC4 (4.28%) and PC5 (2.11%) for water samples containing a decomposing duck carcass at week 0, 3 and 7 of the summer experiment.

The PCA scores plot in Figure 4.13 represents water samples taken from boxes containing duck. The QC samples are clustered toward the middle of the plot, and the control samples are also clustered with only a small overlap into samples from week 0. The samples from each time point can be grouped together, with good separation between them on the plot. Although the samples from week 0 and 3 are not as well separated as those in the rabbit sample, there is good separation between weeks 3 and 7, where the distance between them is further than the spread of the QC samples. Statistical analysis was conducted to look at which compounds were causing these separations on the plot.

4.3.3.5 Statistical analysis

The total number of features detected in the water samples through *XCMS online* was 5491. All features with a CV value of 30% or more were removed, with 3975 remaining. Statistical analysis was performed on water samples from boxes with both rabbit and duck carcasses. 94 compounds were found showing significant differences over time in the water from rabbit boxes, and 105 from duck boxes. Of these markers, 9 of them were present in samples from both species. A summary of these markers is shown below in Table 4.2. Each marker in the table has been assigned a predicted formula and a score that reflects the confidence of that assignment, with high scores showing for the majority of the markers. Table 4.3 investigates where these significant differences lie between each time interval, which will show if the patterns between species are varied, or similar.

Table 4.2: Summary of the 9 markers that show significant differences over time of water samples taken from both rabbit and duck decomposition during the summer.

m/z	Retention time (minutes)	CV value	Formula	Score
171.1324	32.03	22%	$C_7H_{10}N_2O_3$	92.55
208.1185	22.89	11%	$C_{12}H_{12}NO_2$	99.21
241.2115	32.00	17%	$C_{13}H_8N_2O_3$	86.32
262.0122	10.50	17%	$C_{18}H_{15}NO$	75.28
302.2709	32.01	10%	$C_{15}H_{31}NO_3$	96.9
317.2805	31.71	12%	$C_{18}H_{37}NO_3$	99.72
339.2210	32.01	3%	$C_{17}H_{14}N_4O_2S$	90.93
462.1851	33.38	13%	$C_{20}H_{15}NO_{10}S$	47.04
523.1518	33.38	8%	$C_{29}H_2N_2OS_4$	47.61

Table 4.3: Table showing where the significant differences lie between time intervals, in the 9 markers identified in both rabbit and duck water samples.

m/z	Rabbit sample between Week 0 and 3	Rabbit sample between Week 3 and 7	Duck sample between Week 0 and 3	Duck sample between Week 3 and 7
171.1324		p<0.05	p<0.05	p<0.05
208.1185	p<0.05	p<0.05		
241.2115		p<0.05		
262.0122	p<0.05	p<0.05		
302.2709			p<0.05	
317.2805			p<0.05	
339.2210	p<0.05	p<0.05		
462.1851	p<0.05	p<0.05		p<0.05
523.1518	p<0.05	p<0.05	p<0.05	

The table above shows us that the majority of the significant differences lie in the water samples between 3-7 weeks of rabbit decomposing in water, while only few were significantly different in boxes containing duck. This reflects the results obtained in multivariate analysis, where samples from boxes containing duck were less separated on the PCA plot than rabbit. Additionally, the observations carried out on the physical characteristics of decomposition emphasise that there are more drastic changes happening to the colour of the water, the smell surrounding the area and an increase in insect activity in the boxes containing rabbit, compared to those containing ducks.

The fact that only 9 markers were found showing significant differences over time in samples from both species highlights the complexity if the metabolic processes happening during decomposition. Investigating each time point in detail could reveal which compounds show differences between species, and their relevance to the decomposition process.

4.3.3.6 Metabolic profiling of week 0

Figure 4.14 shows the chromatograms of water samples taken from boxes containing both rabbit and duck, following 0 weeks of decomposition in water. It is important to note that these particular samples were taken on day 2. The number of peaks overall in both samples are limited, however this was expected due to the samples being taken in the early stages of decomposition. Whilst the majority of the chromatograms look similar, peak patterns between 5-15 minutes are different. Various peaks are present in the water sample from duck, whilst only one peak of higher intensity appears from rabbit.

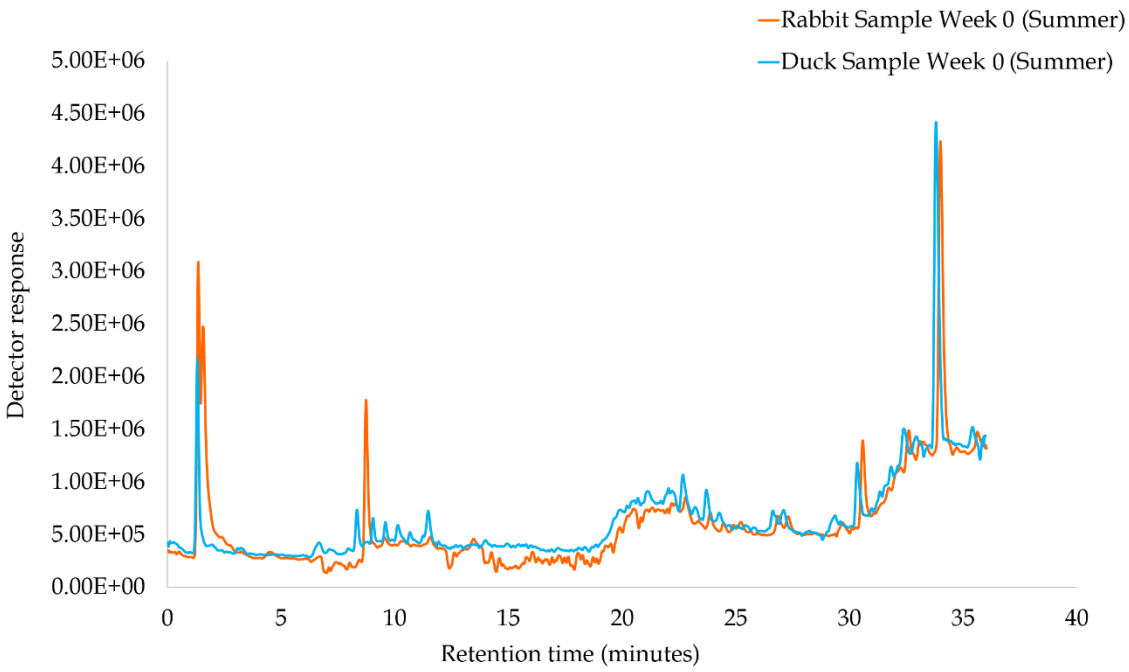

Figure 4.14: Example total ion chromatograms (TIC) of water samples taken after 0 weeks of decomposition in water during the summer.

4.3.3.7 Multivariate analysis of week 0

The PCA scores plot in Figure 4.15 reflects the results obtained from the previous chromatograms at week 0. Water samples from the control box, and those from rabbit and duck boxes are clustered together on the plot. It is still possible to group the samples into each sample group, however, decomposition has not influenced the water chemistry enough to show major separation between species.

For example, during the fresh stage of decomposition the carcass is likely to be intact, with limited insect activity and any chemical decomposition will be happening inside. There are very limited visual differences between species at this stage, it is often important to dig deeper into the data to investigate the full effects of these complex processes.

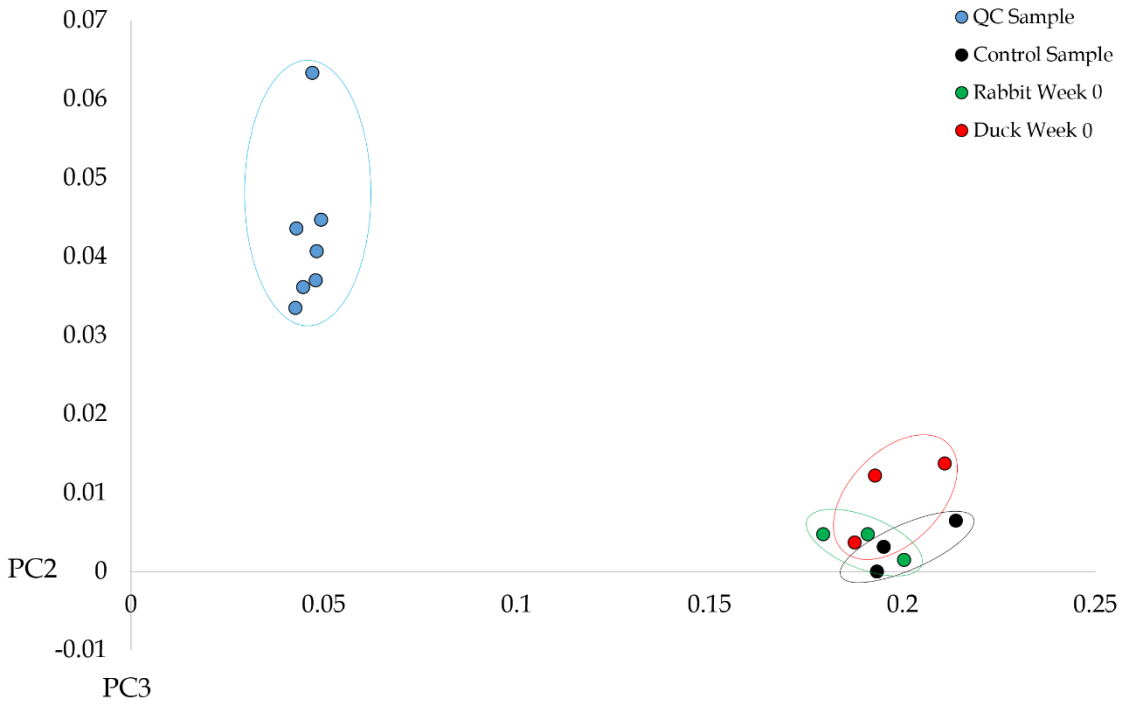

Figure 4.15: PCA scores plot of PC2 (6.60%) and PC3 (2.71%) for water samples taken after 0 weeks of decomposition in water during the summer.

4.3.3.8 Statistical analysis of week 0

Statistical analysis was performed to investigate any significant differences between species following 0 weeks of decomposition. 144 markers were significantly different with a p-value of below 0.05, while 31 markers were significantly different with a p-value of below 0.01. Of these markers, 58% of them had a *m/z* under 400, while 42% had a *m/z* over 400. This shows that the balance between the smaller and larger compounds are reasonably equal at this time point. Table 4.4 presents the top 20 markers that were significantly different between species and shown to be the most robust and reliable.

Table 4.4: Summary of the top 20 compounds that show significant differences between species after 0 weeks of decomposition in water.

m/z	Retention time (minutes)	CV%	p-value XCMS	p-value ANOVA/Welch
106.0487	1.51	10%	p<0.001	p<0.001
115.0340	1.57	28%	p<0.001	0.001
120.0650	1.53	21%	p<0.001	0.003
123.0965	5.87	25%	p<0.001	0.006
246.0210	18.6	15%	p<0.001	0.006
265.1509	7.91	17%	p<0.001	0.002
266.0719	1.59	29%	p<0.001	p<0.001
269.0766	2.82	28%	p<0.001	0.002
325.2588	32.01	6%	p<0.001	0.006
355.2769	32.57	16%	p<0.001	0.004
382.8367	1.43	14%	p<0.001	0.001
540.8950	32.32	14%	p<0.001	0.001
561.2277	32.81	16%	p<0.001	0.003
568.1852	33.66	26%	p<0.001	p<0.001
612.8770	35.86	9%	p<0.001	0.002
616.1733	23.35	12%	p<0.001	0.005
712.3747	33.01	13%	p<0.001	0.009
784.0555	33.8	9%	p<0.001	0.007
850.2475	35.36	26%	p<0.001	0.004
876.6579	35.42	6%	p<0.001	0.002

The average *m/z* of the top 20 compounds showing significant differences is 434.55, which was to be expected as the larger compounds may not have broken down yet. Figure 4.16 presents six markers chosen due to the substantial differences in peak area between each species. The majority of the markers are dominant in the rabbit samples with much higher peak areas than those appearing in the duck samples. It was unexpected to discover such a large number of compounds revealing differences between species at such an early stage of the experiment.

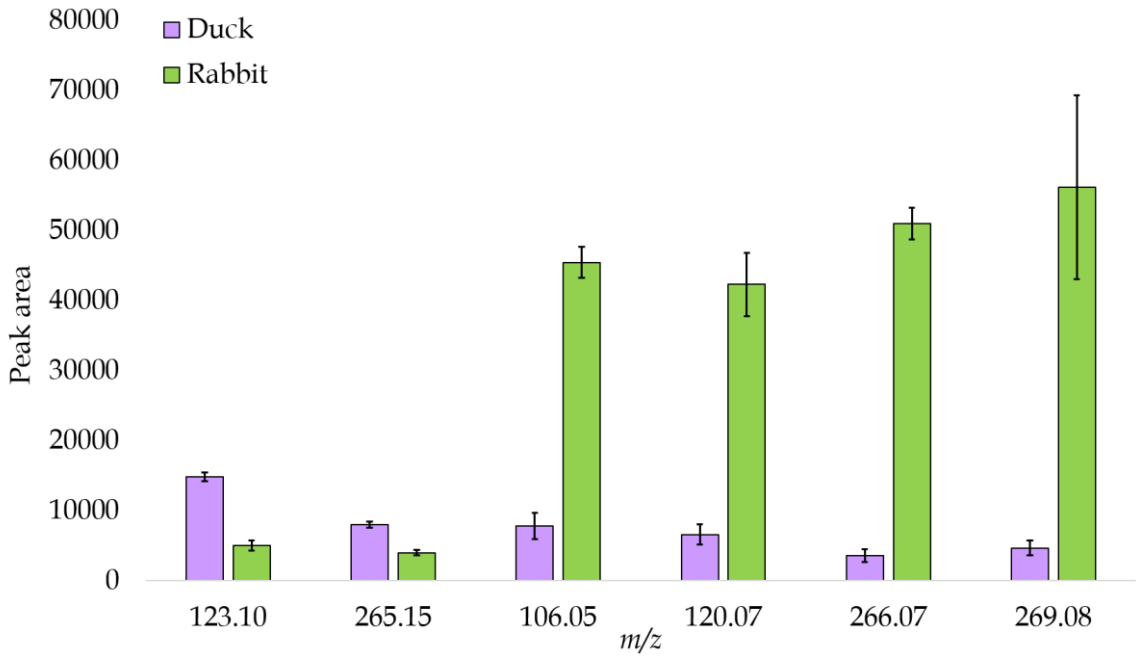

Figure 4.16: Graph showing the peak area of six markers identified as significantly different between species after 0 weeks of decomposition. The error bars represent ±1 standard deviation.

4.3.3.9 Metabolic profiling of week 3

Figure 4.17 shows the chromatograms of water samples taken from boxes containing rabbit and duck at week 3 of the experiment. The chromatograms show an increase in the number of peaks and their intensities compared to week 0. Overall, both chromatograms show some similarities and differences in their peak patterns. The chromatogram produced from the rabbit sample has higher peak intensities (with the exception between 33 to 37 minutes), and additional peaks that are not present in the duck sample chromatogram between 7-22 minutes.

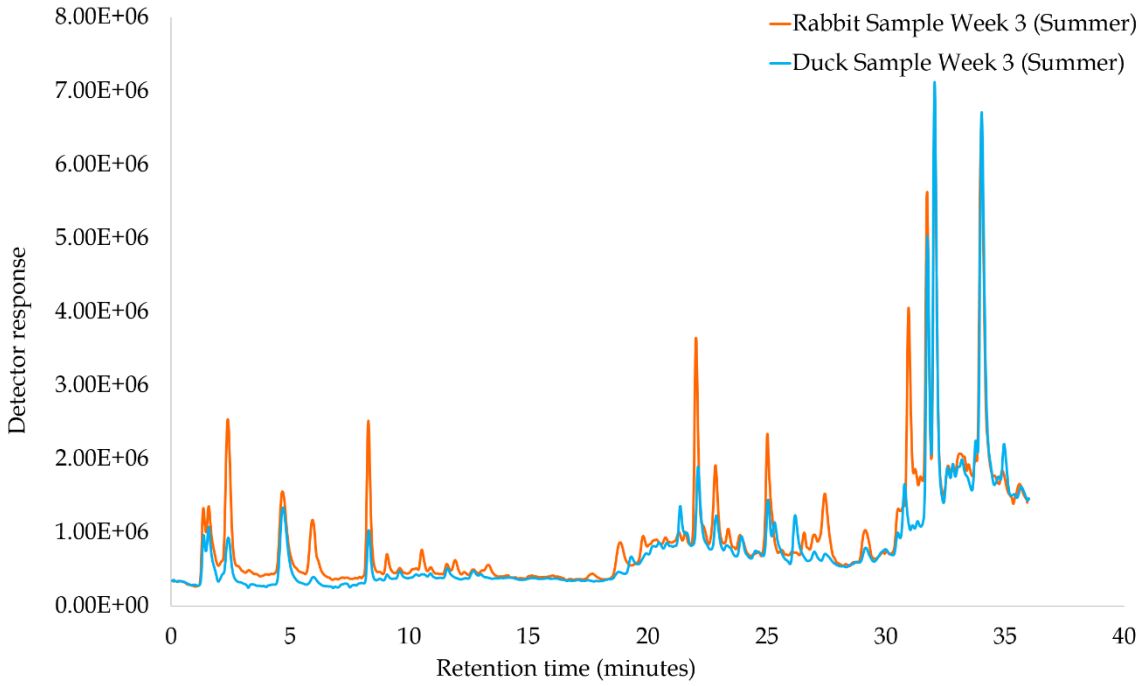

Figure 4.17: Example total ion chromatograms (TIC) of water samples taken after 3 weeks of decomposition in water during the summer.

4.3.3.10 Multivariate analysis of week 3

The PCA scores plot in Figure 4.18 shows the separation between the control sample, water from a rabbit box, and from a duck box at week 3. The QC samples are clustered in the middle of the plot, and the control samples are clustered tightly together to the right. Separation between species after 3 weeks of decomposition in water has improved from week 0. The sample groups are clearly separated and have moved away from the control samples. Although the distance between each sample group is not further than the spread of the QC's, there is now visible separation between species. It is also important to note that there is some spread within the sample groups, highlighting that there is even variation between carcasses exposed to the same conditions. The separation between the control samples and the rabbit boxes is further than the spread of the QC samples, suggesting that the chemical profile of the water is noticeably different between them.

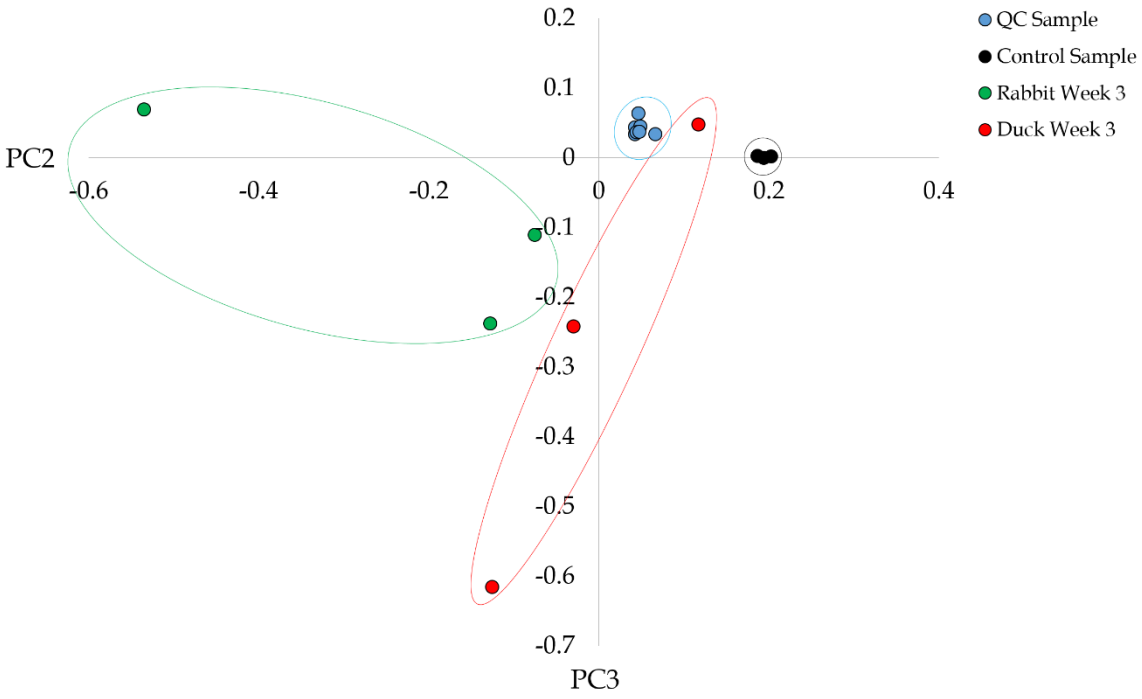

Figure 4.18: PCA scores plot of PC2 (16.53%) and PC3 (8.93%) for water samples taken after 3 weeks of decomposition in water during the summer.

4.3.3.11 Statistical analysis of week 3

334 markers were significantly different with a p-value of below 0.05, while 129 markers were significantly different with a p-value of below 0.01. Of these markers, 57% had a *m/z* under 400, while 43% had a *m/z* over 400. These results show that there are around three times more significant markers detected following three weeks of decomposition, compared to 0 weeks, however a relatively equal distribution of *m/z*. Table 4.5 presents the top 20 markers that show significant differences between species following three weeks of decomposition in water.

Table 4.5: Summary of the top 20 compounds that show significant differences between species after 3 weeks of decomposition in water.

m/z	Retention time (minutes)	CV%	p-value XCMS	p-value ANOVA/Welch
103.0524	1.23	15%	p<0.001	0.045
147.0753	27.32	28%	p<0.001	p<0.001
164.0685	8.41	20%	p<0.001	0.001
173.1493	27.31	12%	p<0.001	p<0.001
195.1308	27.3	18%	p<0.001	0.001
201.1793	31.4	17%	p<0.001	0.001
208.2694	22.08	19%	p<0.001	0.001
211.0963	27.27	18%	p<0.001	0.001
215.1984	31.45	13%	p<0.001	0.001
224.1679	31.45	15%	p<0.001	p<0.001
234.9991	1.33	13%	p<0.001	p<0.001
236.6364	30.93	29%	p<0.001	0.001
257.1025	27.31	22%	p<0.001	0.001
278.1961	27.29	17%	p<0.001	0.001
292.2224	20.54	21%	p<0.001	0.001
297.1989	30.39	5%	p<0.001	0.001
359.1005	22.1	26%	p<0.001	p<0.001
383.2401	27.3	28%	p<0.001	0.001
424.2704	27.3	25%	p<0.001	p<0.001
440.2419	27.29	17%	p<0.001	p<0.001

It is important to note the the *p-values* for the markers found at week 3 are much smaller overall than those calculated at week 0. Therefore even though signficant differences were found at the very beginning of the experiment, they are now showing more significance after three weeks. The average *m/z* here is 266.39. This suggest that there was a decline in the average size of the compounds leaching out from the decomposing carcass.

Figure 4.19 presents six markers chosen due to the substantial differences in peak area between each species. Similar to week 0, the peak areas of markers dominating the rabbit sample are remarkably higher than those appearing in the duck sample.

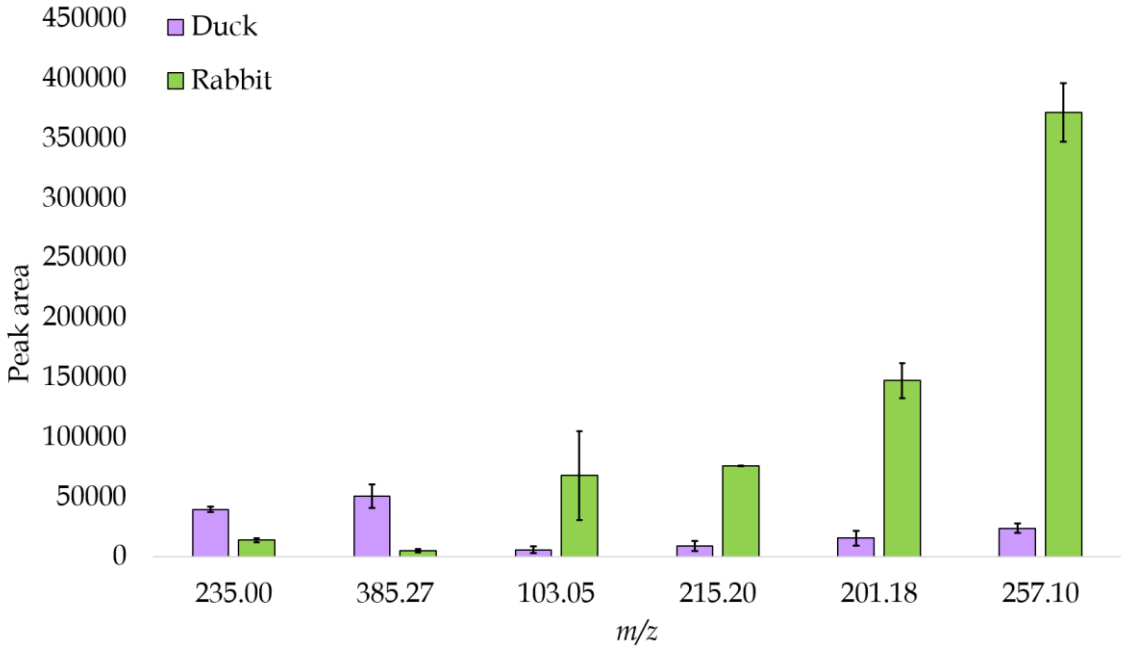

Figure 4.19: Graph showing the peak area of six markers identified as significantly different between species after 3 weeks of decomposition. The error bars represent ±1 standard deviation.

4.3.3.12 Metabolic profiling of week 7

Figure 4.20 presents the overlaid chromatograms of water samples taken after seven weeks of decomposition of both rabbit and duck in water. These chromatograms show an increase in peak intensities once again, noticeably between 5-15 minutes, reflecting the heightened detection of smaller compounds as a result of the breakdown of larger compounds. Both species now show a variety of peak patterns throughout the chromatogram, including peaks which were not present at previous time points. Some of these peaks have higher peak intensities in the rabbit sample, and others in the duck sample. This not only highlights the increase in the abundance of compounds in the water but also the continuous change of the chemical signature of the water, unique to each species.

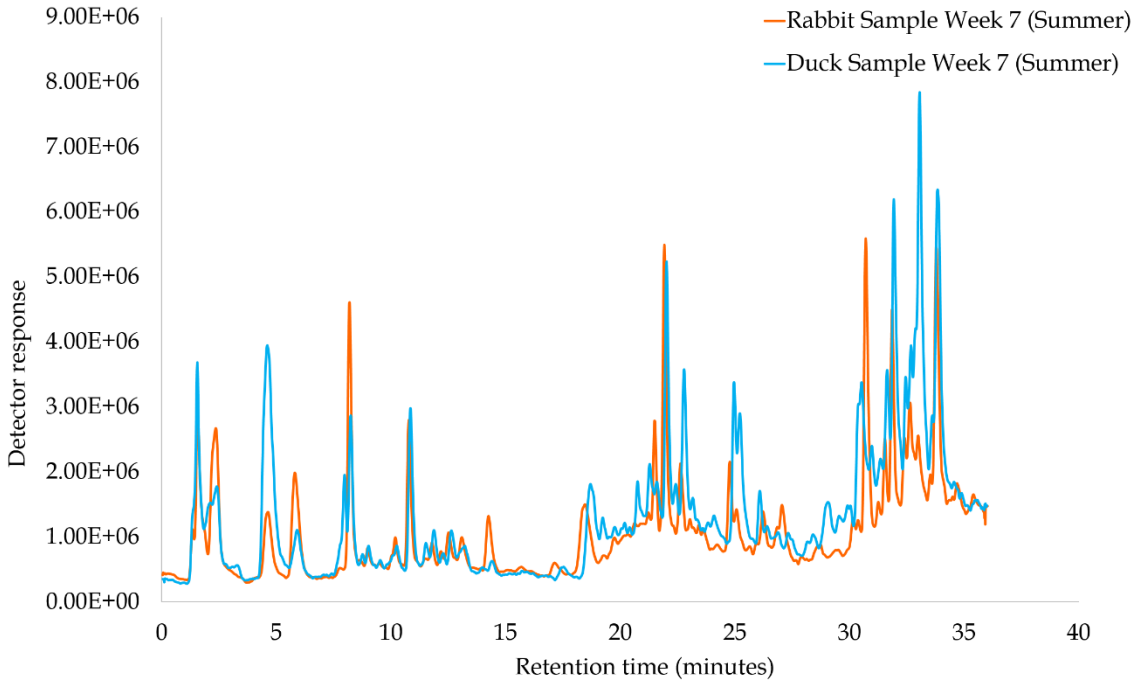

Figure 4.20: Example total ion chromatograms (TIC) of water samples taken after 7 weeks of decomposition in water during the summer.

4.3.3.13 Multivariate analysis of week 7

Figure 4.21 shows the PCA scores plot that includes the control sample, water from boxes containing rabbit and those containing duck after 7 weeks of decomposition. The QC samples are clustered together on the plot. There is very good separation between species, with both species also clearly separated from the control samples. The separation is further than the spread of the QC samples, demonstrating that the results are not caused by instrumental effects, but the chemical signature of the water.

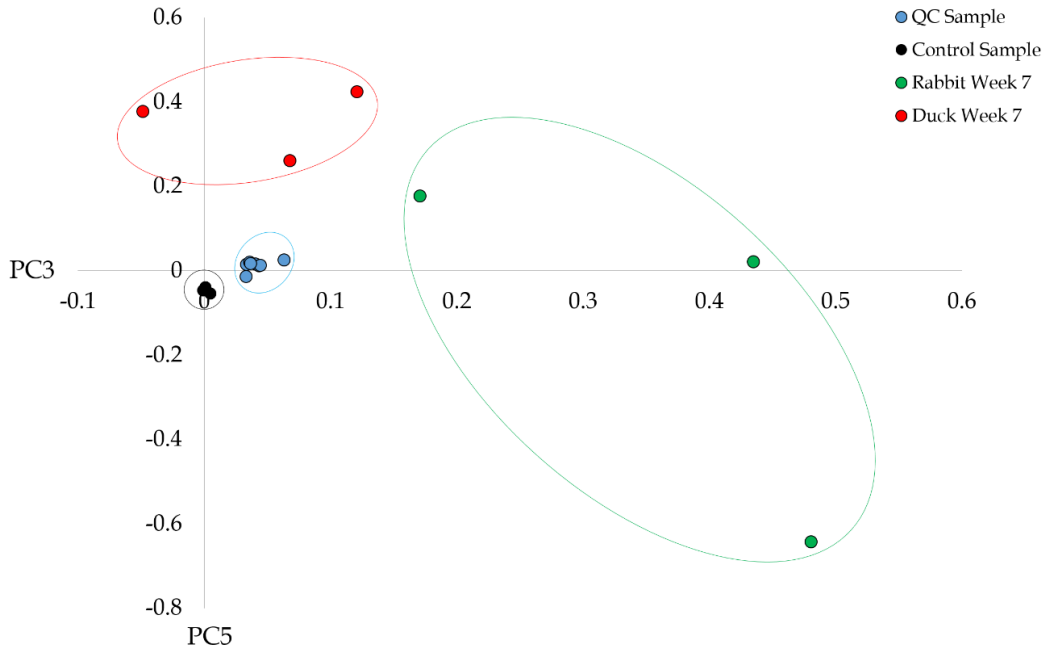

Figure 4.21: PCA scores plot of PC3 (7.79%) and PC5 (3.29%) for water samples taken after 7 weeks of decomposition in water during the summer.

It is important to note that although there is separation between species, there is also variation within each sample group. The spread of the three replicates for both rabbit and duck are significant when comparing to the control samples that are clustered together. When looking at the images in Figure 4.8, it is clear that there are noticeable physical

differences between the three replicate carcasses in each condition. While there are clear differences between the metabolic profiles of the two species, there is also natural variation within species exposed to the same conditions. This shows that even small physical differences can create substantial chemical differences. This is reflected in the majority of the PCA scores plots produced using data from the summer experiment. When comparing the results from the analysis to the observations conducted throughout, it is important to note that there is also variation in the physical changes during decomposition within the three replicates for both species. This strongly suggests that it is possible to link physical attributed of decomposition to patterns emerging from chemical analysis.

However, the unmistakeable differences between species highlights the success of the method's ability to find differences in the chemical signature of the water. Further statistical analysis was carried out to identify the specific markers responsible for the separation.

4.3.3.14 Statistical analysis of week 7

720 markers were significantly different with a p-value of below 0.05, while 202 markers were significantly different with a p-value of below 0.01. Of these markers, 37% had a *m/z* under 400, while 63% had a *m/z* over 400. An important factor when looking at these significant markers is that there are no similarities between the top 20 markers from each time point, however, the markers identified in week 0 and 7 seem to include compounds with larger *m/z* in comparison to week 3. Table 4.6 presents the top 20 markers that show significant differences between species following seven weeks of decomposition in water.

Table 4.6: Summary of the top 20 compounds that show significant differences between species after 7 weeks of decomposition in water.

m/z	Retention time (minutes)	CV%	p-value XCMS	p-value ANOVA/Welch
103.0524	1.23	15%	p<0.001	0.017
125.9735	9.05	18%	p<0.001	0.001
214.0890	20.84	14%	p<0.001	p<0.001
309.1285	8.55	15%	p<0.001	p<0.001
333.1010	19.2	13%	p<0.001	0.001
356.1120	21.38	16%	p<0.001	0.001
379.2772	34.36	10%	p<0.001	0.001
447.2153	30.92	18%	p<0.001	0.001
477.2472	30.92	18%	p<0.001	0.001
490.2409	30.94	19%	p<0.001	0.001
495.2373	8.36	15%	p<0.001	0.001
522.5943	34.2	7%	p<0.001	p<0.001
528.2404	32.05	20%	p<0.001	0.001
537.3115	35.66	14%	p<0.001	0.001
567.1390	33.75	7%	p<0.001	0.001
625.2251	32.17	17%	p<0.001	0.001
749.0862	32.74	18%	p<0.001	p<0.001
753.1572	32.06	8%	p<0.001	0.001
852.5365	30.94	11%	p<0.001	p<0.001
885.0587	32.74	12%	p<0.001	p<0.001

The average *m/z* in the top 20 compounds showing significant differences between species following 7 weeks of decomposition in water was 469.25. This shows that the average size of these markers was increasing. The *p-values* are still showing strong significant differences between species, especially in comparison to those presented at week 0. This implies that the longer the carcasses are left to decompose in water, the more pronounced the differences between their chemical profiles become.

This result is reflected in Figure 4.22, where the difference in peak areas between species is clear. At previous time points, the peak areas for a marker more prominent in duck boxes is relatively small in comparison to those found in rabbit boxes, however, we can see a slight increase in these peak areas at week 7. This could be as a result of the hydrophobic coating on the duck's feathers, protecting the inner tissue and preventing any leaching from the carcass, which over time becomes less effective.

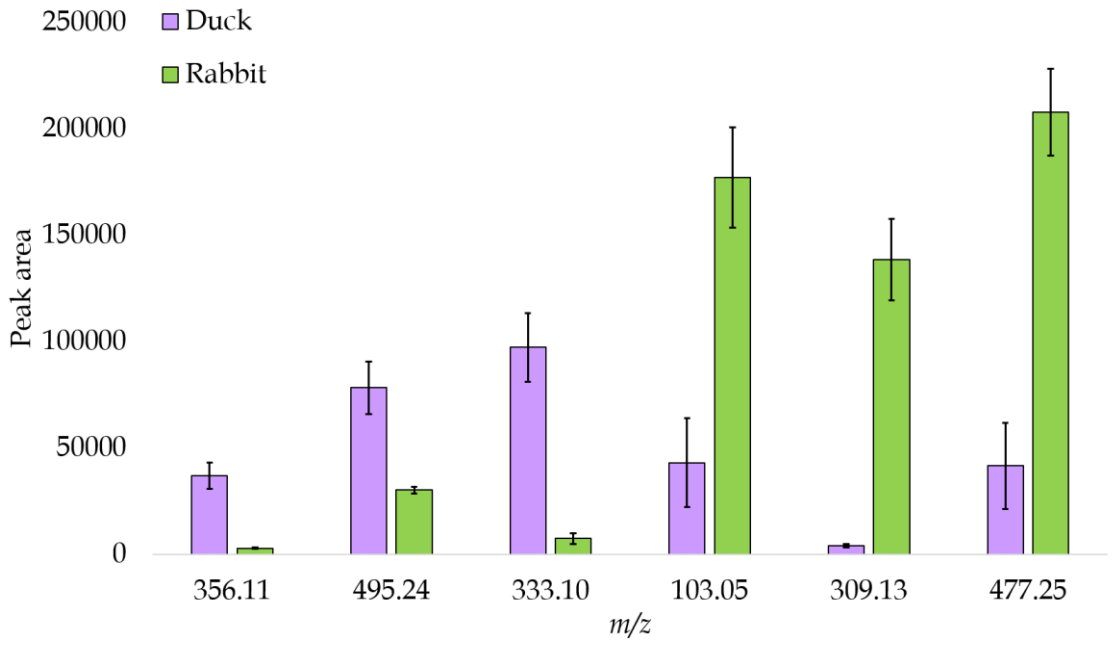

Figure 4.22: Graph showing the peak area of six markers identified as significantly different between species after 7 weeks of decomposition. The error bars represent ±1 standard deviation.

4.3.3.15 Identification of markers

A compound with the *m/z* 103.0524 was assigned a mass of interest following statistical analysis. This ion has shown significant differences between species after three and seven weeks of decomposition. Table 4.7 shows the tentative identification of this marker as cadaverine using *METLIN*. The peak areas in the bar chart of Figure 4.23 suggest that there is a higher prevalence of this marker in the boxes containing rabbit, however there is also an increase in the peak area of this marker in the box containing duck at the seventh week of decomposition. The control sample shows no change throughout the analysis.

Table 4.7: Summary of the marker m/z 103.0524, tentatively identified as cadaverine.

m/z	Adduct	Retention time (minutes)	CV value	Predicted formula	Tentative identification	Probability score
103.0524	(M+H)	1.238	15%	$C_5H_{14}N_2$	Cadaverine	82.02

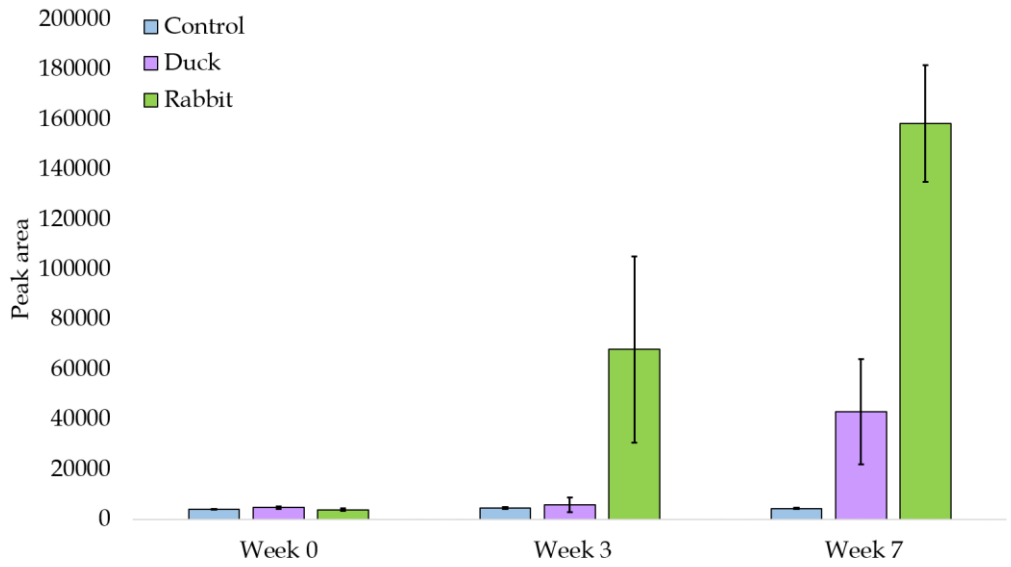

Figure 4.23: Bar chart showing the change in abundance over time of m/z 103.0524 tentatively identified as cadaverine during the summer months. The error bars represent ±1 standard deviation.

To confirm the identification of cadaverine, a cadaverine standard was analysed alongside a sample from the three time points from the boxes containing rabbit. Figure 4.24 shows the mass spectra for the cadaverine standard and a sample from week 3 and 7 at a collision energy of 20 V. The fragmentation patterns are similar between all samples.

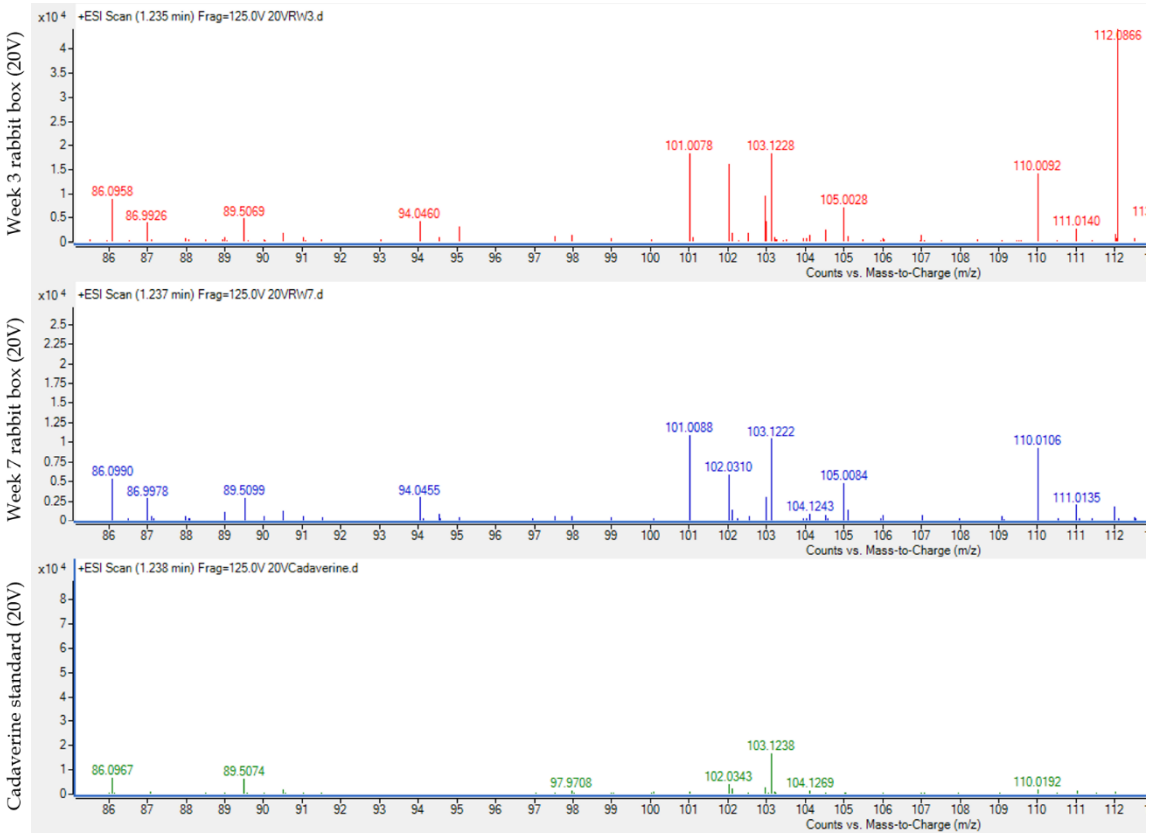

Figure 4.24: A comparison of mass spectra at 20 V collision energy between a cadaverine standard and a sample from a box containing rabbit at weeks 3 and 7.

Figure 4.25 shows the mass spectra for the cadaverine standard and a sample from week 3 and 7 at a collision energy of 40 V. The fragment peaks from the samples at a collision energy of 40 V also match those from the cadaverine standard, confirming that the compound *m/z* 103.0524 can be identified as cadaverine.

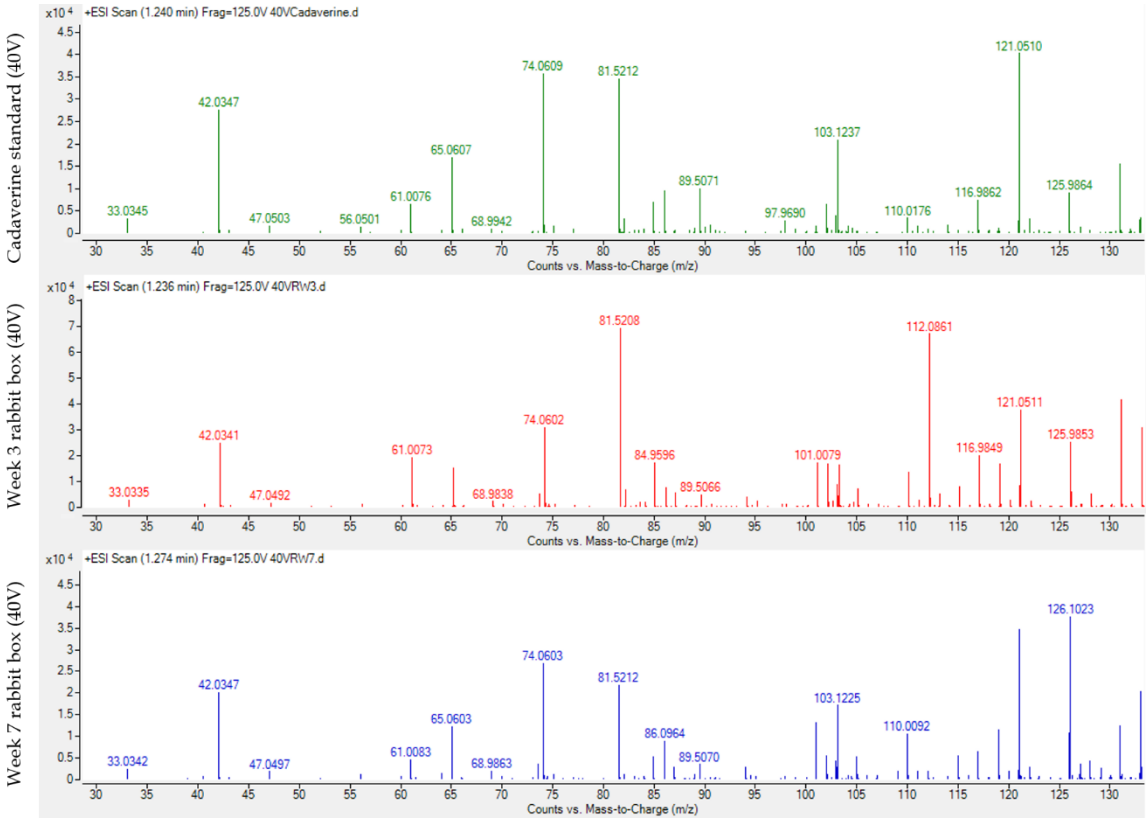

Figure 4.25: A comparison of mass spectra at 40 V collision energy between a cadaverine standard and a sample from a box containing rabbit at weeks 3 and 7.

A compound with the *m/z* 114.0636 was also identified as a mass of interest. Although it does not appear in the top 20 compounds showing significant differences between species, it dominated the sample at week 0 with a strong peak at around 1.4 minutes on the chromatogram. Table 4.8 shows the tentative identification of this compound.

Figure 4.26 shows that even at the very early stages of decomposition, this compound was discovered predominately in the box containing rabbit, with the peak area dramatically decreasing by the third week of decomposition. In contrast, samples taken from the box containing duck only seem to show a very small increase in peak area after three weeks of decomposition.

Table 4.8: Summary of the marker m/z 114.0636, tentatively identified as creatinine.

m/z	Adduct	Retention time (minutes)	CV value	Predicted formula	Tentative identification	Probability score
114.0636	(M+H)	1.43	7%	$C_4H_7N_3O$	Creatinine	93.48

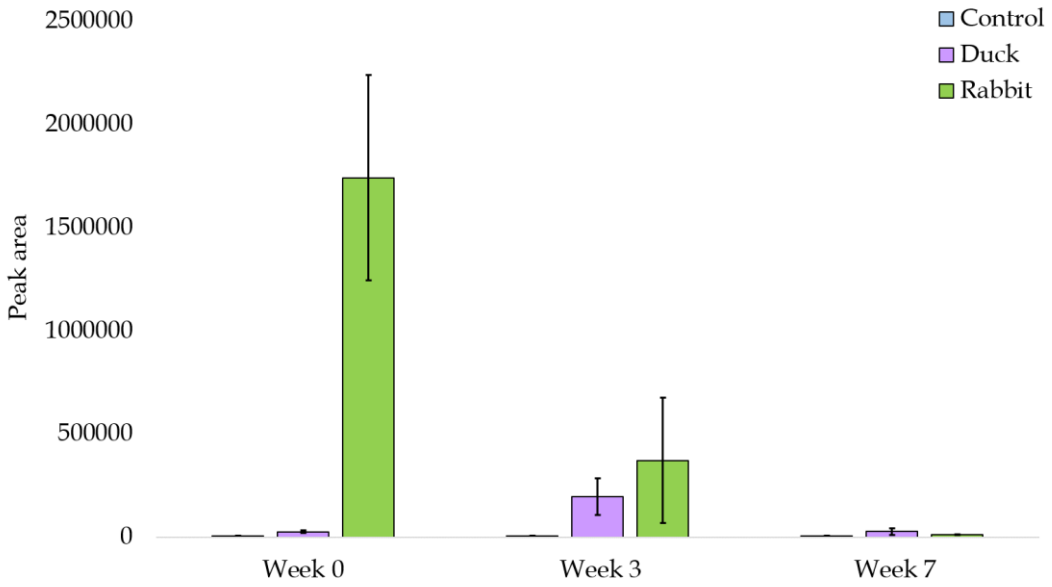

Figure 4.26: Bar chart showing the change in abundance over time of m/z 114.0636 tentatively identified as creatinine during the summer months. The error bars represent ±1 standard deviation.

To confirm the identification of creatinine, a creatinine standard was analysed alongside a sample from all three time points from the boxes containing rabbit. Figure 4.27 shows the mass spectra for the creatinine standard and a sample from week 0 and 3 at a collision energy of 20 V. The mass spectra for each sample and the creatinine standard show a high number of matching fragment peaks.

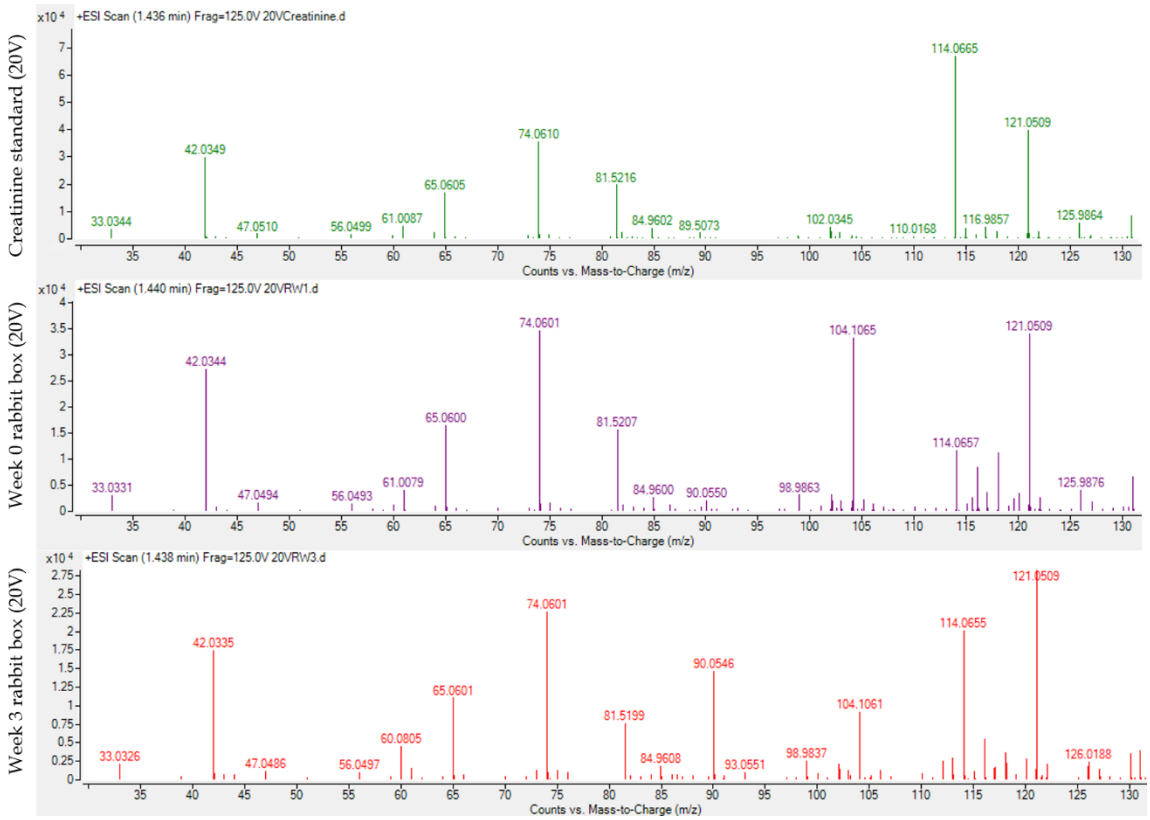

Figure 4.27: A comparison of mass spectra at 20 V collision energy between a creatinine standard and a sample from a box containing rabbit at weeks 0 and 3.

Figure 4.28 shows the mass spectra for the creatinine standard and a sample from week 0 and 3 at a collision energy of 40 V. The fragmentation patterns of the standard and each sample match at a collision energy of 40 V. As a result, it can be confirmed that the compound *m/z* 114.0636 is creatinine.

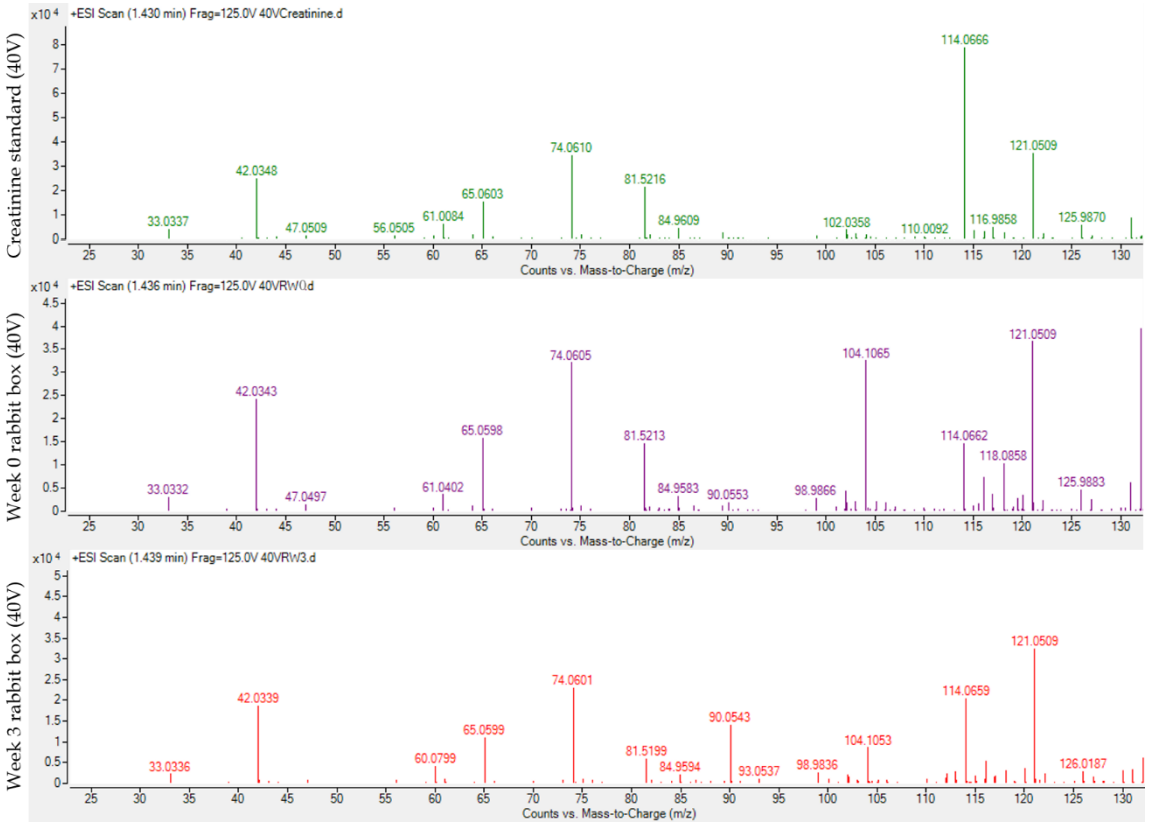

Figure 4.28: A comparison of mass spectra at 40 V collision energy between a creatinine standard and a sample from a box containing rabbit at weeks 0 and 3.

A third compound with the *m/z* 132.1012 was tentatively identified as leucine. This compound was present in both rabbit and duck samples at all three time points (Figure 4.29). Table 4.9 shows the tentative identification of leucine. Amino acids are known as the building blocks of proteins, which themselves make up around 75% of the body, therefore this compound is ubiquitous in nature. Consequently, amino acids such as leucine would not be used as species specific markers. An abundance of amino acids is produced during decomposition, therefore being able to identify the patterns of specific amino acids appearing in water over time could give insight into whether certain amino acids are present at specific time points during decomposition in future studies.

Table 4.9: Summary of the marker m/z 132.1012, tentatively identified as leucine.

m/z	Adduct	Retention time (minutes)	CV value	Predicted formula	Tentative identification	Probability score
132.1012	(M+H)	2.585	29%	$C_6H_{13}NO_2$	Leucine	98.75

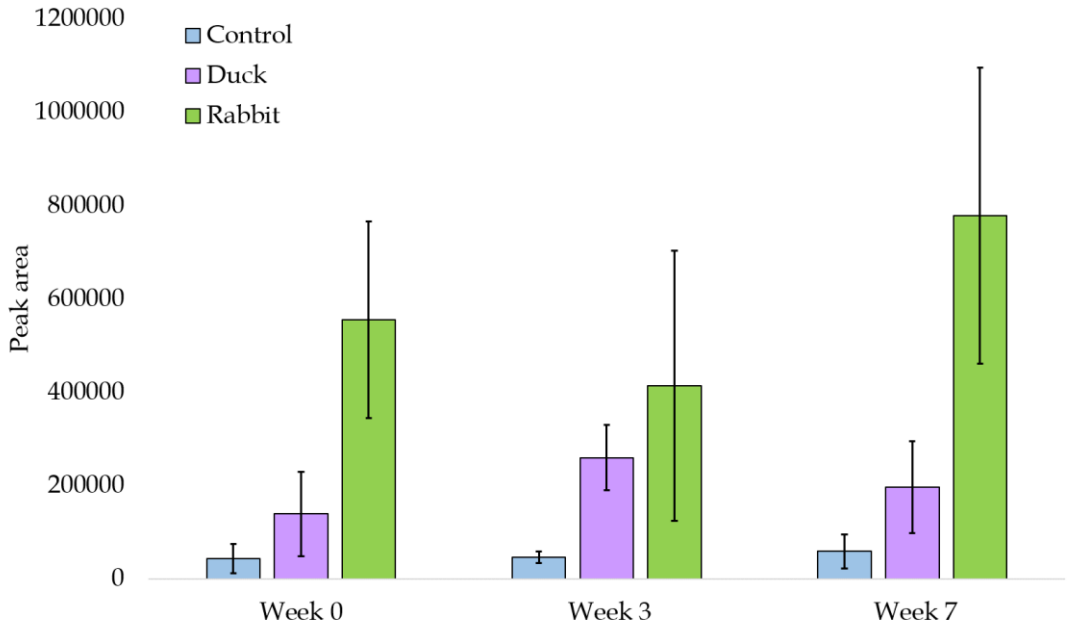

Figure 4.29: Bar chart showing the change in abundance over time of m/z 132.1012 tentatively identified as leucine during the summer months. The error bars represent ±1 standard deviation.

To confirm the identification of leucine, a leucine standard was analysed alongside a sample all three time points from the boxes containing rabbit. Figure 4.30 shows the mass spectra for the leucine standard and a sample from all three time points at a collision energy of 20 V. Each sample shows an excellent match to the fragmentation pattern of the leucine standard.

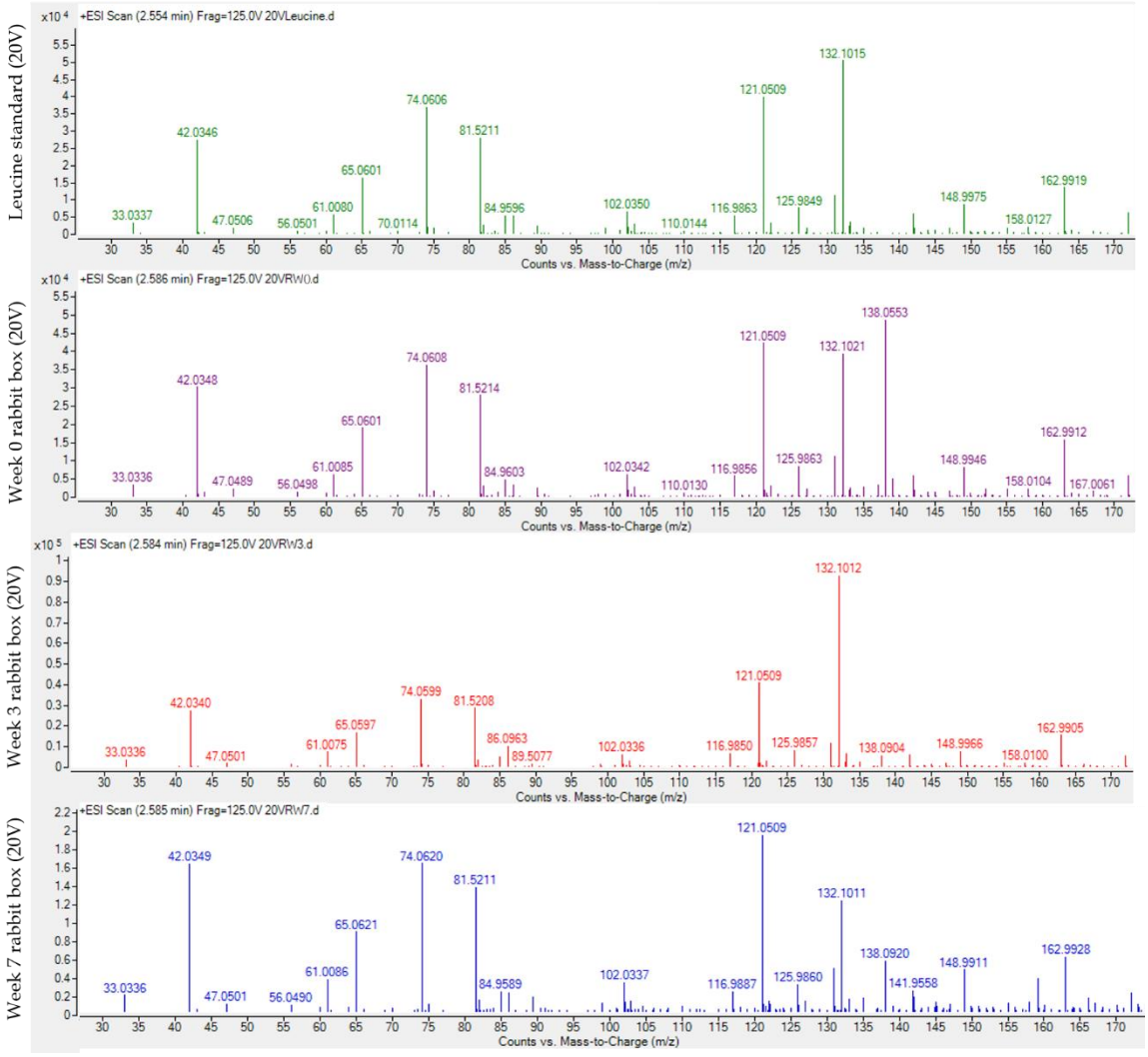

Figure 4.30: A comparison of mass spectra at 20 V collision energy between a leucine standard and a sample from a box containing rabbit at weeks 0, 3 and 7.

Figure 4.31 shows the mass spectra for the leucine standard and a sample from all three time points at a collision energy of 40 V. The fragmentation patterns of the standard and all samples are a very good match. As a result, it can be confirmed that the compound *m/z* 132.1012 is leucine.

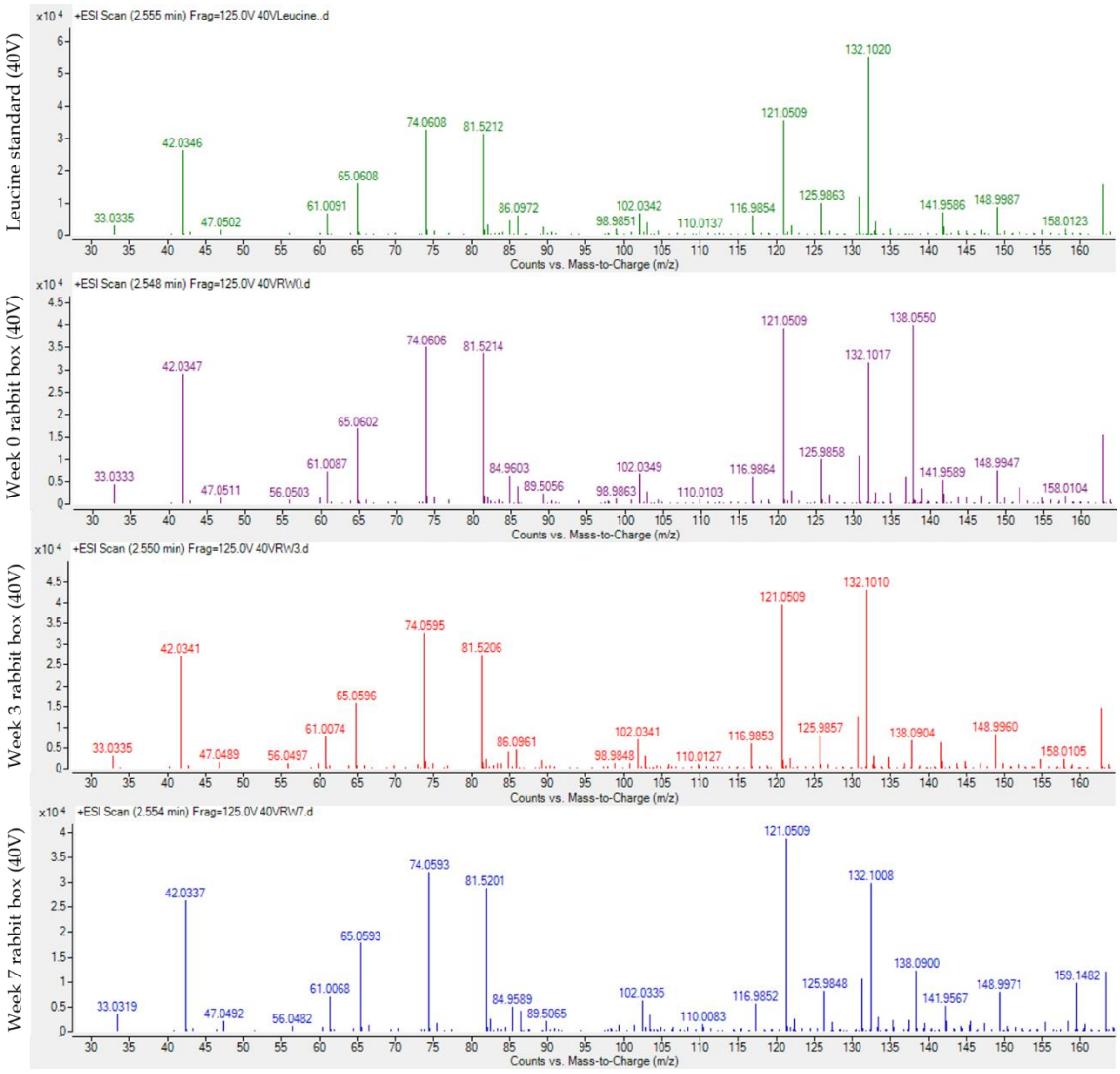

Figure 4.31: A comparison of mass spectra at 40 V collision energy between a leucine standard and a sample from a box containing rabbit at weeks 0, 3 and 7.

4.3.3.16 Monitoring of markers

Each compound successfully identified with the use of standards was investigated further to monitor their progression throughout the whole experiment. Samples from boxes containing rabbit at week 0 through to week 8 were analysed using the same instrumental conditions and method. The same was also done for boxes containing duck[2].

A PCA analysis was initially carried out to observe the progression of the chemical signature of the water throughout the entire experiment. Figure 4.32 shows the PCA scores plot of water samples taken from boxes containing rabbit from week 0 to 8. The QC samples are clustered in the middle of the plot. Samples from each time point are grouped tightly together and show excellent separation throughout the plot, however, samples taken from week 0 and week 1 show poorer separation. The separation between the remaining time points are further apart than the spread of the QC samples, signifying that the results are genuine and not due to any instrument effects.

[2]*This analysis was performed 1 year after the original analysis of these samples. The instrument also received a full service accompanied by part replacements to improve its performance during this time. As a result, it is not appropriate to directly compare the data to previous data collected at these time intervals due to the impact on retention, separation and quality of the sample. This analysis will stand alone.*

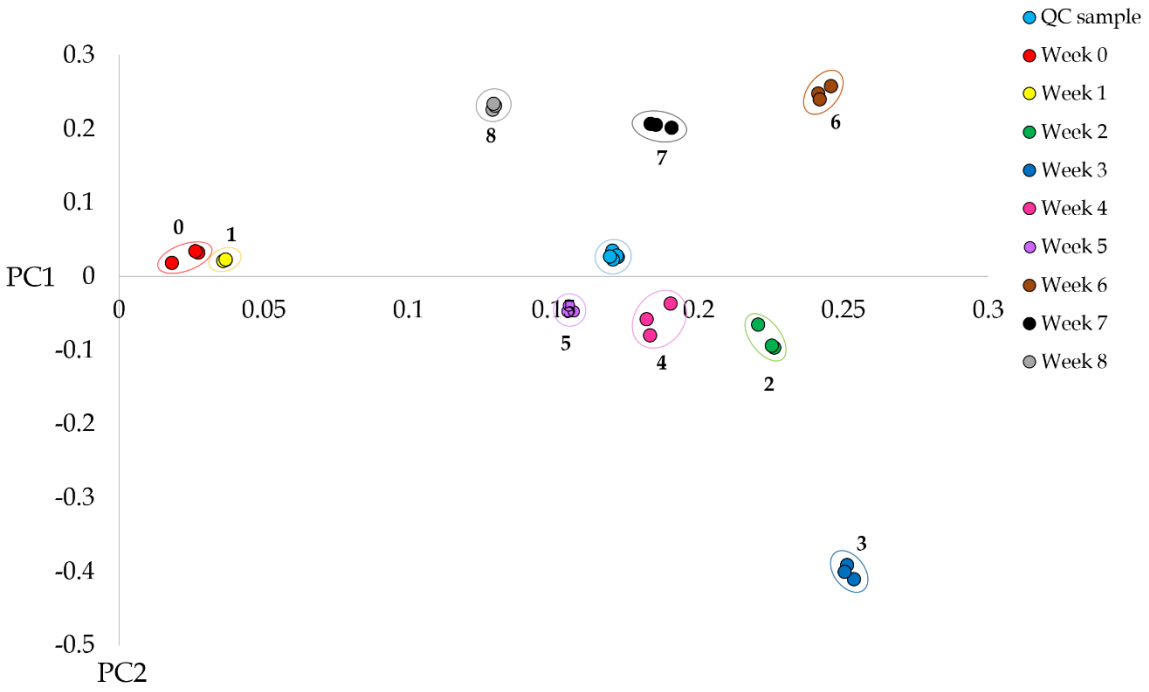

Figure 4.32: PCA scores plot of PC1 (83.18%) and PC2 (6.72%) for water samples from boxes containing rabbit taken every week from week 0 to 8 of decomposition in water during the summer.

Figure 4.33 shows the PCA scores plot of water samples taken from boxes containing duck from week 0 to 8. This PCA plot shows a very similar pattern to that presented for rabbit samples. The QC samples are clustered together, showing minimal instrumental drift. The samples from each time point are grouped well together, with excellent separation between each sample groups. Similar to the previous PCA plot, there is poorer separation between week 0 and week 1, suggesting again that there are only very small changes to the water chemistry at the very early stages of decomposition. However, itis still possible to group them together to show they are two separate time points.

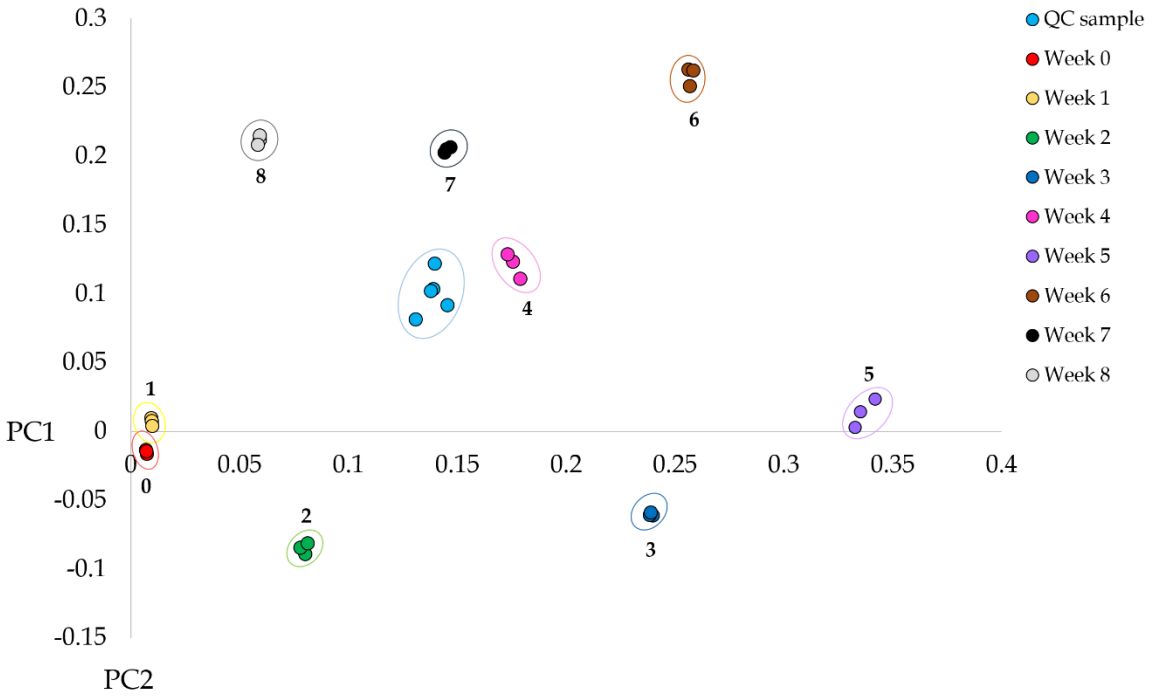

Figure 4.33: PCA score plot of PC1 (87.80%) and PC2 (9.06%) for water samples from boxes containing duck taken every week from week 0 to 8 of decomposition in water during the summer.

Once it was confirmed that there were impactful changes in the water chemistry over time, each successfully identified marker was monitored from week 0 to 8.

Cadaverine

Figure 4.34 monitors the progression of cadaverine over 8 weeks in water containing a decomposing rabbit, and duck. The behaviour of this compound seems to follow a similar pattern in both species, with a steady increase in peak area reaching its highest point in week 6. It is important to note that the overall peak area for cadaverine is much higher in the rabbit sample throughout the experiment.

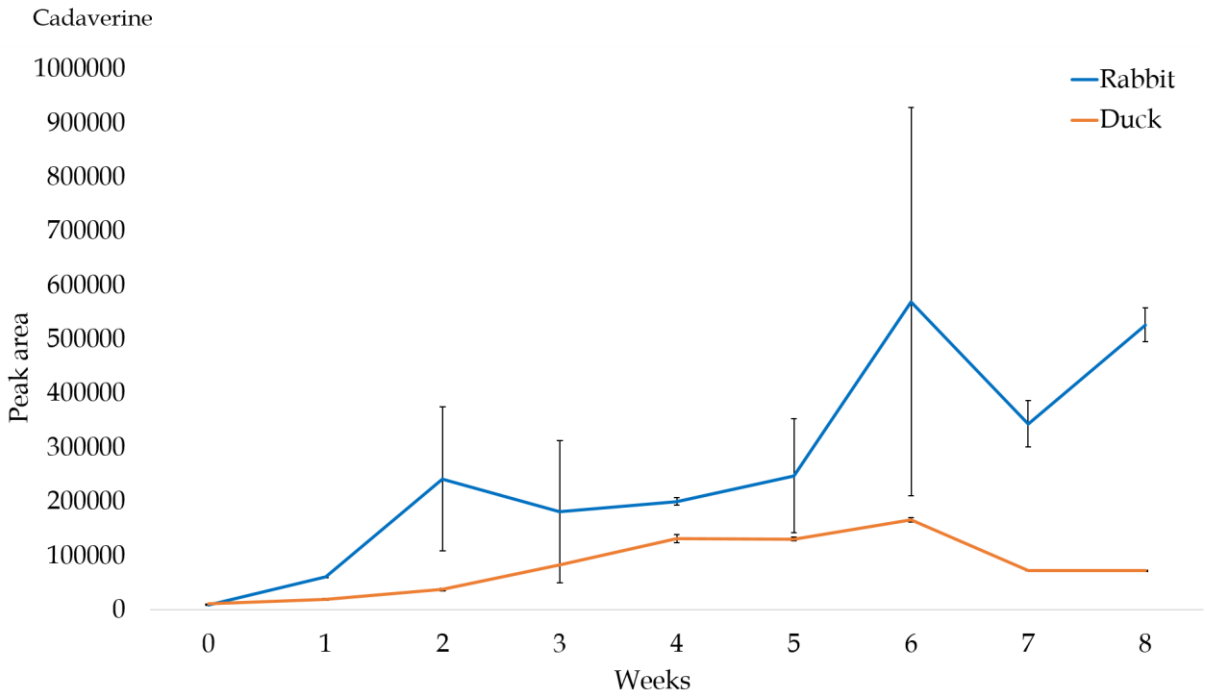

Figure 4.34: Graph monitoring the peak area of cadaverine over eight weeks during the summer months taken from boxes containing rabbit and duck carcasses. The error bars represent ±1 standard deviation.

Cadaverine is an organic compound known as a diamine, first described in 1885 by Ludwig Brieger, a physician from Berlin [49]. It is a colourless syrupy liquid with a very unpleasant odour. The structure of cadaverine is shown in Figure 4.35.

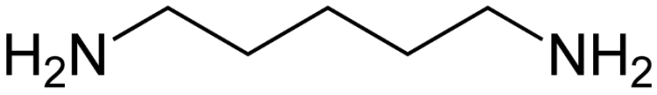

Figure 4.35: Structure of Cadaverine.

Cadaverine is most commonly formed during the putrefaction of animal tissue by the bacterial decarboxylation of lysine during protein hydrolysis [50]. The enzyme lysine decarboxylase removes the carboxyl group from the amino acid to form cadaverine [51, 52]. This is shown in Figure 4.36.

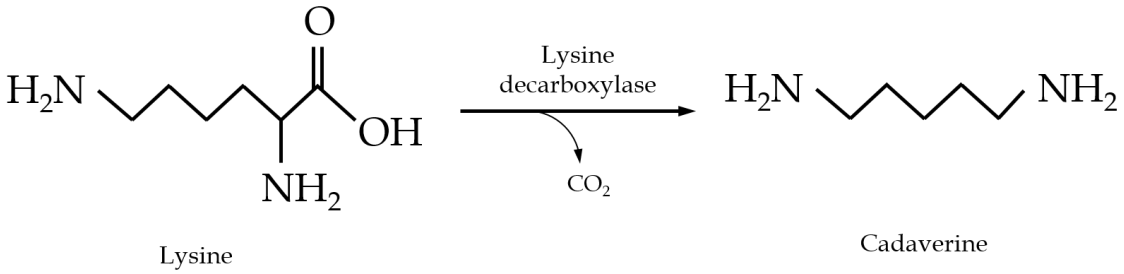

Figure 4.36: A metabolic pathway showing the dexarboxylation of lysine to form cadaverine.

Cadaverine and putrescine are two of the most important biogenic amines in the chemistry of decomposition, they are toxic diamines that confer the characteristic smell of decomposing bodies [50]. Researchers have utilised cadaverine in an attempt to characterise decomposition in many ways. Gonzales-Riano [53] looked at the changes in quantities of cadaverine in brain tissue using LC-MS and GC-MS. They identified a pronounced increase in cadaverine in brain tissue over time.

Vass [54] also used GC-MS to investigate a selection of biomarkers discovered in brain, heart, liver, kidney and muscle tissue from human remains. Cadaverine remained a compound of interest, regardless of its high variability over time. More recently, Pelletti [55] also used GC-MS to assess the effectiveness of cadaverine in the PMI estimation process. They found a 'strong' relationship between cadaverine levels and PMI. This illustrates how useful cadaverine could be in the field of forensic decomposition, showing that the methods used in this analysis are in fact detecting the correct type of compounds.

Creatinine

Figure 4.37 monitors the progression of creatinine over 8 weeks in water containing a decomposing rabbit and duck. In the rabbit sample there seems to be a high abundance of creatinine after 1 week of decomposition, followed by a sharp decline. The graph illustrates that creatinine is not detectable in the water after three weeks of decomposition. On the other hand, the spike in the presence of creatinine in the sample taken from a box containing a duck carcass is seen at week 3. This suggests that it has taken significantly longer for the marker to leach into the water from the duck carcass, as the compound continues to appear in the water until the sixth week of decomposition. This behaviour pattern could be as a result of many factors. Creatinine could have very quickly broken down into smaller compounds, evaporated from the water, or been overwhelmed by other by-products of decomposition leaching into the water. Similar to the results presented for cadaverine, the peak area for the rabbit sample is significantly higher than the duck sample, with the increase in peak area not visible in the duck sample without looking closer into the data.

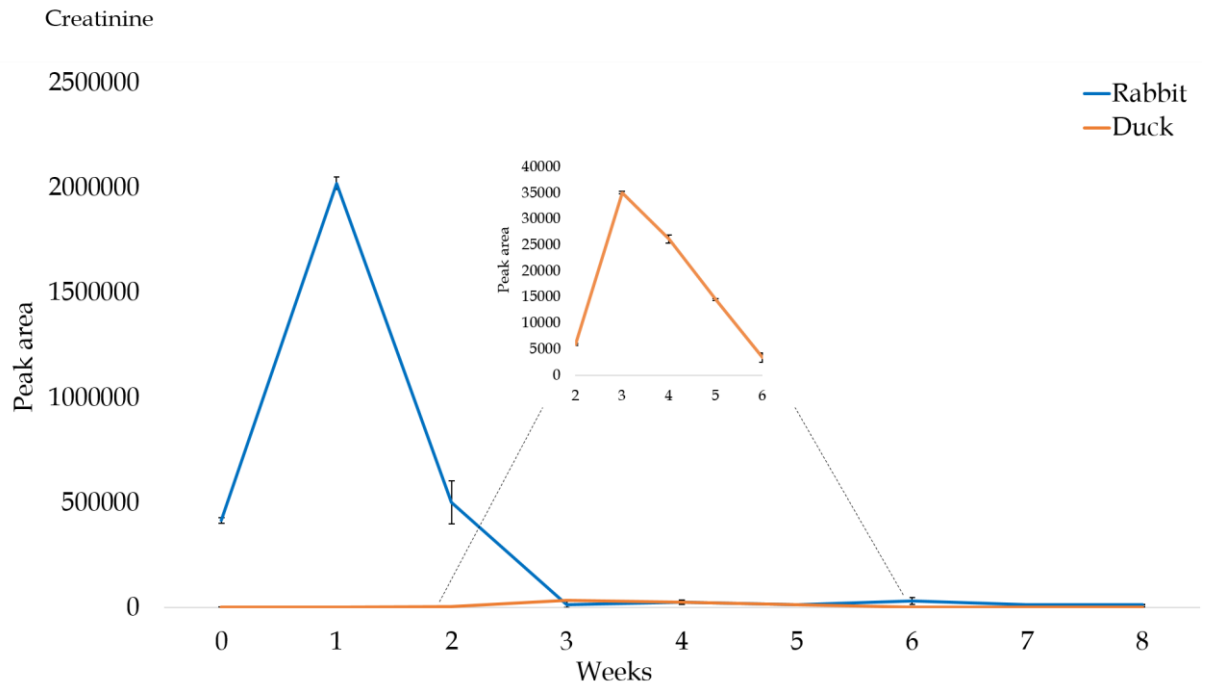

Figure 4.37: Graph monitoring the peak area of creatinine over eight weeks during the summer months taken from boxes containing rabbit and duck carcasses. The error bars represent ±1 standard deviation.

Creatinine is a chemical waste product produced by the constant breakdown of creatine in muscle. It is transported through the bloodstream into the kidneys and excreted in urine [56]. The structure of both compounds is presented in Figure 4.38.

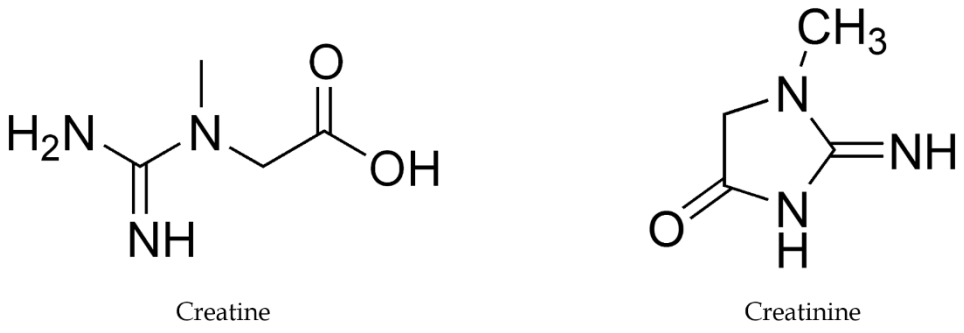

Figure 4.38: The structure of creatine and creatinine.

Creatine is a naturally occurring molecule in the body synthesized primarily in the liver, kidney and pancreas using three amino acids, glycine, methionine and arginine [57]. It is transported through the blood to the muscle, where 95% of the body's creatine is stored [58]. Creatinine is then produced from the natural breakdown of creatine in muscle tissue during the release of energy, for example during exercise. Figure 4.39 taken from Wyss [56] presents a schematic representation of the metabolism of creatine to creatinine. This reaction is a spontaneous, nonezymatic cyclization which is dependent on both pH and temperature [56].

Research into the use of creatinine to assisit with the chemistry of decomposition is lacking, however, the variability of creatinine levels following death is often investigated in regards to kidney health [59].

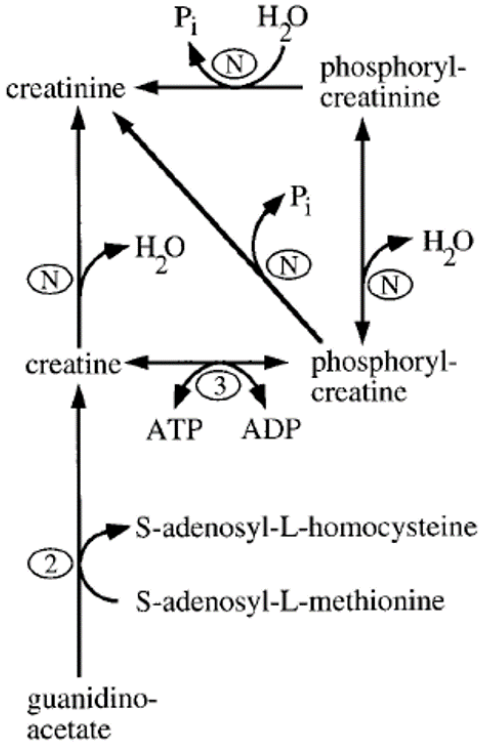

Figure 4.39: Representation of the metabolic pathway of creatine and creatinine, taken from Wyss [56].

Leucine

Figure 4.40 monitors the progression of leucine over 8 weeks in water containing a decomposing rabbit and duck. This marker presents a similar pattern over time in both rabbit and duck experimental conditions, with a spike in peak area at week 2, followed by another at week 7. Leucine also has a much higher peak area throughout the experiment in boxes containing a rabbit carcass, a pattern observed in all three identified markers.

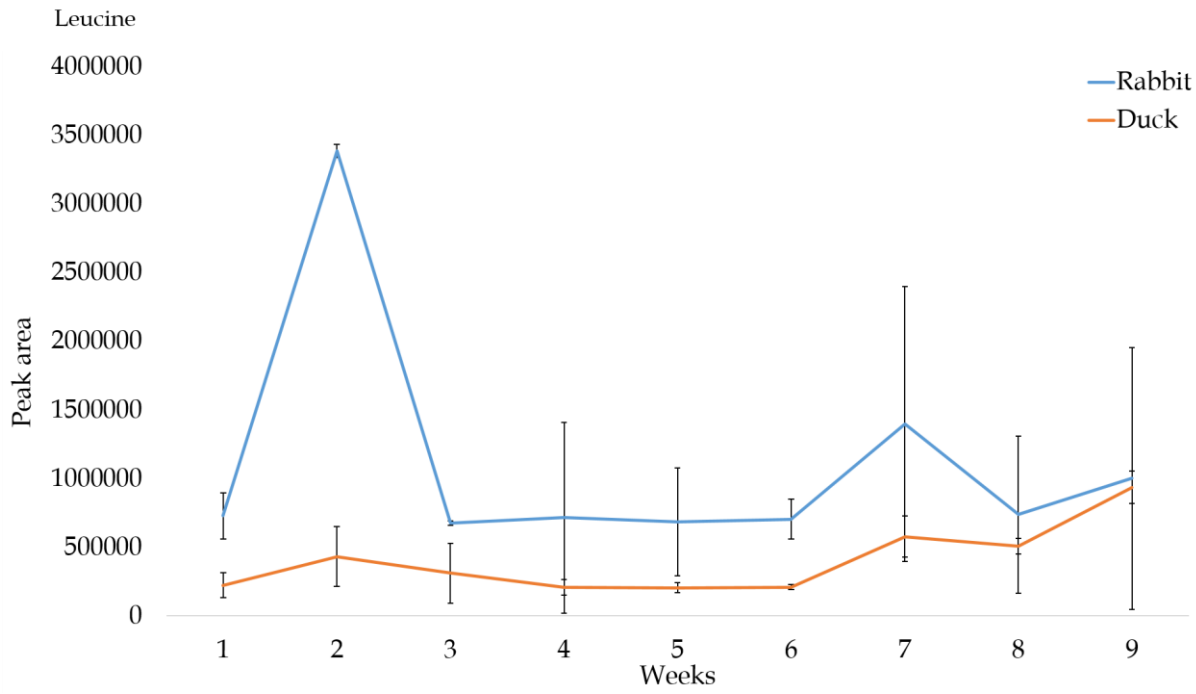

Figure 4.40: Graph monitoring the peak area of Leucine over eight weeks during the summer months taken from boxes containing rabbit and duck carcasses. The error bars represent ±1 standard deviation.

Leucine is a branched chain amino acid, accompanied by isoleucine and valine. It is an essential amino acid, therefore it cannot be synthesised, but obtained by protein in the diet [60]. The structure of leucine is presented in Figure 4.41.

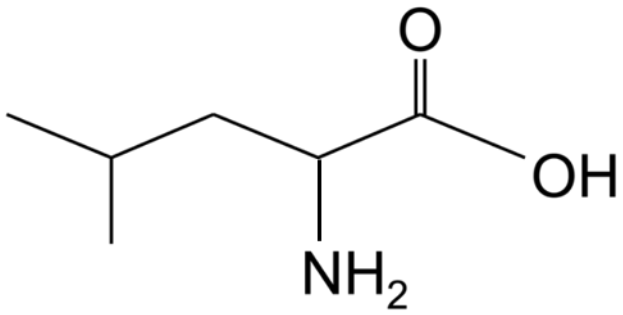

Figure 4.41: Molecular structure of leucine.

Protein breakdown is one of the main factors of chemical decomposition. The majority of proteins break down via proteolysis to form peptones, polypeptides and amino acids [50]. Leucine is naturally present in the liver, adipose tissue and muscle tissue during the early stages of decomposition [54]. Further protein degradation in later stages of decomposition occurring in the epidermis and muscle protein can also produce leucine [61].

The results obtained during this experiment reflect the literature surrounding continuous protein degradation during decomposition. Monitoring leucine over time showed that this compound is continuously leaching into the water, and ever changing throughout the experiment.

As an essential amino acid, leucine is ubiquitous in nature, therefore cannot be considered as a species-specific marker alone. The ability to look at the behaviour of these amino acids as a group could help reveal their patterns in the chemical signature of the water. This could enhance our knowledge of how the water chemistry changes at different stages of decomposition.

4.3.4 Differences in the metabolite profiles of two species decomposing in water during the winter months.

4.3.4.1 The physical changes visible during the decomposition of two species in water during the winter months.

The focus on physical observations during the winter experiment was important to allow a comparison to the physical changes happening at the same time points during the summer months. It was paramount to understand and integrate the physical and chemical differences occurring over time. Figure 4.42 presents the images of both rabbit and duck carcasses following 0 days of decomposition in water.

Figure 4.42: Images of 3 rabbit and 3 duck carcasses in water following 0 days of decomposition in winter conditions.

Each carcass had floated to the surface of the water when initially submerged. There were no visual signs of decomposition. After one week of submersion (Figure 4.43), there were no obvious changes to the physical appearance of both species, or to the water itself. At the same time point in the summer experiment each carcass was colonised with maggots, and the water a brown-yellow colour. The drastic contrast between the two experiments after only one week shows the effects of temperature on decomposition.

Figure 4.43: Images of 3 rabbit and 3 duck carcasses in water following 1 week of decomposition in winter conditions.

Following three weeks of decomposition in water, Figure 4.44 again shows no dramatic physical changes, and no sign of any insect activity. The water in the boxes containing rabbit has a pale-yellow tint. By the second week of decomposition in the summer experiment, the skeletons of both species were visible above the water, surrounded by thousands of drowned maggots. This continued into the third week of the experiment, whilst in the winter experiment there were still no physical signs of decomposition.

Figure 4.44: Images of 3 rabbit and 3 duck carcasses in water following 3 weeks of decomposition in winter conditions.

After 4 weeks of decomposition in water (Figure 4.45), the experiment still failed to show any signs of insect activity, physical changes to the carcasses or smell. There were no further changes for the remainder of the experiment. In the summer experiment, after 1 month the majority of the carcasses had sunk below a brown lipid-like film covering the surface of the water, and remained so until the end of the experiment.

Figure 4.45: Images of 3 rabbit and duck carcasses in water following 4 weeks of decomposition in winter conditions.

4.3.4.2 Metabolic Profiling

The chromatograms in Figure 4.46 and Figure 4.47 look at the changes happening to the chemical signature of the water at three time points for both rabbit and duck respectively. It is clear that the lack of physical changes during the course of this experiment is reflected in the water chemistry, with a distinct reduction in the number of peak and peak intensities in all three time points. While there are small changes in each chromatogram over time, these are minimal and do not reflect the chemical profiles obtained for the same species in the summer experiment.

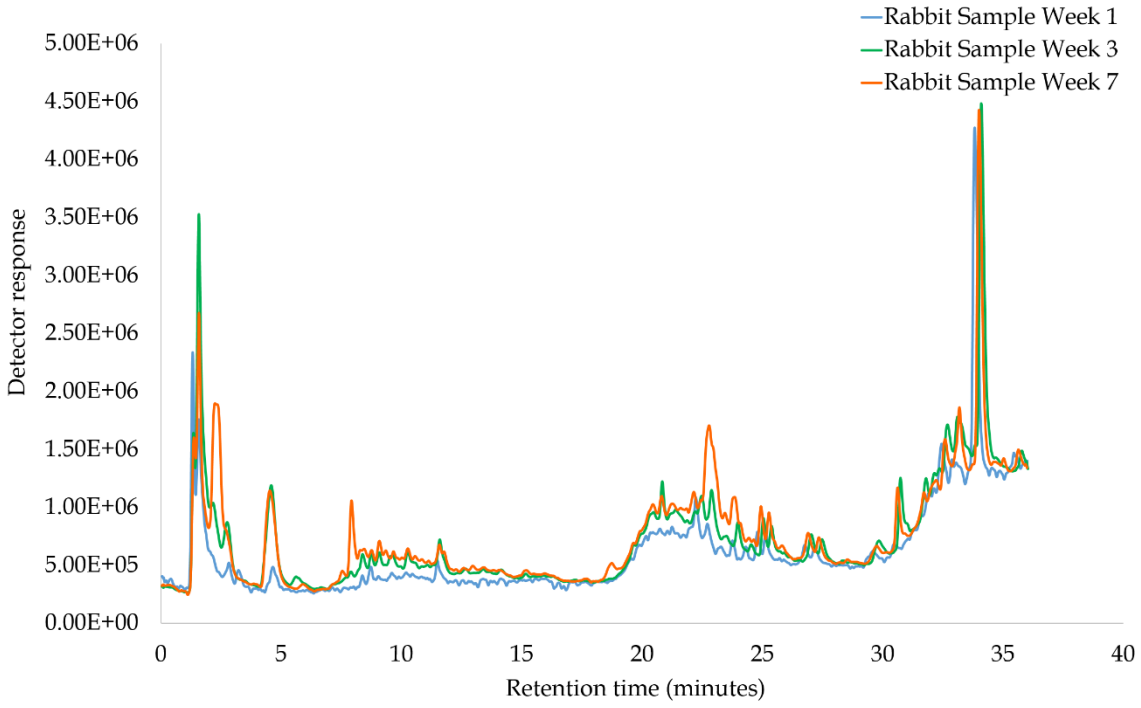

Figure 4.46: Example total ion chromatogram (TIC) of water samples containing a decomposing rabbit carcass at week 0, 3 and 7 of the winter experiment.

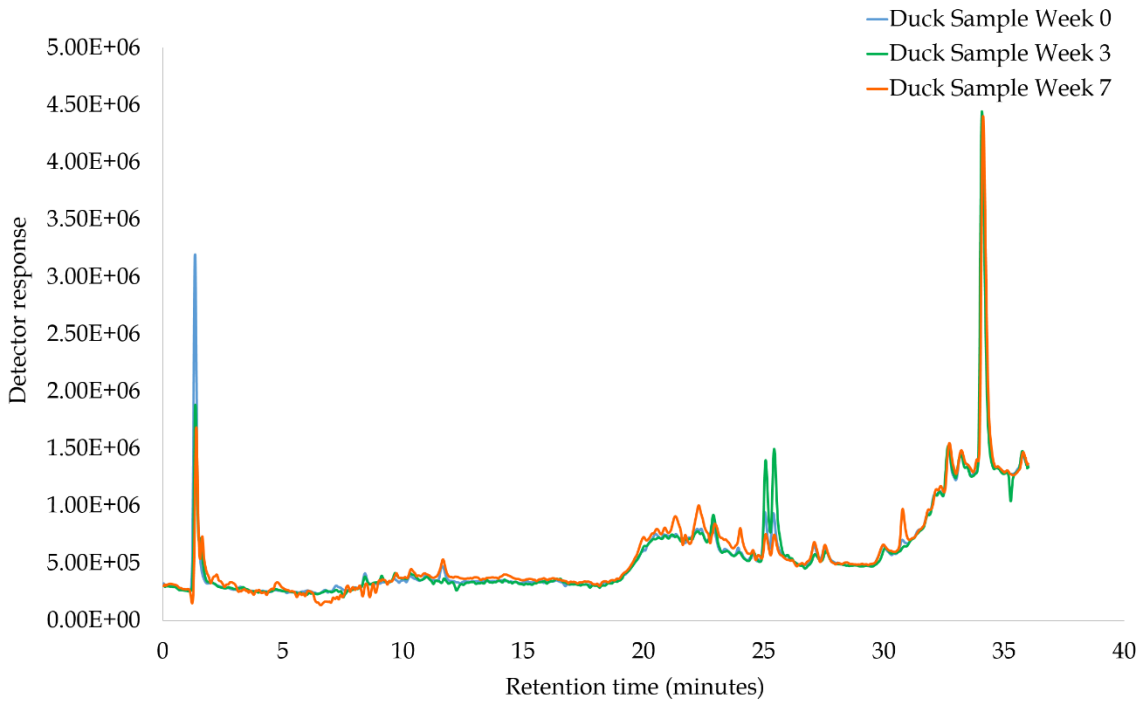

Figure 4.47: Example total ion chromatogram (TIC) of water samples containing a decomposing duck carcass at week 0, 3 and 7 of the winter experiment.

Although the metabolic profiles for each species are limited, there are still some differences between species, specifically the peak patterns between 3-12 minutes, and 20-30 minutes. This shows that even at lower temperatures chemical differences can still be visualised.

4.3.4.3 Multivariate analysis

The PCA scores plot in Figure 4.48 presents the samples taken from boxes containing rabbit at weeks 0, 3 and 7. The QC samples are clustered together, indicating minimal instrumental effects. The control samples and samples at week 0 seem to cluster together, implying that their chemical profiles are very similar. There is slight overlap between samples from week 3 and 7 on the plot, however they are both separated well from the week 0 samples.

It is interesting to note that although there were limited physical changes during the first 3 weeks of decomposition during the winter, this PCA plot implies that subtle chemical changes were still occurring. This highlights the importance of the chemical analysis of decomposition.

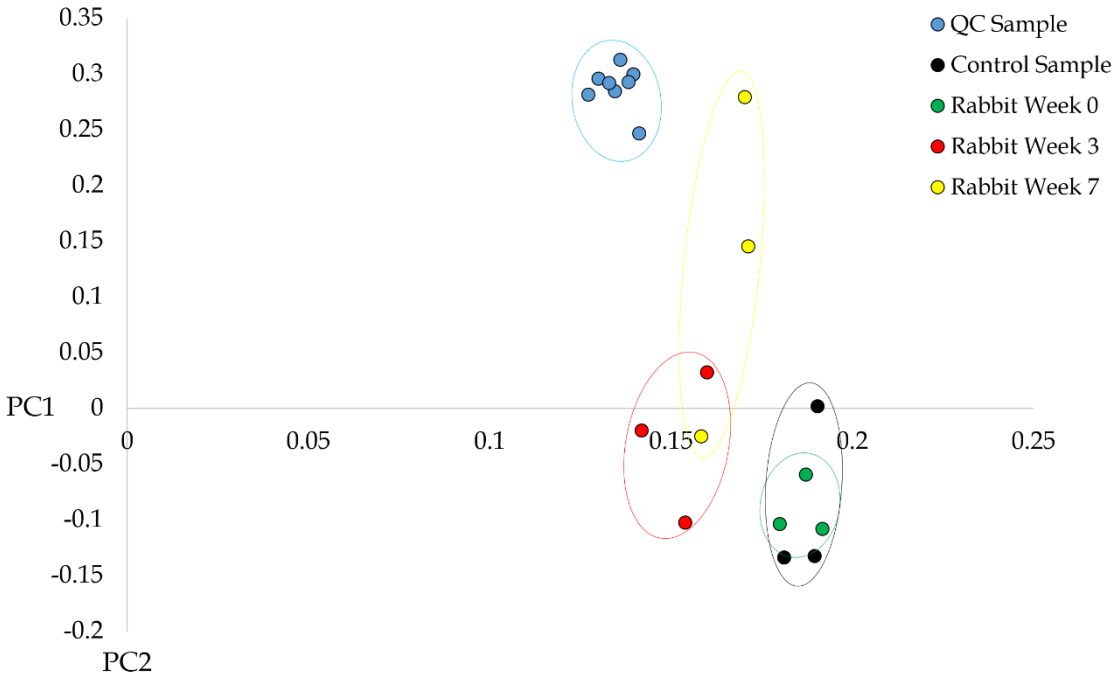

Figure 4.48: PCA scores plot of PC1 (87.16%) and PC2 (4.34%) for water samples containing a decomposing rabbit carcass at week 0, 3 and 7 of the winter experiment.

Figure 4.49 represents water samples taken from boxes containing duck at week 0, 3 and 7 accompanied by a control sample. The QC samples show slight spreading across PC2. It is clear that all three time points are overlapping on the plot, showing limited separation. The control samples seem to have clustered towards the top of the plot, indicating some changes between the control water and the experimental boxes.

When comparing the progression of the samples over time on the PCA plots here to those obtained during the summer experiment (Section 4.3.3.3), it is clear that the separation between each time point is poorer in the winter months, however this dramatic difference as a result of temperature was expected.

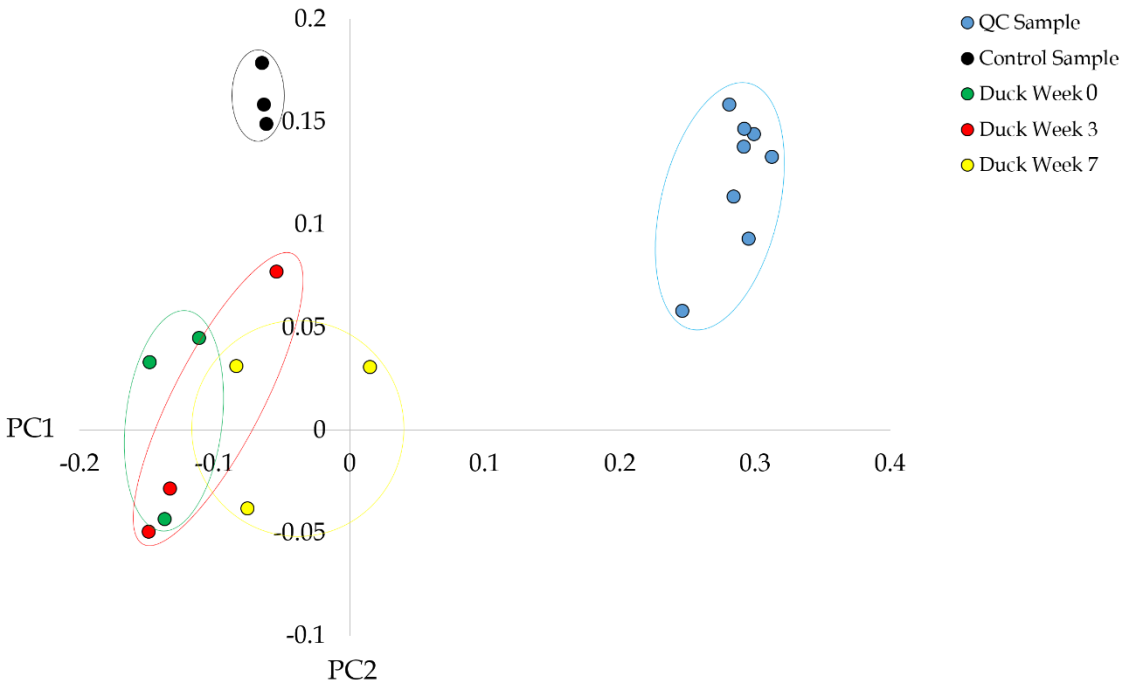

Figure 4.49: PCA scores plot of PC1 (88.35%) and PC2 (4.44%) for water samples containing a decomposing duck carcass at week 0, 3 and 7 of the winter experiment.

The PCA scores plots from the summer experiment show excellent separation between time points, where the distance between the sample groups are further apart than the spread of the QC samples. The fact that the samples from the winter experiment are showing separation on the PCA plot to any degree is remarkable considering the low temperatures experienced and lack of physical signs of decomposition. These initial visual results show promising data that even under cold conditions, this method is still able to monitor the chemical signature of the water as it is influenced by decomposition.

4.3.4.4 Statistical analysis

The total number of features detected in the water samples through *XCMS online* was 5491. All features with a CV value of 30% or more were removed, with 3975 remaining. Statistical analysis was performed on water samples from boxes with both rabbit and duck carcasses. 20 compounds were found showing significant differences over time in the water from rabbit boxes, and 23 from duck boxes. Of these markers, only 1 of them were present in samples from both species. A summary of this marker is shown in Table 4.10. It has been assigned a predicted formula and a score that reflects the confidence of that assignment. Table 4.11 investigates where these significant differences lie between each time interval.

Table 4.10: Summary of the marker that shows significant differences over time of water samples taken from both rabbit and duck decomposition during the winter.

m/z	Retention time (minutes)	CV value	Formula	Score	p-value
416.0673	34.02	22%	$C_{29}H_{25}N_3$	60.39	p<0.05

Table 4.11: Table showing where the significant differences lie between time intervals for the marker identified in both rabbit and duck water samples.

m/z	Rabbit sample between Week 0 and 3	Rabbit sample between Week 3 and 7	Duck sample between Week 0 and 3	Duck sample between Week 3 and 7
416.07	p<0.05	p<0.05	p<0.05	p<0.05

It is clear from the statistical analysis carried out that there are much fewer potential markers that can be monitored over time in both rabbit and duck samples, compared to those obtained in the summer experiment. Deeper analysis into each specific time point will assess the possibility of species differentiation as a result of decomposition in water during winter.

4.3.4.5 Metabolic profiling of week 0

Figure 4.50 shows the chromatograms of water samples taken from boxes containing both rabbit and duck after 0 weeks of decomposition. Note that these particular samples were taken on day 2 of the experiment. The majority of the chromatogram looks similar between species, however there are two peaks that are clearly only present in the rabbit sample at 4.5 minutes and 22.5 minutes, *m/z* 100.0764 and *m/z* 125.9891 respectively. These chromatograms are similar to those obtained during the summer experiment, reflecting the early stage of the experiment.

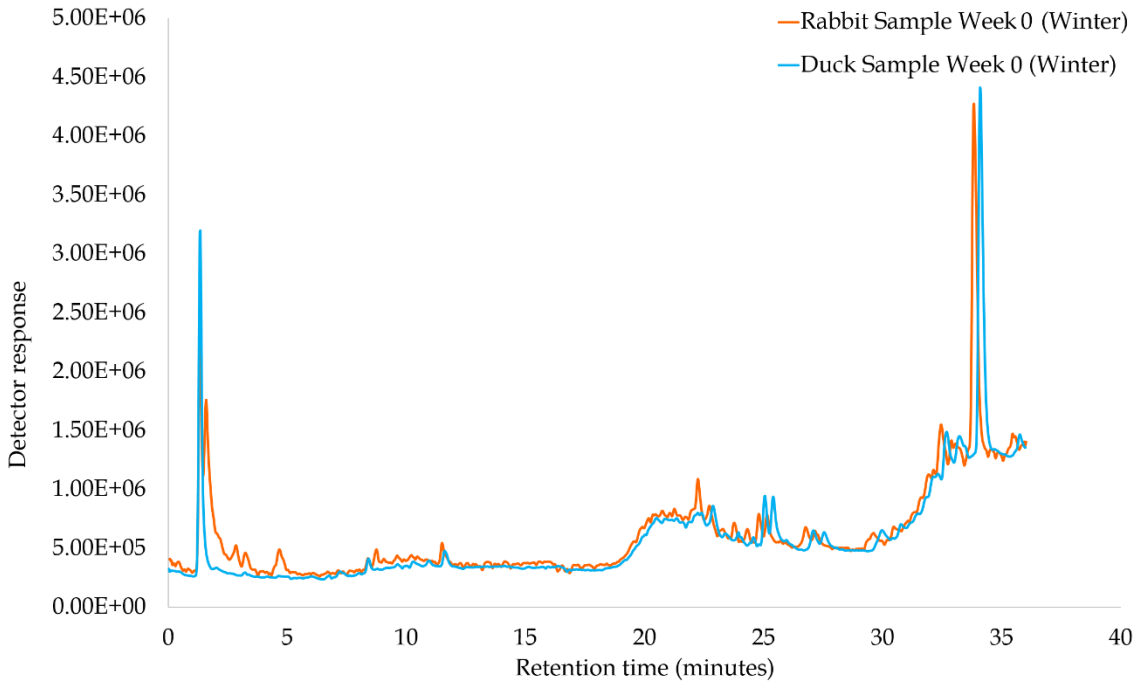

Figure 4.50: Example total ion chromatograms (TIC) of water samples taken after 0 weeks of decomposition in water during the winter.

4.3.4.6 Multivariate analysis of week 0

Figure 4.51 presents the PCA scores plot of samples from both species accompanied by a control at week 0. The QC samples are clustered well together. Water samples from the control, rabbit and duck boxes are also clustered together towards the lower end of the plot, highlighting the lack of separation between species in the winter conditions. The lack of visual separation at the first time point was also evident during the summer experiment.

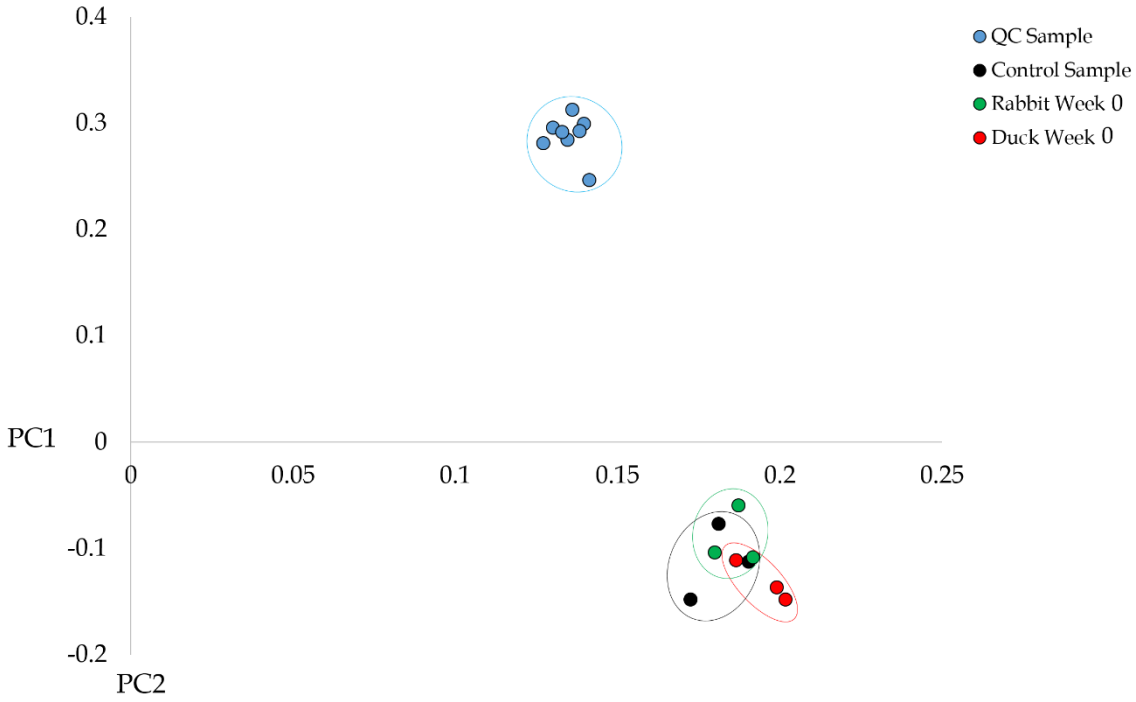

Figure 4.51: PCA scores plot of PC2 (7.09%) and PC3 (1.33%) for water samples taken after 0 weeks of decomposition in water during the winter.

4.3.4.7 Statistical analysis of week 0

Statistical analysis was performed to investigate any significant differences between species following 0 weeks of decomposition. 50 markers were significantly different with a p-value of below 0.05, while 40 markers were significantly different with a p-value of below 0.01. Of these markers, 60% of them had a *m/z* under 400, while 40% had a *m/z* over 400. This shows that the smaller compounds are slightly more prevalent at this time point. Table 4.12 presents the top 20 markers that were significantly different between species and shown to be the most robust and reliable.

Table 4.12: Summary of the top 20 compounds that show significant differences between species after 0 weeks of decomposition in water during the winter.

m/z	Retention time (minutes)	CV%	p-value XCMS	p-value ANOVA/Welch
102.0522	1.53	13%	p<0.001	0.004
120.0650	1.53	21%	p<0.001	0.003
130.9539	9.05	13%	p<0.001	0.002
141.9487	9.08	23%	p<0.001	0.002
152.0543	2.85	22%	p<0.001	0.005
194.1347	1.49	21%	p<0.001	0.004
255.2282	30.87	21%	p<0.001	0.004
268.1626	8.8	28%	p<0.001	p<0.001
274.8671	1.44	16%	p<0.001	0.003
299.0659	4.57	9%	p<0.001	0.004
389.1095	22.73	27%	p<0.001	0.005
400.3058	32.58	12%	p<0.001	0.001
412.2702	30.93	24%	p<0.001	0.004
431.3172	32.06	5%	p<0.001	0.005
434.2124	33.19	15%	p<0.001	p<0.001
457.3430	33.09	9%	p<0.001	0.001
507.2661	32.12	3%	p<0.001	0.005
513.0038	33.64	10%	p<0.001	0.001
550.6233	34.64	7%	p<0.001	0.004
729.5557	33.94	20%	p<0.001	0.002

The average *m/z* of the top 20 compounds showing significant differences between species is 337.85. As it is in the early stages of decomposition, it was expected that the chemical profile of the water would consist of larger compounds. Figure 4.52 presents six markers chosen due to the substantial differences in peak area between each species. The majority of these markers are more prevalent in the rabbit samples, with those also showing the most dramatic difference in peak area.

While each marker also shows a clear difference in peak area between species, these differences are not as pronounced as those obtained during the summer experiment, indicating that there is a higher abundance of these compounds in the samples obtained during the summer. Only one marker is present in the top 20 compounds after 0 weeks of decomposition of both the summer and winter experiment, *m/z* 120.0650.

Whilst the chemical processes occurring during decomposition in the summer and winter are most likely the same, it is the speed and quantity of compounds present that seem to be affected by temperature. Preliminary data seems to suggest that the pool of detected features is much smaller in the samples taken during the winter experiment.

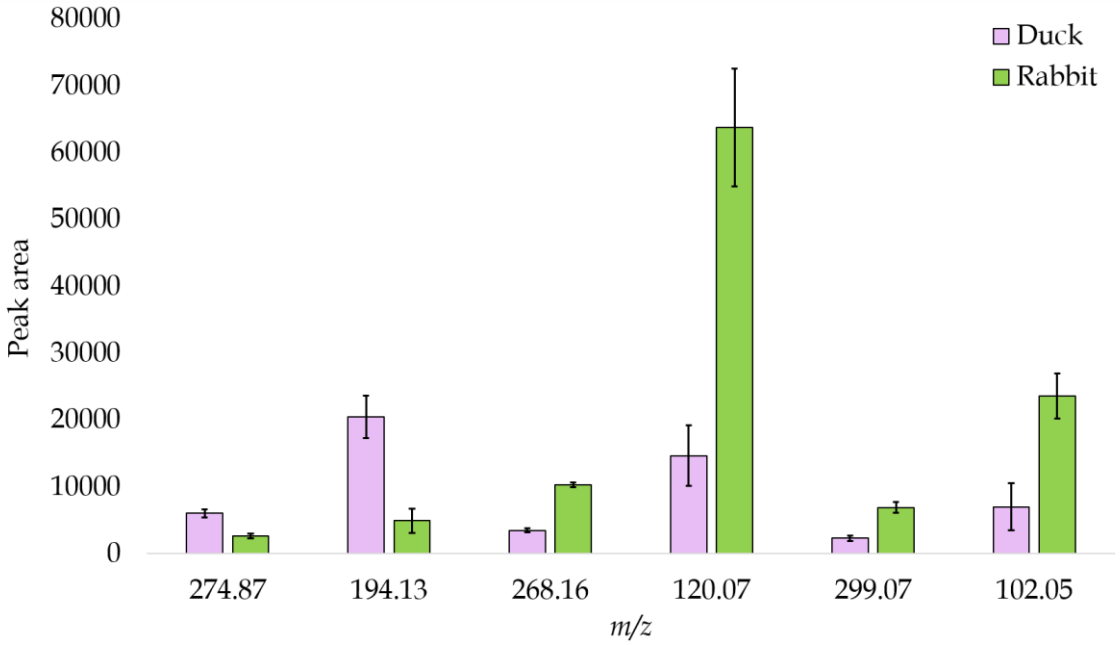

Figure 4.52: Bar chart presenting the peak area of six chosen markers that show significant differences between species following 0 weeks of decomposition. The error bars represent ±1 standard deviation.

4.3.4.8 Metabolic profiling of week 3

Figure 4.53 presents the two chromatograms of water samples taken from boxes containing rabbit and duck carcasses following three weeks of decomposition in water. The peak intensities throughout the chromatograms have increased slightly, providing a clearer image of the subtle differences in the chemical profile of each species. The peak area of a peak eluting at 4.5 minutes that appeared in Figure 4.50 has increased, with no sign of that particular peak in the duck sample.

Although it is possible to visualize the difference in the chemical profiles of both species, it is clear that the overall peak intensities are lower and peak shape is generally poorer when comparing to the chromatograms obtained at this time point during the summer experiment.

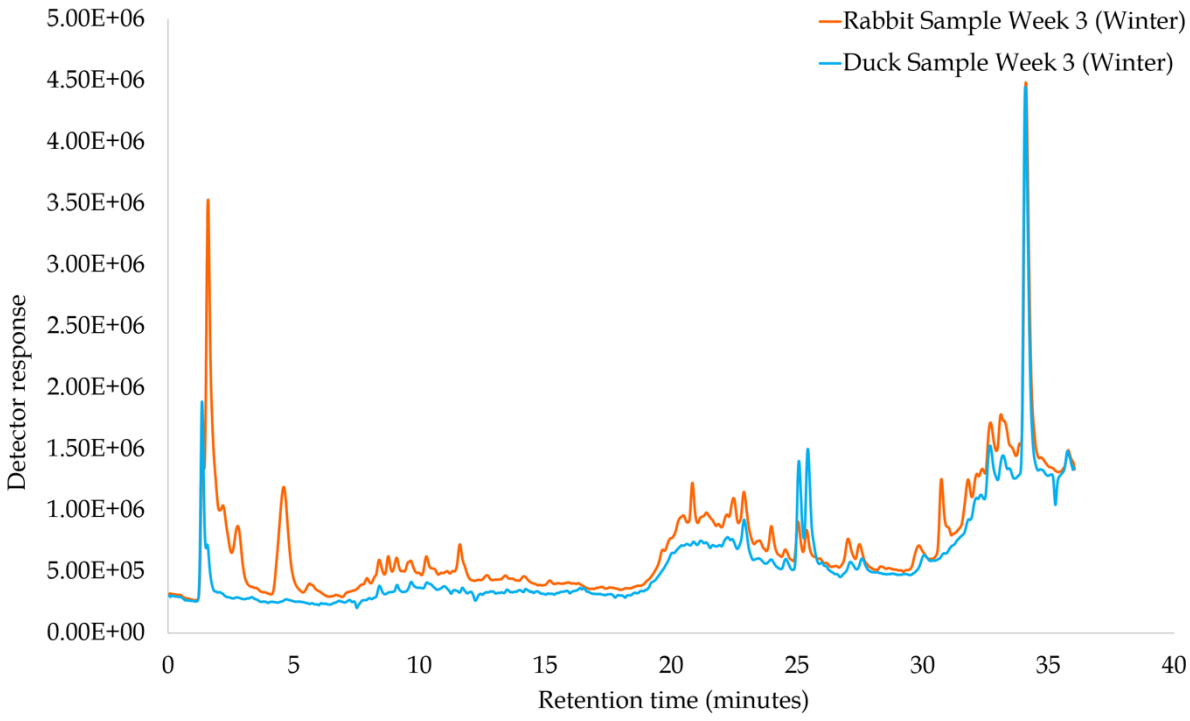

Figure 4.53: Example total ion chromatograms (TIC) of water samples taken after 3 weeks of decomposition in water during the winter.

4.3.4.9 Multivariate analysis of week 3

The PCA scores plot in Figure 4.54 shows slightly better separation between both species after 3 weeks of decomposition. The QC samples are clustered together, however the distance between the sample groups is not further apart than the spread of the QC samples, therefore the separation cannot be attributed to the chemical differences between the samples alone. Although there is slight separation between species on the plot, the samples from the summer experiment showed better separation between the experimental and the control samples. This may suggest that although there is increased separation between species at this time point, the chemical signature of the water has not progressed as much over time as it would have done at this time point during summer conditions.

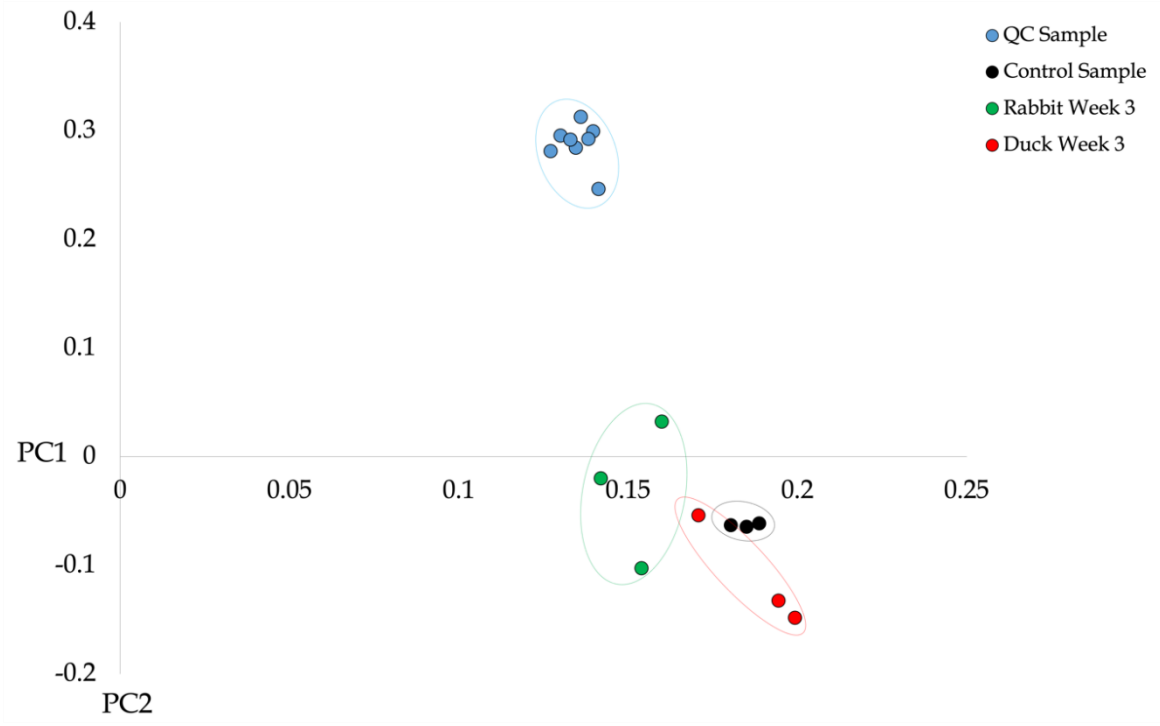

Figure 4.54: PCA scores plot of PC1 (87.64%) and PC2 (6.70%) for water samples taken after 3 weeks of decomposition in water during the winter.

4.3.4.10 Statistical analysis of week 3

Statistical analysis was performed to investigate any significant differences between species following 3 weeks of decomposition. 50 markers were significantly different with a p-value of below 0.05, while 47 markers were significantly different with a p-value of below 0.01. Of these markers, 68% of them had a *m/z* under 400, while 32% had a *m/z* over 400. This shows that there is a slight increase in the number of smaller compounds appearing as the experiment progresses. Table 4.13 presents the top 20 markers that were significantly different between species and shown to be the most robust and reliable.

Table 4.13: Summary of the top 20 compounds that show significant differences between species after 3 weeks of decomposition in water during the winter.

m/z	Retention time (minutes)	CV%	p-value XCMS	p-value ANOVA/Welch
112.1674	1.55	26%	p<0.001	0.007
174.1238	2.49	28%	p<0.001	p<0.001
182.6295	1.31	20%	p<0.001	0.002
208.1130	1.48	16%	p<0.001	0.006
215.9909	1.35	28%	p<0.001	0.004
267.1718	27.5	12%	p<0.001	0.007
291.2240	27.22	15%	p<0.001	0.003
298.2691	31.06	23%	p<0.001	0.001
320.2538	31.07	9%	p<0.001	p<0.001
330.8406	8.01	20%	p<0.001	0.006
345.0822	10.32	8%	p<0.001	p<0.001
362.3017	34.51	20%	p<0.001	0.007
407.2311	33.23	8%	p<0.001	0.006
452.3586	33.99	8%	p<0.001	0.001
473.1764	22.19	20%	p<0.001	0.003
490.3329	34.37	9%	p<0.001	0.002
495.7554	8.02	3%	p<0.001	0.006
523.3574	34.22	4%	p<0.001	0.003
537.1623	35.75	22%	p<0.001	0.002
685.2104	33.99	5%	p<0.001	0.007

The average *m/z* of the top 20 compounds showing significant differences between species is 358.64, which is a very similar value to the average *m/z* after 0 weeks of decomposition. There is a remarkable difference between the small number of markers identified here, and the total of 334 markers identified at this time point in the summer experiment. This seems to suggest that there are substantially more compounds leaching into the water during decomposition in warmer temperatures, and as a result a wider availability of markers to create a fuller chemical profile of the water.

Figure 4.55 presents six markers chosen due to the substantial differences in peak area between each species. There is an overall increase in the peak area at this point, accompanied by bigger difference between the peak areas of each species. This result would support the increasing changes in the chemical signature of the water as decomposition progresses, allowing more opportunity for species specific markers to appear. It is also important to note that the overall peak areas for the markers of interest in the summer experiment are almost double those shown in Figure 4.55, suggesting there is also a higher abundance of these compounds during warmer temperatures.

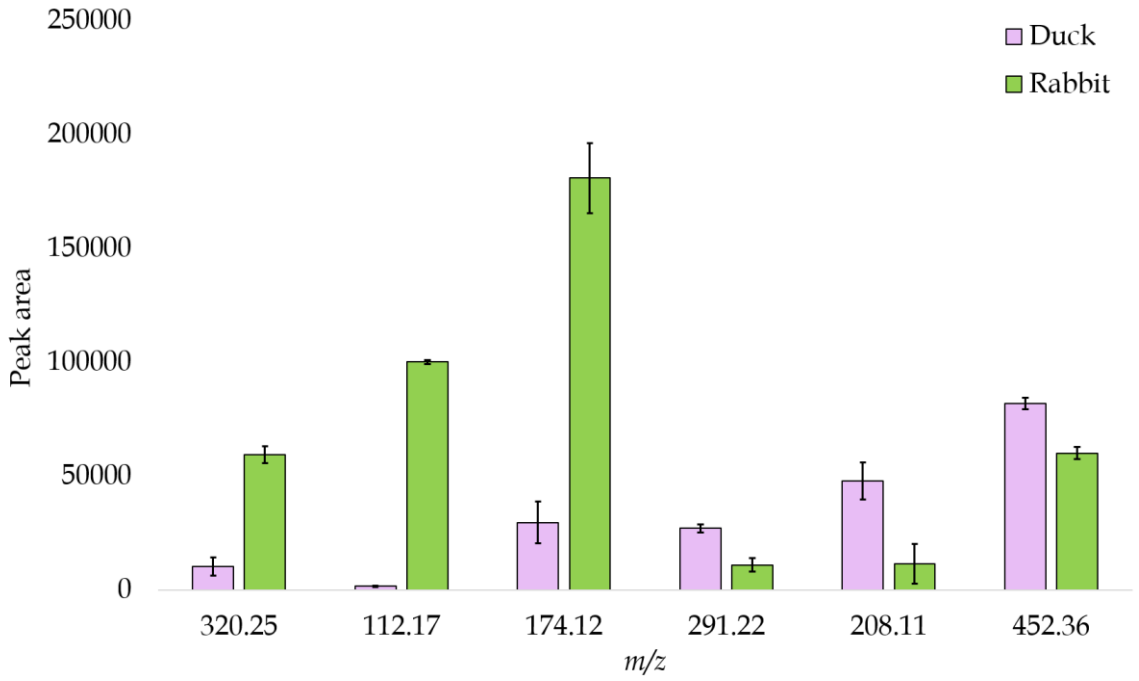

Figure 4.55: Bar chart presenting the peak area of six chosen markers that show significant differences between species following 3 weeks of decomposition. The error bars represent ±1 standard deviation.

4.3.4.11 Metabolic profiling of week 7

Figure 4.56 presents the overlaid chromatograms of water samples taken from boxes containing duck and rabbit after 7 weeks of decomposition in water. There is an increase in peak intensities throughout the chromatogram for both species, however the rabbit sample seems to show overall higher peak intensities. One peak in particular at 4.5 minutes has appeared at all three time points and only in the chromatogram from the rabbit sample. This peak is also visible in the chromatograms obtained at weeks 3 and 7 during the summer experiment. The dominant *m/z* for this peak was *m/z* 100.0764 in both experiments. The software used was unable to identify this compound further.

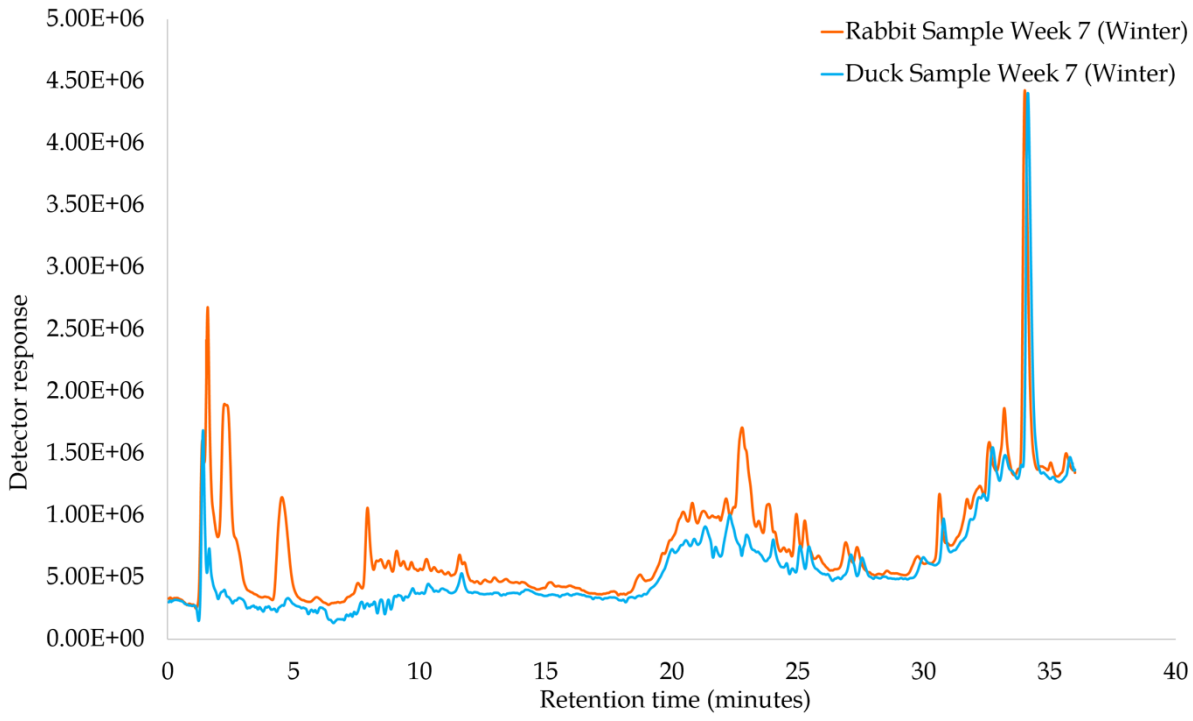

Figure 4.56: Example total ion chromatograms (TIC) of water samples taken after 7 weeks of decomposition in water during the winter.

By the seventh week of the summer experiment, there was a substantial difference in the chromatograms for each species, highlighting their unique chemical profiles. With a larger number of peaks, and those having higher peak intensities and better peak shape during the summer, it is clear that although it is possible to detect the chemical signature of the water during winter conditions the abundance of compounds leaching into the water is much lower.

4.3.4.12 Multivariate analysis of week 7

The PCA scores plot in Figure 4.57 looks at the separation between the control sample, and both species following 7 weeks of decomposition in water. The results are similar to those shown after 3 weeks of decomposition. There is still overlap between the control and duck sample, and only very minimal separation between both species on the plot. At the same time point during the summer experiment, there was a much higher level of separation between species. The distance between the sample groups was further apart than the spread of the QC samples, providing confidence that the separation was due to the chemical signature of the water and not due to instrument variability. Although it is possible to visually differentiate between species in the winter using multivariate analysis, the separation is limited.

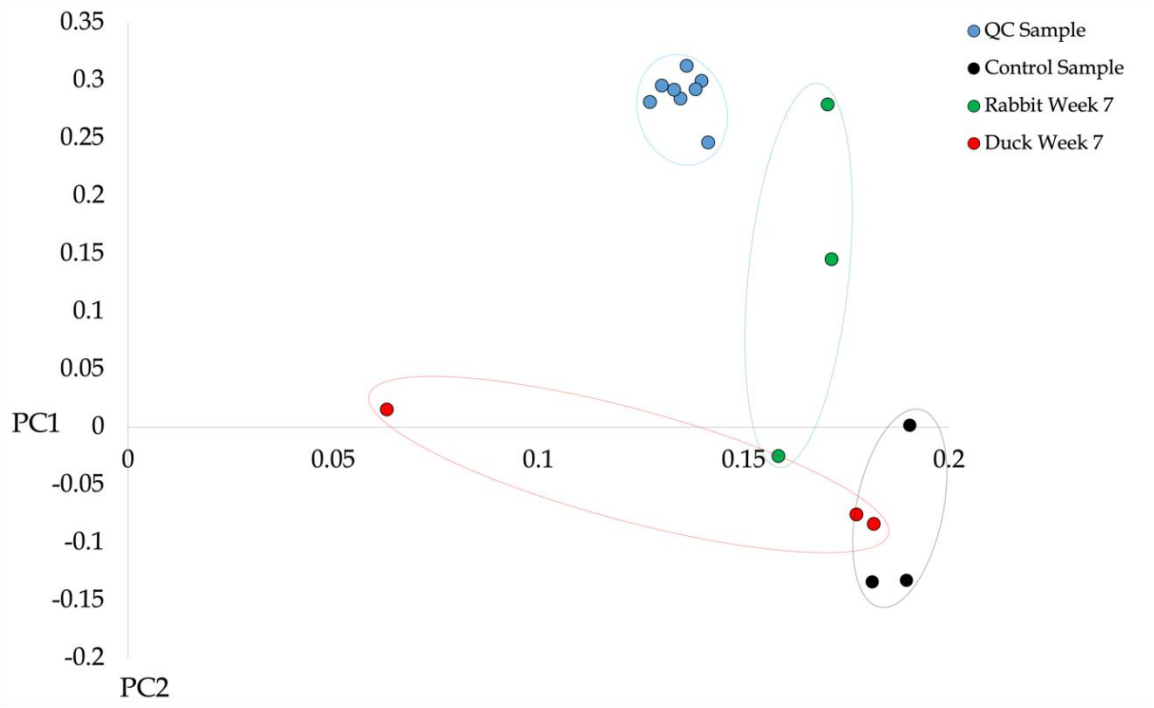

Figure 4.57: PCA scores plot of PC1 (83.95%) and PC2 (6.62%) for water samples taken after 7 weeks of decomposition in water during the winter.

4.3.4.13 Statistical analysis of week 7

Statistical analysis was performed to investigate any significant differences between species following 7 weeks of decomposition. 28 markers were significantly different with a p-value of below 0.05, while 19 markers were significantly different with a p-value of below 0.01. Of these markers, 77% of them had a *m/z* under 400, while 23% had a *m/z* over 400. This shows a further increase in the amount of smaller compounds. Table 4.14 presents the top 20 markers that were significantly different between species and shown to be the most robust and reliable.

Table 4.14: Summary of the top 20 compounds that show significant differences between species after 7 weeks of decomposition in water during the winter.

m/z	Retention time (minutes)	CV%	p-value XCMS	p-value ANOVA/Welch
116.9713	9.05	24%	p<0.001	0.008
148.0819	2.9	13%	p<0.001	0.001
151.5538	22.16	8%	p<0.001	p<0.001
180.0861	3.46	16%	p<0.001	0.009
244.1478	8.44	19%	p<0.001	0.011
285.1458	22.9	15%	p<0.001	0.011
289.1385	24.2	28%	p<0.001	0.006
296.1243	8.46	10%	p<0.001	0.009
309.1285	8.55	16%	p<0.001	0.003
320.2335	33.19	12%	p<0.001	0.006
328.1431	22.73	20%	p<0.001	0.002
346.1065	18.61	28%	p<0.001	0.004
362.3017	34.51	20%	p<0.001	0.008
372.3153	34.06	27%	p<0.001	0.008
387.1761	22.52	4%	p<0.001	0.01
446.2459	22.56	9%	p<0.001	0.007
477.2472	30.92	20%	p<0.001	0.006
657.4160	32.01	14%	p<0.001	0.01
668.3703	22.5	14%	p<0.001	0.009
939.7498	32	8%	p<0.001	0.011

The average m/z of compounds showing significant differences between species at this time point is 336.28, resulting in a consistent average throughout the analysis. It was expected that the average mass would decrease over time due to the breakdown of compounds as a result of decomposition. Figure 4.58 presents six markers chosen due to the substantial differences in peak area between each species.

It is clear that the samples from the box containing rabbit continue to show high peak areas throughout the analysis. The same cannot be said about the duck-specific markers, as their peak areas have remained low even when the markers are specific to that species.

It is natural to assume that a species developed to live in water will have a strong resistance to water.

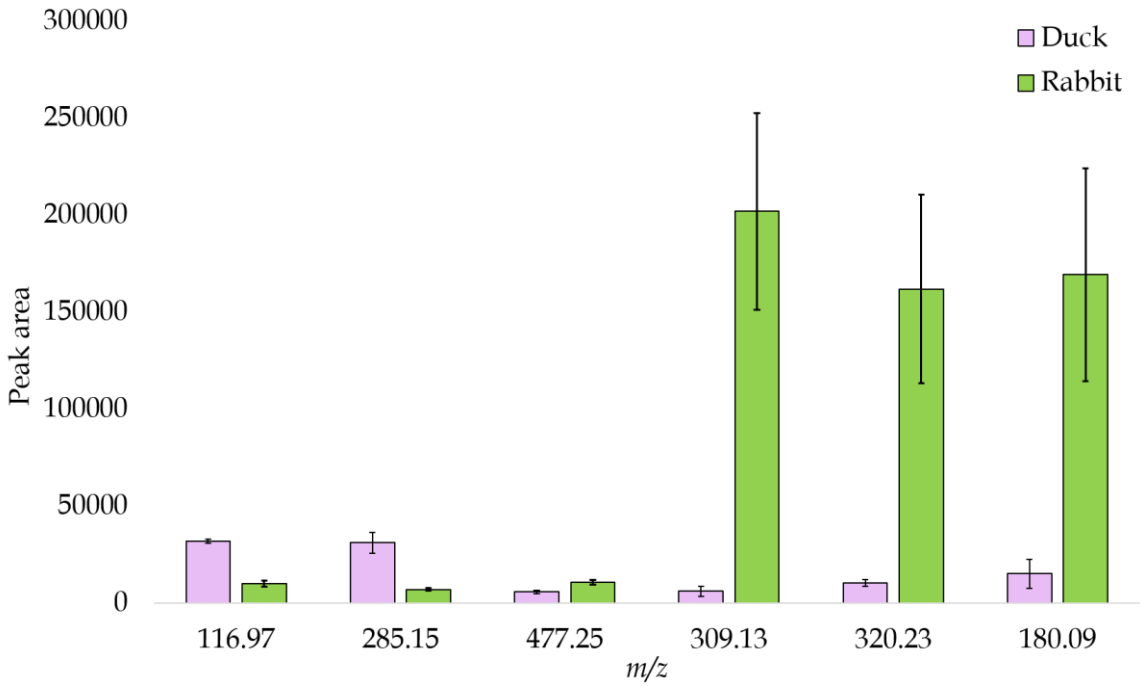

Figure 4.58: Bar chart presenting the peak area of ten chosen markers that show significant differences between species following 7 weeks of decomposition. The error bars represent ±1 standard deviation.

Two markers of interest were found following 7 weeks of decomposition in both summer and winter experiments, *m/z* 309.1285 and *m/z* 477.2472. Both are highly prevalent in the rabbit sample. Whilst the peak area for *m/z* 309.1285 is similar in both experiments, *m/z* 477.2472 presents a significantly smaller peak area in the winter experiment. This particular feature of the data highlights the ability of the method developed to identify similar markers across both seasons. This shows that not only is this method capable of detecting and monitoring the chemical signature of decomposition in the water over time in two different species, but can also detect the same compounds from different experiments.

4.4 Conclusion and Future work

A workflow created for non-targeted metabonomics using liquid chromatography-mass spectrometry successfully created a chemical profile of the water subjected to leachates from a decomposing carcass. Not only was this workflow able to use this chemical profile to monitor the progression of decomposition over time, but also show differences between the species in the water, in this case mammals and birds. When comparing the results from the summer experiment, it is clear that the temperature of the environment had a significant effect on the chemical processes and the amount of compounds in the water, however, it is still possible to detect this important chemical signature at lower temperatures.

The experiment conducted in the summer was the main focus of this study. The overlaid TIC's showed that not only are there changes over time in the chemical signature of the water during decomposition, there are also clear differences between the chromatograms for each species at various time points. The mammal and the bird showed predominantly very different peak patterns, and those peaks that were present in both sample varied in peak intensities which were almost always higher for the mammal.

The results from the PCA plots initially showed that it was possible to monitor the chemical signature of each species over time, with clear separation between the sample groups at each time interval. The control sample seemed to overlap the samples taken at week 0, however it was still possible to distinguish them as two separate sample groups. When looking at the differences between species, the PCA plots showed that the longer the carcasses were left to decompose, the better the separation between mammals and birds. Statistical analysis on the data yielded a large number of compounds showing significant differences between mammals and birds at each time interval. As each time

interval progressed, the number of markers showing significant differences nearly doubled, starting with 144 at week 0, 334 at week 3 and 720 at week 7. While it was expected to find a large number of compounds following 7 weeks of decomposition, it was remarkable that over 100 compounds were found to differentiate between species at week 0. This highlights the complexity of these metabolic processes, and how rapidly they begin after death.

The success of this experiment in identifying compounds such as Cadaverine, Creatinine and Leucine shows that this metabonomic workflow is heading in the right direction. All three compounds have shown a direct link to processes happening during various stages of decomposition, providing confidence that the combination of these methods and techniques can provide a good overview of the chemical profile of the water. Not only were these compounds showing significant differences between species at certain time intervals, their behaviour when monitoring them over time was also different. For example, samples representing the rabbit showed creatinine's peak area rapidly increasing to its highest point at week 1, followed by a steep decline. Samples representing the duck showed a delay in this peak until week 3, with a subsequent steady decline towards week 6.

When comparing the experiment conducted in the summer to that in winter, there were a variety of things to consider. Regardless of the very low temperatures during the winter experiment, it was still possible to identify a chemical signature of decomposition in the water. The number of peaks and their peak intensities on the chromatograms were much lower than those collected during the summer, however the ability of the workflow to be able to produce peaks under these conditions was remarkable. Looking at the PCA plots, it was still possible to observe minimal separation at each time interval when monitoring

over time, and between species. The distance between the sample groups for each species was much further apart at all time intervals during the summer experiment, whilst some overlap was still observed after 7 weeks of decomposition in the winter conditions.

The workflow was able to identify markers that showed significant differences between species, however, the number of compounds differed significantly. Whilst 720 compounds were showing significant differences between species in week 7 during the summer experiment, only 28 were identified at the same time interval during the winter. This major contrast suggests that the pool of compounds in the water is much smaller during the winter, which is expected due to the vast amount of research already looking at the physical effects of temperature on decomposition. Considering the average temperature recorded during the winter experiment was 5.4 °C, and 16 °C during the summer, it was impressive that the workflow was able to find so many markers showing significant differences between species during the winter experiment. This suggests that the chemical processes happening during decomposition do not cease when temperatures are low, they only slow down.

In order to explore this further, similar studies using a variety of species, with a larger number of replicates would allow the workflow to establish how effective the method is at differentiating between species. Implementing more frequent time intervals would allow a more detailed investigation of the early stages of decomposition, to determine when these drastic changes are happening within the first week of submersion. Developing this study further, and slowly applying these methods to a more realistic setting of decomposition in water allows the potential of identifying markers that could assist in the wider community.

4.5 References

[1] F. Rezazade, J. Summer, Identifying food fraud vulnerability factors in food fraud incidents - a review of global incidents 2000-2018, British Food Journal 124 (2021).

[2] M. Tabatabaei, R. Islam, M. Ahmed, Applications of gold nanoparticles in ELISA, PCR, and immuno-PCR assays: A review, Analytical Chimica Acta 1143 (2021) 250-266.

[3] L. Chang, J. Li, L. Wang, Immuno-PCR: An ultrasensitive immunoassay for biomolecular detection, Analytica Chimica Acta 910 (2016) 12-24.

[4] I. Giovannacci, C. Guizard, M. Carlier, V. Duval, J. Martin, C. Demeulemester, Species identification of meat products by ELISA, International Journal of Food Science and Technology 39 (2004) 863-867.

[5] F. Chen, P. Hsieh, Detection of Pork in Heat-Processed Meat Products by Monoclonal Antibody-Based ELISA, Journal of AOAC International 83(1) (2000) 79-85.

[6] M. Lopes, A. Soden, A. Martens, P. Henschke, P. Langridge, Differentiation and species identification of yeasts using PCR, International Journal of Systematic Biology 48 (1998) 279-286.

[7] F. Accensi, J. Cano, L. Figuera, M. Abarca, F. Cabanes, New PCR method to differentiate species in the *Aspergillus niger* aggregate, FEMS Microbiology Letters 180 (1999) 191-196.

[8] W. Jensen, M. Fall, J. Rooney, D. Kordick, E. Breitschwerdt, Rapid Identification and Differentiation of *Bartonella* Species Using a Single-Set PCR Assay, Journal of Clinical Microbiology 38(5) (2000) 1717-1722.

[9] C. Bargen, J. Brockmeyer, H. Humpf, Meat Authentication: A New HPLC-MS/MS Based Method for the Fast and Sensitive Detection of Horse and Pork in Highly Processed Food, Journal of Agricultural and Food Chemistry 62 (2014) 9428-9435.

[10] E. Bendixen, The use of proteomics in meat science, Meat Science 71 (2005) 138-149.

[11] M. Carbonaro, Proteomics: present and future in food quality evaluation, Trends in Food Science and Technology 15 (2004) 209-216.

[12] M. Montowska, E. Pospiech, Species-specific expression of various proteins in meat tissue: Proteomic analysis of raw and cooked meat and meat products made from beef, pork and selected poultry species, Food Chemistry 136 (2013) 1461-1469.

[13] M. Montowska, W. Rao, M. Alexander, G. Tucker, D. Barrett, Tryptic Digestion Coupled with Ambient Desorption Electrospray Ionization and Liquid Extraction Surface

Analysis Mass Spectrometry Enabling Identification of Skeletal Muscle Proteins in Mixtures and Distinguishing between Beef, Pork, Horse, Chicken and Turkey Meat, Analytical Chemistry 86 (2014) 4479-4487.

[14] M. Montowska, M. Alexander, G. Tucker, D. Barrett, Rapid Detection of Peptide Markers for Authentication Purposes in Raw and Cooked Meat Using Ambient Liquid Extraction Surface Analysis Mass Spectrometry, Analytical Chemistry 86 (2014) 10257-10265.

[15] A. Kleinnijenhuis, F. Holthoon, G. Herregods, Validation and theoretical justification of an LC-MS method for the animal species specific detection of gelatin, Food Chemistry 243 (2018) 461-467.

[16] D. Marchis, A. Altomare, M. Gili, F. Osrorero, A. Khadjavi, C. Corona, G. Ru, B. Cappelletti, S. Gianelli, F. Amadeo, C. Rumio, M. Carini, G. Aldini, C. Casalone, LC-MS/MS Identification of Species-Specific Muscle Peptides in Processed Animal Proteins, Journal of Agricultural and Food Chemistry 65 (2017) 10683-10650.

[17] G. Kim, J. Seo, H. Yum, J. Jeong, H. Yang, Protein markers for discrimination of meat species in raw beef, pork and poultry and their mixtures, Food Chemistry 217 (2017) 163-170.

[18] A. Stachniuk, A. Sumara, M. Montowska, E. Fornal, Liquid Chromatography-Mass Spectrometry Bottom-Up Proteomic Methods in Animal Species Analysis of Processed Meat for Food Authentication and the Detection of Adulterants, Mass Spectrometry Reviews 40 (2021) 3-30.

[19] E. Antunes, R. Duarte, T. Moritz, A. Sawaya, Differentiation of two *Maytenus* species and their hybrid via untargeted metabolomics, Industrial Crops & Products 158 (2020) 1-8.

[20] G. Buche, C. Colas, L. Fougere, T. Giordanengo, E. Destandau, Untargeted UHPLC-Q-TOF-HRMS based determination of discrimating compounds for oak species *Quercus robur* L. and *Quercus petraea* Liebl. identification, Phytochemical Analysis 32 (2020) 660-671.

[21] B. Aranha, H. J, R. Barbieri, C. Rombaldi, F. Chaves, Untargeted Metabolomic Analysis of *Capsicum* spp. by GC-MS, Phytochemical Analysis 28 (2017) 439-447.

[22] K. Yang, M. Xu, F. Zhong, J. Zhu, Rapid differentiation of *Lactobacillus* species via metabolic profiling, Journal of Microbiological Methods 154 (2018) 147-155.

[23] M. Narvaez-Rivas, Q. Zhang, Comprehensive untargeted lipidomic analysis using core-shell C30 particle column and high field orbitrap mass spectrometer, Journal of Chromatography A 1440 (2016) 123-134.

[24] M. Mazzeo, B. Giulio, G. Guerriero, G. Ciarcia, A. Malorni, G. Russo, R. Siciliano, Fish Authentication by MALDI-TOF Mass Spectrometry, Journal of Agricultural and Food Chemistry 56 (2008) 11071-11076.

[25] M. Carrera, L. Barros, B. Canas, J. Gallardo, Discrimination of South African Commercial Fish Species (*Merluccius capensis* and Merluccius *paradoxus*) by LC-MS/MS Analysis of the Protein Aldolase, Journal of Aquatic Food Product Technology 18 (2009) 67-78.

[26] K. Man, C. Chan, H. Tang, N. Dong, F. Capozzi, K. Wong, K. Kwok, H. Chan, D. Mok, Mass spectrometry-based untargeted metabolomics approach for differentiation of beef of different geographic origins, Food Chemistry 338 (2021) 1-12.

[27] M. Petrovic, S. Gonalez, D. Barcelo, Analysis and removal of emerging contaminants in wastewater and drinking water, Trends in Analytical Chemistry 22(10) (2003) 685-696.

[28] C. Zwiener, F. Frimmel, LC-MS analysis in the aquatic environment and in water treatment - a critical review, Analytical and Bioanalytical Chemistry 378 (2004) 862-874.

[29] R. Loos, G. Locoro, S. Contini, Occurrence of polar organic contaminants in the dissolved water phase of the Danube River and its major tributaries using SPE-LC-MS^2 analysis, Water Research 44 (2010) 2325-2335.

[30] L. Tong, P. Li, Y. Wang, K. Zhu, Analysis of veterinary antibiotic residues in swine wastewater and environmental water samples using optimized SPE-LC/MS/MS, Chemosphere 74 (2009) 1090-1097.

[31] F. Hernandez, J. Sancho, M. Ibanez, C. Guerro, Antibiotics residue determination in environmental waters by LC-MS, Trends in Analytical Chemistry 26(6) (2007) 466-485.

[32] L. Yao, Y. Wang, L. Tong, Y. Li, Y. Deng, W. Guo, Y. Gan, Seasonal variation of antibiotics concentration in the aquatic environment: a case study at Jianghan Plain, central China, Science of the Total Environment 527 (2015) 56-64.

[33] T. Kivits, H. Broers, H. Beeltje, M. Vilet, J. Griffioen, Presence and fate of veterinary antibiotics in age-dated groundwater in areas with intensive livestock farming, Environmental Pollution 241 (2018) 988-998.

[34] H. Lee, D. Kim, C. Kim, H. Ryu, E. Chung, K. Kim, Concentrations and Risk Assessments of Antibiotics in an Urban-Rural Complex Watershed with Intensive Livestock Farming, International Journal of Environmental Research and Public Health 18(20) (2021) 10797.

[35] M. Krauss, H. Singer, J. Hollender, LC-high resolution MS in environmental analysis: from target screening to the identification of unknowns, Analytical and Bioanalytical Chemistry 397 (2010) 943-951.

[36] A. Hogenboom, J. Leerdam, P. Voogt, Accurate mass screening and identification of emerging contaminants in environmental samples by liquid chromatography-hybrid linear ion trap Orbitrap mass spectrometry, Journal of Chromatography A 1216 (2009) 510-519.

[37] F. Gosetti, E. Mazzucco, M. Gennaro, E. Marengo, Contaminants in water: non-targeted UHPLC/MS analysis, Environmental Chemistry Letter 14 (2016) 51-65.

[38] C. Gwyther, A. Williams, P. Golyshin, G. Edward-Jones, D. Jones, The environmental and biosecurity characteristics of livestock carcass disposal methods: a review, Waste Management 31 (2011) 767-778.

[39] W. Ritter, A. Chirnside, Impact of dead birds disposal pits on ground-water quality on the delmarva peninsula, Bioresource Technology 53 (1995) 105-111.

[40] H. Hatzell, Effects of Waste-Disposal Practices on Ground-Water Quality at Five Poultry (Broiler) Farms in North-Central Florida, 1992-93, Water-Resources Investigations Report 95-4064, 1995.

[41] L. Myers, P. Bush, W. Segars, D. Radcliffe, Impact of poultry mortality pits on farm groundwater quality, Georgia water resources conference, Athens Georgia (1999) 234-239.

[42] H. Kim, K. Kim, Microbial and chemical contamination of groundwater around livestock mortality burial sites in Korea - a review, Geosciences Journal 16(4) (2012) 479-489.

[43] Z. Hseu, Z. Chen, Experiences of Mass Pig Carcass Disposal Related to Groundwater Quality Monitoring in Taiwan, Sustainability 9(46) (2017) 1-11.

[44] M. Kwon, S. Yun, B. Ham, J. Lee, J. Oh, W. Jheong, Impacts of leachates from livestock carcass burial and manure heap sites on groundwater geochemistry and microbial community structure, PLoS ONE 12(8) (2017) 1-19.

[45] J. Oh, H. Kim, J. Lee, K. Kim, K. Choi, H. Kim, S. Yun, Hydrochemical Characteristics of Groundwater in an Area Affected by Pig Carcass Burial: Leakage Detection, Journal of Soil and Groundwater Environment 23(1) (2018) 30-40.

[46] H. Lim, H. Shin, T. Jeon, S. Shin, Y. Jeung, Arachidonic acid and fatty acid profiles as indicators of contamination from the leachates of animal carcasses, Water Science & Technology Water Supply 16(5) (2016) 1287-1296.

[47] J. Choi, J. Kim, Y. Nam, W. Lee, J. Han, Comparison for compositional characteristics of amino acids between livestock wastewater and carcass leachate, Environmental Monitoring and Assessment 185 (2013) 9413-9418.

[48] T. Sana, J. Roark, X. Li, K. Waddell, S. Fischer, Molecular Formula and METLIN Personal Metabolite Database Matching Applied to the Identification of Compounds Generated by LC/TOF-MS, Journal of Biomolecular Techniques (19) 258-266.

[49] S. Law, From the stench of death to an antidote for plant aluminium toxicity, Physiologia Plantarum 167 (2019) 469-470.

[50] B. Ioan, C. Manea, B. Hanganu, L. Statescu, L. Solovastru, I. Manoilescu, The Chemistry Decomposition in Human Corpses, Revista de Chimie 68(6) (2017) 1353-1354.

[51] X. Wang, L. Yang, W. Cao, H. Ying, K. Chen, P. Ouyang, Efficient Production of Enantiopure D-Lysine from L-Lysing by a Two-Enzyme Cascade System, Catalysts 6 (2016) 168-180.

[52] H. Chou, M. Hegazy, C. Lu, L-Lysine Catabolism is Controlled by L-Arginine and ArgR in *Pseudomonas aeruginosa* PAO1., Journal of Bacteriology 192(22) (2010) 5874-5880.

[53] C. Gonzalez-Riano, S. Tapia-Gonzalez, A. Garcia, A. Munoz, J. DeFelipe, C. Barbas, Metabolomics and neuroanatomical evaluation of post-mortem changes in the hippocampus, Brain Structure and Function 222 (2017) 2831-2853.

[54] A. Vass, S. Barshick, G. Sega, J. Caton, J. Skeen, J. Love, J. Synstelien, Decomposition Chemistry of Human Remains: A New Methodology for Determining the Postmortem Interval, Journal of Forensic Sciences 47(3) (2002) 542-553.

[55] G. Pelletti, M. Garagnani, R. Barone, R. Boscolo-Berto, F. Rossi, A. Morotti, R. Roffi, P. Fais, S. Pelotti, Validation and preliminary application of a GC-MS method for the determination of putrescine and cadaverine in the human brain: a promising technique for PMI estimation, Forensic Science International 297 (2019) 221-227.

[56] M. Wyss, R. Kaddurah-Daouk, Creatine and Creatinine Metabolism, Physiological Reviews 80(3) (2000) 1107-1182.

[57] J. Brosnan, R. Silva, M. Brosnan, The metabolic burden of creatine synthesis, Amino Acids 40 (2011) 1325-1331.

[58] R. Cooper, F. Nacleiro, J. Allgrove, A. Jimenez, Creatine supplementation with specific view to exercise/sports performance: an update, Journal of the International Society of Sports Nutrition 9(33) (2012).

[59] A. Nishida, H. Funaki, M. Kobayashi, Y. Tanaka, Y. Akasaka, T. Kubo, H. Ikegaya, Blood creatinine level in postmortem cases, Science and Justice 55 (2015) 195-199.

[60] C. Platell, S. Kong, R. McCauley, J. Hall, Branched-chain amino acids, Journal of Gastroenterology and Hepatology 15 (2000) 706-717.

[61] S. Forbes, Decomposition Chemistry in a Burial Enviornment, Soil Analysis in Forensic Taphonomy, CRC Press, New York, 2008, pp. 203-223.

Chapter 5

The effect of moving and still water on the metabolic profile of water containing decomposing carrion in summer and winter.

The aim of this chapter was to use metabonomic profiling methods to investigate the effects of moving and still water on decomposing carrion, using a workflow that monitors changes to the chemical signature of the water over time. The main aim was to investigate whether the movement of water, or lack thereof, influenced the chemical signature of decomposition detectable in the water. This would help determine whether fast moving water increases or decreases the rate of decomposition. The second aim was to explore the influence of temperature. An experiment comparing summer and winter temperatures in the UK was conducted to see whether the carrion follow the same decomposition patterns in moving and still water in both seasons. If the chemical signature of the water during decomposition is shown to be influenced by different water conditions, it could encourage future research in this field. This could be taken further and applied to real-life investigations that work to find missing individuals in lakes and rivers in the UK.

5.1 Introduction

On average, 400 people drown in UK waters every year, with a further 200 people taking their own lives in these waters [1]. These have been consistent figures in the data for the last 10 years. It also a global issue, with the World Health Organisation claiming a further shocking 372,000 lives are lost each year. It is assumed that the majority of these incidents in the UK occur in coastal locations, however it has been discovered that 62% of the recorded deaths happen inland in areas such as canals, rivers, lakes and reservoirs [1]. In 44% of these incidents the person never intended to enter the water, meaning that others around might not be aware of their location.

When comparing searches for bodies in rivers and lakes, there are slight differences in the time it takes to locate them. In the last twelve months in the UK, bodies found in lakes were discovered within a few days of searching [2-4], while those in rivers were not discovered for at least a month [5-7]. While these are only a small selection of cases, a pattern emerges. Our ability to discover and retrieve human remains from water has improved by leaps and bounds in recent years. Scientific developments have not only improved the way divers approach an underwater search but have also discovered safer techniques to assist underwater. These are known as geoforensic techniques, carefully developed for effective use in water which has the potential to speed up the process. Each technique can be used in a specific body of water.

A magnetometer can be used for underwater searches, as it can detect local variations in magnetic fields caused by ferrous objects [8]. Very little has been published regarding its use for forensic casework. Sonar and side-scan sonar are also traditional instruments that can efficiently create an image of large areas of the sea floor [9]. This technique has been successfully used to detect submerged bodies [10-12], however, it cannot detect remains

wedged between large rocks and boulders. Water penetrating radar (WPR) has also been very successful using radar pulses to image the surface below the water [13-16]. With the ideal conditions being in shallow freshwater areas, limitations arise in deep or salt water. Dogs are frequently used in forensic casework to detect human remains [8, 17]. Research into their abilities at different temperatures and environments has enhanced the effectiveness of this technique [18-20]. Although dogs have been used in an attempt to locate missing persons underwater, success is limited [21]. While all these scientific advances are incredibly successful at assisting in searching for human remains under water, each technique requires very specific conditions that limit their use in certain locations. There is growing interest in looking at the chemical signature of decomposition, and how this is influenced by water [22, 23]. Further research into the use of chemical analysis in the search for missing people has the potential to eliminate these limitations and create an effective and constructive workflow.

If the use of chemical analysis is to be successful in discovering human remains in water, in depth research is essential to investigate how the different water environments affect the chemical processes happening during decomposition. These factors include salinity, pH, flow rate, temperature, pollution, and debris. Some investigation has taken place in the past on the effects of salinity on aquatic decomposition, however these are mostly based on case studies [24, 25]. A study by Ayers [26] investigated the difference between the physical signs of decomposition in terrestrial, freshwater and saltwater environments. The results showed that pigs decomposing in freshwater skeletonized on average after 11-20 days, however it was not until day 38 in the saltwater. It was also found that bodies decomposing in saltwater showed lack of protrusions following the bloating stage, compared to those in freshwater. Another study by Alley [27] at the same establishment comparing the effects of freshwater and chlorinated water observed body protrusions in

both conditions, suggesting that the lack thereof is specific to bodies exposed to saltwater. This phenomenon is likely due to the effects of osmosis. While bodies in fresh water will absorb water which increases blood volume, the saltwater will draw fluid from the blood [28]. The combination of the effects of osmosis and the retardation of bacterial activity due to the salinity decreases the rate of decomposition significantly [29].

The direct influence of flowing water and stagnant water on decomposition has yet to be investigated in detail. Previous knowledge of the stages of decomposition provides useful insight into the factors that influence the rate of decomposition. These influences will likely affect the chemical processes during decomposition, and therefore the chemical signature of the water. It is known that water will cool down much quicker than air, even more so in flowing rivers and streams. Temperature is a key factor affecting the rate of decomposition. As rigor mortis is greatly affected by water temperature, cooler water can delay its onset and prolong its duration. Livor mortis is also an important milestone during decomposition that can be influenced by the movement of the water. Fast flowing water will restrict the blood's ability to pool at the lowest point, inhibiting the development of livor mortis [30].

It has been proven that bodies are capable of traveling very long distances in rivers [31]. The majority of bodies float on the surface of the water in the early stages of decomposition due to the production of gases, increasing the body's ability to travel downstream at speed. Streams or rivers with a rough bed could cause abrasions or trap the body between large objects such as rocks, bridges or trees, causing considerable damage [30]. It is also important to consider that each body of flowing water has a unique dynamic system which will influence it's biological, physical and chemical properties [32, 33]. These differences might not always be visual, however they have the potential to

affect the chemical signature of their surroundings. The stagnation of the water in lakes or reservoirs provides the ideal conditions for bacteria growth. Insects also have easier access to bodies floating in still water compared to flowing water, increasing the ability of maggot colonisation. Scavengers also have access to remains if they are floating still near the edge of the water. Research studies in the past have often compared decomposition in a single water environment to that on land, with focus on insect activity [34, 35]. Work carried out on decomposition in water alone is limited, with most published reports looking at individual case studies based on information gained by forensic casework [24, 32, 36].

There have only been very few studies looking at how the nature of the water affects decomposition, and none of these studies feature any chemical analysis. Anderson and Hobischak [37] investigated the change in rate of decomposition in a marine environment in British Columbia, Canada. When comparing decomposition between running water and still water they immediately discovered an increase in insect activity in the still water conditions, followed by considerable damage by scavengers, which lead to skeletonization much quicker than in the running water condition. A research project at Louisiana State University by Neuman [38] investigated the effects of the flow rate in a river on carcass decomposition. A 'fast' and a 'slow' water site were chosen along a river. The initial proposition suggested that the carcass would decompose faster in fast running water due to the disturbance. The conclusion seemed to imply that the flow rate of the water had little impact on the rate of decomposition. When looking at the tabulated results, the carcass in slow moving water began to bloat sooner, it sank sooner, and was declared skeletonised at day 19. This was not the case in the fast-moving water until day 21. The differences described by observation alone might not be considered significant enough to encourage future work. When looking at this from a chemical perspective,

these small physical differences can create remarkable chemical changes which will significantly influence the chemical signature of the water in very short time intervals.

With only limited publications looking at the effects of the nature of the water on decomposition, it is important to consider the value that chemical analysis would bring to the field. Knowing that there are observational differences between decomposition in specific water environments, it is crucial to investigate whether implementing a chemical approach could provide a different perspective. If a metabonomic approach could identify a chemical signature in the water as a direct result of decomposing remains, changes within that specific signature could be monitored over time and in a variety of water environments. This would not only provide deeper insight into decomposition processes inside the body but additionally developing chemical workflows for specific bodies of water that could assist in locating missing individuals in water.

5.2 Methods and materials

5.2.1 Experimental method

5.2.1.1 Materials

The materials used are exactly as listed in **Chapter 4, Section 4.2.1.1.**

Water pumps (Set flow rate of 240L/hr, 12 volts) purchased from Thunderclap Technology, eBay UK.

5.2.1.2 Experimental setup

A total of 6 rabbit carcasses were placed in separate 60 L boxes along with 6 control boxes. Water pumps were attached to 3 of the control boxes and 3 boxes containing a rabbit carcass to create the moving water condition. The remaining boxes were assigned to the still water condition. Two holes were drilled into the lids of each box to allow airflow and insect activity. Each box was filled with 40 L of water from a single source and placed outside. Temperature probes were used to monitor the temperature of the water and the air every 15 minutes.

Experiment 1 ran for eight weeks from July to September, while Experiment 2 ran for eight weeks from January to March. Each week, a total of 12 samples were taken: 3 control water samples from the moving water condition, 3 control samples from the still water condition, 3 samples from the boxes containing rabbit in moving water and 3 samples from the boxes containing rabbit in still water. In this particular experiment, only samples from week 0^1, 3 and 4 were analysed to limit analysis time in order to minimise the risk of instrumental drift. As the aim of the experiment was to investigate whether it is

possible to detect chemical changes over time in the water, a sample from the beginning, middle and end of the experiment was sufficient to achieve proof of concept. In total 54 samples (3 treatments at 3 time intervals with 3 replicates each in summer and winter conditions) were analysed.

5.2.1.3 Sample collection and preparation

This was carried out exactly as described in **Chapter 4**, section **4.2.1.3.**

5.2.1.4 Solid-phase extraction

This was carried out exactly as described in **Chapter 3, Section 3.2.2.3**.

5.2.2 Instrumental setup

5.2.2.1 Quality control

This was carried out exactly as described in **Chapter 3, Section 3.2.3.1**.

5.2.2.2 Chromatographic parameters

This was carried out exactly as described in **Chapter 3, Section 3.3.5.2.**

5.2.2.3 Mass spectrometry parameters

This was carried out exactly as described in **Chapter 3, Section 3.2.3.3**.

5.2.3 Data pre-processing

This was carried out exactly as described in **Chapter 3, Section 3.2.4.**

5.2.4 Data analysis and statistical analysis

This was carried out exactly as described in **Chapter 3, Section 3.2.5.**

5.2.5 Identification of markers

This was carried out exactly as described in **Chapter 4**, section **4.2.5**.

5.3 Results and discussion

5.3.1 Temperature

A major focus point of this experiment was how the temperature of the environment affects the chemical signature of a decomposing carcass over time. Additionally, it was important to investigate how the temperature may influence decomposition in both moving and still water conditions. Figure 5.1 presents the average temperature at each week of the experiment, along with the highest and lowest value for that week. There are clear differences between the temperature during the summer and winter. While the temperature seems to stay reasonably consistent in winter, there is much more fluctuation in temperature during the summer.

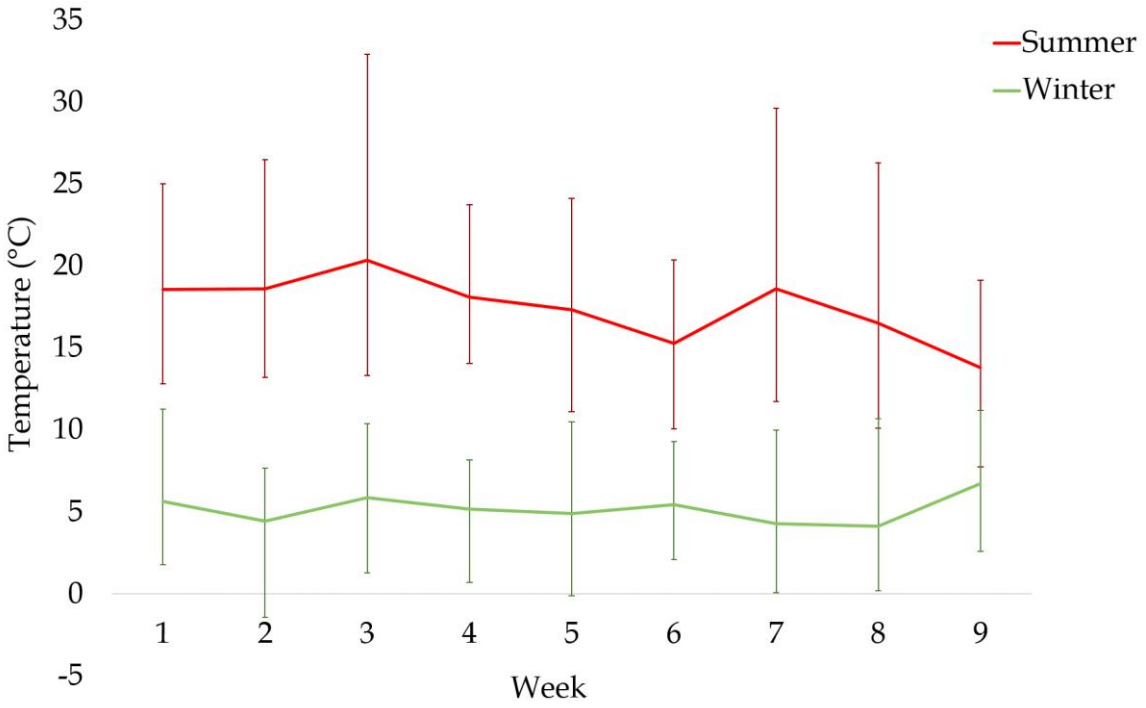

Figure 5.1: Graph showing the average change in temperature over a 9-week period during the summer and winter experiments.

5.3.2 Difference in the metabolite profile of a carcass decomposing in moving and still water during the summer months.

5.3.2.1 The physical changes visible during the decomposition process of rabbits in moving and still water during the summer months.

Observations were recorded throughout the experiment to collect data on the physical changes occurring as a result of decomposition at various time points. This allowed additional exploration of the differences between carcass decomposition in moving and still water conditions. Recording the physical changes over time also created an opportunity to match a particular stage of decomposition to any differences found in the chemical signature of the water over time.

On the first day of the experiment, each carcass was floating on the surface of the water. Insect activity began on the second day, increasing substantially each day. Figure 5.2 presents the images of each carcass in the moving and still water conditions after 6 days of decomposition in water. Insects continue to swarm around each carcass. All carcasses were exhibiting bloating of the abdomen, and the water turned a pale yellow colour. One carcass from the moving water condition had already experienced ruptures in the skin, exposing the internal organs.

A **B**

Figure 5.2: Images of 3 rabbit carcasses in moving water (A) and 3 in still water (B) following 6 days of decomposition in summer conditions.

Eight days after submersion (Figure 5.3), eggs laid by the flies had hatched on the carcasses in the still water condition, with maggots colonising the internal organs. One carcass in the still water condition was surrounded by foam. On the ninth day of the experiment, maggots had also colonised each carcass in the moving water condition. A strong odour of putrefaction (rotting meat) was evident when standing above the boxes.

A **B**

Figure 5.3: Images of 3 rabbit carcasses in moving water (A) and 3 in still water (B) following 8 days of decomposition in summer conditions.

Figure 5.4 presents one carcass from the moving water condition, and one from the still water condition at day 9, 10, 13 and 17 of the summer experiment.

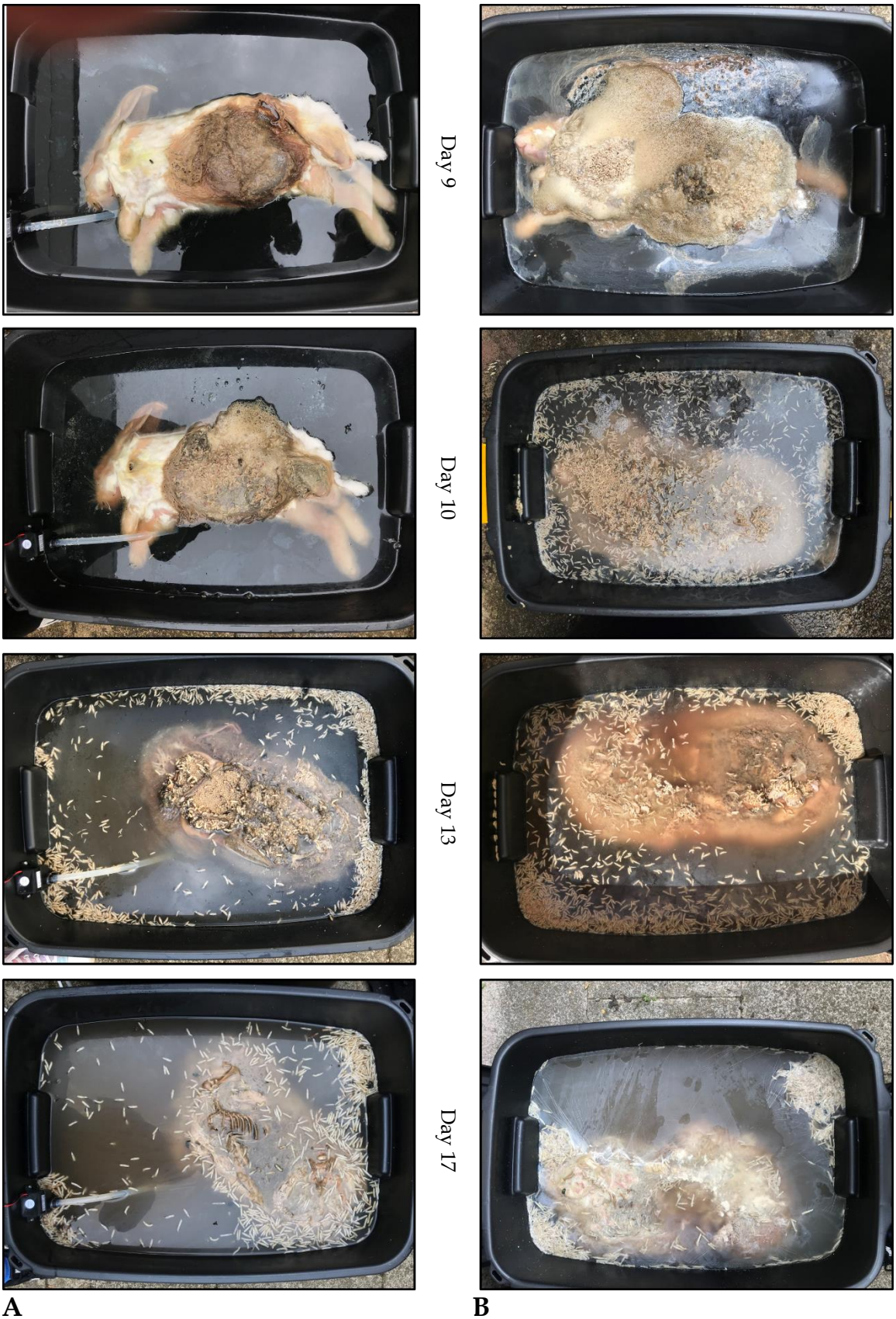

Figure 5.4: Images of one rabbit from the moving water box (A), and one from the still water box (B) on days 9, 10, 13 and 17 of the experiment in summer conditions.

On the ninth day of the experiment, the maggots had colonised each carcass, and were surrounding the exposed organs. In the still water condition, foam had surrounded the carcasses with a large number of maggots everywhere. In the moving water box, the maggots were condensed toward the internal organs, with no foam.

On the tenth day, the bloating had subsided and the rib cage was visible on carcasses in both the moving and still water. Foam had surrounded the maggots in the moving water condition, as the infestation intensified. The carcass in the still water condition began to sink below the surface of the water, with drowned maggots floating on the surface. A very strong odour was present even when standing further away from the site.

Thirteen days after submersion, maggot activity had come to an end on all carcasses in the still water condition, with many of them floating on the surface. Maggot activity was still present in the moving water boxes, as the carcass was still above water, exposing more of the ribcage. While the colour of the water was still a pale yellow in the moving water boxes, the water in the still condition had turned orange-brown. The odour was now more intense surrounding the still water boxes.

On day 17, the carcasses had sunk under the surface of the water. A thick layer of the white film had now formed on the surface of the still water box, while the water was only starting to turn an orange-brown colour in the moving water. The odour from both water conditions was now pungent and difficult to avoid when entering the enclosed area.

Figure 5.5 consist of two images taken on the 20th day of the experiment. At this stage, all carcasses had sunk under the surface of the water There was a layer of film on the top of each box from both water conditions, with the water appearing brown under the surface. No further changes were observed toward the end of the experiment.

A **B**

Figure 5.5: Images of 3 rabbit carcasses in moving water (A) and 3 in still water (B) following 20 days of decomposition in summer conditions.

5.3.2.2 QC analysis

Figure 5.6 shows the chromatograms of QC samples 1-11. QC samples 1-5 were used at the beginning to condition the column, and QC samples 6-11 were placed every five samples during the analysis. There seems to be slight variation in the baseline at the beginning, however the retention time seems stable throughout.

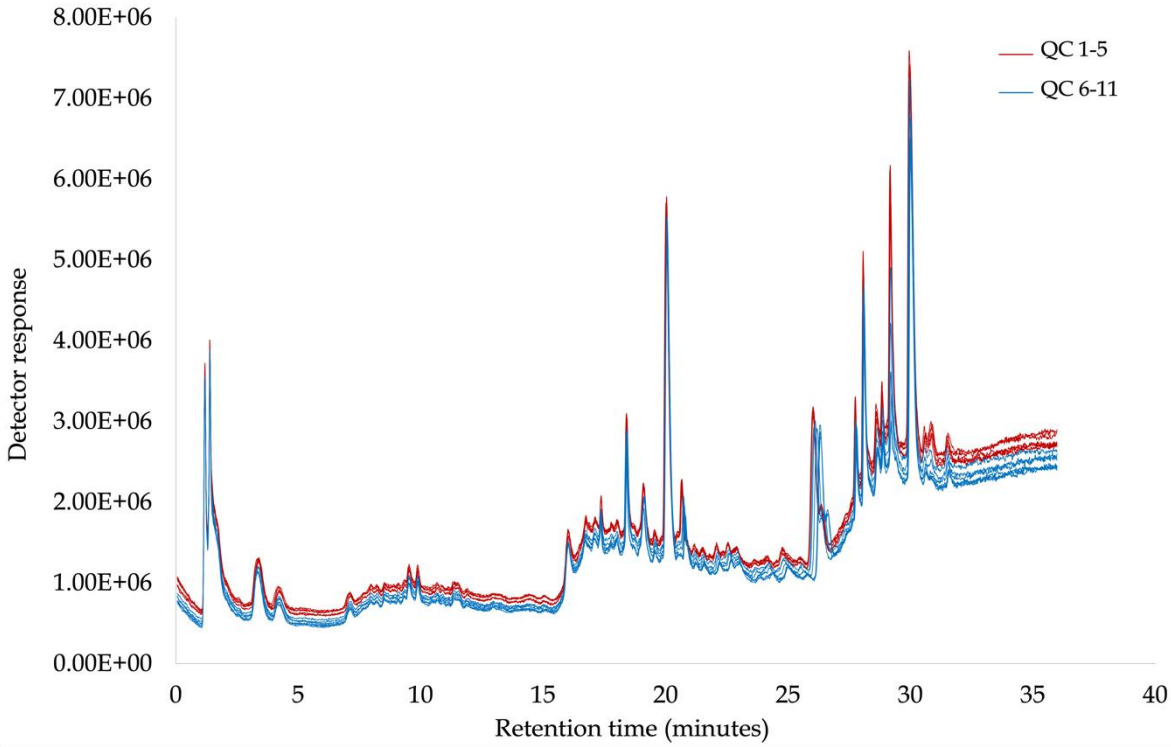

Figure 5.6: Total ion chromatograms of 11 QC samples throughout the analytical run for water samples taken from both summer and winter experiments.

Table 5.1 looks in detail at the variability in the peak area and retention time throughout the analysis by calculating the coefficient of variance (CV) value for six selected peaks. The highest CV value for the peak areas was 13%, and 0.12% for retention time. This result reflects the observations from the chromatograms above, and are well under the accepted variation for untargeted metabonomic analyses.

Table 5.1: Variability of peak area (A) and retention time (B) from 6 selected peaks in the QC samples during the analytical sequence for water samples taken from both summer and winter experiments.

A

Peak	QC6	QC7	QC8	QC9	QC10	QC11	Average	St. Dev	CV%
1	1293313	1314247	1276757	1253914	1267156	1177988	**1263896**	**47024**	**4%**
2	1664429	1603694	1617638	1568491	1558979	1523981	**1589535**	**49544**	**3%**
3	2065615	2035277	2045248	2035363	2033529	1914512	**2021591**	**53820**	**3%**
4	3100131	2887527	3076720	3054917	2972586	2891601	**2997247**	**93845**	**3%**
5	2234682	2106044	2187655	2176867	2118443	2040265	**2143993**	**69374**	**3%**
6	2268865	2045264	2008983	1991039	1949601	1506968	**1961787**	**249542**	**13%**

B

RT	QC6	QC7	QC8	QC9	QC10	QC11	Average	St. Dev	CV%
1	3.39	3.38	3.39	3.39	3.39	3.39	3.39	0.0040	0.12%
2	16.02	16.01	16.02	16.02	16.01	16.02	16.02	0.0040	0.03%
3	17.36	17.35	17.36	17.36	17.36	17.37	17.36	0.0041	0.02%
4	18.41	18.40	18.40	18.40	18.40	18.41	18.40	0.0042	0.02%
5	19.08	19.08	19.08	19.08	19.08	19.09	19.08	0.0044	0.02%
6	20.64	20.63	20.64	20.64	20.64	20.65	20.64	0.0040	0.02%

5.3.2.3 Metabolic profiling

Figure 5.7 shows the chromatograms for the samples taken at week 0, 3 and 7 from the moving water condition. The chromatogram from week 0 shows only a small number of peaks, with low peak intensities. The chromatogram at week 3 shows not only an increase in the number of peaks, but also an increase in peak intensities. The chromatogram presented for week 4 shows a significant increase in peak intensities throughout the chromatogram. These results suggest that the quantity of compounds increases over time in moving water.

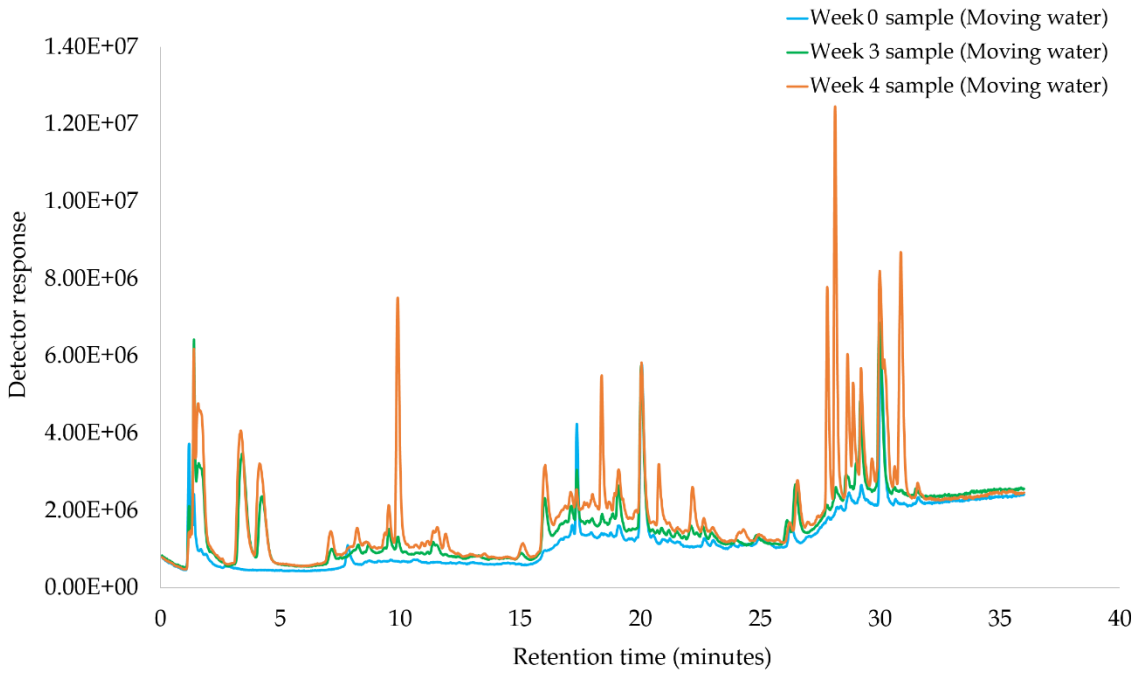

Figure 5.7: Example total ion chromatogram (TIC) of water samples containing a decomposing carcass in moving water at week 0, 3 and 4 of the summer experiment.

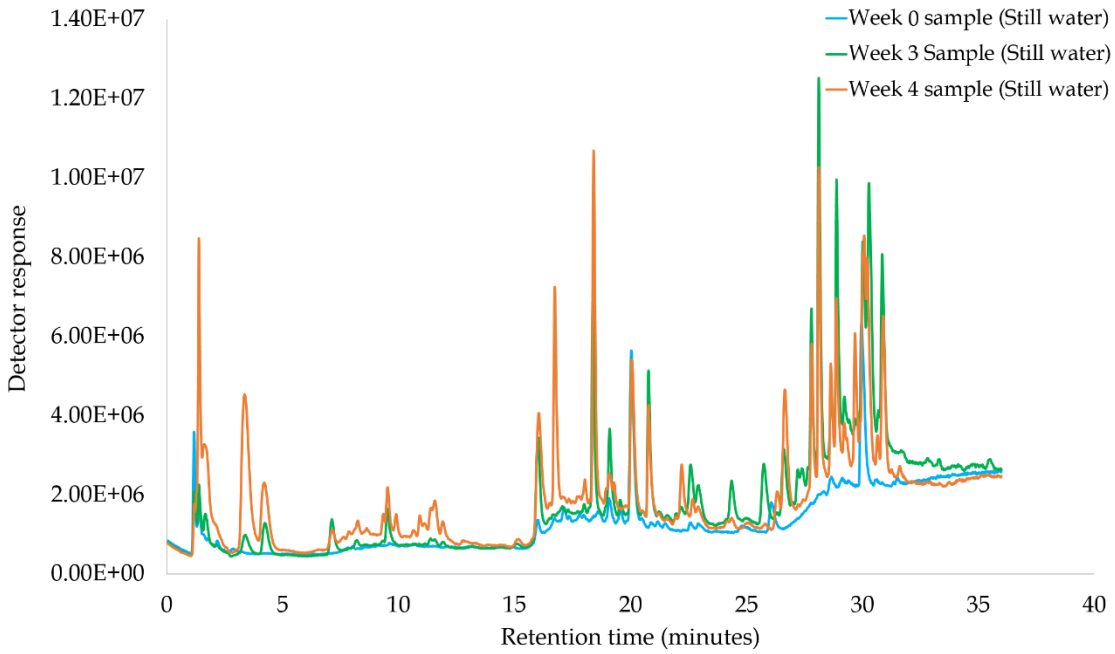

Figure 5.8: Example total ion chromatogram (TIC) of water samples containing a decomposing carcass in still water at week 0, 3 and 4 of the summer experiment.

Figure 5.8 shows the chromatograms for samples taken at three time intervals in still water. Whilst the sample taken at week 0 presents very limited information in the chromatogram, the sample from week 3 shows an increase in the number of peaks present between 15-35 minutes, dominating the chromatogram between these times. The peak intensities in the chromatogram representing week 4 are higher overall between 0-20 minutes. One particular peak at 17 minutes is only present in the chromatogram representing week 4.

5.3.2.4 Multivariate analysis

The PCA scores plot in Figure 5.9 shows the separation between the control samples, and samples taken at three time intervals of a carcass decomposing in moving water. The QC samples are clustered together, indicating good instrument stability. The control samples and samples taken after 0 weeks of decomposition are overlapping completely. All three time intervals show good separation. The distance between each sample group is further apart than the spread of the QC samples, giving confidence that these differences are due to changes to the chemical signature of the water, and not instrumental effects. The replicates within each sample group seem to spread out more over time. The complexity of the metabolic processes can create more variability over time, even under the same conditions.

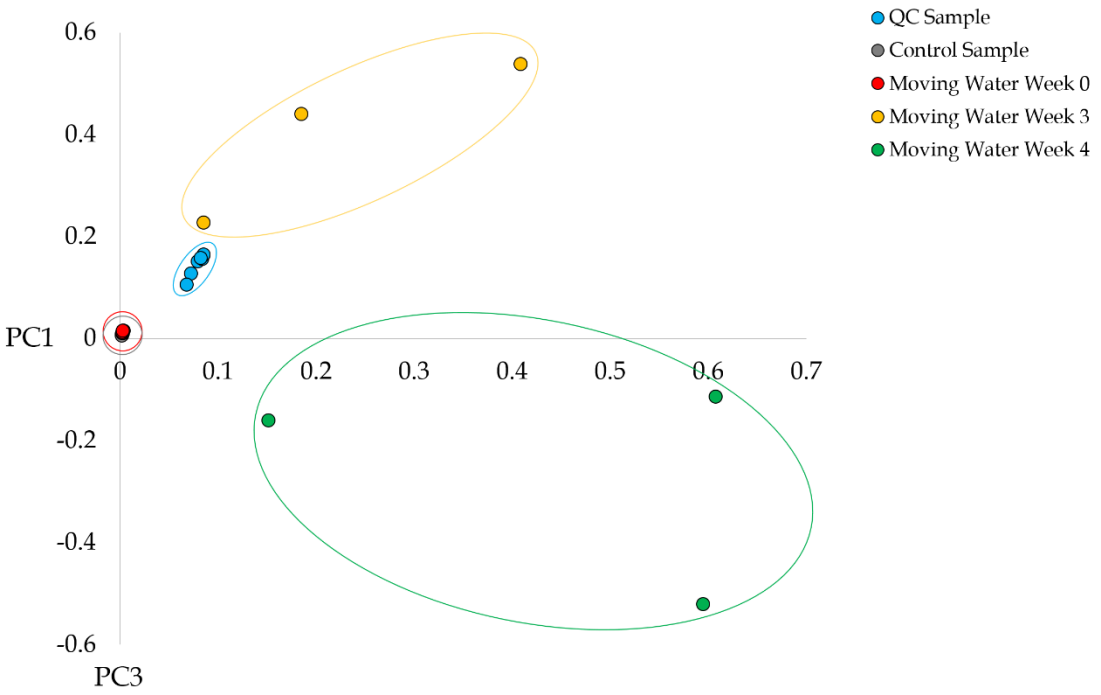

Figure 5.9: PCA scores plot of PC1 (81.95%) and PC3 (3.52%) for water samples containing a decomposing carcass in moving water at week 0, 3 and 4 of the summer experiment.

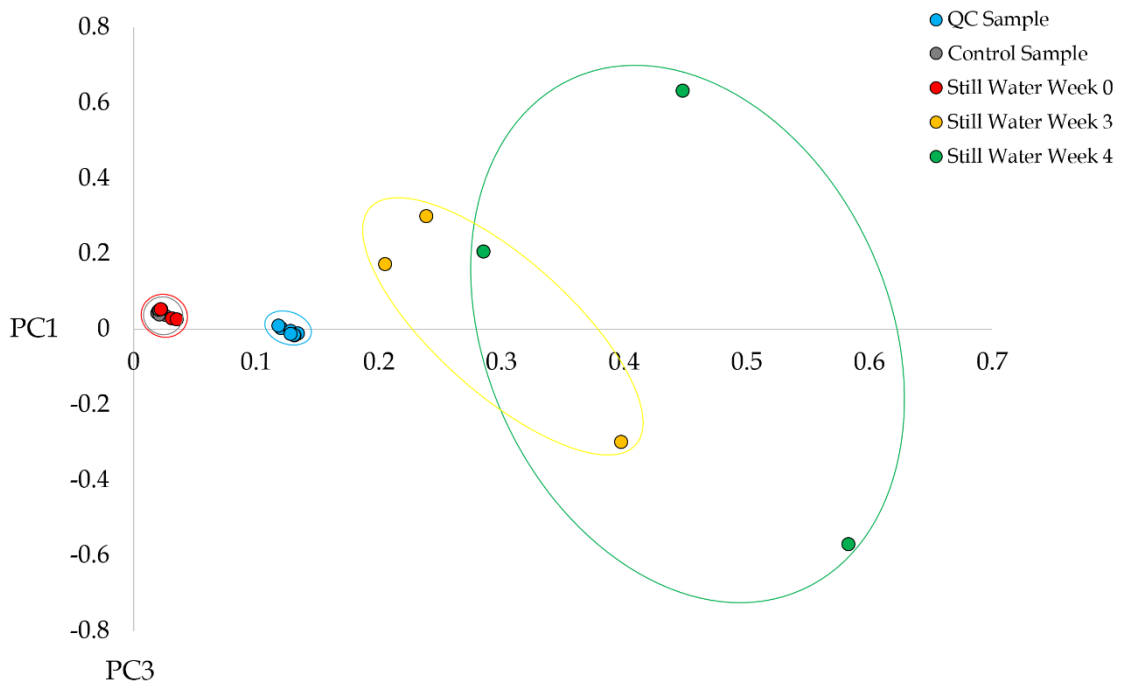

Figure 5.10: PCA scores plot of PC1 (67.89%) and PC3 (9.19%) for water samples containing a decomposing carcass in moving water at week 0, 3 and 4 of the summer experiment.

The PCA scores plot in Figure 5.10 represents the water samples taken from the still water condition. The QC samples are tightly clustered toward the middle of the plot. Similar to the moving water condition, the control samples and samples taken after 0 weeks of decomposition are overlapping. Still water samples from weeks 3 and 4 also show slight overlap, and as a result do not show strong separating power over time in comparison to the moving water condition.

The PCA scores plot in Figure 5.11 presents the samples taken at three time points in both moving and still conditions, accompanied by the control sample. The QC samples are clustered together toward the middle of the plot, showing good instrument stability. The control samples, and those taken after 0 weeks of decomposition in moving and still water are overlapping on the scores plot. Sample groups from weeks 3 and 4 of the experiment are clearly separated in both conditions, and furthermore, separated from each other.

It is important to note that higher order principal components were used to achieve this level of separation on the plot for both moving and still water samples. This suggests that the differences causing these separations are very discreet.

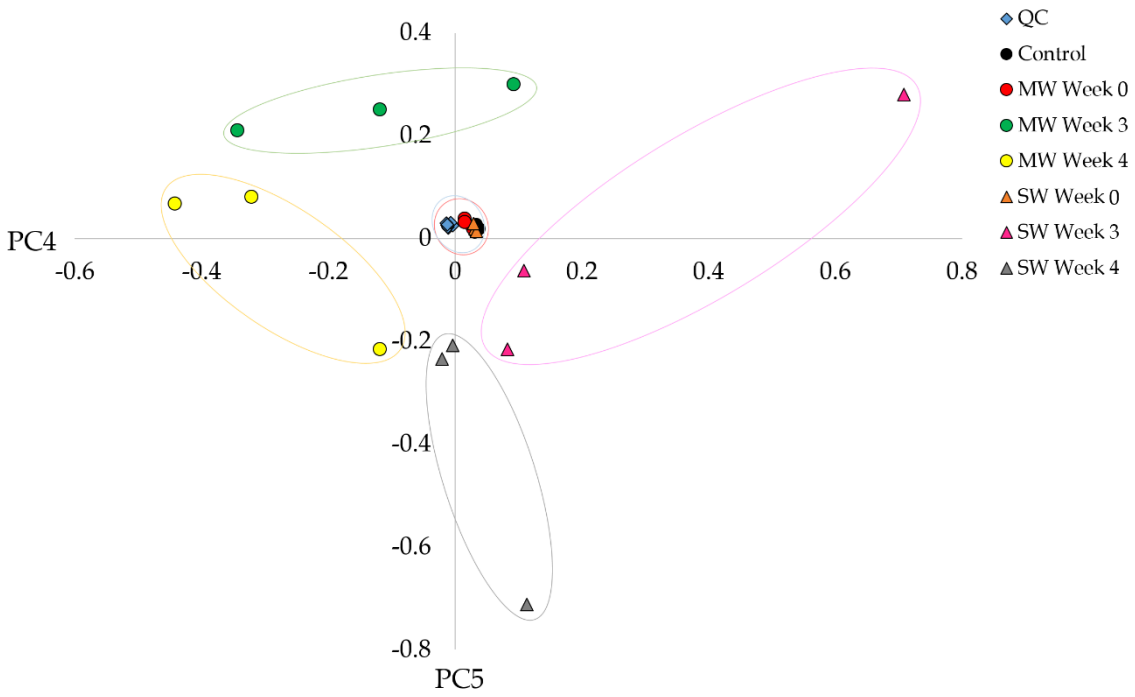

Figure 5.11: PCA scores plot of PC4 (2.83%) and PC5 (1.10%) for water samples containing a decomposing carcass in moving and still water at week 0, 3 and 4 of the summer experiment.

5.3.2.5 Statistical analysis

The total number of features detected in the water samples through *XCMS online* was 2195. All features with a CV value of 30% or more were removed, with 1794 remaining. Statistical analysis was performed on water samples from boxes with both moving and still water conditions. 12 compounds were found showing significant differences over three time points in moving water, and 71 in still water. Of these markers, the top 20 from each condition are shown in Table 5.2 and Table 5.3. There are only 12 markers for the moving water condition.

Table 5.2: Summary of the markers that show significant differences over time of water samples taken from a carcass decomposing in moving water during the summer experiment.

m/z	Retention time (minutes)	CV%	p-value	
			Compounds showing significant differences between	
			Week 0 and Week 3	Week 3 and Week 4
136.1053	1.33	9%	0.048	0.008
138.1138	2.2	12%	0.019	0.038
155.1465	1.44	2%	0.002	0.04
162.1768	1.33	7%	0.031	0.026
172.2419	20.3	16%	0.001	0.041
199.2037	17.96	14%	p<0.001	0.022
207.2340	12.24	2%	0.013	0.033
258.1943	1.44	12%	0.035	0.015
370.4100	29.12	16%	0.002	0.002
407.3535	28.43	9%	0.009	0.044
421.2395	16.01	16%	0.022	0.001
423.2414	16.01	16%	0.002	0.032

The fact that there were only 12 markers showing significant differences between the time points analysed from the moving water conditions suggests that the nature of the water a carcass is decomposing in will have a notable effect on the chemical signature of the water and how it changes over time. There are many things to consider when comparing

both tables. The masses presented in the samples taken from the still water condition seem to be greater than in the moving water, with the highest recorded *m/z* being 639.6454, compared to *m/z* 423.2414 in the moving water sample. The p-values in the table representing the still water sample are overall much lower than the p-values in the table representing moving water. Further investigation would determine whether this is caused by more impactful chemical changes occurring in the still water boxes. Both *m/z* 155.1465 and *m/z* 162.1768 are present in both tables, showing that similar products are appearing, however it is important to investigate the difference in their behaviours. These compounds are small and likely breakdown products of larger compounds.

Table 5.3: Summary of the markers that show significant differences over time of water samples taken from a carcass decomposing in still water during the summer experiment.

m/z	Retention time (minutes)	CV%	p-value	
			Compounds showing significant differences between	
			Week 0 and Week 3	Week 3 and Week 4
145.1935	1.44	10%	0.003	0.006
155.1465	1.44	2%	0.046	0.009
157.0961	9.36	10%	0.001	0.011
162.1768	1.33	7%	0.016	0.018
195.2080	22.83	8%	0.002	0.019
237.1545	17.4	26%	0.006	0.01
245.1630	1.52	8%	0.018	0.004
282.3409	27.75	18%	<0.001	0.007
292.2977	28.18	13%	0.016	0.014
301.3706	28.08	15%	<0.001	0.020
304.1555	17.39	11%	0.007	0.009
323.5543	28.06	15%	<0.001	0.005
330.3485	29.83	15%	0	0.008
335.2987	27.09	27%	<0.001	0.002
345.3415	28.08	11%	<0.001	0.009
349.3186	27.72	8%	0.005	0.008
383.3244	27.74	25%	0.002	0.007
450.4820	34.27	20%	0.001	0.011
623.6699	28.07	9%	<0.001	0.011
639.6454	28.07	7%	0.003	0.013

Figure 5.12 presents bar charts showing the progression of the two markers identified in the top 20 table for both moving and still water conditions, *m/z* 155.1465 and *m/z* 162.1549. Both markers show a very similar pattern. The sample from moving water seems to have a higher peak area up until week 3, whilst still water has a large increase in peak area at week 4. The control water is stable over time, confirming that the changes occurring are influenced by the decomposing carcass, not natural changes in the water itself. The presence of any compound in the control water sample is so small, it is likely attributed to instrument or column carryover. Further analysis is needed to assess whether this is the case or the extent of it.

Although similar markers are showing significant differences over time in moving and still water conditions, their behaviour in each condition is very different. This suggest that the nature of the water can affect the speed and behaviour of these complex metabonomic processes during decomposition. A detailed investigation into each time point during the experiment will establish the extent of these differences.

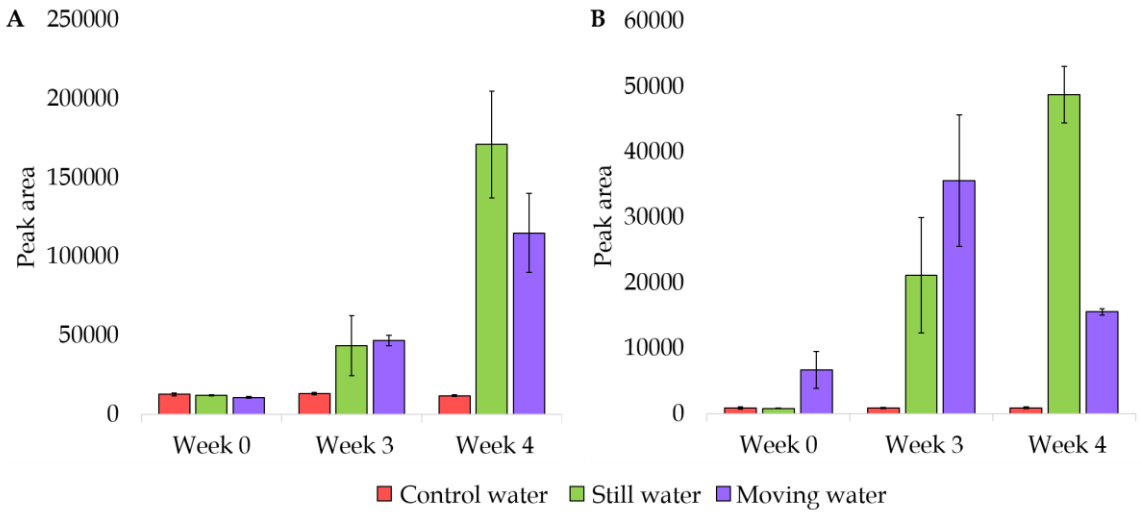

Figure 5.12: Bar charts showing the progression of two markers over three time points showing significant differences in both moving and still water conditions in summer. (A: m/z 155.1465, B: m/z 162.1549).

5.3.2.6 Metabolic profiling of week 0

The total ion chromatograms (TIC) from the analysis of samples taken from moving and still water following 0 weeks of decomposition are shown in Figure 5.13. It is important to note that these particular samples were taken on day 2. The chromatogram representing the moving water sample contains two peaks that are not present in still water samples at 7 and 17 minutes into the analysis. Despite this, the peak intensities for those that are present in both samples are higher in the still water samples.

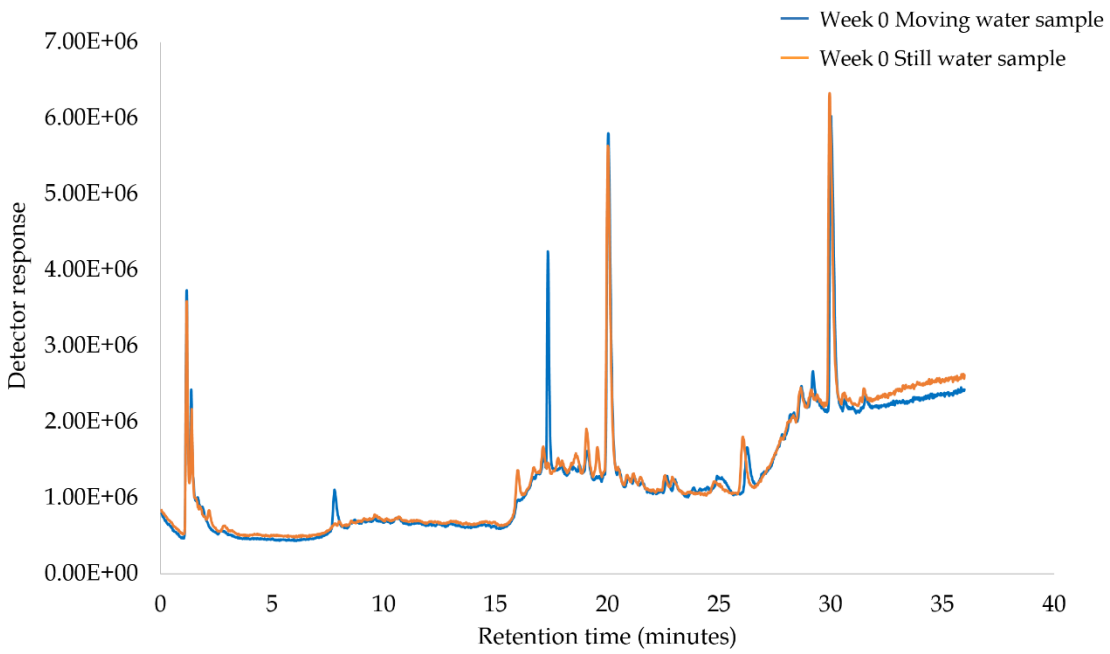

Figure 5.13: Example total ion chromatograms (TIC) of water samples taken after 0 weeks of decomposition in moving and still water during the summer.

5.3.2.7 Multivariate analysis of week 0

The PCA scores plot in Figure 5.14 presents the samples taken after 0 weeks of decomposition in moving and still water accompanied by a control sample. The QC samples are clustered together. The samples taken from the still water boxes are overlapping the control samples, while the moving water sample is slightly separated from the control. This is not unexpected as the samples were taken during the early stages of decomposition. The poor separation on this plot reflects the very few peaks showing differences between water conditions on the chromatograms.

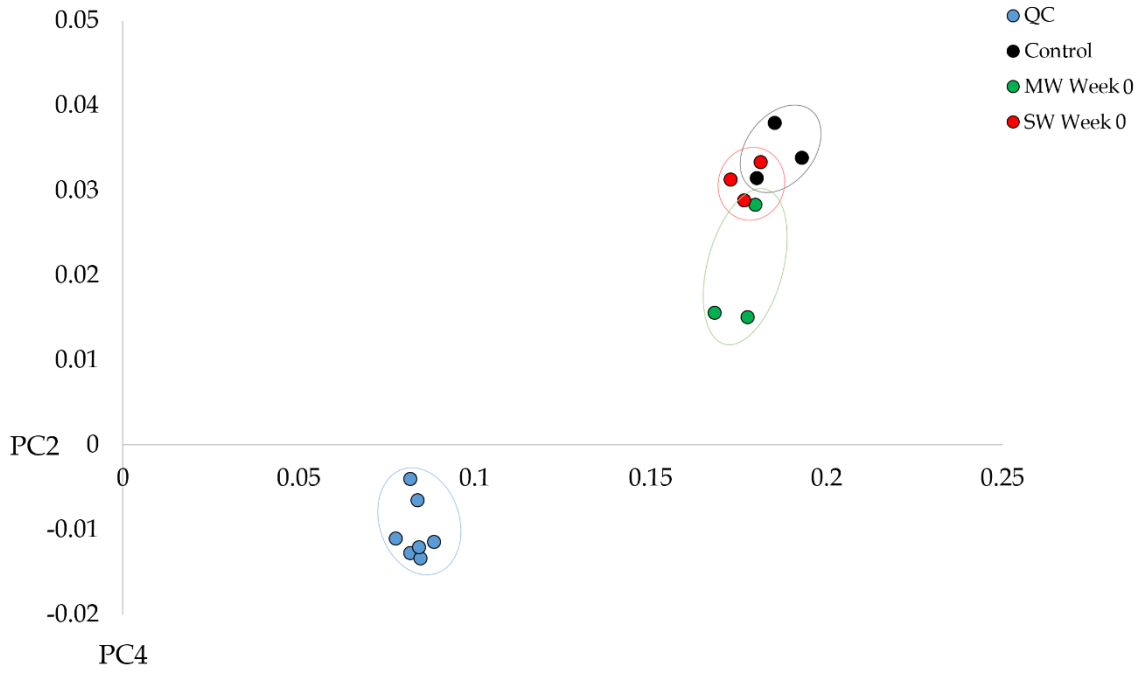

Figure 5.14: PCA score plot of PC2 (19.41%) and PC4 (2.82%) for water samples taken after 0 weeks of decomposition in moving and still water during the summer.

5.3.2.8 Statistical analysis of week 0

Statistical analysis was performed to investigate any significant differences between decomposition in different water conditions following 0 weeks of decomposition. 58 markers were significantly different with a p-value of below 0.05. Of these markers, 81% of them have a *m/z* under 400, while 19% have a *m/z* over 400. This is an unusual split during the early stages of decomposition, as larger compounds are expected at this time. Table 5.4 presents the top 20 markers that were significantly different between water conditions and shown to be the most robust and reliable.

Table 5.4: Summary of the top 20 compounds that show significant differences between water conditions after 0 weeks of decomposition in water during the summer.

m/z	Retention time (minutes)	CV%	p-value XCMS	p-value ANOVA/Welch
126.0454	1.17	29%	0.011	0.045
133.1567	1.27	10%	0.048	0.048
163.1792	17.79	8%	0.005	0.005
167.1381	19.59	16%	0.043	0.043
187.1653	33.74	24%	<0.001	<0.001
195.1759	19.58	3%	0.026	0.026
201.1191	16.14	3%	0.029	0.029
203.1826	17.79	17%	0.001	0.001
218.1700	19.59	12%	0.02	0.02
222.2627	23.82	7%	0.009	0.009
229.9744	1.18	21%	0.01	0.011
279.1497	19.58	9%	0.032	0.032
299.3523	29.01	4%	0.041	0.041
315.2399	21.52	7%	0.015	0.015
331.3084	16.76	6%	0.02	0.022
387.2938	18.8	4%	0.007	0.007
404.3250	18.8	4%	0.006	0.006
409.2788	18.8	2%	0.003	0.003
415.3927	33.22	2%	0.005	0.006
425.2573	18.8	5%	0.019	0.019

The retention times presented in the table above are mostly toward the end of the analytical run. This result was expected, as most compounds eluting at this time are the larger compounds. However, the average mass calculated from the table is *m/z* 265.71, which is much smaller than expected considering the retention time trends.

The bar chart in Figure 5.15 shows the peak area of the top 10 compounds from the table, including the control, moving and still water sample. Samples taken from the moving water condition seem to have the highest peak area overall. The majority of the markers have low peak areas, which is expected in the early stages of decomposition. There were no obvious signs of decomposition during the physical observations, therefore these changes are occurring discreetly under the surface.

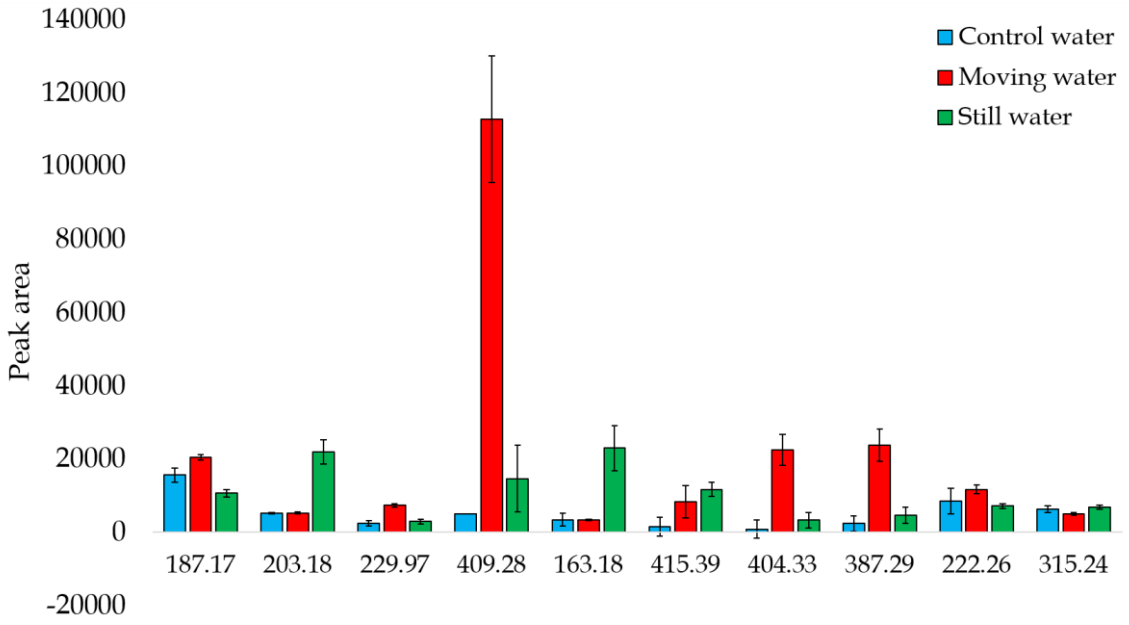

Figure 5.15: Bar chart showing the peak area of the top 10 markers identified as significantly different between moving and still water condition after 0 weeks of decomposition in summer.

5.3.2.9 Metabolic profiling of week 3

The chromatograms in Figure 5.16 show a dramatic increase in the number of peaks and overall peak intensities at week 3 of the experiment in both moving and still water conditions. The peak intensities of the moving water sample seem to dominate the chromatogram between 0-15 minutes, while the still water chromatogram has higher peak intensities between 15-35 minutes. This result implies that smaller compounds are dominating the moving water sample, while larger compounds are more prominent in the still water sample. One of the potential reasons for this is the larger compounds have already broken down into smaller ones in the moving water sample.

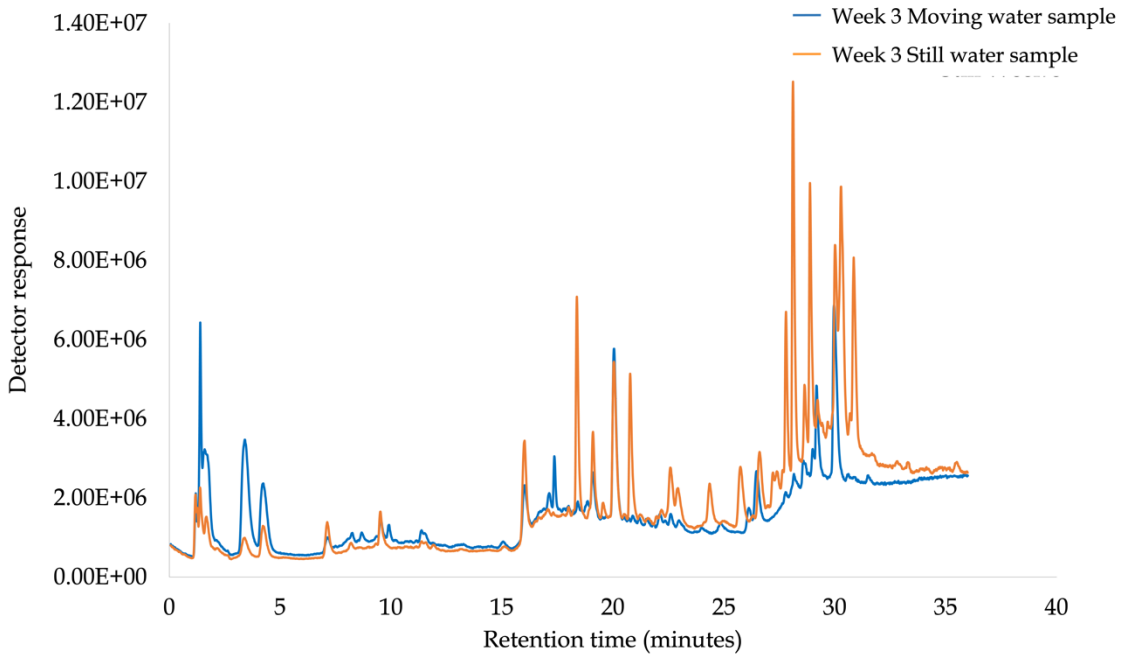

Figure 5.16: Example total ion chromatograms (TIC) of water samples taken after 3 weeks of decomposition in moving and still water during the summer.

5.3.2.10 Multivariate analysis of week 3

Figure 5.17 presents the PCA scores plot for the control samples and samples taken from moving and still water conditions following 3 weeks of decomposition in water. The QC samples are clustered together, highlighting good instrument stability. There is increased separation between the sample groups and the control samples in comparison to week 0. The moving and still water samples are slightly overlapping on the plot, suggesting that there are some similarities between their chemical profile. The samples taken from the moving water box seem to spread out more across the plot, indicating more variability within the experimental condition.

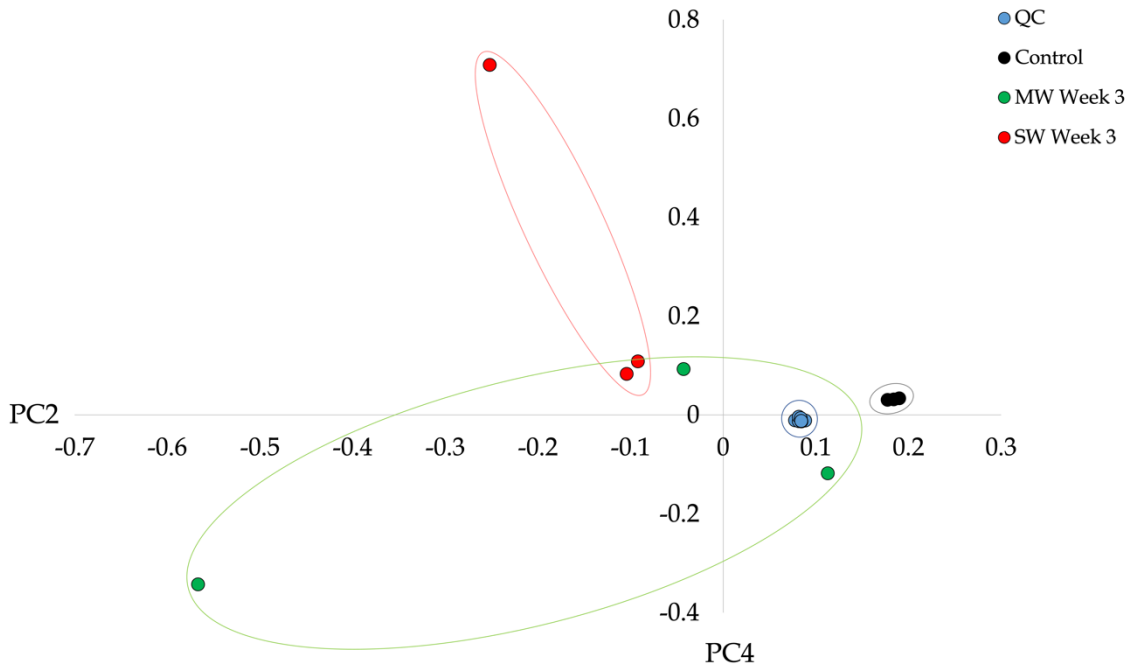

Figure 5.17: PCA score plot of PC2 (16.52%) and PC4 (1.63%) for water samples taken after 3 weeks of decomposition in moving and still water during the summer.

5.3.2.11 Statistical analysis of week 3

Statistical analysis was performed to investigate any significant differences between decomposition in different water conditions following 3 weeks of decomposition. 78 markers were significantly different with a p-value of below 0.05. Of these markers, 49% of them have a *m/z* under 400, while 51% have a *m/z* over 400. This shows that the balance between the smaller and larger compounds are reasonably equal at this time interval. Table 5.5 presents the top 20 markers that were significantly different between water conditions and shown to be the most robust and reliable.

Table 5.5: Summary of the top 20 compounds that show significant differences between water conditions after 3 weeks of decomposition in water during the summer.

m/z	Retention time (minutes)	CV%	p-value XCMS	p-value ANOVA/Welch
130.1094	1.65	17%	0.019	0.019
163.1792	17.79	8%	0.01	0.01
167.1381	19.59	16%	0.028	0.028
194.2234	20.29	19%	0.007	0.008
205.0349	32.37	19%	0.005	0.005
257.2365	21.52	11%	0.023	0.023
299.3523	29.01	4%	0.032	0.032
323.2036	19.16	7%	0.01	0.01
387.2938	18.8	4%	0.003	<0.001
409.2788	18.8	2%	<0.001	<0.001
467.4391	27.64	5%	0.041	0.041
485.4706	28	5%	0.025	0.025
532.1636	29.91	8%	0.048	0.048
543.5234	28.52	6%	0.044	0.044
583.5406	28.73	5%	<0.001	<0.001
612.5694	28.92	3%	0.005	0.005
642.0978	29.1	4%	0.027	0.006
670.6223	29.28	8%	0.015	0.015
700.1489	29.44	6%	0.027	0.027
728.6695	29.6	3%	0.044	0.044

The average mass of the markers presented in the table above is *m/z* 425.11. It was expected that the average mass in the samples would be much lower, to follow the traditional pattern of decomposition products breaking down into smaller compounds over time. When comparing the markers showing significant differences here to those presented at week 0, five compounds are the same. These were *m/z* 409.2788, *m/z* 387.2938, *m/z* 163.1792, *m/z* 167.1381, and *m/z* 299.3523. The significance of these markers will be discussed further into this chapter.

The bar chart in Figure 5.18 shows the top 10 markers showing significant differences from the table above. The majority of these markers are now showing higher peak areas in the still water sample. The peak areas in moving water samples are higher at week 0, while the peak areas in still water are higher at week 3. This suggests that the movement of the water can influence the behaviour and quantity of the compounds present as a result of decomposition.

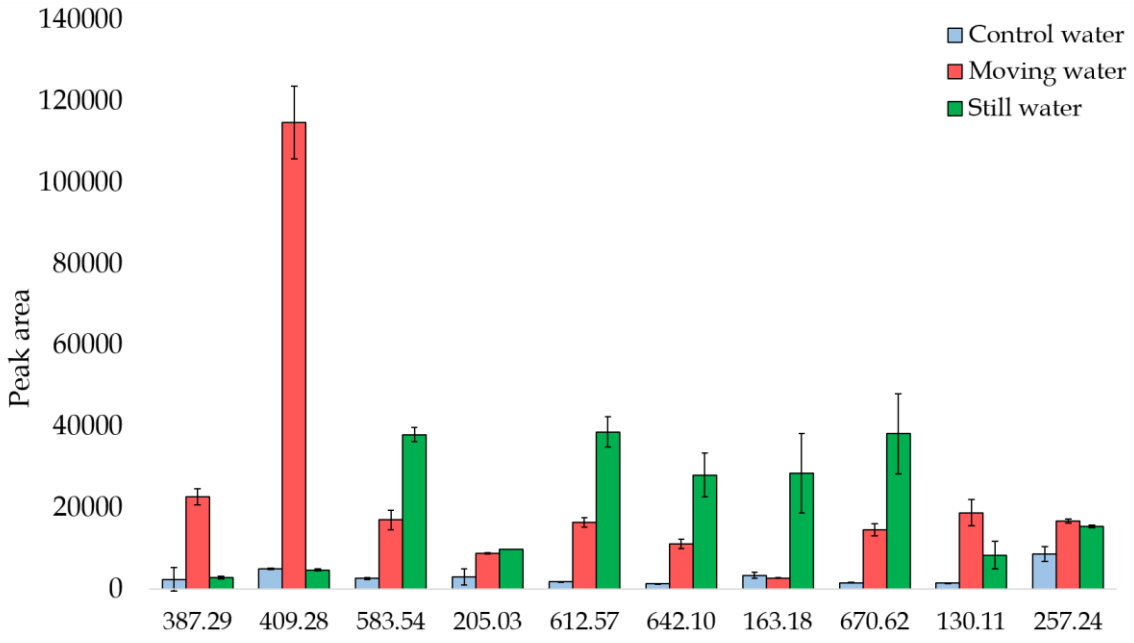

Figure 5.18: Bar chart showing the peak area of the top 10 markers identified as significantly different between moving and still water condition after 3 weeks of decomposition in summer.

5.3.2.12 Metabolic profiling of week 4

Figure 5.19 presents the overlaid chromatograms of water samples taken from both moving and still water conditions following 4 weeks of decomposition. A peak appearing on the chromatogram at around 10 minutes for moving water is not present in the still water condition. The peak patterns are otherwise similar between both chromatograms. The main visible difference between both conditions is their peak intensities. It seems that after 4 weeks of decomposition, the moving water sample shows higher peak intensities between 26-15 minutes, while the still water sample dominates the chromatogram at 10-25 minutes. This is the opposite pattern to what was presented in the chromatograms following 3 weeks of decomposition.

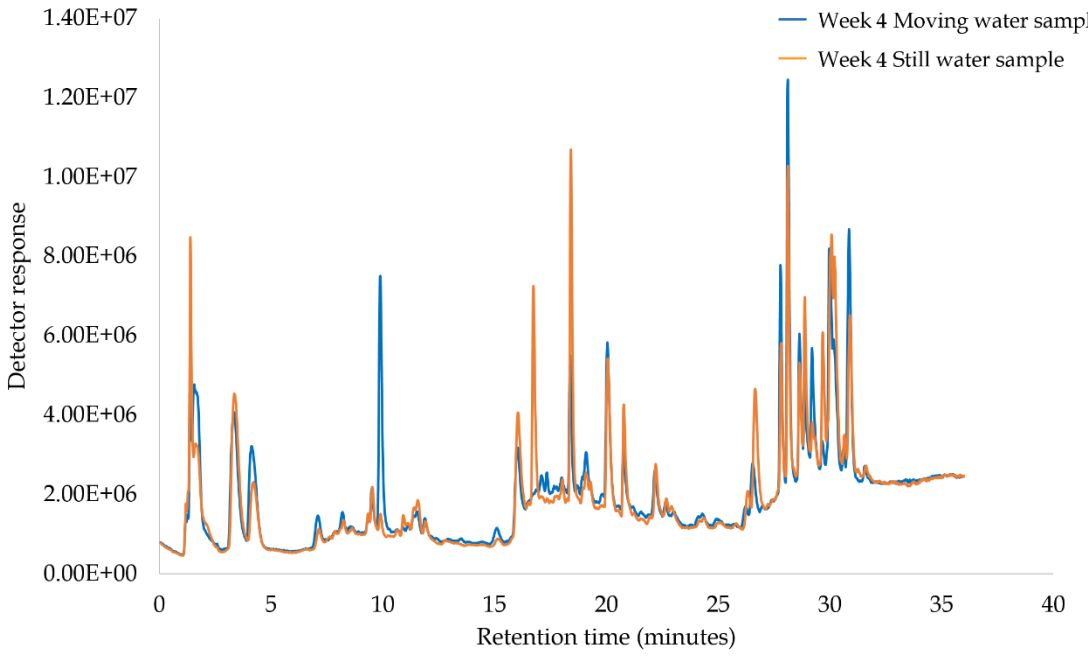

Figure 5.19: Example total ion chromatograms (TIC) of water samples taken after 4 weeks of decomposition in moving and still water during the summer.

5.3.2.13 Multivariate analysis of week 4

Figure 5.20 shows the PCA scores plot for the control sample and samples taken from the moving and still water conditions after 4 weeks of decomposition in water. It is evident that both experimental sample groups are clearly separated from the control samples, and the QC samples are tightly clustered in the middle of the plot. The separation between all sample groups is further apart than the spread of the QC samples, asserting that this is a genuine separation and not as a result of instrument variation. This implies that the chemical signature of the water from both moving and still conditions are significantly different to the control sample. This is to be expected as the experiment progresses.

It is important to note here that even in the same environmental conditions, the same species of carcass and the same method of analysis, the movement of the water is enough to create differences in the chemical profile of the water over time.

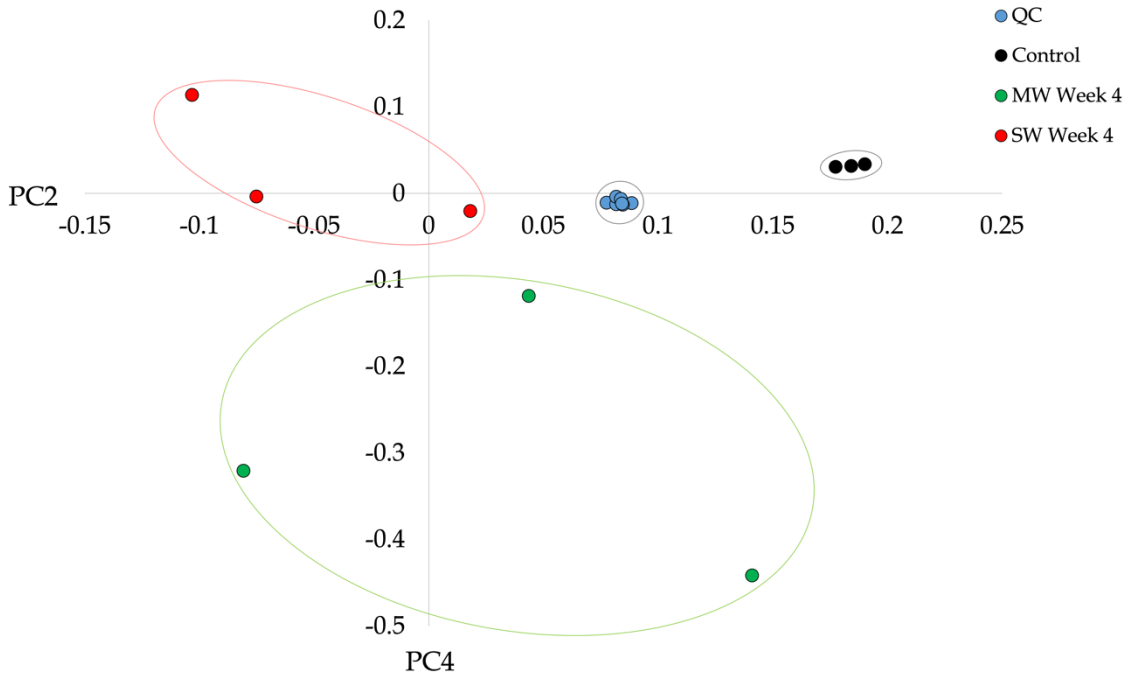

Figure 5.20: PCA score plot of PC2 (11.28%) and PC4 (2.37%) for water samples taken after 4 weeks of decomposition in moving and still water during the summer.

5.3.2.14 Statistical analysis of week 4

Statistical analysis was performed to investigate any significant differences between decomposition in different water conditions following 4 weeks of decomposition. 88 markers were significantly different with a p-value of below 0.05. Of these markers, 45% of them have a *m/z* under 400, while 55% have a *m/z* over 400. These compounds are of similar size to those identified after 3 weeks of decomposition. Table 5.6 presents the top 20 markers that were significantly different between water conditions and shown to be the most robust and reliable.

Table 5.6: Summary of the top 20 compounds that show significant differences between water conditions after 4 weeks of decomposition in water during the summer.

m/z	Retention time (minutes)	CV%	p-value XCMS	p-value ANOVA/Welch
130.1225	11.58	19%	0.042	0.042
187.2438	22.83	19%	0.017	0.017
195.2080	22.83	8%	0.025	0.025
205.2238	17.21	26%	0.006	0.006
257.1905	22.83	19%	0.007	0.007
279.1497	19.58	9%	0.003	0.004
299.3523	29.01	4%	0.048	0.048
315.2399	21.52	7%	0.024	0.024
467.4391	27.64	5%	0.006	0.006
485.4706	28.00	5%	0.012	0.012
514.4948	28.28	14%	0.015	0.015
532.1636	29.91	8%	0.004	0.004
543.5234	28.52	6%	0.004	0.004
583.5406	28.73	5%	0.015	0.015
612.5694	28.92	3%	0.014	0.014
642.0978	29.10	4%	0.013	0.013
670.6223	29.28	8%	0.007	0.007
700.1489	29.44	6%	0.003	0.003
728.6695	29.60	3%	0.003	0.003

The average mass calculated from the table above is *m/z* 439.44. This mass is very similar to the calculated average following three weeks of the experiment. There are 17 markers in the table above that are also found in the table for samples taken at week 3. Five of these markers are also present in the table presenting significantly different markers from week 0. Table 5.7 presents all the markers that have shown significant differences between moving and still water at more than one time point.

Table 5.7: Table showing the markers that show significant differences between moving and still water at more than one time point during the summer experiment.

Markers showing significant differences at week 0 and week 3	Markers showing significant differences in week 3 and week 4	Markers showing significant differences in week 0 and week 4
m/z	*m/z*	*m/z*
163.1792	728.6695	187.2438
387.2938	700.1489	315.2399
409.2788	543.5234	195.2080
167.1381	532.1636	279.1497
299.3523	757.6967	299.3523
	467.4391	
	205.2238	
	670.6223	
	257.1905	
	485.4706	
	642.0978	
	612.5694	
	514.4948	
	583.5406	
	130.1225	
	299.3523	
	167.1381	

The bar chart in Figure 5.21 presents the top 10 markers showing significant differences between moving and still water following 4 weeks of decomposition. The sample from the still water condition has a higher peak area in the majority of the markers presented.

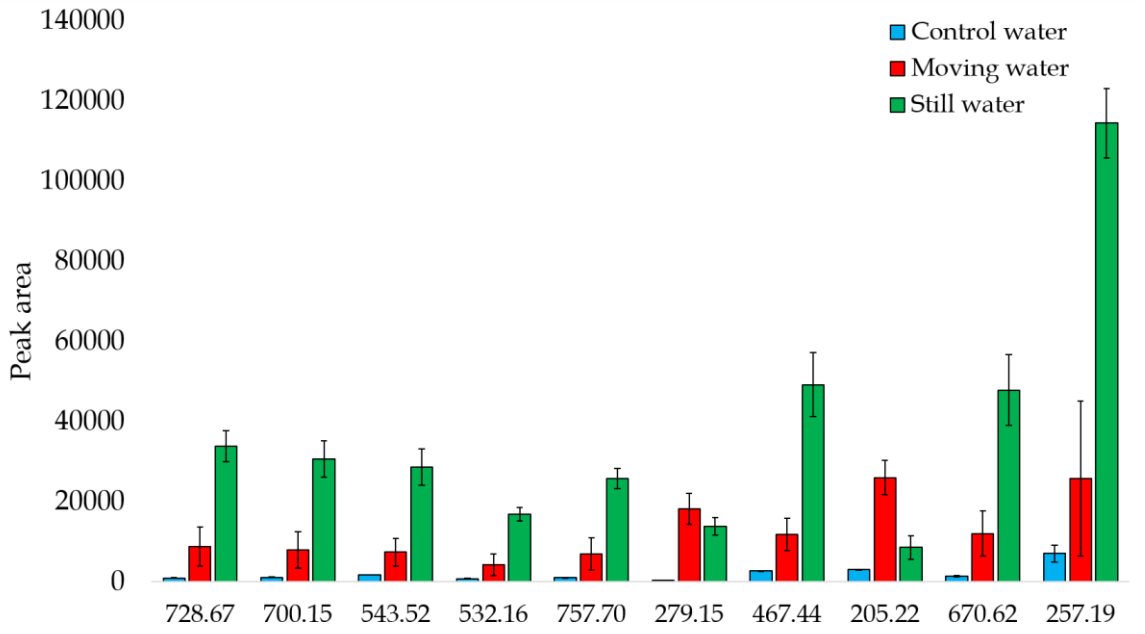

Figure 5.21: Bar chart showing the peak area of the top 10 markers identified as significantly different between moving and still water condition after 4 weeks of decomposition in summer.

While these drastic differences could be attributed to the effects of running and still water, it is also important to consider the implications of the experimental procedures, such as sample collection.

The circulation of water in the moving water condition would prevent the decomposition products from clustering together. The lack of movement in still water could lead to the stagnation of the decomposition products in certain areas. All samples were taken from the same location in both water conditions; therefore this was likely to be an influential factor. An additional experiment focused entirely on the sampling position in the box would determine if this was the case.

The marker *m/z* 299.2035 is showing significant differences between moving and still water samples at all three time points. Table 5.8 shows the tentative identification of this marker.

Table 5.8: Summary of the marker m/z 299.3523 that shows significant differences over time of water samples taken from both moving and still water conditions during the summer experiment.

m/z	Retention time (minutes)	CV value	Formula	Tentative identification	Score	p-value
299.3523	27.74	4%	$C_{19}H_{38}O_3$	Pristanic acid	90.26	$p<0.05$

The bar chart in Figure 5.22 shows the progression of this marker over time. It shows that the peak area for samples taken in both moving and still water conditions increase over time, however, they do so at different rates. While the peak area is similar between them at week 0, the sample taken from still water seems to have a much greater increase in peak area over time than the moving water. This demonstrates that there is a higher quantity of this particular marker in the still water sample. The confirmation of this marker using a standard was not possible due to rising costs and lack of instrument availability.

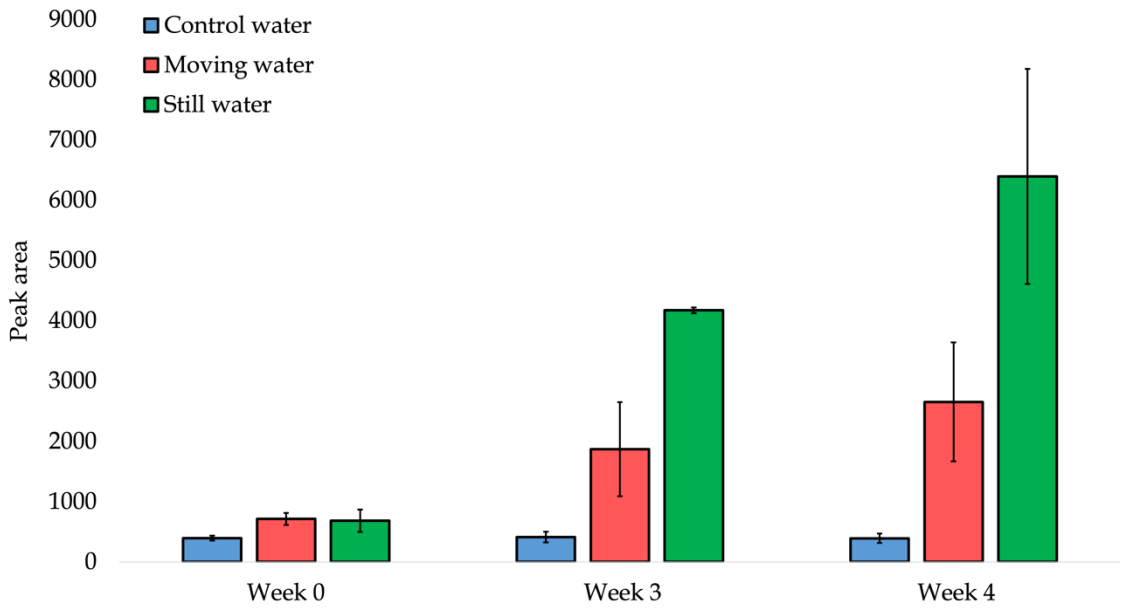

Figure 5.22: Bar chart showing the progression of m/z 299.3523 over three time points in the control, moving and still water sample in summer.

5.3.3 Difference in the metabolite profile of a carcass decomposing in moving and still water during the winter months.

5.3.3.1 The physical changes visible during the decomposition process of rabbits in moving and still water during the winter months.

In addition to carrying out the experiment in the summer, the same experiment was also carried out in winter. This created an opportunity to investigate the effects of temperature on the physical and chemical processes of decomposition.

Observations were carried out throughout the experiment to create a full picture of the effects of moving and still water on the process of decomposition over time, in addition to comparing the effects of temperature on the physical changes associated with decomposition. Figure 5.23 presents the images of the carcasses in both moving and still water conditions after 6 days of decomposition.

A **B**

Figure 5.23: Images of 3 rabbit carcasses in moving water (A) and 3 in still water (B) following 6 days of decomposition in winter conditions.

There are no significant observational differences between the carcasses in moving and still water after 6 days of decomposition in water during the winter months, other than a small amount of foam in two of the moving water boxes. In both water conditions, there were no signs of insect activity, no physical changes to any of the carcasses, and no obvious odour near the site. The decomposition process does not seem to have progressed as much as during the summer experiment, where day 6 presented bloating and discolouration of the abdomen, skin tears and a high level of insect activity.

Figure 5.24 shows the image of each carcass after 10 days of decomposition in water. The only visible sign of change is the increase of foam in the moving water condition. There was still no sign of insect activity. The differences between the summer and winter experiment at this time point is significant, as observations during the summer described a substantial maggot colony and a strong odour surrounding the boxes on day 10.

A **B**

Figure 5.24: Images of 3 rabbit carcasses in moving water (A) and 3 in still water (B) following 10 days of decomposition in winter conditions.

Figure 5.25 presents the experimental samples at day 24 of the winter experiment. The majority of the carcasses had sunk under the water. There were no changes to the colour of the water, the surrounding odour or any insect activity around the boxes. There were no further observable changes through to the end of the experiment. It is clear that there

are substantial differences between the physical changes observed during the experiment in both summer and winter conditions. While each carcass seemed to follow the expected stages of decomposition accompanied by insect colonisation during the summer, there were no obvious observable changes during the winter. The layer of film on the surface of the boxes during the summer suggests that not only are there physical differences between decomposition at different temperatures, but also chemical differences in the chemical signature of the water.

Figure 5.25 Images of 3 rabbit carcasses in moving water (A) and 3 in still water (B) following 24 days of decomposition in winter conditions.

5.3.3.2 Metabolic profiling

The chromatograms in Figure 5.26 shows the chemical profile of the water samples taken at week 0, 3 and 4 from the moving water condition. The chromatogram representing the sample taken at week 0 shows very limited chromatography. A peak at around 1.5 minutes and 30 minutes do show an unusual characteristic of high peak intensities. The number of peaks and their peak intensities increase as the experiment progresses. Whilst some peaks have higher peak intensities at week 3, others show higher peak intensities at week 4. When comparing the chromatograms shown here to those obtained during the summer experiment, it is clear that temperature has influenced the chemical changes seen in the water as a result of decomposition. The peak intensities are much higher in the chromatograms produced during the summer experiment, along with the number of peaks that appear over time. The lack of peaks appearing between 5-10 minutes and 25-30 minutes during the winter experiment suggests that the quantity of leachates in the water is much lower during cold temperatures.

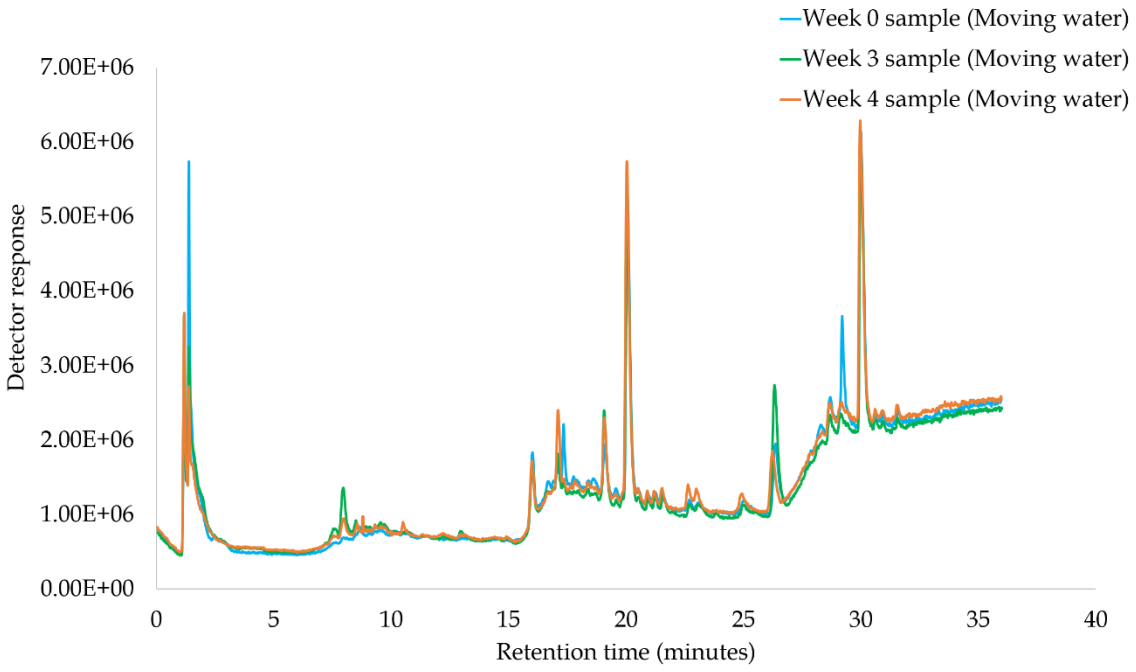

Figure 5.26: Example total ion chromatogram (TIC) of water samples containing a decomposing carcass in moving water at week 0, 3 and 4 of the winter experiment.

Figure 5.27 shows the chromatograms for samples taken from the still water condition at three time points in the winter experiment. Similar to the moving water condition, the sample from week 0 shows a very limited number of peaks on the chromatogram. An increase in peak intensities is observed at week 3 of the experiment, followed by the highest peak intensities at week 4. While there are differences in peak patterns over time in the still water condition during the winter, they are not very substantial when comparing to those presented during the summer experiment. Additionally, in the summer the sample taken at week 3 seems to dominate the chromatogram with high peak intensities between 25-35 minutes. This is not the case in the winter experiment, where the sample taken at week 4 has higher peak intensities between these times.

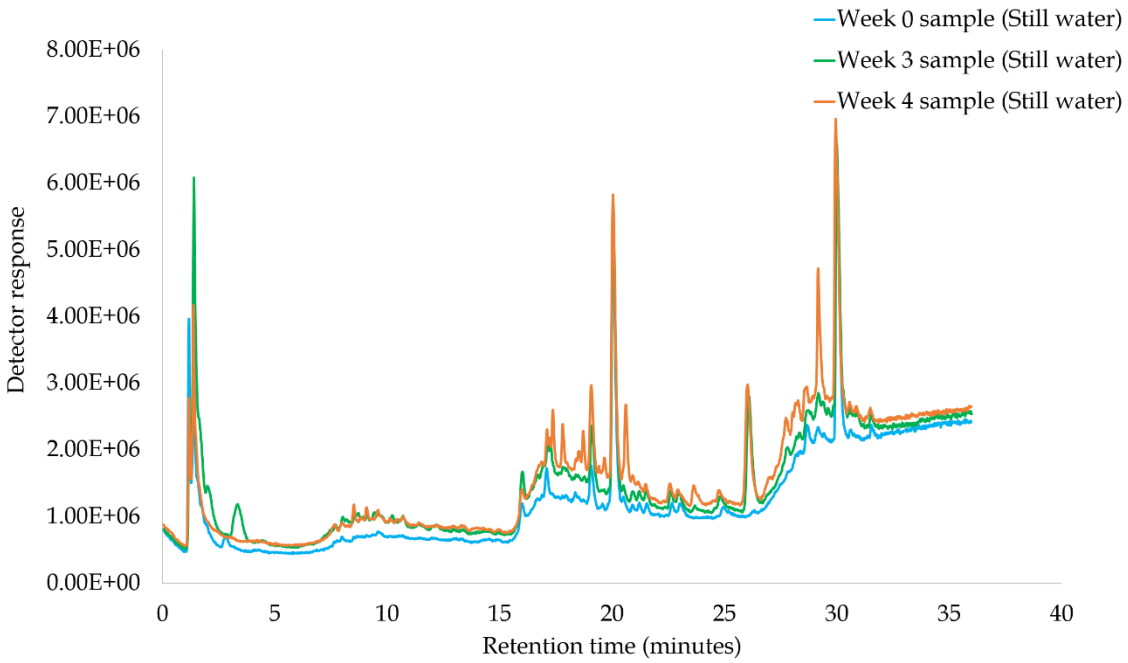

Figure 5.27: Example total ion chromatogram (TIC) of water samples containing a decomposing carcass in still water at week 0, 3 and 4 of the winter experiment.

5.3.3.3 Multivariate analysis

The PCA scores plot in Figure 5.28 shows the separation between the control sample, and experimental samples taken at three time points from the moving water condition. The QC samples are clustered together, highlighting no instrumental variability. Poor separation is seen across the plot, with the control samples overlapping the samples from all three time points. Each of the three replicates from each sample group are clustered together close enough to group them, however the overall separation is minimal.

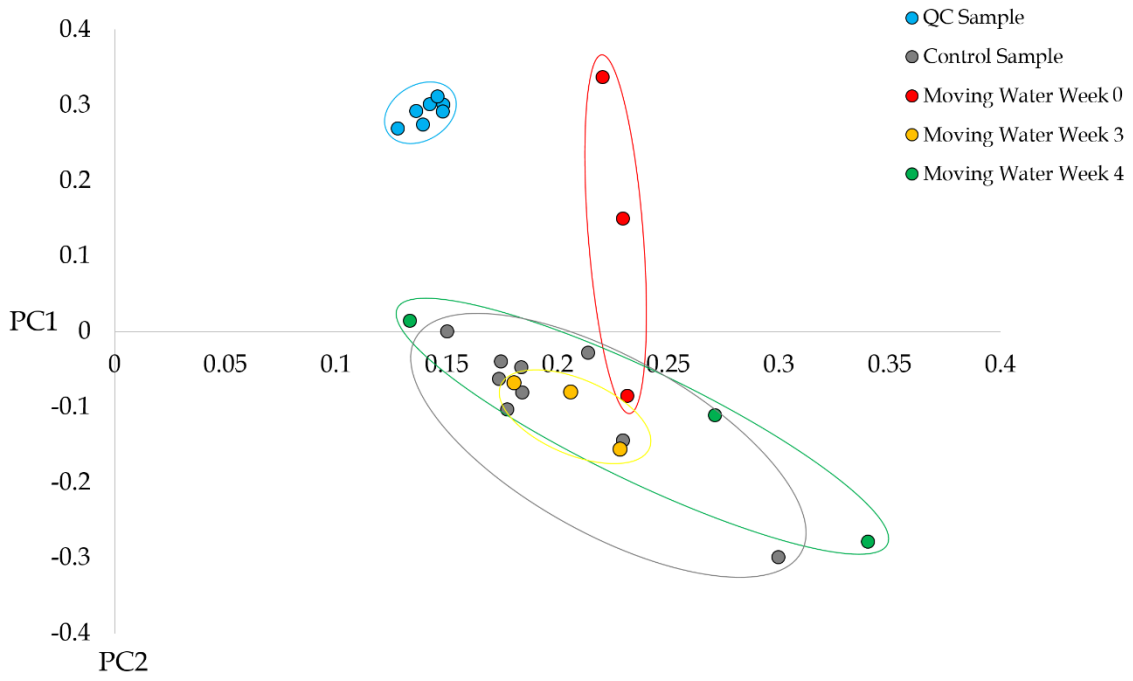

Figure 5.28: PCA score plot of PC1 (65.00%) and PC2 (15.35%) for water samples containing a decomposing carcass in moving water at week 0, 3 and 4 of the winter experiment.

Figure 5.29 presents the PCA scores plot for the control samples, and samples taken at three time points from the still water condition in winter. The QC samples are again clustered towards the middle of the plot. The samples taken at week 0 are overlapping the control samples. The samples taken at week 3 of the experiment are also overlapping those taken at week 0. Samples taken at week 4 show good separation from the rest of the groups. The distance between the samples taken at week 4 and the rest of the sample groups are further apart than the spread of the QC samples, justifying this separation as genuine and not as a result of instrumental effects.

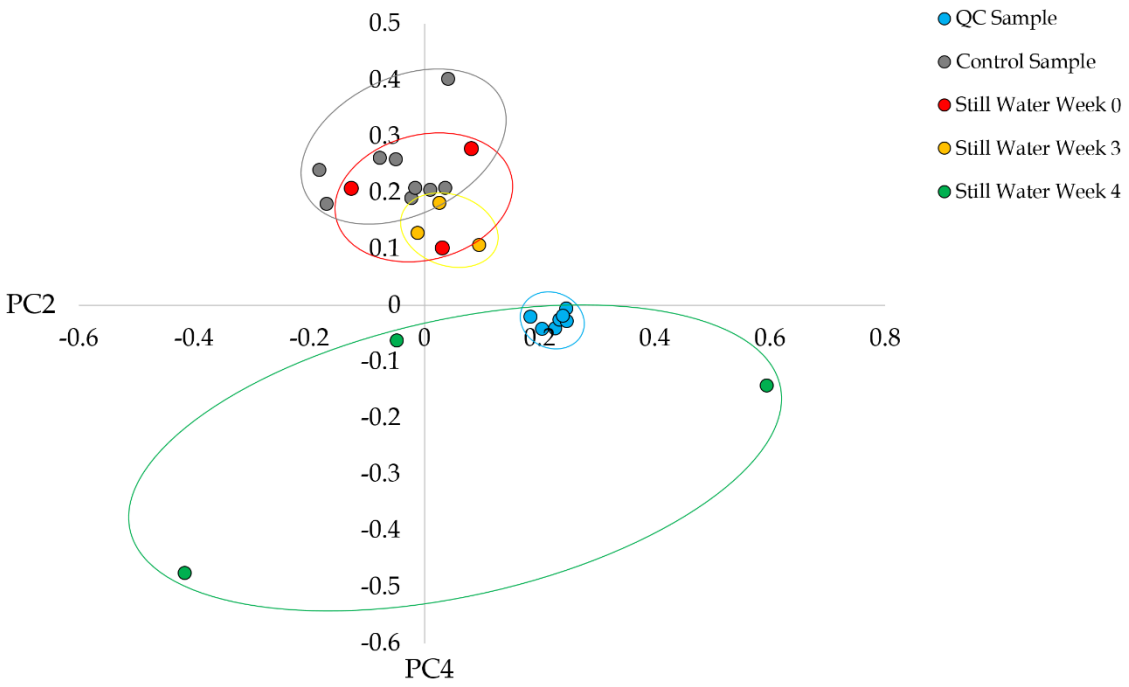

Figure 5.29: PCA score plot of PC2 (7.42%) and PC4 (2.33%) for water samples containing a decomposing carcass in still water at week 0, 3 and 4 of the winter experiment.

The striking differences on the PCA scores plot between the summer and winter experiments reflect the results presented in the chromatograms. The lack of chromatographic changes over time, accompanied by poor separation on the PCA plots strengthens the argument that temperature has a significant effect on the chemical processes during decomposition.

When focusing on the still water condition, there are different patterns emerging in the data when comparing between the summer and winter experiment. Whilst in summer we see overlap between weeks 3 and 4 on the PCA scores plot, in the winter conditions the overlap is between weeks 0 and 3. This suggests that the temperature of the environment has a significant effect on the rate of change in the chemical signature of the water subjected to decomposition over time.

5.3.3.4 Statistical analysis

The total number of features detected in the water samples through *XCMS online* was 2195. All features with a CV value of 30% or more were removed, with 1794 remaining. Statistical analysis was performed on water samples from boxes with both moving and still water conditions. 19 compounds were found showing significant differences over three time intervals in moving water, and 8 in still water. The significant markers from each condition are shown in Table 5.9 and Table 5.10.

Table 5.9: Summary of the markers that show significant differences over time of water samples taken from a carcass decomposing in moving water during the winter experiment.

m/z	Retention time (minutes)	CV%	p-value	
			Compounds showing significant differences between	
			Week 0 and Week 3	Week 3 and Week 4
195.1759	19.58	3%	0.013	0.041
199.1308	6.85	26%	0.02	0.025
202.1618	8.67	8%	0.006	0.023
214.2037	20.14	7%	0.03	0.017
236.2366	1.40	9%	0.008	0.005
282.2927	18.76	3%	0.013	0.032
327.1138	19.12	12%	0.021	0.031
329.1089	19.12	2%	0.025	0.022
349.0935	19.12	3%	0.017	0.011
353.0921	19.12	3%	0.015	0.028
355.0891	19.12	3%	0.028	0.019
411.0797	19.12	8%	0.004	0.025
452.4057	20.12	7%	0.008	0.041
495.4677	17.28	5%	0.007	0.026
675.1523	19.11	3%	0.024	0.027
677.1489	19.11	3%	0.03	0.024
679.1494	19.11	5%	0.025	0.023

Table 5.10: Summary of the markers that show significant differences over time of water samples taken from a carcass decomposing in still water during the winter experiment.

m/z	Retention time (minutes)	CV%	p-value	
			Compounds showing significant differences between	
			Week 0 and Week 3	Week 3 and Week 4
149.1813	8.96	14%	0.002	0.034
213.2225	17.81	10%	0.005	0.017
215.1704	17.39	7%	0.049	0.003
221.2376	20.51	10%	0.048	0.039
244.2746	18.64	5%	0.022	0.026
279.1497	19.58	9%	0.002	0.022
298.1427	17.39	18%	0.023	0.007
360.2533	1.37	12%	0.006	0.048

When comparing the results of the statistical analysis to those carried out in the summer experiment, there are some obvious differences. There are only eight markers showing significant differences over three time points in the moving water condition in winter, however it was the still water sample that presented a limited number of markers during the summer experiment. It is also important to note that none of the markers appear in both tables, whilst two markers were investigated after showing significant differences in the moving and still water conditions in summer. In winter, the highest *m/z* in the moving water table was *m/z* 679.1494, and *m/z* 360.2533 in the still water table. The results from the summer experiment showed the opposite effects, with still water recording the highest mass.

Figure 5.30 presents a bar chart showing the change in peak area of the top five markers identified in the moving water condition. The highest peak area is recorded at week 3 for each marker, with a decrease in peak area at week 4. This is not the case for the top five markers in still water (Figure 5.31), where only two markers show this pattern. The remaining markers show a direct increase in peak area at week 4 instead.

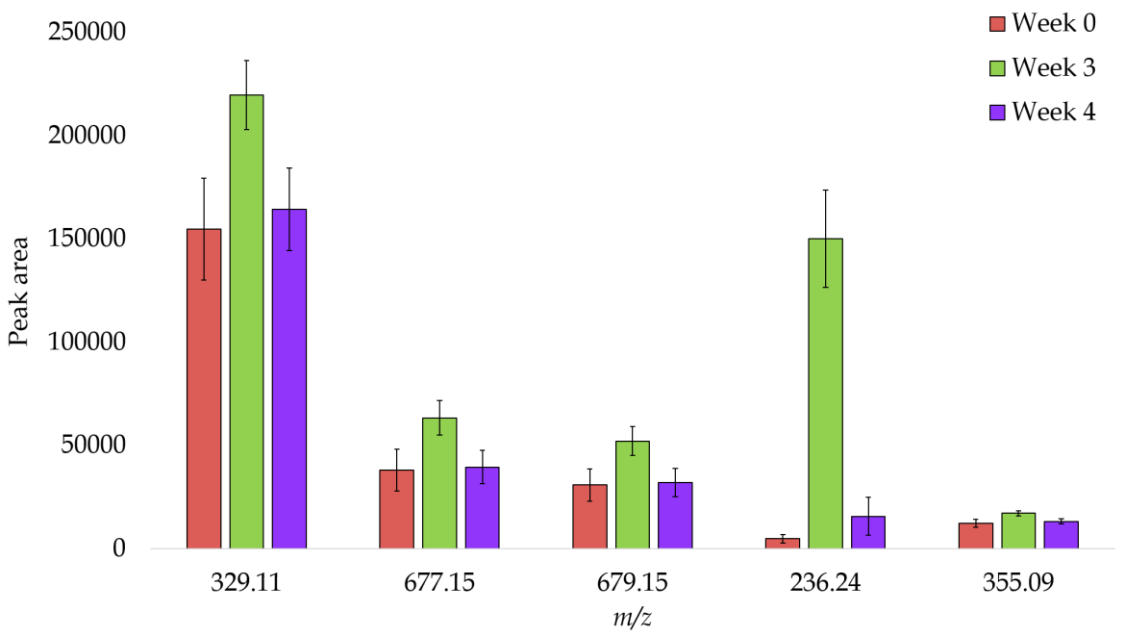

Figure 5.30: Bar chart showing the peak area of the top five markers showing significant differences over time in the moving water condition in winter.

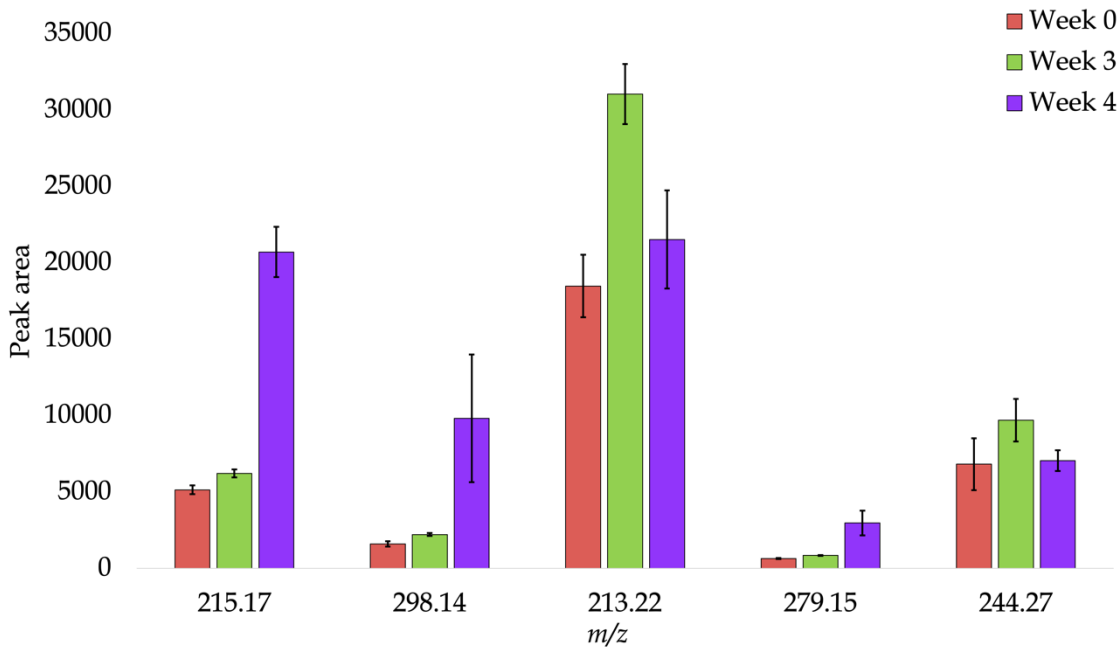

Figure 5.31: Bar chart showing the peak area of the top five markers showing significant differences over time in the still water condition in winter.

5.3.3.5 Metabolic profiling week 0

Figure 5.32 presents the total ion chromatograms (TIC) for samples taken after 0 weeks of decomposition in moving and still water conditions. It is important to note that these particular samples were taken on day 2. Both chromatograms show characteristics of what is expected during the early stages of decomposition. Most peaks appear between 15-30 minutes, and the majority have low peak intensities. It seems that the sample taken from moving water has some additional peaks that are not present in the still water sample, for example at 26, 28 and 29 minutes. This result is similar to that obtained during the summer experiment at week 0. One peak at 7 minutes in the chromatogram for the moving water condition in the summer has a high peak intensity. That particular peak can be seen in the same chromatogram during the winter conditions; however the peak area is very small.

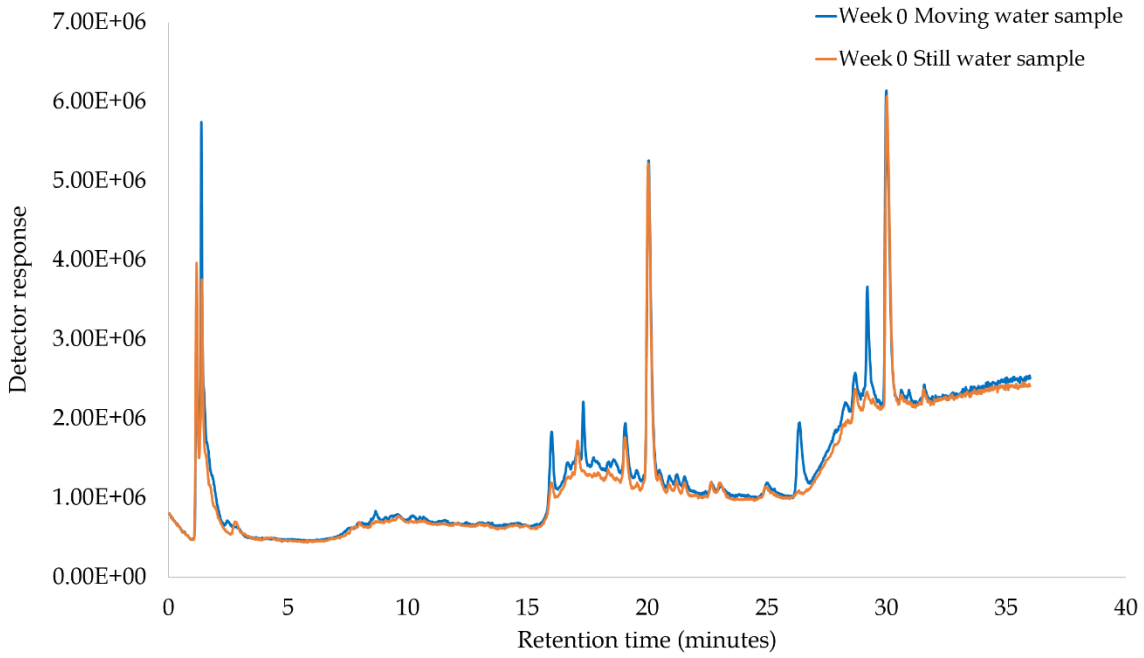

Figure 5.32: Example total ion chromatograms (TIC) of water samples taken after 0 weeks of decomposition in moving and still water during the winter.

5.3.3.6 Multivariate analysis of week 0

Figure 5.33 shows the PCA scores plot of the samples taken after 0 weeks of decomposition in both moving and still water conditions during the winter experiment. The QC samples are clustered together, showing minimal instrumental drift. There is overlap between all three sample groups on the plot. The sample from the moving water condition seems to be separated slightly better from the control sample, but it still shows lack of separation overall. The results presented here are very similar to the results obtained at the same time point during the summer experiment.

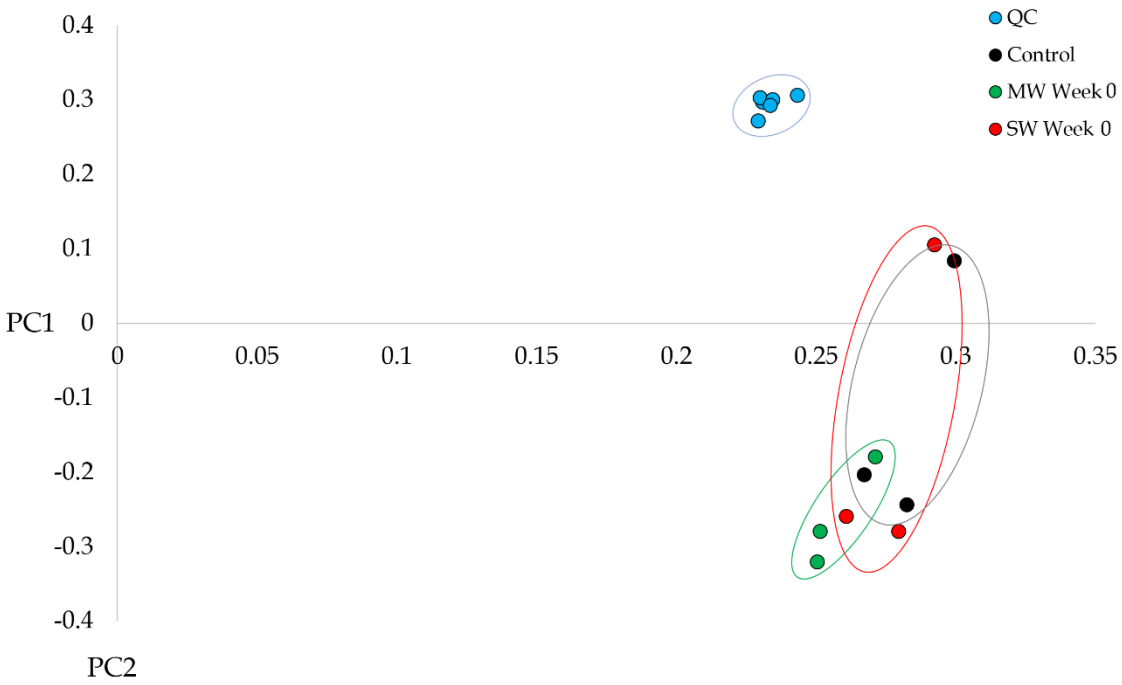

Figure 5.33: PCA score plot of PC1 (91.32%) and PC2 (4.50%) for water samples taken after 0 weeks of decomposition in moving and still water during the winter.

5.3.3.7 Statistical analysis of week 0

Statistical analysis was performed to investigate any significant differences between decomposition in different water conditions following 0 weeks of decomposition. 86 markers were significantly different with a p-value of below 0.05. Of these markers, 50% of them have a *m/z* under 400, while 50% have a *m/z* over 400. This shows that the balance between the smaller and larger compounds are equal at this time interval. Table 5.11 presents the top 20 markers that were significantly different between water conditions and shown to be the most robust and reliable.

Table 5.11: Summary of the top 20 compounds that show significant differences between water conditions after 0 weeks of decomposition in water during the winter.

m/z	Retention time (minutes)	CV%	p-value XCMS	p-value ANOVA/Welch
117.1589	1.16	5%	0.020	0.02
139.1337	16.13	6%	0.005	0.005
158.0899	17.39	17%	0.021	0.021
188.2500	1.26	23%	0.015	0.015
196.1800	19.58	9%	0.009	0.009
215.1704	17.39	7%	0.010	0.01
221.1949	18.15	10%	0.026	0.026
236.1573	17.4	4%	0.011	0.047
242.1989	1.39	11%	0.003	0.003
252.1281	17.41	16%	0.017	0.017
298.1427	17.39	18%	0.004	0.028
304.1555	17.39	11%	0.005	0.005
392.3964	26.89	8%	0.010	0.01
398.3556	18.62	7%	<0.001	<0.001
406.3949	29.43	5%	0.018	0.018
413.3858	29.97	2%	0.007	0.007
450.4799	29.97	4%	0.003	0.003
469.4618	31.55	3%	0.001	0.001
507.4076	28.24	6%	0.006	0.006
529.3146	29.38	11%	0.010	0.01

The average *m/z* for the markers in the table above is *m/z* 308.87. Larger markers are to be expected at this early stage of decomposition. Figure 5.34 presents a bar chart of the top 10 markers, and their peak areas from the moving and still water samples. Ten markers were chosen to give a good overview of the different patterns between markers, whilst still allowing deeper insight into the behaviours of individual markers. The markers that are more prevalent in the still water samples have a significantly higher peak area than those more prevalent in moving water samples. This is particularly the case with *m/z* 413.39 where an adjusted scale was used. This was not the case during the summer experiment, where moving water samples produced higher peak areas overall.

These results are consistent to those obtained during the summer experiment, where a similar number of significantly different markers and average *m/z* across the top 20 markers are presented. However, while the size of these compounds were equal in the winter experiment, 81% of the markers in the summer experiment were over *m/z* 400.

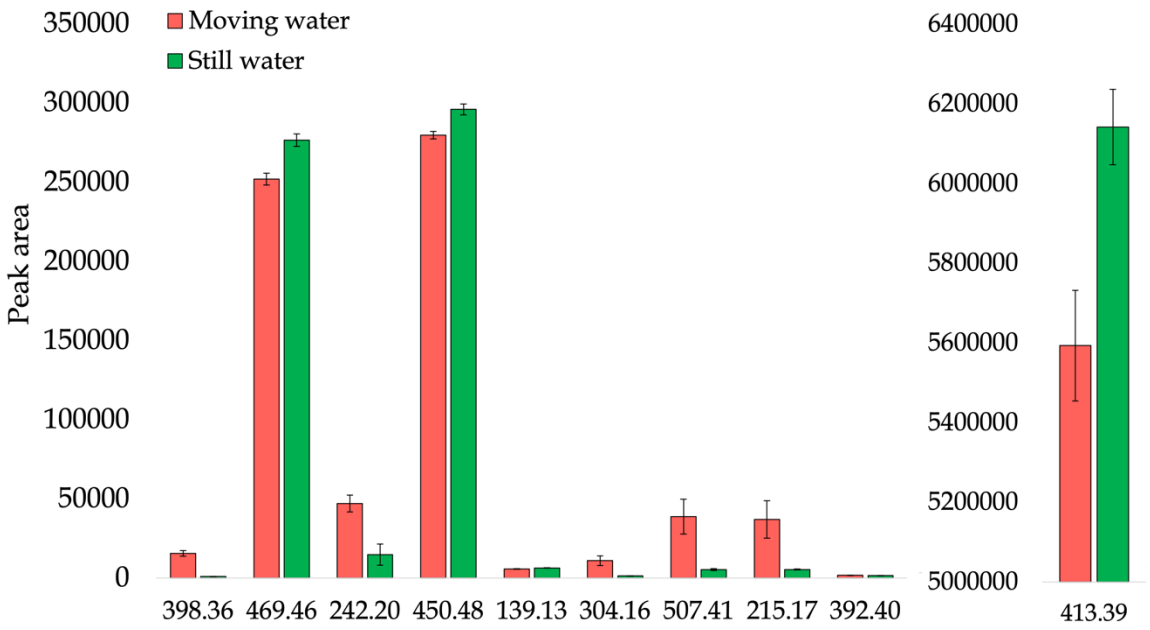

Figure 5.34: Bar chart showing the peak area of the top 10 markers identified as significantly different between moving and still water condition after 0 weeks of decomposition in winter.

5.3.3.8 Metabolic profiling of week 3

Figure 5.35 presents the chromatograms of samples taken at week 3 from moving and still water conditions. There is only a slight increase in peak intensities and number of peaks from week 0. A peak in the still water sample at 3.5 minutes is not present in the moving water sample, and a peak at 7 minutes in the moving water sample does not appear in the still water sample. This peak is also noticeably present in the moving water sample during the summer experiment. These noticeable differences were unexpected in cold conditions. When comparing these chromatograms to those obtained during the summer experiment, there are differences in the peak patterns, the peak quality and their intensities, particularly between 15-35 minutes. During the summer, the moving water sample dominates the beginning of the chromatogram, while the still water sample presents higher peak intensities and number of peaks further into the chromatogram. This result is not reflected in the chromatograms obtained during the winter experiment.

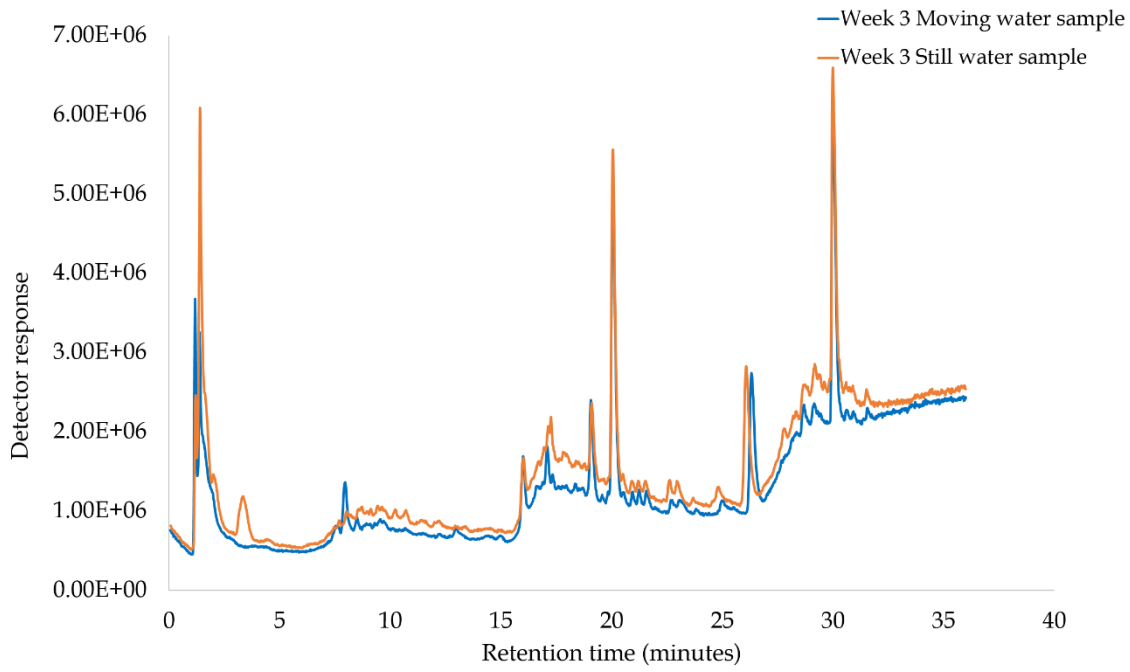

Figure 5.35: Example total ion chromatograms (TIC) of water samples taken after 3 weeks of decomposition in moving and still water during the winter.

5.3.3.9 Multivariate analysis of week 3

The PCA scores plot in Figure 5.36 shows the control sample and samples taken following 3 weeks of decomposition in moving and still water conditions. The QC samples are not clustered as during previous analyses, suggesting the potential of some instrumental effects. The plot shows good separation between the control group and the experimental sample groups, but poor separation between the moving and still water samples specifically. This suggests that there is a clear difference between the chemical signature of the control water and experimental samples, but not between different water conditions within the experimental samples. During the summer experiment the control group was also showing good separation from the experimental groups, however, there was also better separation between the moving and still water conditions. The higher temperatures seem to be influencing whether there are significant differences in the chemical signature of the samples from different water conditions.

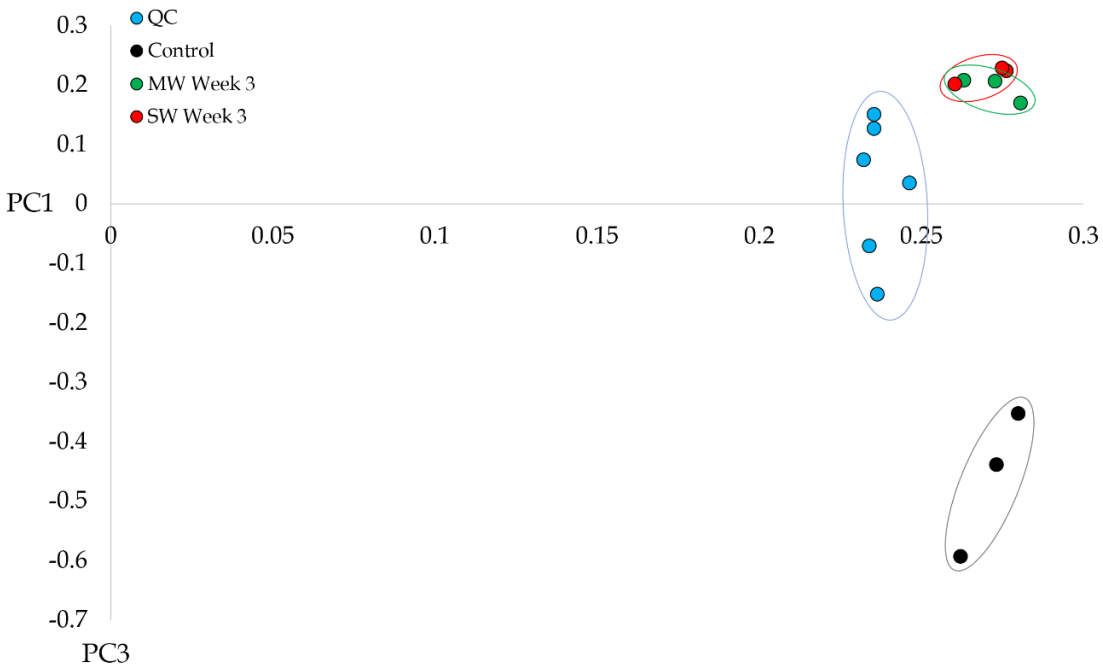

Figure 5.36: PCA score plot of PC1 (92.20%) and PC3 (1.77%) for water samples taken after 3 weeks of decomposition in moving and still water during the summer.

5.3.3.10 Statistical analysis of week 3

Statistical analysis was performed to investigate any significant differences between decomposition in different water conditions following 3 weeks of decomposition. 90 markers were significantly different with a p-value of below 0.05. Of these markers, 53% of them have a *m/z* under 400, while 47% have a *m/z* over 400. A slight increase in the number of markers with a *m/z* under 400 reflects the natural progression of breakdown products associated with decomposition. Table 5.12 presents the top 20 markers that were significantly different between water conditions and shown to be the robust and reliable.

Table 5.12: Summary of the top 20 compounds that show significant differences between water conditions after 3 weeks of decomposition in water during the winter.

m/z	Retention time (minutes)	CV%	p-value XCMS	p-value ANOVA/Welch
112.1043	1.40	4%	0.002	0.002
139.1337	16.13	6%	0.032	0.032
158.0899	17.39	17%	0.005	0.005
171.1445	1.41	4%	0.008	0.008
188.2500	1.26	23%	0.026	0.026
199.2442	24.76	4%	0.028	0.028
214.1702	17.40	3%	0.01	0.01
215.2040	1.34	13%	0.027	0.027
221.1949	21.51	6%	0.027	0.027
236.1573	17.40	4%	0.04	0.04
237.2340	1.43	10%	0.008	0.008
242.2971	18.04	3%	0.027	0.027
250.2461	8.30	15%	<0.001	0.008
252.1281	17.41	16%	0.014	0.014
282.2927	18.76	3%	0.02	0.02
304.1555	17.39	11%	0.029	0.029
398.3556	18.62	7%	0.001	0.001
409.2788	18.80	2%	0.039	0.039
413.0747	19.12	7%	0.005	0.005
417.0941	19.12	5%	0.015	0.015

The average *m/z* calculated from the table above is *m/z* 253.04. This is slightly smaller than the average mass of week 0. It is expected that the compounds break down into smaller products as the process of decomposition continues. There are 13 markers present in the table that also appear at week 0. These markers will be discussed in section **5.3.4.13**

Figure 5.37 presents the bar chart for the top 10 markers showing significant differences at week 3. Similar to week 0, the moving water samples exhibit greater peak areas overall. These results notably contrast those presented at week 3 of the summer experiment, where the still water samples show much higher peak areas. Additionally, only five markers were present in both tables (week 0 and 3) during the summer. This suggests that due to the increased rate of decomposition in the summer, the metabolic processes are rapidly changing over time. As a result, completely different markers will appear throughout, whilst in winter it may take longer for new markers to appear.

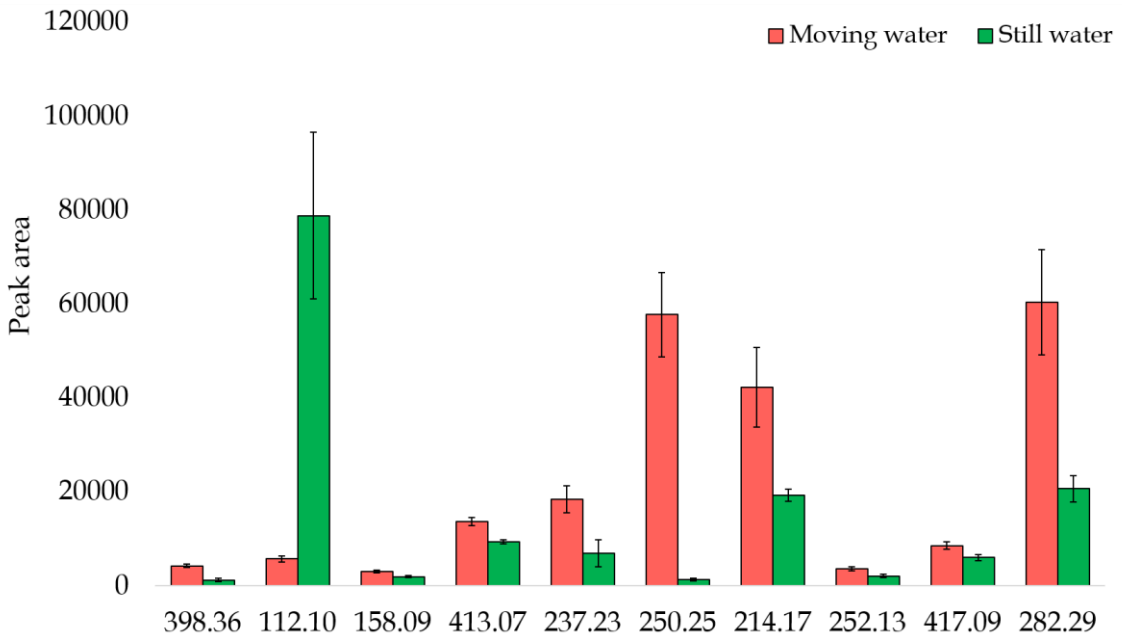

Figure 5.37: Bar chart showing the peak area of the top 10 markers identified as significantly different between moving and still water condition after 3 weeks of decomposition in winter.

5.3.3.11 Metabolic profiling of week 4

Figure 5.38 presents the overlaid chromatograms of water samples taken following 4 weeks of decomposition in moving and still water. Both chromatograms show very similar peak patterns, however those in the still water sample seem to show higher peak intensities overall. Although additional peaks are produced between 15-30 minutes at week 4, there are no distinct changes to the peak patterns and intensities when compared to week 3.

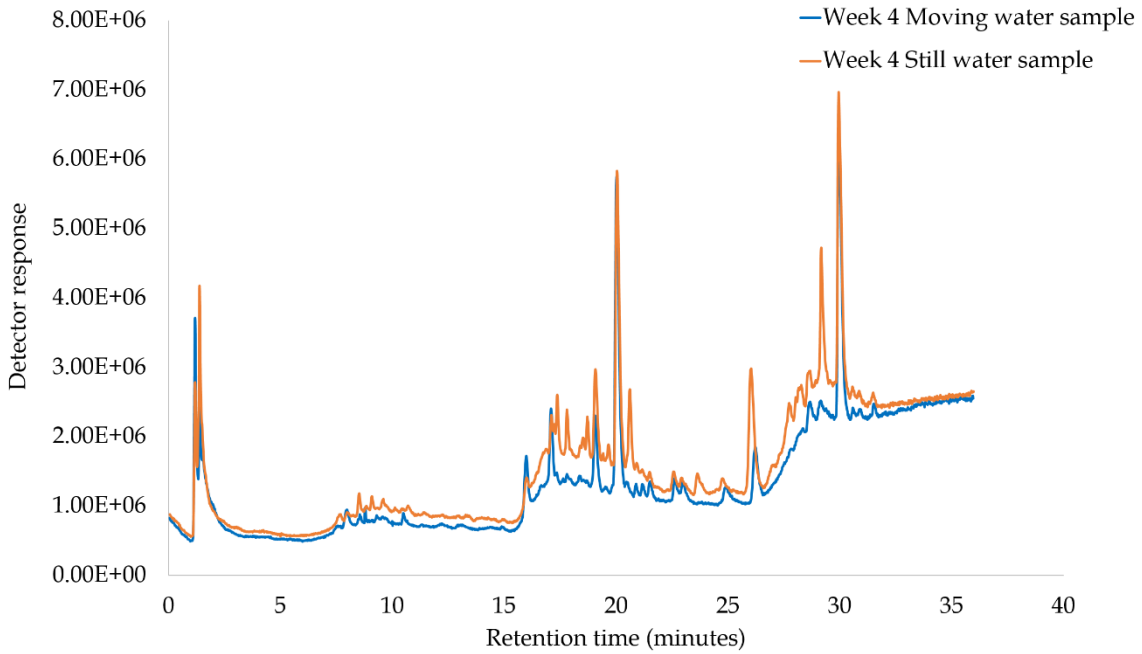

Figure 5.38: Example total ion chromatograms (TIC) of water samples taken after 4 weeks of decomposition in moving and still water during the winter.

The chromatograms produced from the samples taken at week 4 in the summer experiment show a greater number of peaks and higher peak intensities compared to the winter experiment, specifically between 0-15 minutes. The most obvious differences here are the two peaks appearing at 3-4 minutes in the summer that are completely absent in the winter conditions. This may suggest that there are higher quantities of smaller

compounds present in the samples obtained during the summer, as they elute sooner on the chromatogram. This aligns with previous research into the effects of temperature on decomposition, where the cold temperatures restrict certain chemical processes.

5.3.3.12 Multivariate analysis of week 4

The PCA scores plot in Figure 5.39 presents the control, moving and still water samples taken after 4 weeks of decomposition in water. The QC samples are clustered together towards the middle of the plot, showing limited instrumental interference. There is excellent separation between the control samples, moving and still water samples. The separation between all three sample groups are further apart than the spread of the QC samples, indicating that these reflect genuine differences in the chemical profile of the samples, and not due to instrumental effects.

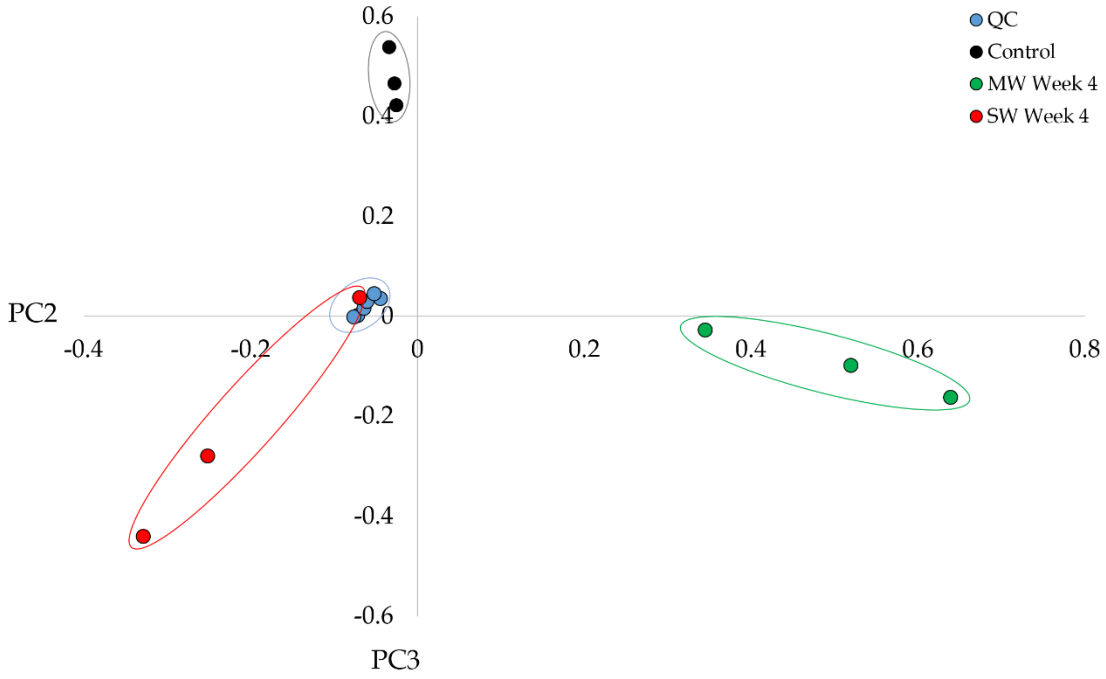

Figure 5.39: PCA score plot of PC2 (26.55%) and PC3 (15.48%) for water samples taken after 4 weeks of decomposition in moving and still water during the summer.

There is good separation between the moving and still water conditions at week 4 of the experiment in both summer and winter conditions. Unexpectedly, the sample groups are clustered tighter together, and placed much further apart on the plot in the winter condition.

The observations conducted during the summer experiment showed there are far more physical changes to the carcasses and the water itself, compared to the limited changes in the winter. As a result, it is likely that there are more complex metabonomic processes occurring during the summer which will increase the variety of compounds in each sample replicate. This would explain the spread of the samples within a specific sample group on the PCA scores plot representing the summer experiment.

5.3.3.13 Statistical analysis of week 4

Statistical analysis was performed to investigate any significant differences between decomposition in different water conditions following 4 weeks of decomposition. 99 markers were significantly different with a p-value of below 0.05. Of these markers, 28% of them have a *m/z* under 400, while 72% have a *m/z* over 400. This is an unusual result as the number of smaller compounds are expected to increase over time. Table 5.13 presents the top 20 markers that were significantly different between water conditions and shown to be the most robust and reliable.

Table 5.13: Summary of the top 20 compounds that show significant differences between water conditions after 4 weeks of decomposition in water during the winter.

m/z	Retention time (minutes)	CV%	p-value XCMS	p-value ANOVA/Welch
112.1043	1.40	4%	0.007	0.007
117.1508	1.17	26%	0.003	0.003
173.1466	2.17	3%	0.003	0.003
215.1704	17.39	7%	0.001	0.001
221.1949	1.23	5%	0.009	0.009
236.1573	17.40	4%	0.006	0.006
250.2461	8.30	15%	0.001	0.016
252.1281	17.41	16%	0.001	0.001
282.3698	29.18	20%	0.01	0.044
304.3556	29.18	15%	0.003	0.022
379.2437	20.62	4%	0.001	0.001
381.4057	26.88	8%	<0.001	<0.001
383.4253	29.45	11%	0.002	<0.001
392.3964	26.89	8%	0.004	0.004
409.0360	35.14	12%	0.006	0.006
417.4399	27.73	9%	0.004	0.004
493.4654	29.62	4%	0.001	0.001
507.4076	28.24	6%	<0.001	<0.001
529.5454	29.48	8%	0.001	0.014
603.5935	29.09	8%	0.002	0.002

The average mass calculated from Table 5.13 was *m/z* 333.04, which is similar to the average calculated from the table at week 0 of the experiment. Both summer and winter conditions yielded a similar number of significantly different markers at this time point, however overall the winter experiment produced larger compounds at week 4. The bar chart in Figure 5.40 shows the peak area of the top 10 statistically significant markers identified at week 4. The still water samples dominate the figure with much higher peak areas in all but one marker, which was also the case in the summer experiment. Nine of the markers identified in this table were also identified at week 0, and ten of these markers

were previously identified at week 3. These include five markers that show significant differences at all three time points. These are shown in Table 5.14. and Figure 5.41.

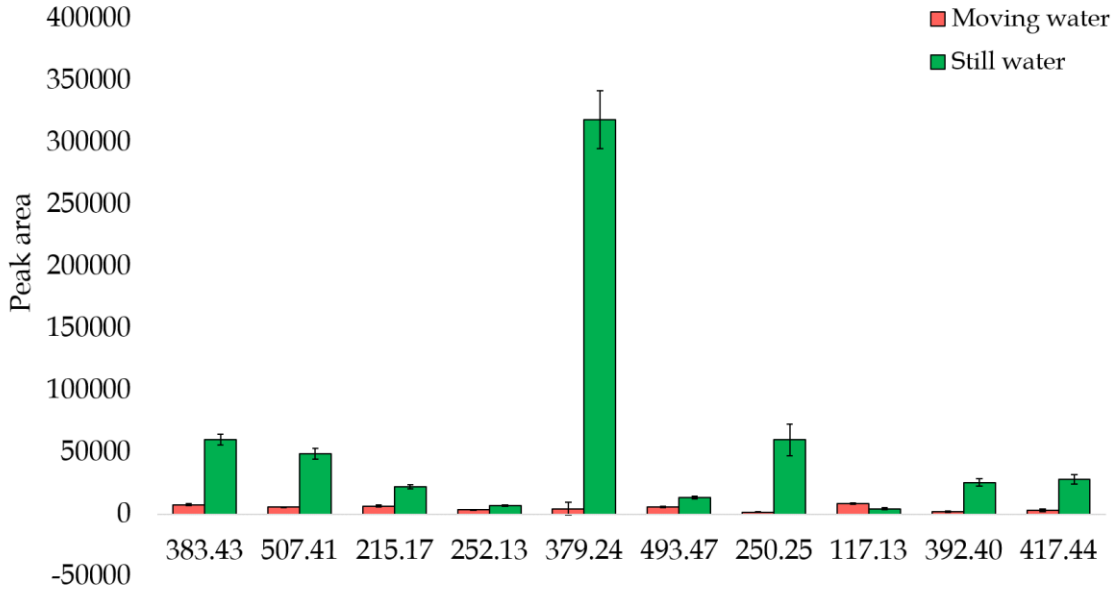

Figure 5.40: Bar chart showing the peak area of the top 10 markers identified as significantly different between moving and still water condition after 4 weeks of decomposition in winter.

Table 5.14: Table showing the markers that show significant differences between moving and still water at more than one time point during the winter experiment.

Markers showing significant differences at week 0 and week 3	Markers showing significant differences in week 3 and week 4	Markers showing significant differences in week 0 and week 4
m/z	***m/z***	***m/z***
215.1704	215.1704	215.1704
221.1949	221.1949	221.1949
236.1573	236.1573	236.1573
252.1281	252.1281	252.1281
304.1555	304.1555	304.1555
398.3556	112.1043	507.4076
242.1989	250.2461	529.3146
139.1337	417.0941	392.3964
413.3858	282.2927	117.1589
158.0899	409.2788	
298.1427		
188.2500		

Figure 5.41 shows the five markers showing significant differences over time.

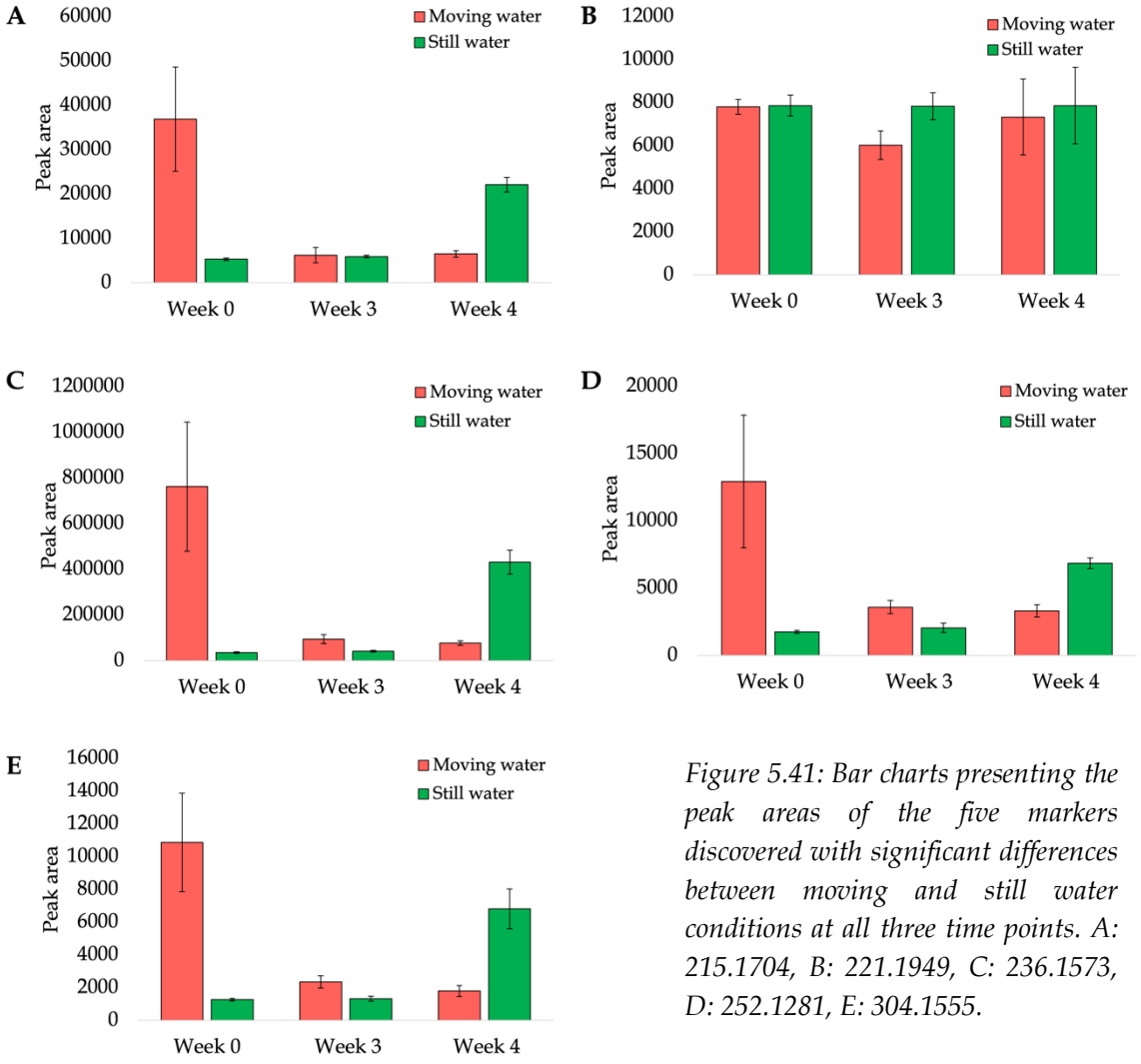

Figure 5.41: Bar charts presenting the peak areas of the five markers discovered with significant differences between moving and still water conditions at all three time points. A: 215.1704, B: 221.1949, C: 236.1573, D: 252.1281, E: 304.1555.

Markers **A**, **C**, **D** and **E** all show a higher peak area in the moving water sample at week 0, very low peak area during week 3 and a sudden increase in peak area for the still water sample at week 4. On the other hand, marker **B** does not show any drastic changes in peak area over time. These results show how the movement of the water can affect the presence of decomposition products at certain time points. The behaviour of marker **B** also emphasizes that each compound does not progress or behave the same. The chemical changes during decomposition are so complex that the effects of these changes are variable.

5.4 Conclusion and future work

This experiment successfully used untargeted metabonomic analysis with liquid chromatography-mass spectrometry to investigate the influence of running or still water on the chemical signature of a decomposing carcass in water. This workflow was able to monitor the progress of decomposition over time, whilst highlighting the differences between each water condition. The effects of temperature on these conditions were also investigated thoroughly.

It is fascinating that although the experiment focused on the same species in the same amount of water and in the same environment, there was such a pronounced difference in the chemical changes as a result of water movement, or lack thereof. It was expected that moving water would increase the rate of decomposition due to the agitation of the carcass, however, there were clear signs during the experiment that showed this to be untrue. Insect activity was more prominent in carcasses placed in still water compared to moving water. It is possible that the movement of the water could have deterred the insects or damaged the eggs, resulting in the delay of maggot colonisation. The increased insect activity in the still water boxes potentially accelerated the decomposition process, resulting in the drastic changes observed earlier in the chapter. Another visible difference between the moving and still water condition was the formation of white film on the surface of the water. This film formed on day 17 in the still water condition, whilst not until day 20 in the moving water condition. The movement of the water alongside the delay in insect colonisation most likely delayed the formation of this film.

There is also clear variation in the chemical signature of the water over time when comparing moving and still water conditions. The chromatograms highlight obvious differences between the moving and still water samples. In the moving water condition,

the peak intensities and number of peaks increase slowly over time, whilst in still water this is not the case. It seems that in still water, the sample collected at week 3 shows higher peak intensities toward the end of the chromatogram, and week 4 at the beginning. This is emphasized when looking at the PCA plots at week 0, 3 and 4, where the distance between the sample groups increases over time. However, this is not only due to the increase in decomposition products in an enclosed space, as often the peak area of certain markers in the sample would also decrease over time. While it was interesting to investigate the number of statistically significant markers at each time point, it is also important to consider that there are over a thousand compounds identified in these samples that show no statistical significance between moving and still water. Therefore, while there are markers that clearly show the difference in the chemical signature of the water from both conditions, the vast majority of the sample content is similar. However, it is clear from the results throughout this chapter that the markers showing significant differences heavily influence the sample matrix.

Conducting this experiment in both summer and winter conditions also provided useful insight into the effect of temperature on the decomposition process and the differences caused by water movement. The observations showed that the rate of decomposition was significantly reduced by the low temperatures in winter. The lack of insect activity, odour, discolouration of the water and changes to the carcass itself provided useful insight of what to expect in the chemical analysis. Overall, the results proposed that the samples taken during the winter experiment had a much lower quantity of decomposition products compared to the samples taken in summer. The chromatograms from the winter experiment produced a limited number of peaks and low peak intensities in comparison to the chromatograms obtained during the summer. Additionally, during the summer there was greater separation on the PCA plot between the sample groups over time,

accompanied by greater separation between the moving and still water conditions at specific time points. This suggests that not only was the rate of decomposition faster in the summer, the chemical differences between moving and still water conditions were also greater. It is important to note that the ability of this metabonomic workflow to identify changes in the chemical signature of the water over time in both moving and still water conditions in the winter temperatures is a high level of success. With the temperatures often dropping under 0°C, and very limited visual changes to the decomposing carcasses, this workflow was able to detect a large number of markers showing significant differences not only over time, but also between moving and still water conditions.

Future work in this area could improve the current experimental procedures and provide greater insight into the effects of moving water on decomposition. One of the main factors to improve would be to provide a bigger sample set to gain more reliable results from statistical analysis. Adding more time points to the experiment such as sampling twice a week would give greater insight into these subtle metabonomic changes, and how quickly the chemical signature of the water can change. An important consideration when discussing these results was whether the sampling location in the box could have affected the results. The stagnation of the water could cause leachates to cluster in one particular area, therefore an essential research goal moving forward would be to investigate whether the sampling location such as area and depth influences the results obtained. Furthermore, looking into the effects of other water conditions such as salinity and pH would be an opportunity to broaden the research goals outlined in this chapter. Incorporating these additional factors would help this new research area move forward, using the successful data from preliminary experiments and applying them to more realistic circumstances.

5.5 References

[1] National Water Safety Forum, A Future Without Drowning: The UK Drowning Prevention Strategy 2016-2026, 2015, pp. 1-10.

[2] M. Cassidy, Body found in Lake district during search for Newcastle swimmer. <https://www.chroniclelive.co.uk/news/north-east-news/body-found-lake-district-during-21113187>, 2021 (accessed 07/03/22.).

[3] BBC News, Woman found dead in Oxfordshire lake identified after CCTV appeal. <https://www.bbc.co.uk/news/uk-england-oxfordshire-58340568>, 2021 (accessed 07/03/22.).

[4] J. Macpherson, Man's body found in Lake District after huge underwater search. <https://www.lancs.live/news/local-news/mans-body-found-lake-district-21135444>, 2021 (accessed 07/03/22.).

[5] J. Tyler, Body found in river by police searching for missing woman Margaret Tyszkow. <https://www.birminghammail.co.uk/news/midlands-news/body-found-river-police-searching-22904877>, 2022 (accessed 07/03/22.).

[6] BBC News, Harvey Parker: Body recovered from Thames is missing student. <https://www.bbc.co.uk/news/uk-england-london-59902225>, 2022 (accessed 07/03/22.).

[7] T. Beattie, Body found in search for missing Gateshead man Jamie Grant. <https://www.chroniclelive.co.uk/news/north-east-news/jamie-grant-body-found-gateshead-23299108>, 2022 (accessed 07/03/22.).

[8] A. Ruffel, J. Pringle, J. Cassella, R. Morgan, The use of geoscience methods for aquatic forensic searches, Earth-Science Reviews 171 (2017) 323-337.

[9] R. Parker, A. Ruffell, D. Hughes, J. Pringle, Geophysics and the search of freshwater bodies: a review, Science & Justice 50 (2010) 141-149.

[10] C. Healy, J. Schultz, K. Parker, B. Lowers, Detecting submerged bodies: controlled research using side-scan sonar to detect submerged proxy cadavers, Journal of Forensic Science 60 (2015) 743-752.

[11] A. Ruffell, Lacustrine flow (divers, side scan sonar, hydrogeology, water penetrating radar) used to understand the location of a drowned person, Journal of Hydrology 513 (2014) 164-168.

[12] O. McGrane, A. Cronin, D. Hile, Use of handheld sonar to locate a missing diver, Wilderness & Environmental Medicine 24 (2013) 28-31.

[13] A. Annan, J. Davis, Impulse radar and time-domain reflectometry experiments in permafrost terrain during 1976, In: Section 12, Report of Activities, Part B; Geological Survey of Canada Paper 77-1B (1977) 67.

[14] P. Sellmann, A. Delaney, S. Arcone, Sub-bottom surveying in lakes with ground-penetrating radar, In: U.S. Army Corps of Engineers Cold Regions (1992).

[15] A. Ruffell, Under-water scene investigation using ground-penetrating radar (GPR) in the search for a sunken jetski, Northern Ireland, Science & Justice 46 (2006) 150-159.

[16] J. Pope, R. Lewis, T. Welp, Beach and Underwater occurrences of ordnance at a former defense site, Erie Army Deport, Ohio, Army Corps of Engineers CERC Report 96-1, (1996).

[17] M. Sorg, D. Edward, Forensic Osteology: Advances in the Identification of Human Remains, Charles C. Thompson Publisher, Illinois, 1998.

[18] A. Lasseter, K. Jacobi, Cadaver dog and handler team capabilities in the recovery of buried human remains in the southern United States, Forensic Science Journal 48(3) (2003) 617-621.

[19] D. France, T. Griffin, Forensic Taphonomy: The Postmortem Fate of Human Remains, CRC Press, Florida, 1997.

[20] D. Komar, The use of cadaver dogs in locating scattered remains: Preliminary field test results, Journal of Forensic Science 44(2) (1999) 405-408.

[21] A. Snovak, Guide to Search and Rescue Dogs, Barron's Educational Series, New York, 2004.

[22] H. Dick, J. Pringle, Inorganic elemental analysis of decomposition fluids of an in situ animal burial, Forensic Science International 289 (2018) 130-139.

[23] L. Swann, S. Forbes, S. Lewis, Observations of the temporal variation in chemical content of decomposition fluid: A preliminary study using pigs as a model system, Australian Journal of Forensic Sciences 42(3) (2010) 199-210.

[24] J. Giertsen, I. Morild, Seafaring bodies, American Journal of Forensic Medicine and Pathology 10(1) (1989) 25-27.

[25] W. Rodriguez III, Decomposition of buried and submerhed bodies, in: W. Haglund, M. Sorg (Eds.), Forensic Taphonomy: The Postmortem Fate of Human Remains, CRC Press, Boca Raton, 1997.

[26] L. Ayers, Differential decomposition in terrestrial, freshwater and saltwater environments: A pilot study, Texas State University, Texas, 2010, p. 99.

[27] O. Alley, Aquatic decomposition in chlorinated and freshwater environments, Texas State University, Texas, 2007, p. 84.

[28] S. Boyle, A. Galloway, R. Mason, Human aquatic taphonomy in the Monterey Bay area, in: W. Haglund, M. Sorg (Eds.), Forensic Taphonomy: The Postmortem Fate of Human Remains, CRC Press, Boca Raton, 1997.

[29] J. Davis, M. Goff, Decomposition patterns in terrestrial and intertidal habitats on Oahu Island and Coconut Island, Hawaii, Journal of Forensic Sciences 45(4) (2000) 836-842.

[30] W. Lawler, Bodies recovered from water: a personal approach and consideration of difficulties, Journal of Clinical Pathology 45 (1992) 654-659.

[31] T. Simmons, V. Heaton, Postmortem Interval: Submerged Bodies, Wiley Encyclopedia of Forensic Science, John Wiley & Sons, New Jersey, 2013.

[32] V. Heaton, A. Lagden, C. Moffat, T. Simmons, Predicting the Postmortem Submersion Interval for Human Remains Recovered from UK Waterways, Journal of Forensic Sciences 55(2) (2010) 302-307.

[33] J. Caruso, Decomposition Changes in Bodies Recovered from Water, Academic Forensic Pathology International 6(1) (2016) 19-27.

[34] R. Farris, Decomposition and entomological associations of swine in Louisiana micro-environments, LSU Digital Commons, Louisiana State University and Agricultural and Mechanical College, Louisiana, 2014, p. 56.

[35] G. Anderson, L. Bell, Impact of Marine Submergence and Season on Faunal Colonization and Decomposition of Pig Carcasses in the Salish Sea, PLOS ONE 11(3) (2016) 1-20.

[36] G. Cotton, A. Aufderheide, V. Goldschmidt, Preservation of human tissue immersed for five years in fresh water of known temperature, Journal of Forensic Sciences 32(4) (1987) 1125-1130.

[37] G. Anderson, N. Hobischak, Decomposition of carrion in the marine environment in British Columbia, Canada, International Journal of Legal Medicine 118 (2004) 206-209.

[38] M. Neuman, A comparative study of the effects of river flow rates on decomposition, Geography and Anthropology, Louisiana State University and Agricultural and Mechanical College, Louisiana, 2017, p. 53.

[39] T. Sangster, H. Major, R. Plumb, A.J. Wilson, I.D. Wilson, A pragmatic and readily implemented quality control strategy for HPLC-MS and GC-MS-based metabonomic analysis, Analyst 131(10) (2006) 1075-1078.

[40] F. Michopoulos, L. Lai, G. Gika, I. Theodoridis, UPLC-MS-Based Analysis of Human Plasma for Metabonomics Using Solvent Precipitation or Solid Phase Extraction, Journal of Proteome Research 8(4) (2009) 2114-2121.

[41] K. Sidwick, A. Johnson, C. Adam, L. Pereira, D. Thompson, Use of Liquid Chromatogrphy Quadrupole Time-of-Flight Mass Spectrometry and Metabolic Profiling to Differentiate between Normally Slaughtered and Dad on Arrival Poultry Meat, Analytical Chemistry 89(22) (2017) 12131-12136.

[42] R. Tautenham, G. Patti, D. Rinehart, G. Siuzdak, XCMS Online: A Web-Based Platform to Process Untargeted Metabolomic Data, Analytical Chemistry 84 (2012) 5035-5039.

[43] G. Theodoridis, H. Gika, E. Want, I. Wilson, Liquid chromatography-mass spectrometry based global metabolite profiling: A review, Analytica Chimica Acta 711 (2012) 7-16.

Chapter 6

Using metabonomic profiling methods to investigate the chemical signature of leachate samples from buried human remains.

The focus of this experiment was to investigate the potential of using non-targeted metabonomic analysis to profile the chemical signature of leachate samples taken from various locations under decomposing human remains. There were two primary aims. The first was to investigate how the leachate interacts with different column chemistries, to obtain as much information as possible from each sample. The second was an attempt to define a chemical profile of the leachates to investigate the chemical changes during human decomposition over time, using biological markers. The identification of these markers could provide a direction for future studies that will influence the way human remains are investigated.

6.1 Introduction

Research into the human decomposition process has accelerated in the scientific community, evolving from forensic anthropology into other disciplines in the last 30 years. Significant advances in this field have expanded our knowledge of decomposition, contributing to its increasing popularity. This has triggered a substantial growth in research activity involving decomposition studies, and how various new techniques and approaches can be used together to try and answer the big questions [1].

The vast majority of our knowledge of the decomposition process have relied on studies conducted on a range of vertebrates. The use of animal models in experiments dates back to the ancient Greek times, where human anatomy was studied using chicks and dogs [2]. The most frequently used analogues for forensic decomposition studies since the 1980's are pigs, known for their anatomical and physical similarities to humans. They are excellent subjects that provide good replication, reliability and are easily obtained for forensic experiments. This provided a more experimental approach for forensic taphonomy. There have been countless studies producing successful results using pigs as human analogues for a variety of purposes such as changes in environment, seasons, PMI calculations and search techniques [3-6]. Researchers have also worked successfully with mice [7, 8], rats [9], dogs [10] and rabbits [11].

A chemical approach to decomposition has unearthed concerns that the similarities between pigs and humans could be outweighed by their chemical differences. While it has been established that pigs and humans have similar body mass and gut microbiome composition compared to other carnivores and herbivores [12], various publications in the last decade have expressed the differences between each mammalian species' unique

composition. Research focusing on the formation of adipocere identified higher levels of fatty acids and moisture content present in pigs compared to humans, leading to variations in adipocere formation [13]. Additionally, the nitrogen content is also higher in humans, which can lead to a variety of differences in breakdown pathways [14]. Furthermore, Vass [15] also discovered differences between pig and human profiles when looking at the volatile organic compounds (VOC) released, with the differing odours between species exposed by human remains detection dogs [15]. The combination of these chemical differences in each species can therefore influence the environment surrounding the decomposing remains. A chemical study of the surrounding soil of graves showed various differences in the biogeochemical activity of the soils between human and pig remains [16]. This study was published in 2021, emphasizing that we are only just discovering the methodologies that will unearth accurate and reliable knowledge of the chemistry of human decomposition. Another recent study in 2018 quotes "human remains behave less predictably than those of pigs or rabbits such that the nonhuman models could not replicate the impacts of differential insect activity, scavenging or physical state changes (e.g., mummification) exhibited by the human subjects" [17, 18].

There are acknowledgeable difficulties with using human remains in decomposition studies, such as the variability between each human being (age, illness, type of death), the difficulties in getting adequate donations and the costs that arise as a result. The variation of laws in different countries limits the number of facilities, which could make it difficult to replicate experiments in different climates. Despite this, raising the awareness of the importance of these human decomposition facilities using the valuable knowledge already gained from studies at these facilities can be beneficial for future research into the chemistry of human decomposition.

There are a total of five active facilities working on human decomposition research in the USA, in addition to one in Australia, and recently in Canada and the Netherlands. The first facility was opened by Dr. William Bass at the University of Tennessee, Knoxville. His work on human decay rates began in 1972 [19, 20]. This seemed a unique opportunity to study human decomposition in a controlled environment when he came across a case that interested him. In 1977, a vandal disturbed a Civil War era burial. Investigators identified active decomposition in one of the graves, suggesting a homicide victim was placed there. With Dr. Bass' knowledge and experience of decomposition patterns, he believed the remains were a year old. However, it was later discovered that it was in fact the original grave with Colonel Shy, a Civil War casualty buried there. His body was embalmed and placed in a cast iron coffin, preserving his remains until the recent vandalism [19]. After a badly missed estimate concerning time of death, Dr. Bass realised the lack of research surrounding an important question – how to calculate the time of death! As a result, The Anthropology Research Facility (ARF) was established in 1980 on an old hospital site at the University of Tennessee. After receiving the first body donation in 1981 the numbers increased rapidly each year, reaching its maximum in 2006 with 107 bodies donated.

The initial research focus was based on morphological changes associated with decomposition, and how different environments and insects can affect these processes [21, 22]. By 1994, research at the facility had developed to look at how bodies decompose in water, and the formation of adipocere with Dr O'Brien [23]. In the meantime, research began to attempt to determine the 'time since death' by collecting data on volatile fatty acids deposited in soil solution from under decomposing remains [24]. By 2002, Vass had successfully developed a new method to help determine a post mortem interval (PMI) using volatile organic compounds (VOC) [25]. The distinct changes in chemical patterns discovered could be correlated to the length of time since death. An Odour Analysis

Database was created in 2004, with over 400 compounds of interest identified to help estimate the PMI of human remains [26]. It was clear from the valuable knowledge gained from the ARF that research on human remains was a success, and the way forward to learn more about human decomposition.

Despite this, concerns were quickly raised about the risks of saturation at the site, of decomposition by-products, and an increased population of insects. Shahid et al [27] conducted an in depth experiment to determine whether these allegations were scientifically true. They discovered that the prevalence of sarcosaprophagous arthropods (blow flies, flesh flies, skipper flies, carrion beetles, and rove beetles) was not significant different in the ARF facility, than beyond the fence and surrounding sites [27].

Whilst four other research facilities have opened in the USA, the Australian Facility for Taphonomic Experimental Research (AFTER) was opened in 2016 at the University of Technology Sydney by Professor Shari Forbes, an Australian and Canadian forensic researcher [28]. This 49-hectare site was the first facility to open in the southern hemisphere, and in 2016 alone received over 40 body donations. They have formed strong partnerships with New South Wales Police, Australian Federal Police and the Fire and Rescue NSW. Forbes has expressed that there are many other valuable applications for research conducted at a 'body farm', such as improving search and recovery methods and identifying victim remains [28]. Investigating the VOC's released during decomposition is a strong focus at this research facility [29], with Forbes leading a vast number of studies on the chemical odour profile of decomposition [30]. A significant purpose to these experimental studies are to increase our understanding of cadaver detection dog training, and to investigate what odours the dogs are identifying [31]. The success of this particular facility is reflected in the successful design of an 'electronic nose system', for odour analysis

and assessment [32]. The development of science and technology at these facilities have the potential to revolutionize the search and rescue methods around the world.

Initially explored in 2010, the Human Taphonomic Research Facility (HTRF) in the Netherlands was announced in 2017. This new facility was not only special because it was the first and only European taphonomic research facility, but also as it specifically allowed the study of buried bodies [33]. Located in the vicinity of the Amsterdam Medical Center (AMC), this allowed ease of access to the morgue, technical assistance and experimental facilities. In March 2018, the first inhumation was performed to test the logistics and operational workflows as a reference for future methodologies. Following this, in November 2018, the Amsterdam Research Initiative for sub-surface Taphonomy and Anthropology (ARISTA) was opened [33]. There are currently five active graves in use by a variety of international research groups. The strategy for ARISTA presented a different focus to what has been done elsewhere. The main focus of this taphonomic research facility is to use remote and telemetric sensing, with the use of minimally invasive sampling techniques to allow the opportunity for a full archaeological excavation of undisturbed remains.

- **REMOTE SENSING.** Using the technology of ground penetrating radar (GPR) and spectral imaging allows the preservation of the integrity of the taphonomic processes within each grave. These techniques can be repeated indefinitely.
- **TELEMETRIC SENSING.** Placing temperature and humidity sensors in and around the body causes a very limited amount of disturbance to the decomposition processes in the grave.

- **SAMPLING.** Minimally invasive sampling opportunities such as VOC measuring, leachate lysimeters will have minimal influences on the experiment. Sampling body parts temporarily exposed for tissue biopsies is also carried out, causing disturbance to the natural decomposition processes.

These new research methodologies have the potential to expand the focus of decomposition to cover a broad range of disciplines, giving a unique opportunity for researchers from all areas to work together.

6.2 Methods and materials

6.2.1 Experimental method

6.2.1.1 Materials

Methanol (HPLC grade), formic acid and a reference mass solution consisting of purine (*m/z* 121.0509) and hexakis (1*H*, 1*H*, 3*H*- tetrafluropropoxy)phosphazine (*m/z* 922.0098) were purchased from Fisher Scientific (Loughborough UK). Ultra-pure water (18.2 MΩ) was purified using a Purelab Option-Q system by Veolia Water (Saint Maurice, France). Lysimeters were purchased from HANNA Instruments (Bedfordshire UK).

6.2.1.2 Experimental setup

The measurements of the site were 32 m x 18 m, enclosed with a fence extending 3 m above ground and 1m below ground to avert unauthorised persons and larger animals. The plot can accommodate 30-50 graves, depending on the distance between each grave. The burial site was 2 m long, 8 m wide and 60 cm deep. Each body is buried at the lowest level to avoid cross contamination of future graves.

The top level of terrain is 4m below sea level. It consists of 1m of a homogeneous blend of various sand types and peat, covered by 10-20 cm of humus-rich topsoil. The groundwater table fluctuates around 70 cm and is tilted downward in the north westerly direction. The surface homogeneity was determined using ground penetrating radar (GPR) and ground condctivity, further validated with soil profiles retrived with an auger. To ensure the site was kept as natural as possible, most of the vegetation was kept in situ.

Continuous telemetric registration of temperature and humidity was collected using a Sweco Nederland B.V data logging system, which can be accessed through the web-based platform. This data was also coupled with simultaneous non-tephonomic ambient data retrieved from a weather station, and two ground water gauges to measure the water table and temperature. The experiment began on the 28th August 2019. Ethical approval for this work was approved by the University (NS-190054).

6.2.1.3 Sample collection and storage

One lysimeter was placed at the head of the body, the second at the foot of the body, and a control lysimeter placed at opposite side of the site. The water was removed from the soil through a porous ceramic cup with a vacuum placed on the cup. A sample was collected

from the lysimeters every two weeks, if a leachate sample was present. Figure 6.1 Shows a labelled diagram of a sampling lysimeter.

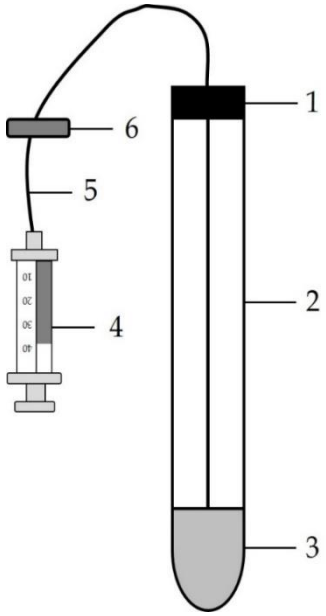

Figure 6.1: A labelled diagram of a basic sampling lysimeter. 1: Rubber cap, 2: Soil solution sampler tube, 3: Porous ceramic cup, 4: 30 ml syringe, 5: Rubber suction capillary, 6: Finger clamp.

The syringe was connected to the rubber capillary, and the syringe piston was drawn back 30ml. Following this, the finger clamp was pinched and the syringe disconnected. A vacuum of -60cb was created in the sampler tube. The soil solution was drawn out after 30 minutes as followed; The syringe was connected to the rubber capillary, the finger clamp opened and the syringe piston drawn 30 ml. The piston was held until all the solution that was available was sucked into the syringe, then disconnected with the finger clamp left open. All samples were placed in a 1.5 ml Eppendorf tube and centrifuged for 10 minutes at 16100 rcf to remove any particulates, then stored in a freezer at -25^{o}C prior to analysis.

It is important to note that this experiment was a preliminary experiment, conducted to develop an effective and robust method for the metabonomic analysis of leachates collected

underneath decomposing remains. Due to the unpredictable nature of the leachates, a sample was not always available at the specific time points chosen. Furthermore, as a result of factors beyond our control, further experiments could not be conducted at this time and therefore leachate samples were limited.

Table 6.1 shows the location underneath the body and the date each sample was collected. Each sample was injected three times into the instrument as accurate replicates.

Table 6.1: The location and date of each sample taken during the experiment.

Area of body	18 / 09	01 / 10	24 / 10	07 / 12	09 /12
Control	**X**				
Head	**X**	**X**			
Foot	**X**	**X**	**X**	**X**	
Runoff Water					**X**

6.2.2 Instrumental setup

6.2.2.1 Quality control

This was carried out exactly as described in **Chapter 3, Section 3.2.3.1**.

6.2.2.2 Chromatographic parameters

The chromatographic separation was carried out using an Agilent Technologies 1260 Infinity Binary HPLC system. Early method development was conducted on each column to produce a robust and effective solvent gradient unique to each column, shown below.

C18 Column. Thermo Fisher C18 Hypersil Gold (100 mm x 2.1 mm, 1.9 µm particle size). The column temperature was maintained at 40°C, and the injection volume was 5 µl. The mobile phase consisted of (A) Water with 0.1% formic acid and (B) Methanol with 0.1% formic acid. The flow rate was 0.2 ml min^{-1}. The solvent gradient is shown in Table 6.2.

Table 6.2: Solvent gradient used for the analysis of leachate samples, using a C18 column.

Time (minutes)	Solvent A (%)	Solvent B (%)
0	97	3
6	97	3
12	20	80
22	20	80
25	0	100
30	0	100
32	97	3

Hypercarb Column. Hypercarb Porous Graphitic Carbon HPLC Column (100mm x 2.1mm), 5µm particle size. The column temperature was maintained at 40°C, and the injection volume was 5µl. The mobile phase consisted of (A) Water with 0.1% formic acid and (B) Methanol with 0.1% formic acid. The flow rate was 0.4 ml min^{-1}. The solvent gradient used is shown in Table 6.3.

Table 6.3: Solvent gradient used for the analysis of leachate samples, using a Hypercarb column.

Time (minutes)	Solvent A (%)	Solvent B (%)
0	97	3
3	40	60
5	35	65
10	35	65
12	0	100
20	0	100
21	97	3

HILIC Column. HILIC Accucore HPLC Column (100mm x 2.1mm, 2.6µm particle size). The column temperature was maintained at 40ºC, and the injection volume was 5µl. The mobile phase consisted of (A) Water with 0.1% formic acid and (B) Methanol with 0.1% formic acid. The flow rate was 0.5 ml min^{-1}. The solvent gradient used is shown in Table 6.4.

Table 6.4: Solvent gradient used for the analysis of leachate samples, using a HILIC column.

Time (minutes)	Solvent A (%)	Solvent B (%)
0	3	97
5	3	97
7	50	50
10	50	50
11	3	97

6.2.2.3 Mass spectrometry parameters

This was carried out exactly as described in **Chapter 3, Section 3.2.3.3**.

6.2.3 Data pre-processing

This was carried out exactly as described in **Chapter 3, Section 3.2.4.**

6.2.4 Data analysis and statistical analysis

This was carried out exactly as described in **Chapter 3, Section 3.2.5.**

6.3 Temperature

The temperature of the environment, along with the humidity, wind, rainfall, and moisture content have a significant effect on the rate of decomposition. During this study, the air temperature was monitored constantly to investigate how the temperature effects the production and content of leachate samples taken from near a decomposing body. Figure 6.2 shows the change in temperature during this study.

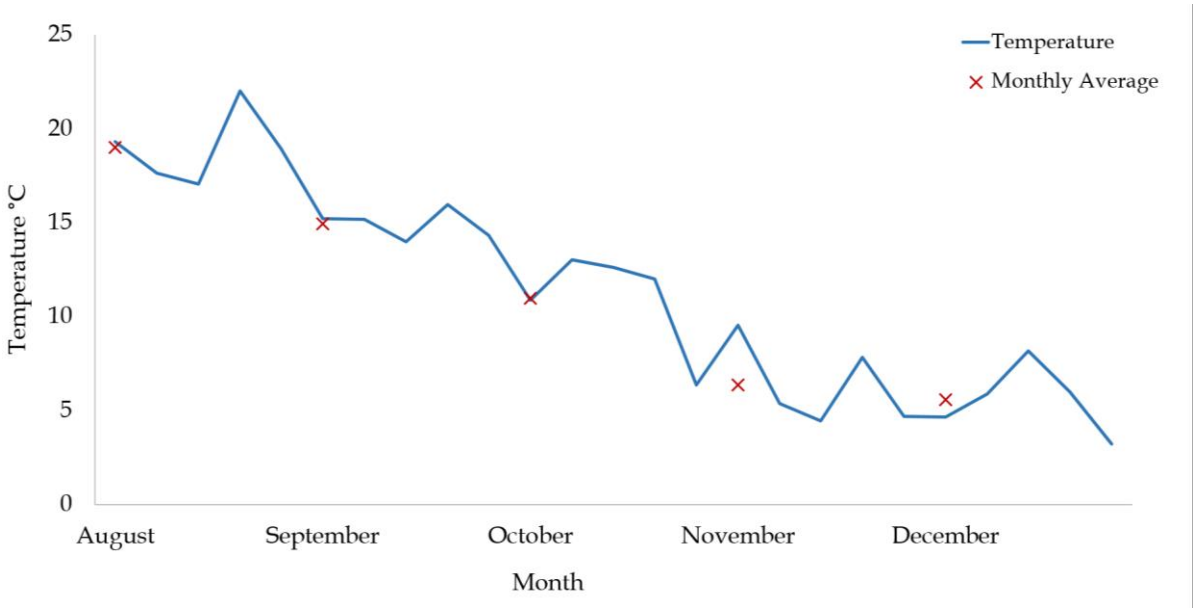

Figure 6.2: Graph showing the change in temperature every week between August and December 2019, also including a monthly average value.

The graph in Figure 6.2 highlights the typical trend expected for temperatures between August and December in this climate. The highest temperature in August was 32.5°C, and lowest 10.6°C. December produced a much lower highest temperature of 10.2°C, and lowest of -2.6°C. This substantial difference is very likely to have affected the rate of decomposition, and as a result, the chemical processes that occur in the body during decomposition.

6.4 Results and discussion using a C18 column

6.4.1 QC analysis

The chromatograms shown in Figure 6.3 show no visible retention time variability in the QC samples, and only minor differences in peak area.

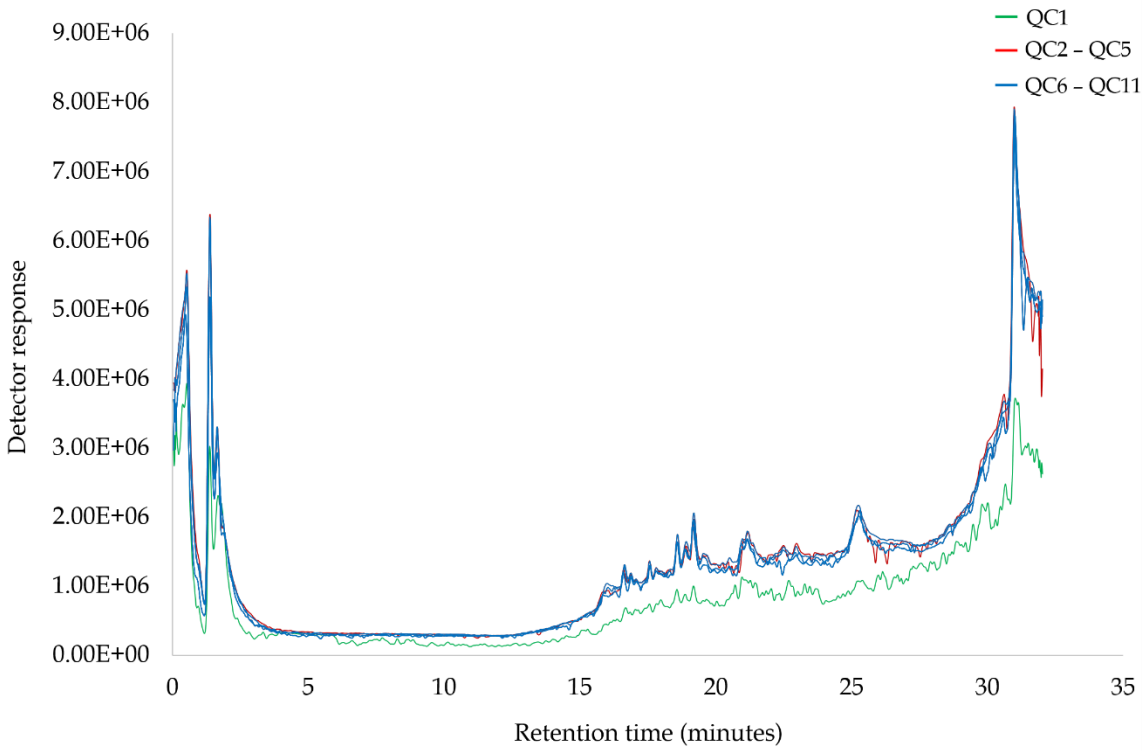

Figure 6.3: Total ion chromatograms of QC samples throughout the analytical run for leachate samples using a C18 column.

The baseline appears to be unstable in QC1, however, QC2 seems to have stabilised. Two blank samples were injected at the beginning of the sequence to condition the instrument. Table 6.5 presents supplementary data for variability between peak area and retention time. Although the CV values for peak area are much higher than those obtained for retention time values, they are still under the accepted level of variability for non-targeted metabonomic analysis.

Table 6.5: Variability of peak area (A) and retention time (B) from 6 selected peaks in the QC samples during the analytical sequence for leachate samples using a C18 column.

A

Peak	QC6	QC7	QC8	QC9	QC10	QC11	Average	St. Dev	CV%
1	2950315	6188775	6298119	6380347	5184569	6264139	**5544378**	**1346023**	**24%**
2	669566	1285248	1313446	1200778	1138070	669348.8	**1046076**	**298251**	**29%**
3	740312	1292991	1360942	1367524	1296405	1212891	**1211845**	**237716**	**20%**
4	947121	1637234	1748549	1623175	1641160	1675661	**1545484**	**296590**	**19%**
5	992596	1780831	2060227	1971240	1923509	1984541	**1785491**	**399338**	**22%**
6	1065574	2064602	2116983	2088894	1980666	2078894	**1899269**	**411006**	**22%**

B

RT	QC6	QC7	QC8	QC9	QC10	QC11	Average	St. Dev	CV%
1	1.39	1.39	1.39	1.39	1.39	1.37	**1.39**	**0.0056**	**0.41%**
2	16.64	16.64	16.65	16.65	16.64	16.63	**16.64**	**0.0041**	**0.02%**
3	17.57	17.57	17.58	17.58	17.57	17.57	**17.57**	**0.0020**	**0.01%**
4	18.58	18.59	18.59	18.59	18.58	18.57	**18.58**	**0.0035**	**0.02%**
5	19.19	19.2	19.20	19.20	19.19	19.20	**19.20**	**0.0020**	**0.01%**
6	25.32	25.33	25.33	25.33	25.32	25.35	**25.33**	**0.0127**	**0.05%**

6.4.2 Metabolic profiling

Due to the nature of the total ion chromatograms (TIC's) obtained during this analysis, total compound chromatograms (TCC's) were used for visualisation of the peaks. A TCC is a chromatogram showing the extraction of each compound identified within that sample. On account of the small amount of sample used, the abundance of compounds in each sample was low. A high baseline, and lack of resolution in the TIC's could be as a result of the compounds being inundated by background noise. Using the TCC provides more information for each peak present in the sample, allowing a clearer picture of the chemical signature of the sample, and eliminating the baseline. Observing these overlaid TCC's in Figure 6.4, a difference between peak pattern and peak intensity is seen between the samples taken from near the head in September and October.

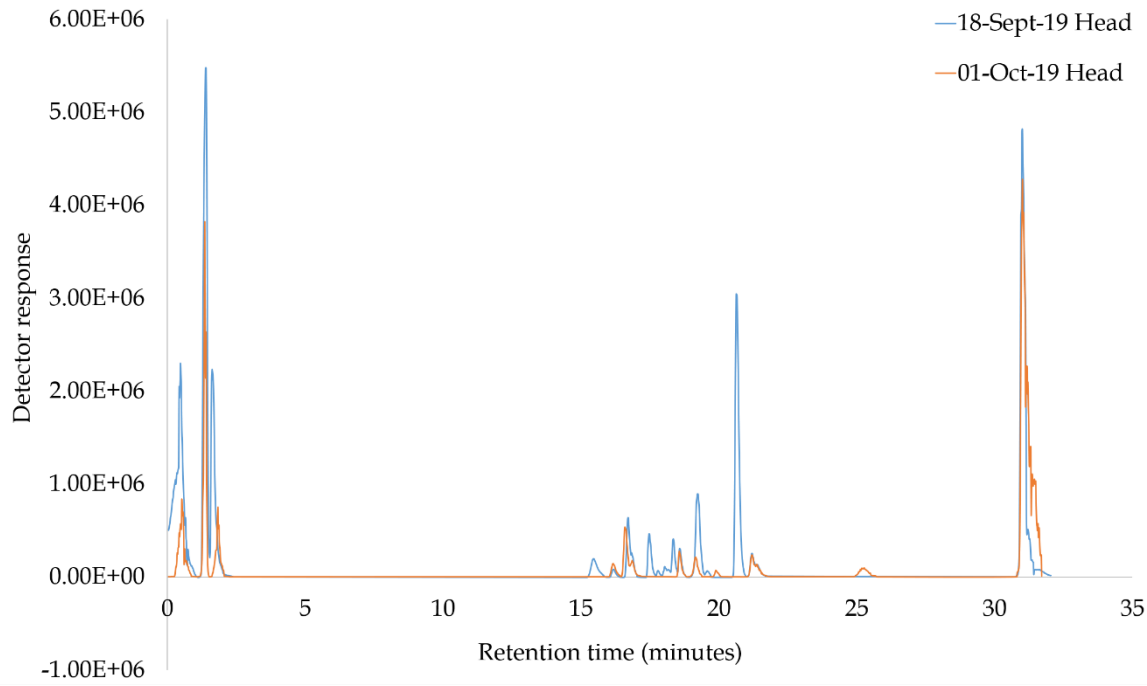

Figure 6.4: Example total compound chromatogram (TCC) of samples taken at the head of the body at two different time points, analysed using a C18 column.

The peak patterns at the beginning and very end of the chromatogram seem to be consistent between both samples, however, peaks from the sample taken in October have very low abundance throughout in comparison to those taken in September. There are differences between their chemical profiles at 15 – 25 minutes. An additional four peaks were present in the sample taken in September, which are not present in the sample taken in October.

Figure 6.5 shows the overlaid chromatograms for samples taken at four time points from the foot of the body. The chromatograms here show fewer differences in peak pattern, and more differences in peak intensities. Similar to what occurred in Figure 6.4, the majority of the peak intensities for samples taken at the beginning of October seem to decrease from those taken in September, additionally followed by a sharp increase in intensity in samples taken toward the end of October, then a slight decrease yet again in December. This is shown in the areas highlighted in grey on the chromatogram below. There is also an additional peak present at 18.9 minutes only on the sample taken on Oct-24.

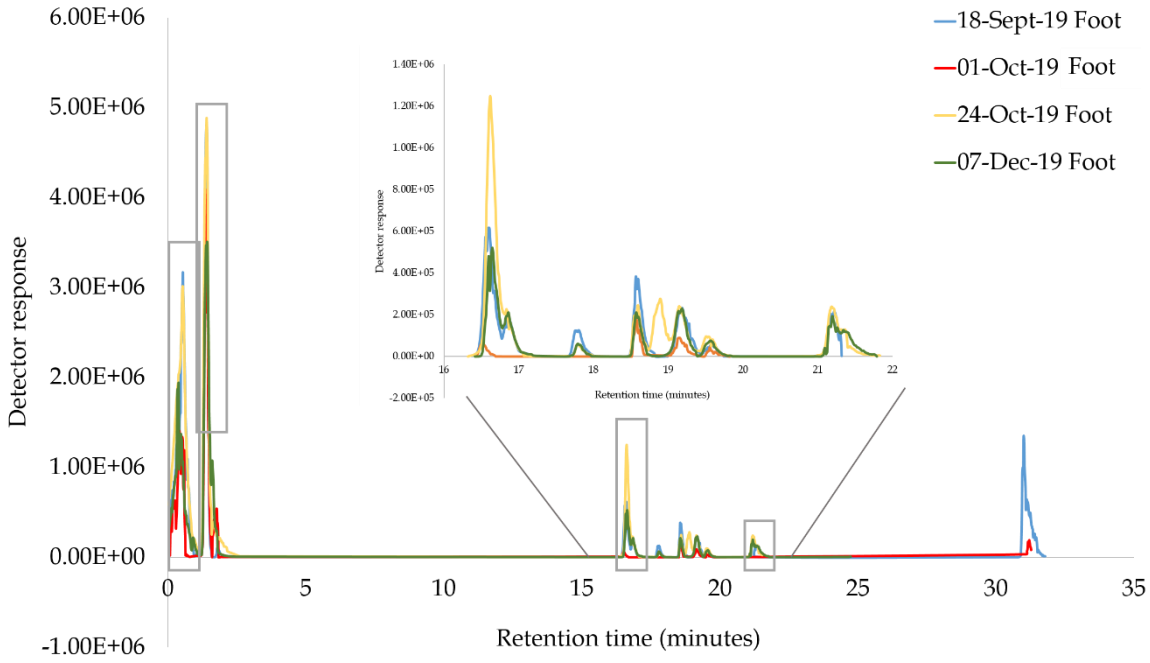

Figure 6.5: Example total compound chromatogram (TCC) of samples taken at the foot of the body at two different time points, analysed using a C18 column.

There is a high level of variability in the patterns between peaks between 15-25 minutes on the chromatograms. Each peak shows varying levels of intensity at different time points, even in very low abundances. This highlights the complexity of the decomposition process, and how even very small changes can affect the metabolite profile of the sample.

It is important to note that the overlaid chromatograms for leachate samples taken at the head and foot of the body show very similar peak patterns. This implies that similar class of compounds are detected at both areas of the body. It was assumed that the abundance of each compound detected in the leachates would increase over time as it clusters in the soil. The uncontrolled nature of this real-life experiment emphasises how quickly these compounds seem to have broken down further or simply washed away with groundwater, allowing compounds leaching from new chemical processes to appear. The decrease in temperature throughout the course of this experiment is very likely to have impacted the speed and efficiency of chemical decomposition happening in the body, as shown in Figure 6.2. which will be discussed further in this chapter.

6.4.3 Multivariate analysis

The PCA scores plot in Figure 6.6 shows the progression of the chemical profile of the leachate samples collected from the foot of the body at five time points and a control sample. The QC samples are clustered toward the middle of the plot, indicating minimal instrumental effects.

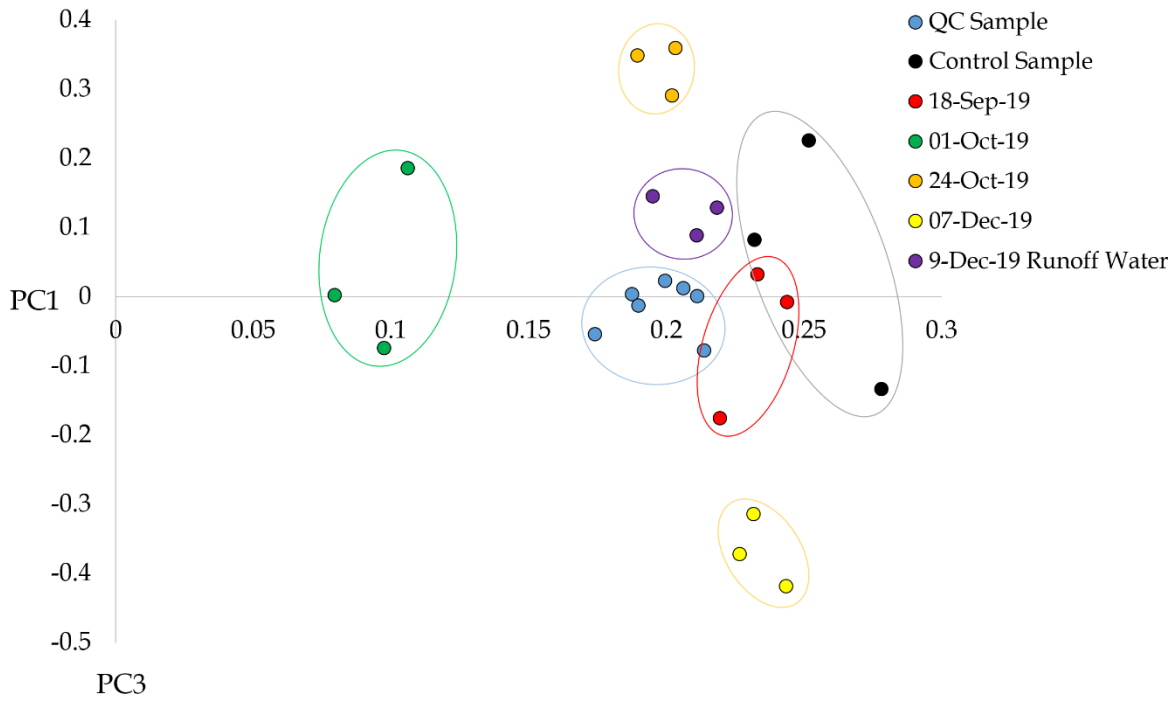

Figure 6.6: PCA score plot of PC1 (88.02%) and PC3 (8.22%) for leachate samples from the foot of the body using a C18 column.

Each experimental group shows good reproducibility on the plot, with little variation within the three replicates. These groups are also well separated on the plot, with limited overlap between the control sample and the sample taken on 18-Sept only. This is not unexpected as this sample was taken near the beginning of the experiment. The distance between each sample group is not further apart than the spread of the QC samples, however, each time point can still clearly be distinguished from the next on the plot. There is no linear progression between each time point as they are spread randomly across the plot. The runoff water sample is positioned close to the control sample, suggesting that their chemical profiles could be similar.

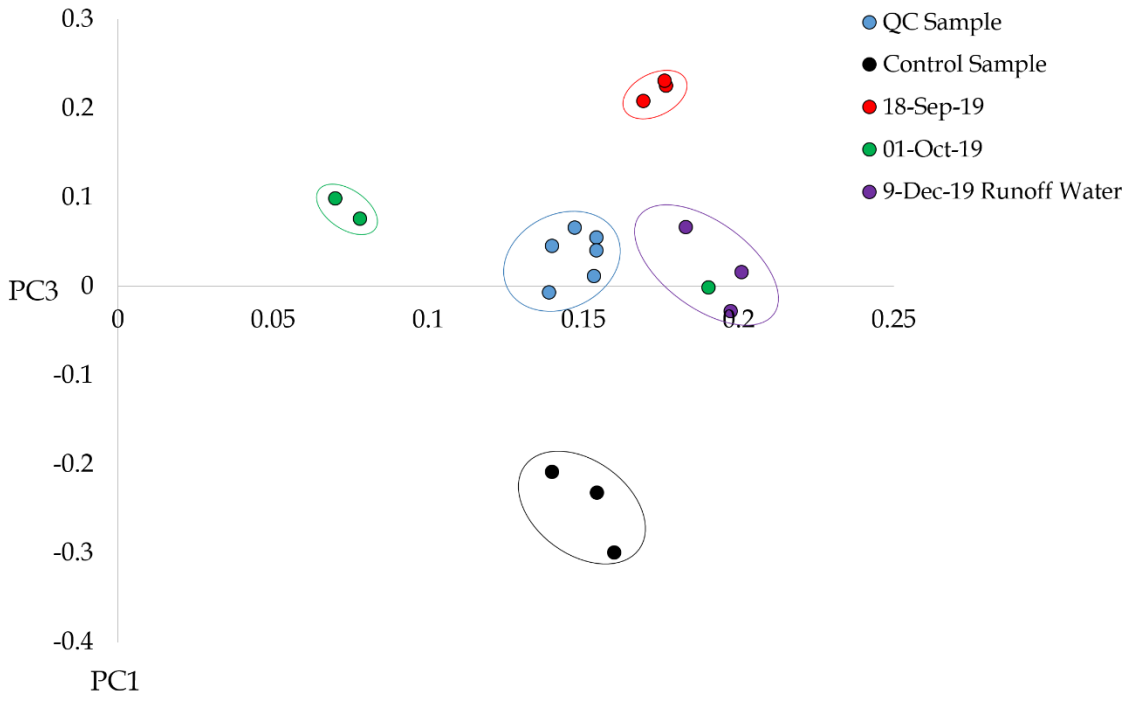

Figure 6.7: PCA score plot of PC1 (88.02%) and PC3 (8.22%) for leachate samples from the head of the body using a C18 column.

The PCA scores plot in Figure 6.7 representing the samples taken from the head of the body shows good separation between each sample group. A sample from 24 Oct and 7 Dec were not available from the head of the body due to the limited nature of leachates, however it is still possible to visualise the difference in the chemical profile between the time points presented. One replicate from 01 Oct seems to spread across the plot, and is considered an anomaly, most likely due to instrumental effects. The control sample is positioned much further away from the experimental samples compared to the samples taken from the foot of the body.

Table 6.6 looks at the *m/z* of the compounds that show significant differences between each time point at the head and foot of the body This data provides a deeper insight to the type of compounds expected at various stages of decomposition, and whether the compounds that are detected reflect the processes we are already aware of.

Table 6.6: Table showing the percentage of compounds of a specific m/z at each time interval showing significant differences, using a C18 column.

Area	% of m/z	Compounds showing significant differences between :		
		18 Sept and 01 Oct	01 Oct and 24 Oct	24 Oct and 7 Dec
Foot of the body	100-300	36%	50%	23%
	301-500	32%	35%	40%
	501+	32%	15%	37%
Head of the body	100-300	30%	N/A	N/A
	301-500	28%	N/A	N/A
	501+	42%	N/A	N/A

The data shows a sharp increase in the percentage of smaller compound (*m/z* 100-300), followed by a sharp decrease in the sample. Furthermore, the larger compounds (*m/z* 501+) show the opposite effect, a sharp decrease in percentage followed by an increase. Compounds with a *m/z* between 301-500 do not fluctuate. Samples taken at the head of the body also show a higher percentage of larger compounds present at the beginning of the experiment.

Decomposition is a process where large biological macromolecules such as proteins, carbohydrates and lipids are broken down into gases (volatile compounds) and leachates (non-volatile compounds) by bacteria, fungi and protozoa [25]. These smaller intermediate compounds such as amino acids, glucose monomers, fatty acids and alcohols will eventually break down to their most stable form [35]. The increase in percentage of smaller compounds at the same time as a decrease in large compounds could be explained as the breakdown of larger compounds into a variety of smaller compounds that overwhelm the sample. Nonetheless, it is slightly more challenging to explain why the percentage of compounds with a larger *m/z* increase towards the end of the experiment, whilst the

percentage of smaller compounds decrease. One possible explanation for this could be that the small compounds have broken down into even smaller compounds that cannot be detected by this method, or they have washed away from the sampling location. This would allow the larger compounds still present to dominate the sample.

It is important to consider that decomposition consists of a variety of processes/reactions happening at each stage. The larger compounds detected at the beginning of the experiment are likely to be very different to the larger compounds detected towards the end of the experiment. Further statistical analysis was conducted to provide deeper insight into the particular markers that influence these results.

6.4.4 Statistical analysis

The total number of features detected in the leachate samples was 3572. Following the removal of all features with a CV value over 30%, 2116 remained. A t-test was performed on samples from the head and foot of the body separately. Features with a *p-value* of more than 0.05 were removed, leaving 411 features from samples taken by the foot of the body, and 156 features from the head of the body. The top 50 compounds from both the head and foot of the body were chosen for further statistical analysis (ANOVA/Welch test) using. Table 6.7 shows the top 20 markers that proved to be the most robust and significantly different from samples taken at the foot of the body.

Table 6.7: Summary of the markers that show significant differences between at least two time points at the foot of the body, analysed using a C18 column.

m/z	Retention time (minutes)	CV	p-value		
			Compounds showing significant differences between :		
			18-Sept and 01-Oct	01-Oct and 24-Oct	24-Oct and 7-Dec
103.0018	1.37	23%	\	\	p<0.05
132.0995	1.63	21%	p<0.05	p<0.05	p<0.05
143.1049	15.28	24%	p<0.05	\	\
164.1223	1.58	19%	p<0.05	p<0.05	\
171.0657	1.78	25%	p<0.05	\	p<0.05
177.1094	15.92	22%	p<0.05	p<0.05	\
180.9437	1.61	24%	p<0.05	\	p<0.05
184.0973	1.62	16%	p<0.05	\	\
217.1748	17.80	21%	p<0.05	\	\
239.1588	17.84	28%	p<0.05	\	\
240.9639	1.39	21%	\	\	p<0.05
319.2578	31.88	26%	p<0.05	p<0.05	\
402.8964	1.48	25%	\	p<0.05	\
408.7838	0.51	29%	p<0.05	\	\
470.8839	1.48	24%	p<0.05	\	\
476.2371	31.02	27%	p<0.05	p<0.05	\
512.8750	1.41	22%	p<0.05	\	\
574.6889	0.51	24%	p<0.05	\	\

Each marker shown in Table 6.8 shows a significant difference between at least two time points. It is clear that the majority of these markers are showing significant differences between the first two time points (18-Sept and 01-Oct), while the number of significant differences identified decreases as the experiment progresses. This initial observation suggests that warmer months show an increase in decomposition activity compared to the colder months. Although samples were only collected at two time points at the head of the body, Table 6.8 shows the markers showing significant differences between two time points (18-Sept and 01-Oct) from samples taken at the head of the body.

Table 6.8: Summary of the top 20 markers that show significant differences between two time points at the head of the body, analysed using a C18 column.

m/z	Retention time (minutes)	CV	p-value
			Compounds showing significant differences between :
			18-Sept and 01-Oct
107.0463	18.43	22%	p<0.05
132.0995	1.63	21%	p<0.05
169.0491	1.37	12%	p<0.05
206.1338	1.68	25%	p<0.05
240.1546	18.44	11%	p<0.05
295.1830	19.19	29%	p<0.05
307.0814	18.44	9%	p<0.05
378.1848	18.09	27%	p<0.05
407.3932	1.38	12%	p<0.05
456.3937	1.39	25%	p<0.05
485.8819	1.39	19%	p<0.05
493.3725	1.39	25%	p<0.05
500.3625	1.39	18%	p<0.05
541.3653	1.40	12%	p<0.05
549.8609	1.39	27%	p<0.05
607.3523	1.39	12%	p<0.05
614.3403	1.40	18%	p<0.05
671.7758	1.41	27%	p<0.05
673.8314	1.40	28%	p<0.05
719.7653	1.43	8%	p<0.05

Overall, the markers identified at the head of the body seem to have a higher *m/z* than those identified at the foot of the body. The average *m/z* of markers showing significant differences at the foot of the body was *m/z 283,* and *m/z 450* at the head of the body. The substantial difference between the two suggests that very different chemical processes are occurring at both ends of the body, highlighting the complexity of metabolic processes after

death. The chemical breakdown of larger macromolecules into smaller products is reflected in the data accumulated during this experiment, showing that previous research into the chemical aspect of decomposition can be used to understand the patterns appearing in new research.

6.4.5 Marker identification

Of these compounds that were found to be statistically significant at different time points, four were tentatively identified through comparing mass spectra from the analysis to those provided by *METLIN*. The marker *m/z* 132.0995 was tentatively identified as Leucine, *m/z* 184.0973 as Epinephrine, *m/z* 169.0491 as Dihydroxyphenyl-acetic acid and *m/z* 171.0657 as 3,4-Dihydroxyphenyl glycol. The observed *m/z* for all four compounds were as a result of the $[M+H]^+$ adduct. The tentative identifications of each marker, their peak area and the *p-values* at each time interval are discussed further.

Table 6.9: Summary of the marker m/z 132.0995, tentatively identified as Leucine.

m/z	Adduct	Retention time (minutes)	Predicted formula	Tentative identification	Probability score
132.0995	[M+H]	1.63	$C_6H_{13}NO_2$	L-Leucine	85.4

Area	Foot of the body			Head of the body
Date	18-Sept and 01-Oct	01-Oct and 24-Oct	24-Oct and 7-Dec	18-Sept and 01-Oct
p-value	0.009	0.033	0.028	p<0.001

This marker was tentatively identified as leucine. The *p-values* from the statistical analysis in Table 6.9 show that the peak areas are statistically significant across all time points. The bar chart in Figure 6.8 shows that there are rapid changes in the abundance of leucine in the leachate samples collected from the head and foot of the body. It is important to note that the abundance in the control sample is very low, implying that it is very likely that the marker identified is leaching from the body into the ground, not only in the soil itself.

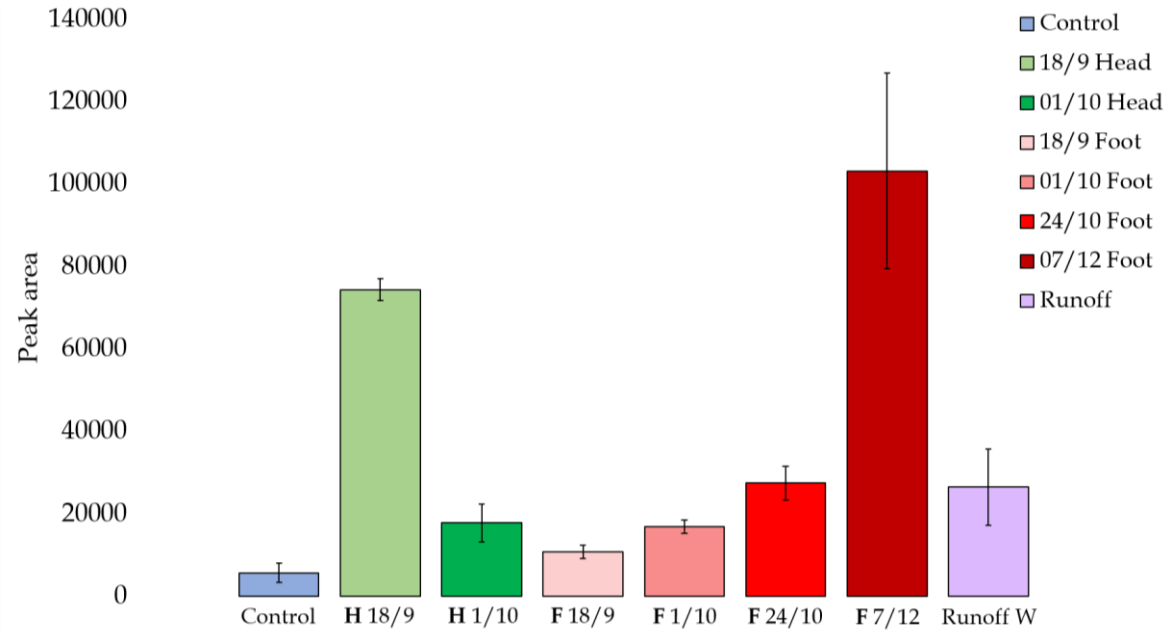

Figure 6.8: Bar chart showing the change in abundance over time of m/z 132.0995 tentatively identified as Leucine, in samples taken from the head and foot of the body with error bars ±1 standard deviation.

Table 6.10: Summary of the marker m/z 184.0973, tentatively identified as Epinephrine.

m/z	Adduct	Retention time (minutes)	Predicted formula	Tentative identification	Probability score
184.0973	[M+H]	1.62	$C_9H_{13}NO_3$	Epinephrine	75

Area	Foot of the body			Head of the body
Date	18-Sept and 01-Oct	01-Oct and 24-Oct	24-Oct and 7-Dec	18-Sept and 01-Oct
p-value	0.027	p>0.05	p>0.05	0.037

This marker was tentatively identified as epinephrine. The *p-values* in Table 6.10 show that this marker only yields statistically significant differences between the first two time points at the head and foot of the body, inferring that this compound may be a product of the early stages of decomposition. This is also reflected in the bar chart in Figure 6.9, demonstrating a dramatic change in abundance in samples from both the head and foot of the body at the first two time points, then decreasing over time.

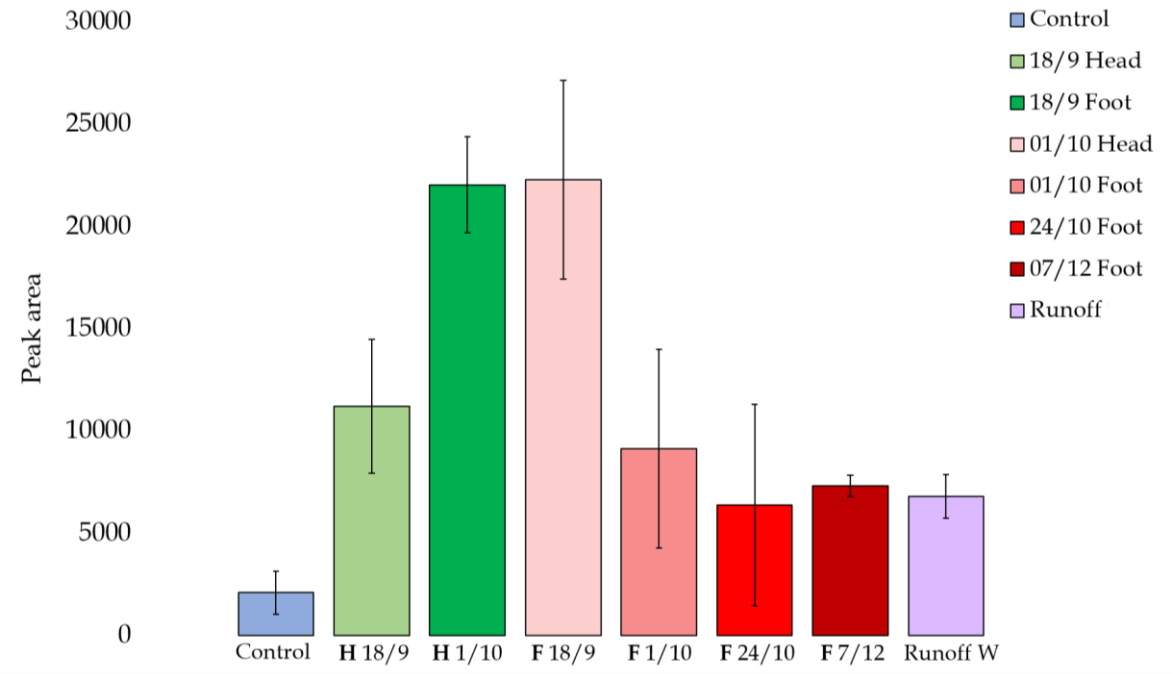

Figure 6.9: Bar chart showing the change in abundance over time of m/z 184.0973 tentatively identified as Epinephrine, in samples taken from the head and foot of the body with error bars ±1 standard deviation.

Table 6.11: Summary of m/z 169.0491, tentatively identified as Dihydroxyphenyl-acetic acid.

m/z	Adduct	Retention time (minutes)	Predicted formula	Tentative identification	Probability score
169.0491	[M+H]	1.37	$C_8H_8O_4$	Dihydroxyphenyl-acetic acid	66.8

Area	Foot of the body			Head of the body
Date	18-Sept and 01-Oct	01-Oct and 24-Oct	24-Oct and 7-Dec	18-Sept and 01-Oct
p-value	p>0.05	p>0.05	p>0.05	0.01

Table 6.11 shows that this marker only yields statistical significance in the sample taken at the head of the body, suggesting that this compound is more likely involved in decomposition processes happening in this area. When looking ar the bar chart in Figure 6.10, there also seems to be high abundance of this particular marker in the runoff water. It is possible that the compound drained very quickly through the site, accumulating at the lowest point, however, it is not possible to confirm at this time.

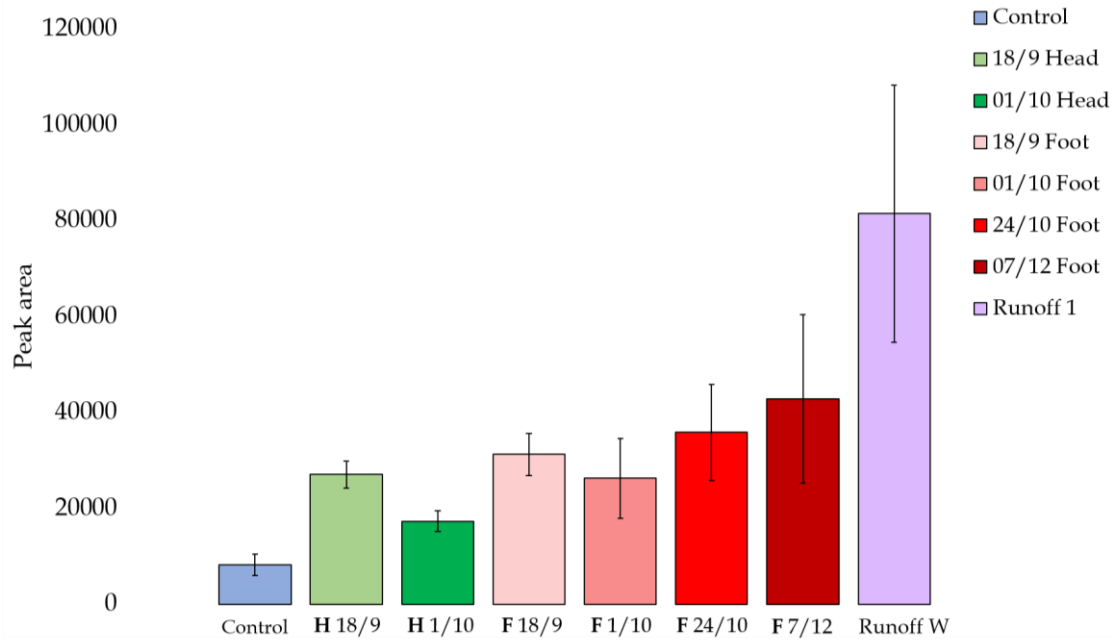

Figure 6.10: Bar chart showing the change in abundance over time of m/z 169.0491 tentatively identified as Dihydroxyphenyl-acetic acid, in samples taken from the head and foot of the body with error bars ±1 standard deviation.

Table 6.12: Summary of the marker m/z 171.0657, tentatively identified as DL-3,4-Dihydroxyphenyl glycol.

m/z	Adduct	Retention time (minutes)	Predicted formula	Tentative identification	Probability score
171.0657	[M+H]	1.78	$C_8H_{10}O_4$	3,4-Dihydroxy-phenyl glycol	83.5

Area	Foot of the body			Head of the body
Date	18-Sept and 01-Oct	01-Oct and 24-Oct	24-Oct and 7-Dec	18-Sept and 01-Oct
p-value	0.019	p>0.05	p>0.05	0.020

This marker was tentatively identified as DL-3,4-Dihydroxyphenyl glycol. Table 6.12 shows that this marker yields statistically significant differences between the first two time points at both the head and foot of the body, which is also evident by the changes in peak area on the bar chart in Figure 6.11. This implies that this marker also seems to be a key marker in the early stages of decomposition.

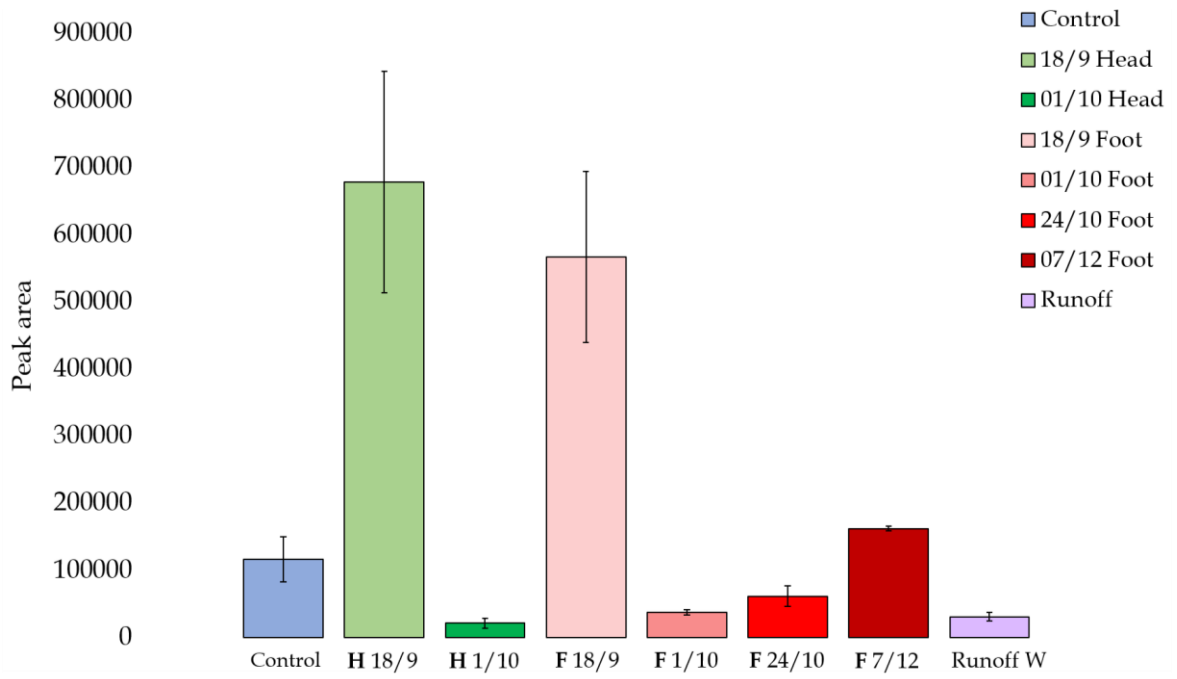

Figure 6.11: Bar chart showing the change in abundance over time of m/z 171.0657 tentatively identified as DL-3,4-Dihydroxyphenyl glycol., in samples taken from the head and foot of the body with error bars ±1 standard deviation.

Each of the tentatively identified markers were investigated further to assess their relevance to the decomposition process. Leucine is one of three branched chain amino acids, essential to human life. It is found naturally in the body provided by food, stimulating protein synthesis and muscle repair [36]. Leucine is also essential to regulate blood sugar levels, acting as a source for gluconeogenesis in the liver [37, 38]. The structure of leucine consists of a four carbon side chain from the basic amino acid structure, shown in Figure 6.12.

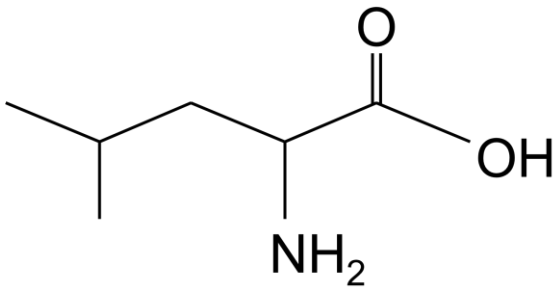

Figure 6.12: Molecular structure of Leucine.

The decomposition of proteins is one of the most studied pathways in attempts to achieve the full picture of human decomposition. The majority of proteins in the body are degraded to peptones, polypeptides and amino acids via proteolysis, catalysed by cellular enzymes called proteases [39]. It is evident from statistical analysis and investigations into its individual patterns in the data, that leucine is present in the leachate samples taken at the head and foot of the body, and ever changing throughout the experiment. During the initial stages of decomposition, leucine is present surrounding the liver, adipose tissue and muscle tissue, followed by the epidermis and muscle protein in later stages as a result of protein degradation. Although leucine is not identified as a human-specific marker, the patterns and behaviours of amino acids will enhance the knowledge of what compounds you would expect to see at certain time intervals during human decomposition, and how they change over time.

The remaining three compounds tentatively identified are all associated with very similar metabolic pathways. Epinephrine (also known as adrenaline) is a hormone secreted by the medulla of the adrenal gland. It is one of a group of monoamines called catecholamines (in addition to dopamine and noradrenaline), which are responsible for the 'fight or flight' response in humans [40].

Monoamine oxidases (MAO)[1] are enzymes that catalyse the oxidation of these catecholamines by removing the amine group, forming their aldehyde intermediates [41]. These intermediates are presented in the metabolic pathways in Figure 6.13. These compounds are known for their toxic nature [42], and as a result are quickly detoxified by enzymes aldehyde dehydrogenase/reductase. The enzyme aldehyde dehydrogenase will oxidise the remaining aldehyde intermediates to form carboxylic acids, while aldehyde reductase reduces these compounds to sugar alcohols [43, 44]. Additionally, in Figure 6.13 we see the remaining two compounds tentatively identified in this experiment, 3,4-dihydoxyphenylglycol and 3,4-dihydroxyphenylacetic acid, now known as metabolites of dopamine, norepinephrine and epinephrine. The true complexity of these metabolic pathways result in many variations of chemical reactions. While there are an infinite number of pathways and breakdown products in our biological systems, this specific interaction is a clear and concise way of showing where these tentatively identified compounds could have originated from, and how they could be a part of the decomposition process.

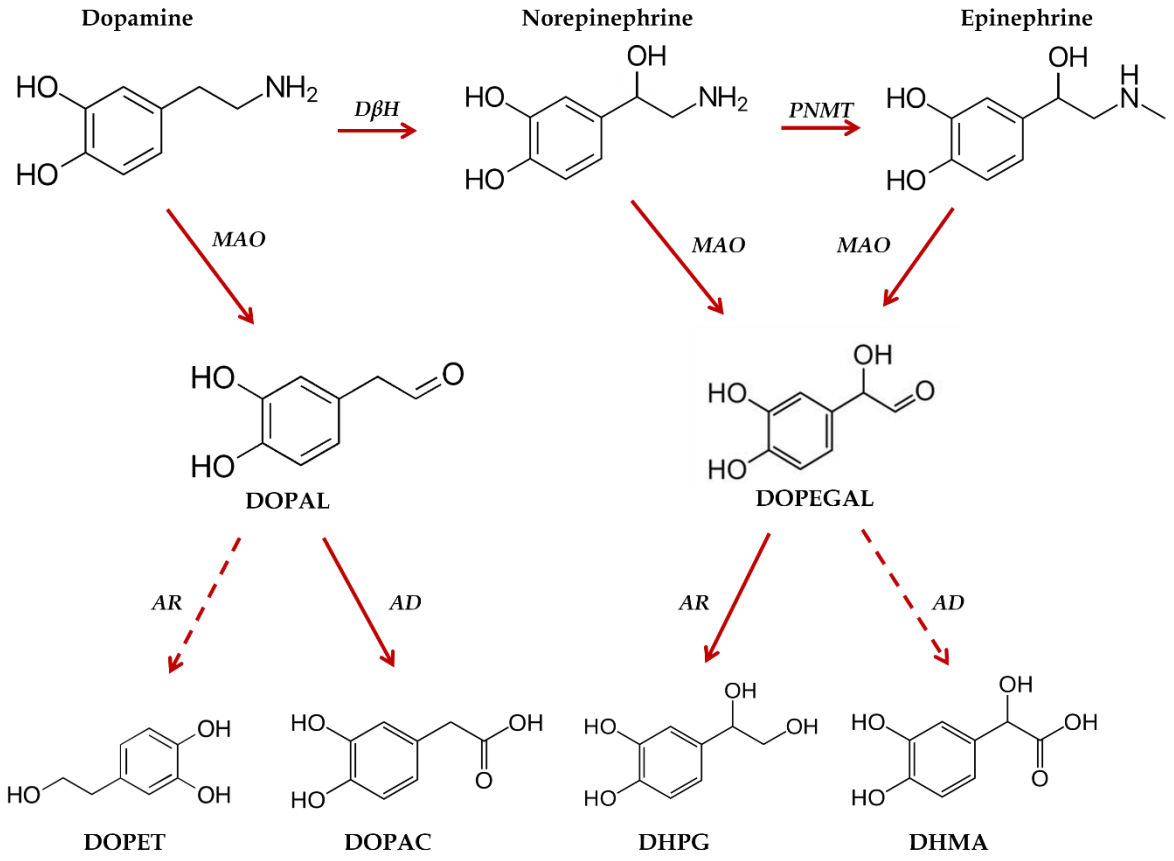

Figure 6.13 Pathways of oxidative deamination of catecholamines to their corresponding biogenic aldehyde intermediates and acid derivative or alcohol metabolites Adapted from Eisenhofer et al [45]. (DOPAL, 3,4-dihydroxyphenylacetaldehyde; DOPEGAL, 3,4-dihydrophenylglycolaldehyde; DOPET, 3,4-dihydroxyphenylethanol; DOPAC, 3,4-dihydroxyphenylacetic acid; DHPG, 3,4-dihydoxyphenylglycol; DHMA, 3,4-dihydroxymandelic acid; MAO, Monoamine oxidase; PNMT, Phenoethanolamine-N-methyltransferase; AR, Aldehyde reductase; AD, Aldehyde dehydrogenase).

[1]*Abbreviations:* (DOPAL, 3,4-dihydroxyphenylacetaldehyde;
DOPEGAL, 3,4-dihydrophenylglycolaldehyde;
DOPET, 3,4-dihydroxyphenylethanol;
DOPAC, 3,4-dihydroxyphenylacetic acid;
DHPG, 3,4-dihydoxyphenylglycol;
DHMA, 3,4-dihydroxymandelic acid;
MAO, Monoamine oxidase;
PNMT, Phenoethanolamine-N-methyltransferase;
AR, Aldehyde reductase;
AD, Aldehyde dehydrogenase.

6.5 Results and discussion using a Hypercarb column

6.5.1 QC analysis

Figure 6.14 shows the overlaid chromatograms for each QC sample analysed using a Hypercarb column. The first 15 minutes of each chromatogram shows only small variation in peak area and no retention time drift. The remainder of the chromatogram seems to show high level of variation in both peak area and retention time, additionally showing poor peak shape and a higher baseline. Due to the inconsistencies observed toward the end of the chromatogram, six peaks were investigated further via QC analysis.

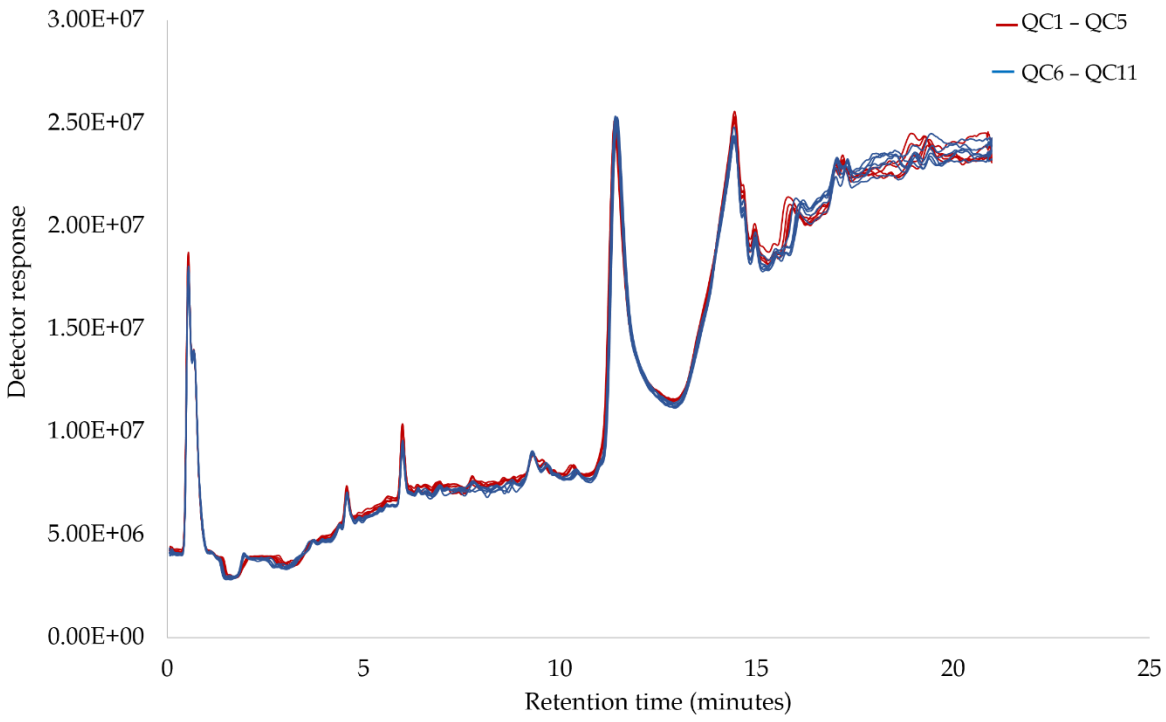

Figure 6.14: Total ion chromatograms of QC samples throughout the analytical run for leachate samples using a Hypercarb column.

The CV values presented in Table 6.13 demonstrate that although the values for peak areas are slightly higher, they are still under the accepted level of variability for non-targeted metabonomic analysis. The QC chromatograms appear to be much more stable and consistent following analysis with a Hypercarb column, in comparison to a C18 column. Additionally, the CV values are much lower following analysis with a Hypercarb column.

Table 6.13: Variability of peak area (A) and retention time (B) from 6 selected peaks in the QC samples during the analytical sequence for leachate samples using a Hypercarb column.

A

Peak	QC6	QC7	QC8	QC9	QC10	QC11	Average	St. Dev	CV%
1	207724	240777	217113	182632	181237	224370	**208976**	**23578**	**11%**
2	36803	38667	40904	43686	42738	40821	**40604**	**2545**	**6%**
3	496375	446572	433223	362585	338788	331485	**401505**	**66915**	**17%**
4	63455	68697	70131	63216	66619	64246	**66061**	**2898**	**4%**
5	88474	96998	99856	92811	81898	91372	**91902**	**6359**	**7%**
6	1289123	1274018	1293944	1292787	1284747	1194951	**1271596**	**38233**	**3%**

B

RT	QC6	QC7	QC8	QC9	QC10	QC11	Average	St. Dev	CV%
1	4.56	4.57	4.57	4.56	4.57	4.57	**4.57**	**0.0057**	**0.12%**
2	5.05	5.06	5.07	5.08	5.07	5.05	**5.06**	**0.0101**	**0.20%**
3	5.98	5.97	5.98	5.99	5.97	5.98	**5.98**	**0.0080**	**0.13%**
4	6.96	6.95	6.95	6.95	6.94	6.94	**6.95**	**0.0076**	**0.11%**
5	9.26	9.29	9.27	9.25	9.24	9.25	**9.26**	**0.0182**	**0.20%**
6	11.40	11.37	11.47	11.42	11.41	11.41	**11.41**	**0.0347**	**0.30%**

6.5.2 Metabolic profiling

The total ion chromatograms (TIC's) obtained from samples analysed with a Hypercarb column also had a high baseline, which as a result showed peaks of very low abundance. By extracting each chromatogram and producing a total compound chromatogram (TCC), it enabled better visualisation of the peaks, giving a clearer image of the metabolic profile of the sample. The overlaid chromatograms for samples taken at the head of the body are shown in Figure 6.15. From 6 to 14 minutes, the majority of peaks show a higher abundance in the sample collected in October, with similar peak patterns in both samples. Outside this time window, it seems that samples taken in September show greater peak height in conjunction with additional peaks that are not present in samples taken in October. An example of this is seen between 14-15 minutes. The compounds that are eluting here could prove useful in detecting the changes to the chemical signature of the leachates over time.

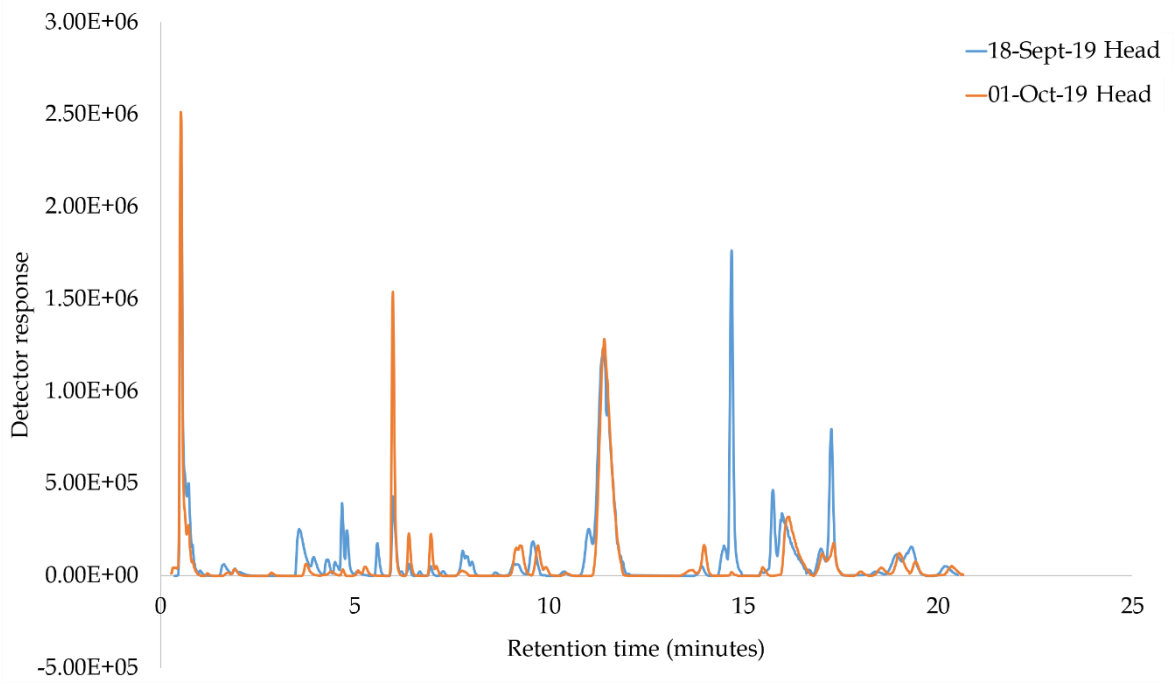

Figure 6.15: Example total compound chromatogram (TCC) of samples taken at the head of the body at two different time points, analysed using a Hypercarb column.

Looking at the overlaid chromatograms for samples taken at the foot of the body in Figure 6.16, there are differences in the chemical profile of each sample. The highest peak at the beginning of the chromatogram shows several differences in peak intensities. The peak area seems to increase from September through October, followed by a decline in December. This peak seems to be the only one following this pattern. After approximately 4-5 minutes, the chromatogram for the sample taken in late October (24th October) produced three additional peaks that are not present in any other sample. Furthermore, both samples taken in October present an additional peak at 17 minutes. Similarly, a broad peak between 13-15 minutes is only present in the sample taken in September. Although peaks between 5-10 minutes on the chromatogram show low abundance, the leachate sample taken in early October (1st October) seem to dominate the majority of the chromatogram in regards to peak height.

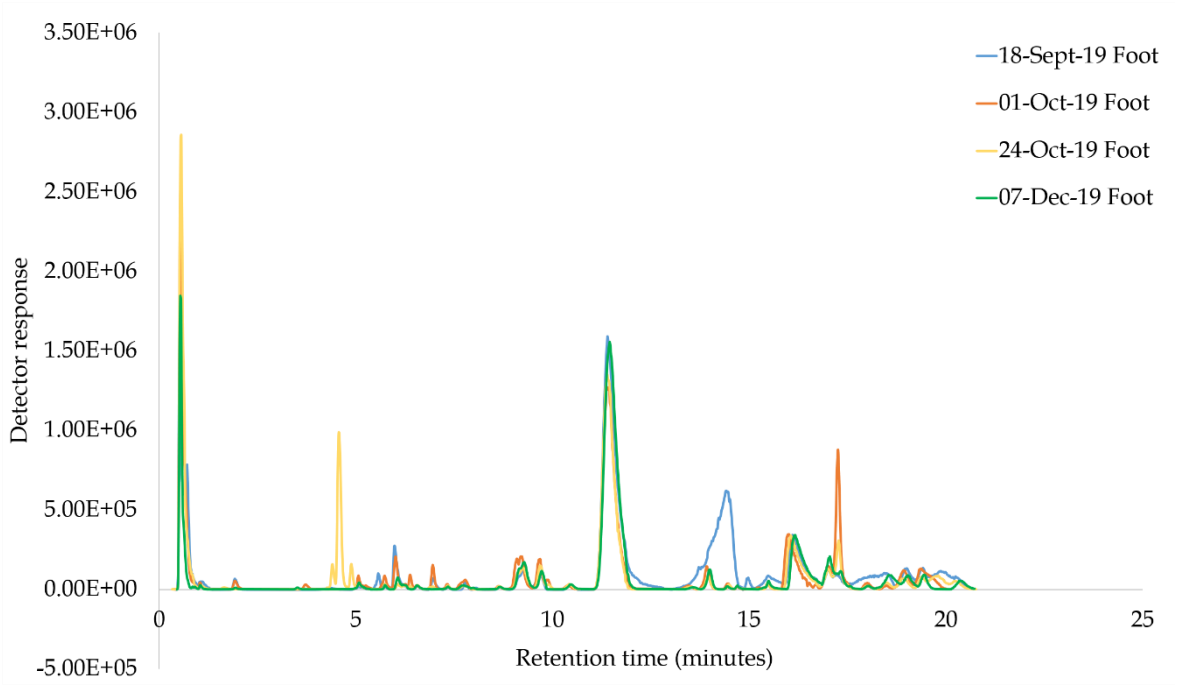

Figure 6.16: Example total compound chromatogram (TCC) of samples taken at the foot of the body at two different time points, analysed using a Hypercarb column.

The profile of each sample differs when comparing the analysis using a C18 column to the Hypercarb column. The most noticeable difference is that the Hypercarb column was able to detect a significantly higher number of peaks, and as a result was able to produce a more thorough chemical profile. It is also important to note that the leachate sample taken on October 1st produced very limited results when analysed with a C18 column, while on the Hypercarb column the chromatograms showed a variety of changes happening in both peak pattern and peak height at the head and food of the body.

6.5.3 Multivariate analysis

Figure 6.17 shows a PCA scores plot of leachate samples collected at four time points at the foot of the body. The QC samples are clustered closely together, establishing minimal instrumental effects during the analysis.

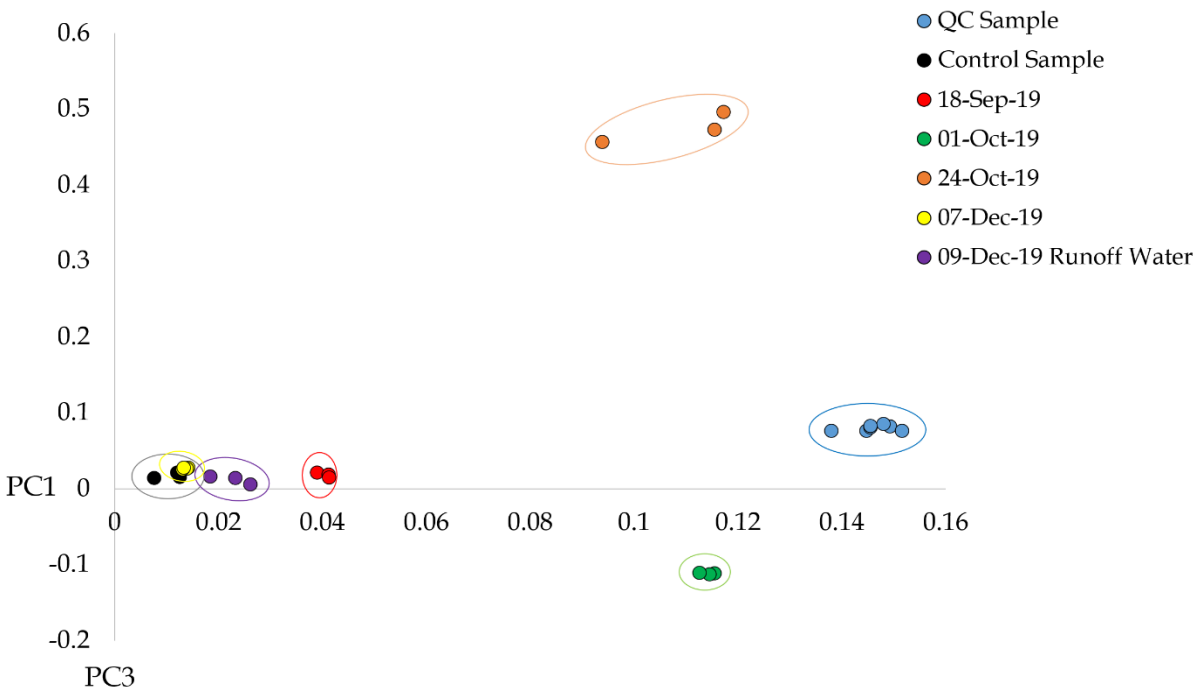

Figure 6.17: PCA score plot of PC1 (67.46%) and PC3 (6.94%) for leachate samples from the foot of the body using a Hypercarb column.

The control sample is positioned near the leachate sample taken in December, accompanied by the runoff water sample. With the lower temperatures recorded in the winter months (the lowest being -2.6°C), it is likely that the rate of decomposition had slowed down, resulting in less compounds leaching from the body. All four time points on the plot show excellent separation power, where the distance between each sample group is further apart than the spread of the QC samples. Each sample group is tightly clustered together, indicating minimal variation between replicates.

The PCA scores plot in Figure 6.18 representing samples taken from the head of the body shows similar results to those taken from the foot of the body. The QC samples are tightly clustered, and the distance between each sample group is further apart than the spread of the QC samples. The runoff water sample again seems to be positioned near the control sample.

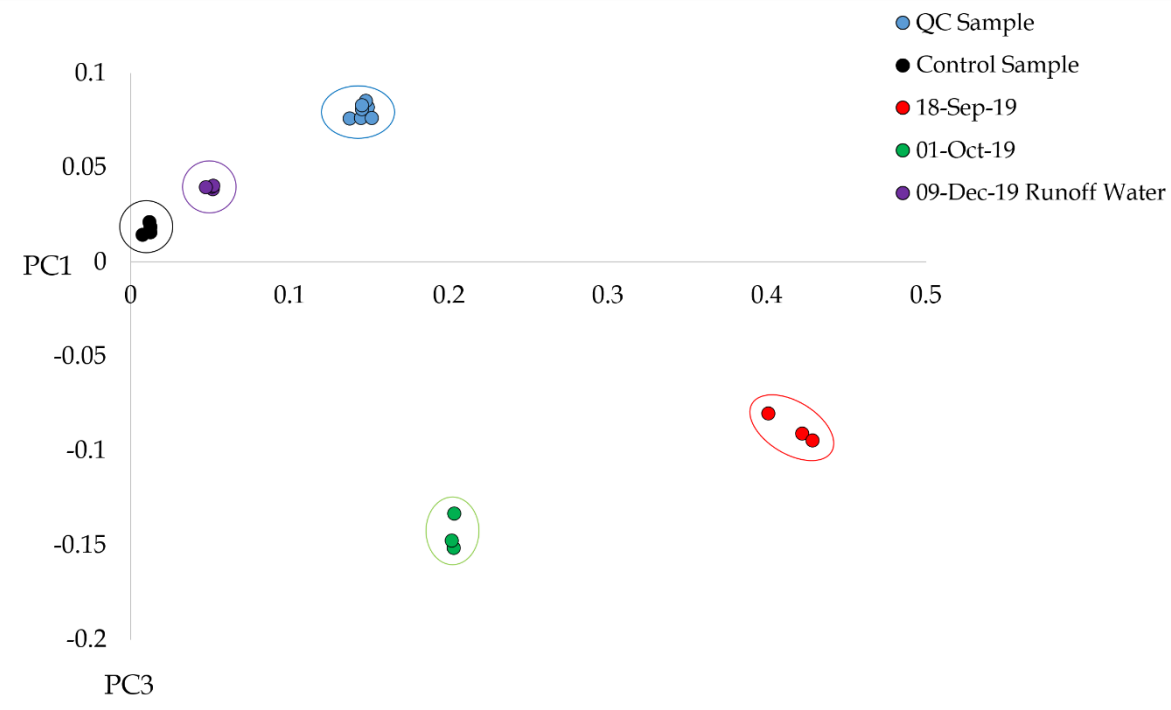

Figure 6.18: PCA score plot of PC1 (79.36%) and PC3 (1.35%) for leachate samples from the head of the body using a Hypercarb column.

Whilst the sample taken on 1st October 2019 presented an anomaly following analysis with a C18 column, this was not the case when using a Hypercarb column. Overall. There is much better separation between sample groups at both the head and foot of the body following analysis with a Hypercarb column.

Table 6.14 emphasises the *m/z* of the compounds showing significant differences at different stages of the experiment, at the head and foot of the body. There is a constant increase in the % of smaller compounds (*m/z* 100-300) from September to December, and a decrease in larger compounds (*m/z* 501+).

The patterns observed in this table reflects the expected behaviour of the compounds leaching from remains during decomposition, taking into account what we already know about chemical decomposition in the body. It is possible that the smaller compounds in the leachates are detected more efficiently with a Hypercarb column compared to a C18 column, allowing a more thorough data set that gives a broader sense of the chemical profile of the leachate samples.

Table 6.14: Table showing the percentage of compounds of a specific m/z at each time interval, using a Hypercarb column.

Area	% of m/z	Compounds showing significant differences between :		
		18 Sept and 01 Oct	01 Oct and 24 Oct	24 Oct and 7 Dec
Foot of the body	100-300	42%	49%	63%
	301-500	26%	30%	25%
	501+	31%	20%	12%
Head of the body	100-300	17%	N/A	N/A
	301-500	24%	N/A	N/A
	501+	38%	N/A	N/A

6.5.4 Statistical analysis

The total number of features detected in the leachate samples was 7337. Following the removal of all features with a CV value over 30%, 5125 remained. Statistical analysis was performed on samples from the head and foot of the body separately. Features with a *p-value* of more than 0.05 were removed, leaving 830 features from samples taken by the foot of the body, and 101 features from the head of the body. The top 50 compounds from both the head and foot of the body were chosen for further statistical analysis. Table 6.15 shows the top 20 markers that proved to be the most robust and significantly different from samples taken at the foot of the body.

Table 6.15: Summary of the top 20 compounds that show significant differences between time points at the foot of the body, analysed using a Hypercarb column.

m/z	Retention time (minutes)	CV	p-value		
			Compounds showing significant differences between :		
			18-Sept and 01-Oct	01-Oct and 24-Oct	24-Oct and 7-Dec
104.0675	0.73	6%	p<0.05	p<0.05	p<0.05
119.0690	3.73	7%	p<0.05	p<0.05	p<0.05
128.1051	1.11	15%	p<0.05	p<0.05	p<0.05
144.0118	0.89	10%	p<0.05	p<0.05	p<0.05
153.0029	0.56	25%	p<0.05	p<0.05	p<0.05
155.0248	1.21	23%	p<0.05	p<0.05	p<0.05
164.1262	0.77	9%	p<0.05	p<0.05	p<0.05
166.0359	4.57	3%	p<0.05	p<0.05	p<0.05
177.0809	0.54	17%	p<0.05	p<0.05	p<0.05
188.9856	0.82	9%	p<0.05	p<0.05	p<0.05
191.9712	0.90	14%	p<0.05	p<0.05	p<0.05
227.0851	6.39	4%	p<0.05	p<0.05	p<0.05
234.1680	3.98	4%	p<0.05	p<0.05	p<0.05
239.1590	0.56	14%	p<0.05	p<0.05	p<0.05
292.9461	0.56	8%	p<0.05	p<0.05	p<0.05
372.8793	0.71	14%	p<0.05	p<0.05	p<0.05
390.8791	0.59	7%	p<0.05	p<0.05	p<0.05
417.8771	0.57	25%	p<0.05	p<0.05	p<0.05
573.8368	0.58	15%	p<0.05	p<0.05	p<0.05
689.2063	6.22	13%	p<0.05	p<0.05	p<0.05

Every single marker selected in this table show significant differences between at least two time points. The table seems to be dominated by smaller compounds, reflecting the percentage of different sized compounds in Table 6.15. When comparing the markers detected at the foot of the body using a C18 and Hypercarb column, similar markers are presented in both tables. These markers are *m/z* 164.1262, *m/z* 177.0809 and *m/z* 239.1590. Whilst it is not possible to confirm the identity of these compounds at this current time, it is interesting to note that although both columns have different chemistries they have also shown to be able to retain and separate similar compounds. Table 6.16 looks at the top 20 compounds detected at the head of the body that show significant differences between the two time points and are robust and reliable.

Table 6.16: Summary of the top 20 compounds that show significant differences between two time points at the head of the body, analysed using a Hypercarb column.

m/z	Retention time (minutes)	CV	p-value
			Compounds showing significant differences between :
			18-Sept - 01-Oct
100.0738	2.86	8%	p<0.01
104.0675	0.73	6%	p<0.01
128.1051	5.28	4%	p<0.01
141.1011	1.17	29%	p<0.01
160.1309	2.74	16%	p<0.01
162.0962	14.71	14%	p<0.01
167.1164	3.67	5%	p<0.01
171.1454	6.97	5%	p<0.01
204.1039	14.70	23%	p<0.01
206.1011	4.78	8%	p<0.01
243.1283	7.86	8%	p<0.01
253.0676	6.43	27%	p<0.01
299.1598	14.70	3%	p<0.01
300.1628	14.70	2%	p<0.01
317.1662	14.43	3%	p<0.01
381.1294	14.55	4%	p<0.01
382.1315	16.97	9%	p<0.01
500.3052	19.06	14%	p<0.01
566.6924	8.97	6%	p<0.01
569.6905	3.82	18%	p<0.01

Each marker in the table show significant differences between the first two time points. There are also similar markers detected at the head of the body using both the C18 and Hypercarb columns. These are *m/z* 206.1011 and *m/z* 500.3052.

It is also important to note that the CV values for the compounds in Tables 6.15 and 6.16 are notably low. The average CV value for the markers discovered at the head of the body was 12.1%, and 10.6% at the foot of the body, highlighting the robustness and reliability of

the method. When using a C18 column, the average CV values were 23.3% and 19.7% respectively. The contrasting results between the two columns thus far highlights the importance of the interactions happening between the sample and the stationary phase.

6.5.5 Marker identification

Four of the compounds that showed significant differences at different time points were tentatively identified through comparing mass spectra from the analysis to those provided by *METLIN*. The marker *m/z* 132.1018 was tentatively identified as Leucine, *m/z* 118.0864 as Valine, *m/z* 148.0605 as Glutamate and *m/z* 183.0651 as Homovanillic acid. The observed *m/z* for all four compounds were as a result of the $[M+H]^+$ adduct. The tentative identifications of each marker, their peak area and the *p-values* at each time interval were explored further.

Table 6.17: Summary of the marker m/z 132.1018, tentatively identified as Leucine.

m/z	Adduct	Retention time (minutes)	Predicted formula	Tentative identification	Probability score
132.1018	[M+H]	1.10	$C_6H_{13}NO_2$	L-Leucine	86.8

Area	Foot of the body			Head of the body
Date	18-Sept and 01-Oct	01-Oct and 24-Oct	24-Oct and 7-Dec	18-Sept and 01-Oct
p-value	p>0.05	p<0.001	p<0.001	p<0.001

This marker shows very similar characteristics to the marker tentatively identified as leucine using a C18 column, with similar retention times and *m/z*. Additionally, both columns seem to show high significant differences between time points in Table 6.17. Figure 6.19 shows that the prevalence of the marker here is consistent throughout the experiment, as opposed to only appearing in a select few samples with the reverse phase column chemistry.

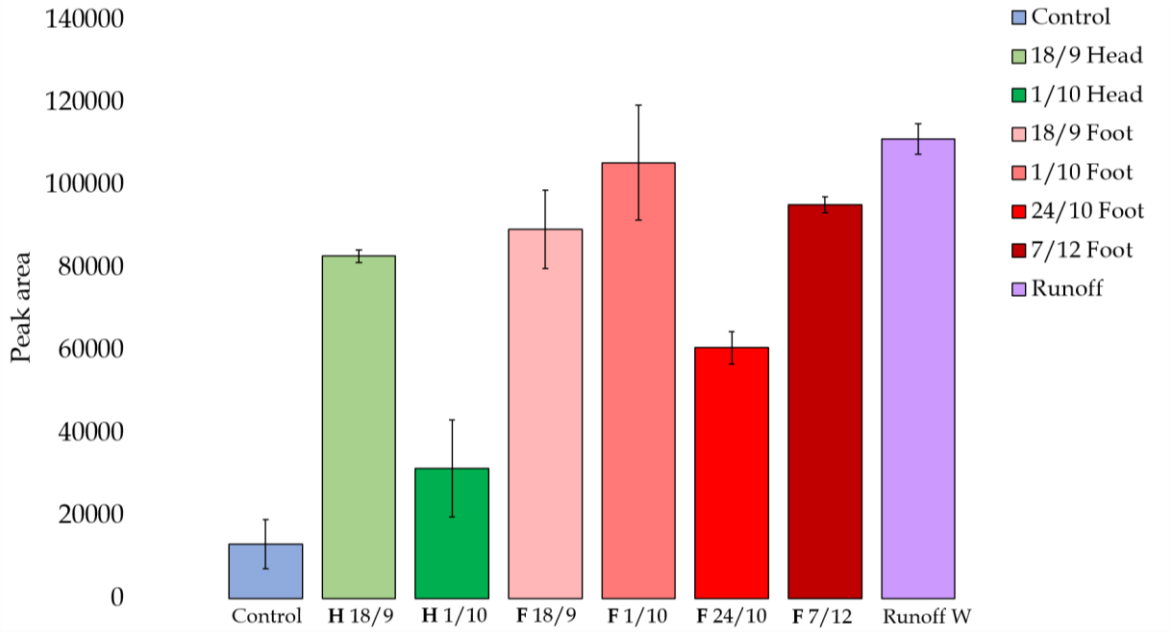

Figure 6.19: Bar chart showing the change in abundance over time of m/z 132.1018 tentatively identified as Leucine, in samples taken from the head and foot of the body with error bars ±1 standard deviation.

Table 6.18: Summary of the marker m/z 118.0864, tentatively identified as Valine.

m/z	Adduct	Retention time (minutes)	Predicted formula	Tentative identification	Probability score
118.0864	[M+H]	2.18	$C_5H_{11}NO_2$	Valine	86.8

Area	Foot of the body			Head of the body
Date	18-Sept and 01-Oct	01-Oct and 24-Oct	24-Oct and 7-Dec	18-Sept and 01-Oct
p-value	p>0.05	p>0.05	p>0.05	p>0.05

The most distinct observation from Table 6.18 is that there are no significant differences between each time point in the head or foot of the body. Whilst this could be perceived as a poor result, the bar chart in Figure 6.20 emphasises that the peak area for samples taken at the foot of the body are consistent. The peak area is higher for samples taken at the head of the body, and are also consistent across both samples. This illustrates that in this study, valine is mostly present in samples taken from the head of the body.

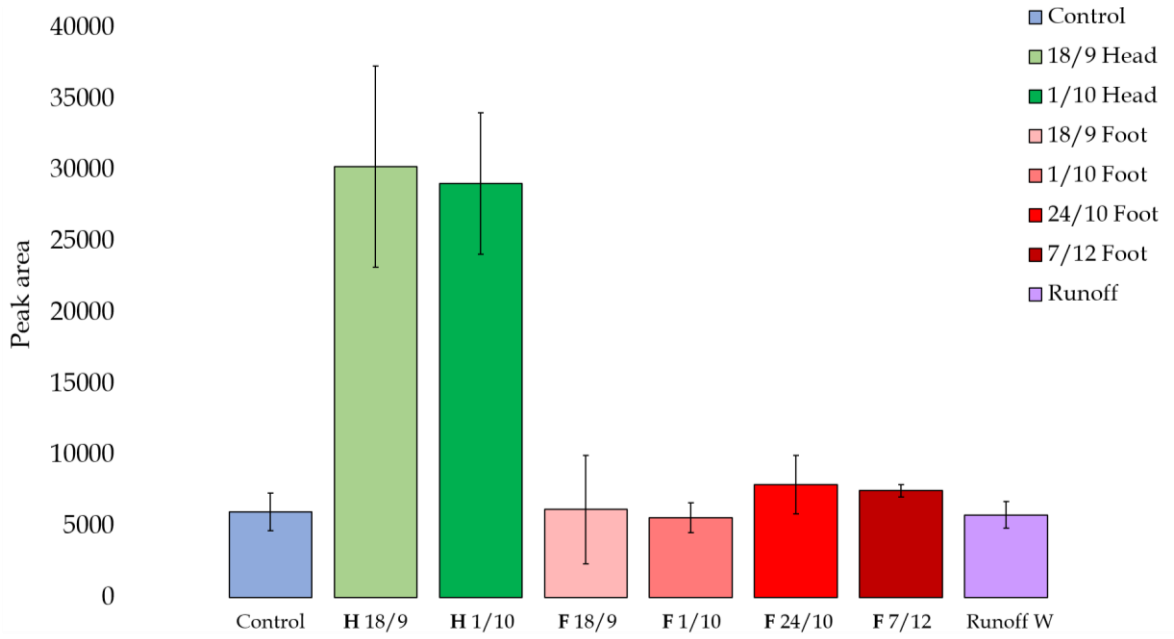

Figure 6.20: Bar chart showing the change in abundance over time of m/z 118.0864 tentatively identified as Valine, in samples taken from the head and foot of the body with error bars ±1 standard deviation.

Table 6.19: Summary of the marker m/z 148.060, tentatively identified as Glutamate.

m/z	Adduct	Retention time (minutes)	Predicted formula	Tentative identification	Probability score
148.0605	[M+H]	1.03	$C_5H_9NO_4$	Glutamate	80.96

Area	Foot of the body			Head of the body
Date	18-Sept and 01-Oct	01-Oct and 24-Oct	24-Oct and 7-Dec	18-Sept and 01-Oct
p-value	p>0.05	0.02	p<0.001	0.007

A marker tentatively identified as glutamate shows rapid changes in samples taken from the foot of the body. The *p-values* in Table 6.19 show significant differences between the majority of time points. Whilst the difference in peak area over time from the head of the body seem small (Figure 6.21), samples from the foot of the body show an increase in peak area, followed by a sharp decrease toward the end of the experiment. The fluctuation of this marker over time could be a useful tool when considering time since death.

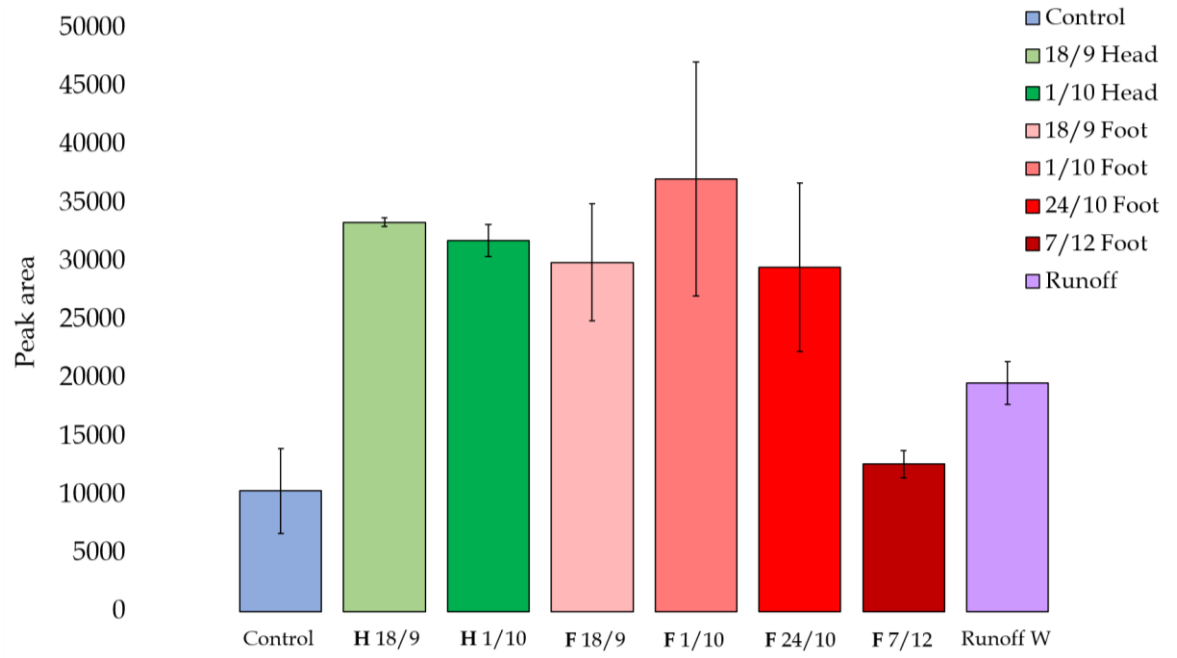

Figure 6.21: Bar chart showing the change in abundance over time of m/z 148.0605 tentatively identified as Glutamate, in samples taken from the head and foot of the body with error bars ±1 standard deviation.

Table 6.20: Summary of the marker m/z 183.0651, tentatively identified as Homovanillic Acid.

m/z	Adduct	Retention time (minutes)	Predicted formula	Tentative identification	Probability score
183.0651	[M+H]	11.02	$C_9H_{10}O_4$	Homovanillic Acid	86.7

Area	Foot of the body			Head of the body
Date	18-Sept and 01-Oct	01-Oct and 24-Oct	24-Oct and 7-Dec	18-Sept and 01-Oct
p-value	p>0.05	p>0.05	p>0.05	p<0.001

The marker tentatively identified as homovanillic acid only seems to show significant differences between the first two time points in samples taken from the head of the body (Table 6.20). This is reflected in the bar chart shown in Figure 6.22, where the peak area for the sample taken in September at the head of the body has a much higher peak area than other samples during analysis. This marker is a potential breakdown product of dihydroxyphenyl-acetic acid, a compound previously tentatively identified with a C18 column.

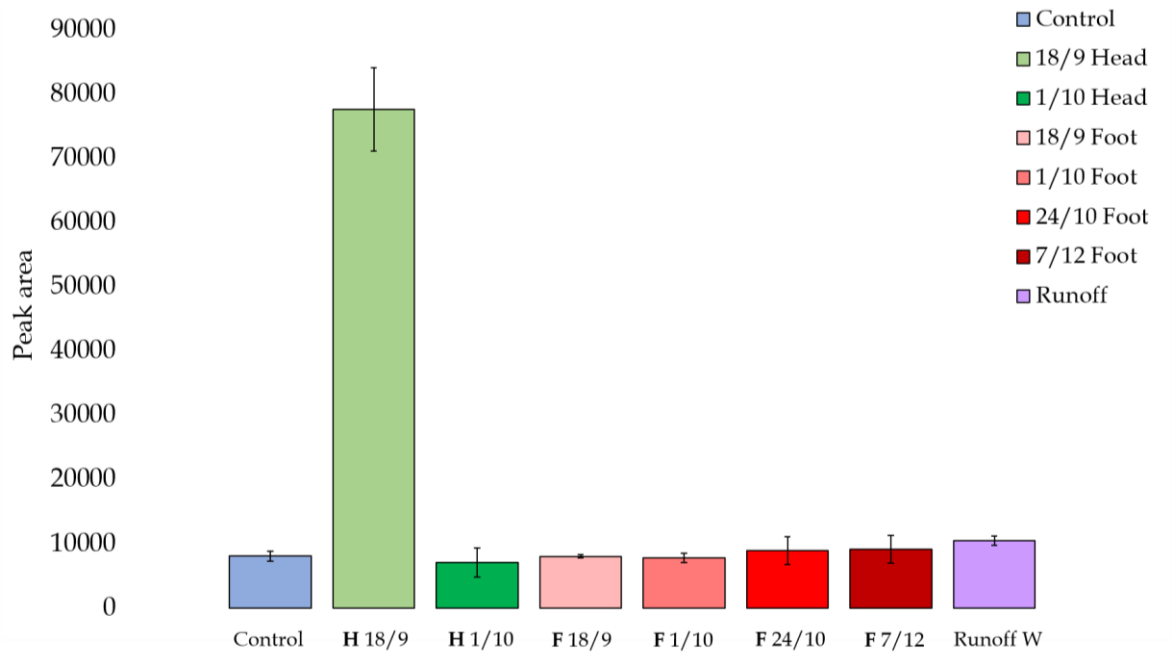

Figure 6.22: Bar chart showing the change in abundance over time of m/z 183.0651 tentatively identified as Homovanillic Acid, in samples taken from the head and foot of the body with error bars ±1 standard deviation.

Two branched chain amino acids (BCAA) have been tentatively identified in this experiment as leucine and valine. BCAA's are important precursors for the synthesis of proteins and other amino acids. They stimulate muscle growth, muscle repair and are used as an efficient energy source during exercise and stress [46]. The structure of leucine was presented above in Figure 6.12, while the structure of valine is seen below in Figure 6.23. It is important to note that leucine was also tentatively identified while using a C18 column, revealing the similarities in the interactions between certain compounds and the stationary phase of both columns.

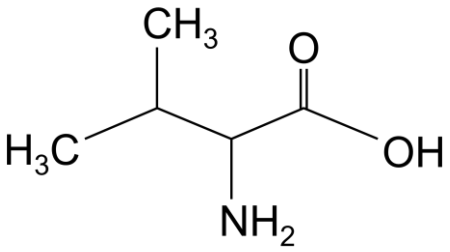

Figure 6.23: Molecule structure of Valine.

A third amino acid, glutamate, was also tentatively identified in this experiment, with its molecular structure shown in Figure 6.24. Glutamate is one of the most abundant amino acids produced in the body, and although known to be a building block for protein growth, it is also acknowledged as a neurotransmitter in the nervous system. It plays an essential role in normal brain function, and is at the crossroad between a variety of metabolic pathways [47]. Amino acids are the major components of all proteins. The degradation of proteins via proteolysis yields a vast number of amino acids. This knowledge has facilitated modern research in attempts to create a 'chemical profile' of human decomposition. Although amino acids are ubiquitous in our environment, gaining knowledge on the behaviour of a variety of amino acids at different stages of decomposition is an opportunity to create a clearer picture of the chemical changes happening in the body after death.

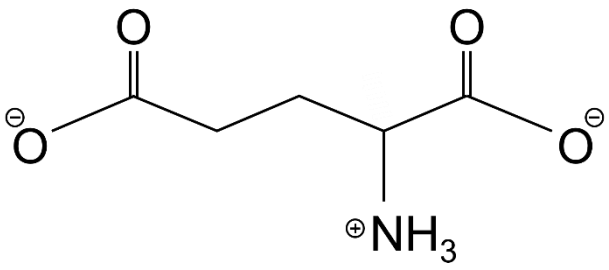

Figure 6.24: Molecular structure of Glutamate.

Homovanillic acid (HVA) is a major catecholamine metabolite, specifically in the dopamine metabolic pathway. Enzymes called COMT (Catechol-O-methyltransferase) metabolize DOPAC to HVA (Metabolic pathway shown in Figure 6.25) [48].

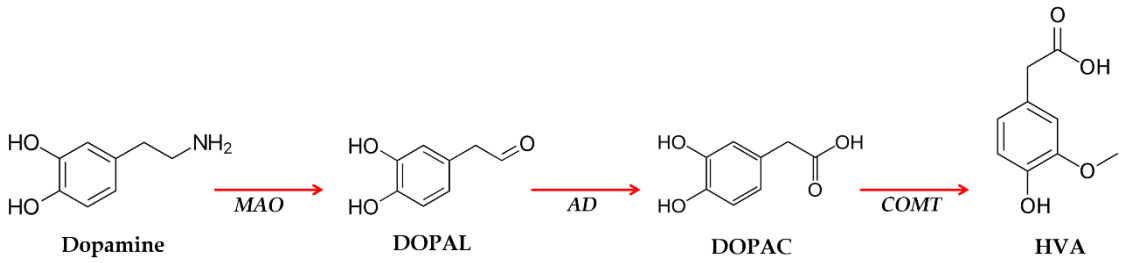

Figure 6.25: Metabolic pathway of Homovanillic Acid (created with information from Halbig et al. [49] and Meiser et al. [50]).

This particular pathway reflects the pathways described in Section 6.3.6. DOPAC was tentatively identified as a marker of interest in the analysis of the leachate samples using a C18 column. The identification of further metabolism of this compound to HVA suggests that the Hypercarb column could have potentially detected smaller breakdown products. This supports recent research recognizing the effectiveness of the Hypercarb column in detecting a wide range of metabolites, in comparison to the traditional C18 column [51].

6.6 Results and discussion using a HILIC column

6.6.1 QC analysis

Figure 6.26 shows the chromatograms for each QC sample analysed using a HILIC column. It is clear that the compounds in the leachate samples lack retention on the stationary phase. The chromatograms below show a maximum of three unresolved peaks, all appearing within the first minute of the analysis. This is most likely the solvent front, which suggests that the majority of the sample has travelled through the column directly with the solvent. A QC analysis was carried out on the data regardless of the poor chromatographic resolution. As a result of only producing three peaks of poor resolution during the analysis, only three peaks were analysed when looking at the reliability and robustness of the QC samples.

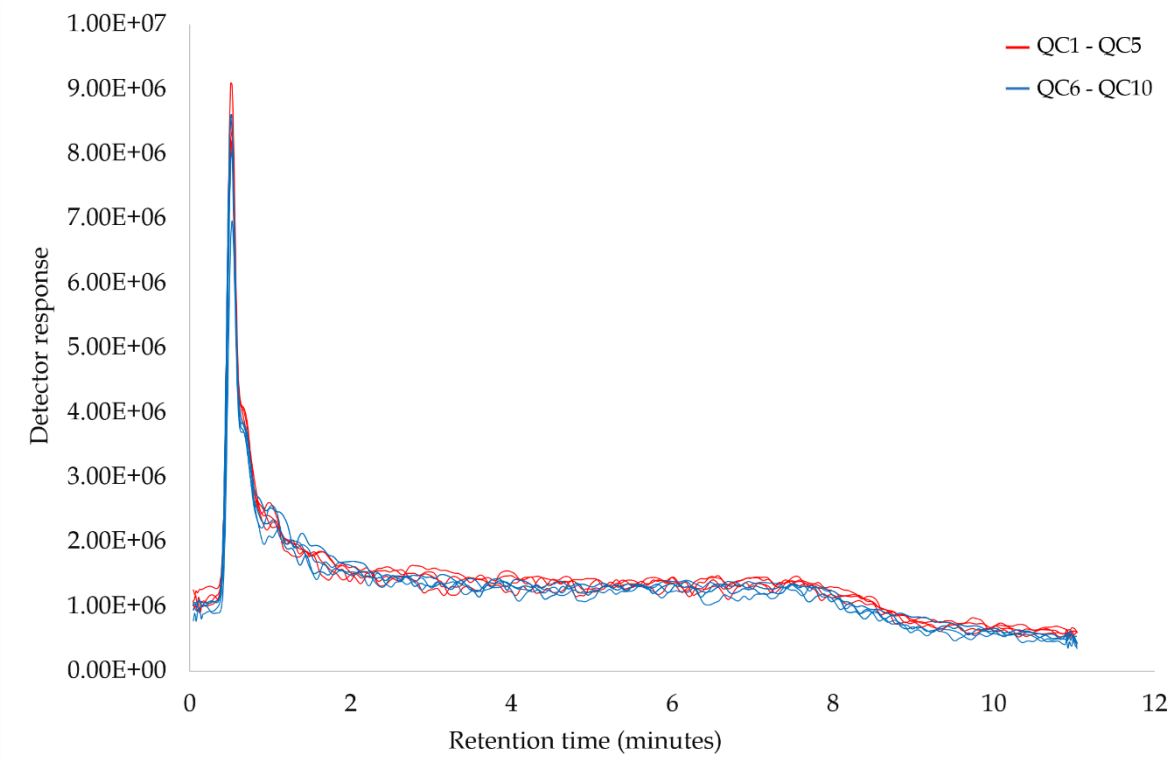

Figure 6.26: Total ion chromatograms of QC samples throughout the analytical run for leachate samples using a HILIC column.

Looking at the data in Table 6.21, the CV values for both peak area and retention time are under the accepted value in non-targeted analysis. It is important to note that the CV values calculated here are very low, which is unexpected considering the poor chromatographic quality. The results obtained here are similar to those obtained when using the C18 and Hypercarb column.

Table 6.21: Variability of peak area (A) and retention time (B) from 6 selected peaks in the QC samples during the analytical sequence for leachate samples using a HILIC column.

A

Peak	QC1	QC2	QC3	QC4	QC5	QC6	Average	St. Dev	CV%
1	7938889	8502967	9058342	8335210	8602958	7991587	**8404992**	**416817**	**5%**
2	3869721	4076288	3999129	3798951	3706943	3820040	**3878512**	**136327**	**4%**
3	2366713	2229047	2293852	2563123	2321138	2514043	**2381320**	**130645**	**5%**

B

RT	QC1	QC2	QC3	QC4	QC5	QC6	Average	St. Dev	CV%
1	0.53	0.52	0.53	0.52	0.52	0.53	**0.52**	**0.0022**	**0.42%**
2	0.67	0.67	0.68	0.67	0.67	0.68	**0.67**	**0.0021**	**0.31%**
3	1.02	1.02	1.02	1.02	1.02	1.03	**1.02**	**0.0022**	**0.22%**

6.6.2 Metabolic profiling

Due to the poor chromatographic resolution of the QC chromatograms, a total compound chromatogram (TCC) was used once more instead of the total ion chromatogram (TIC). Figure 6.27 shows the overlaid TCC for samples taken at the head of the body. There are only two peaks visible on the chromatogram in both samples. While there is slight retention time variation between the second peak, the first peak shows higher peak intensity for the sample taken in October. This produced very limited information in regards to the metabolite profile of the samples.

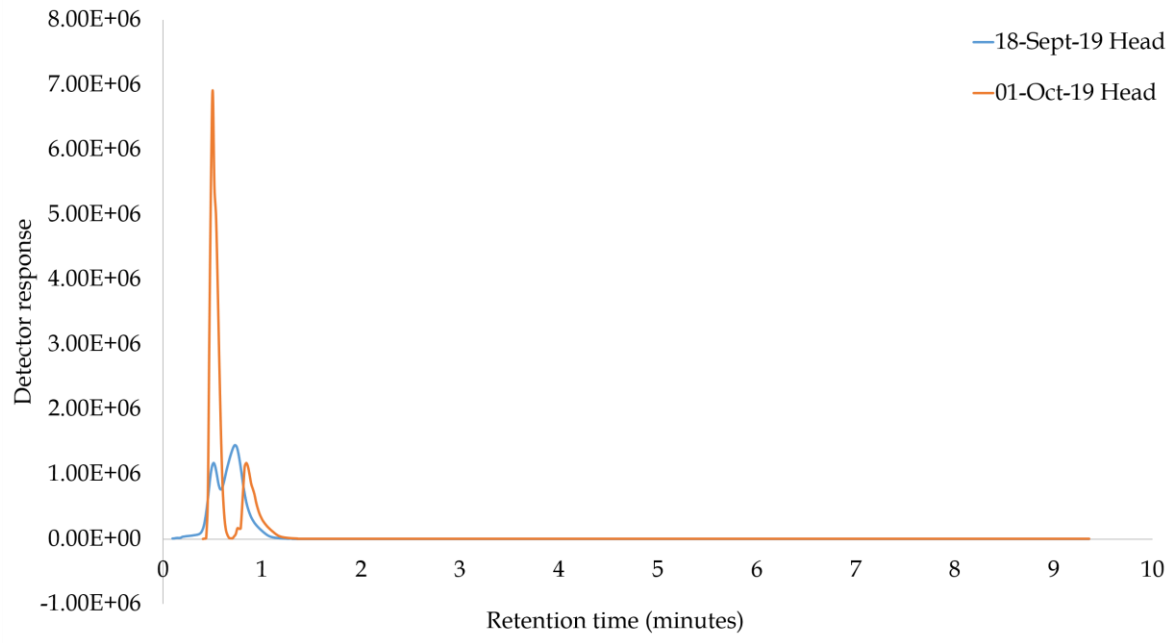

Figure 6.27: Example total compound chromatogram (TCC) of samples taken at the head of the body at two different time points, analysed using a HILIC column.

Figure 6.28 presents the TCC of each sample collected from the foot of the body. The majority of samples show only one peak in the chromatograms below. The sample taken on October 24th produced an additional peak after 1 minute of analysis. There is a visible difference between the peak intensities of each sample in the first peak. The intensity seems to increase throughout the timeline of the experiment, followed by a slight decrease in intensity in December.

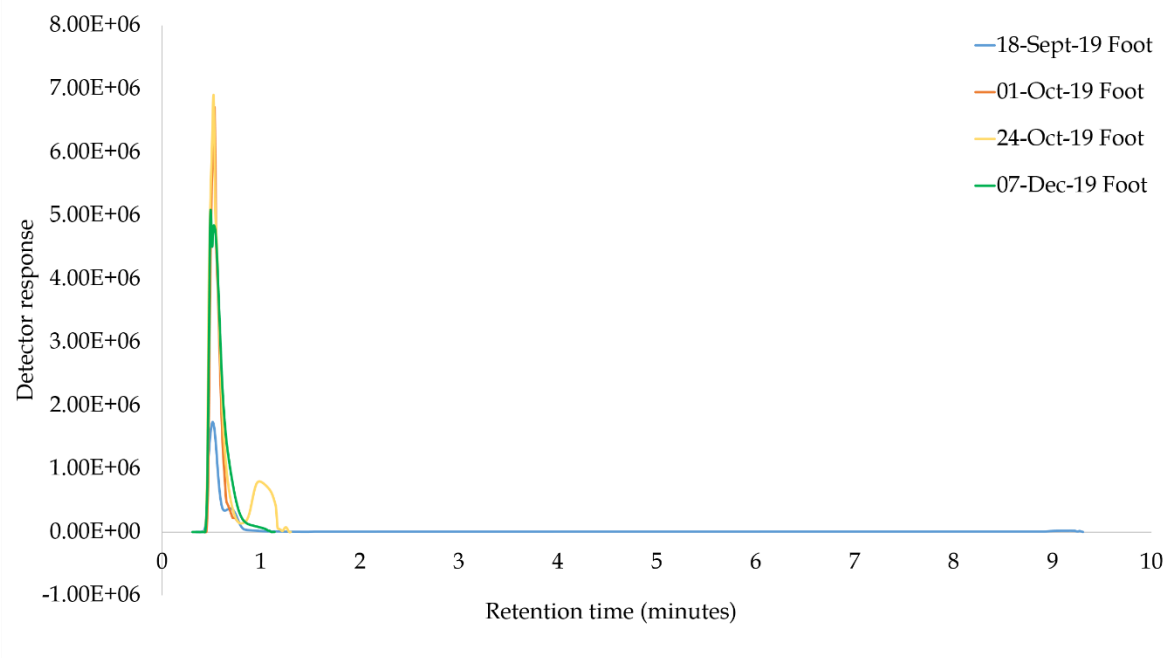

Figure 6.28: Example total compound chromatogram (TCC) of samples taken at the foot of the body at two different time points, analysed using a HILIC column.

The lack of retention of compounds on the HILIC column suggests that this particular type of sample does not interact well with the stationary phase. When comparing the chromatographic separation to the C18 and Hypercarb column, it is clear that using a HILIC column produces poor chromatographic resolution.

6.6.3 Multivariate analysis

Figure 6.29 presents the PCA scores plot produced with all samples. Initial observations show that the QC samples are tightly clustered in the middle of the plot, demonstrating the stability of the instrument. The control samples are also clustered together and appear to be at the opposite end of the plot to the remaining samples. The samples taken at the head and foot of the body are clearly differentiated from each other due to the trend of the sample groups. Both samples taken at the head of the body travel up the plot over time, while samples taken at the foot of the body seem to travel down the plot in a linear trend. The ability to show this on the same PCA plot allows clear visualisation that the chemical signature of the leachate samples not only change over time, but also vary when comparing different areas of the body.

Although the distance between most sample groups are not further apart than the spread of the QC samples, each samples group is separated on the plot with limited overlap, showing good separation power in comparison to the chromatographic results.

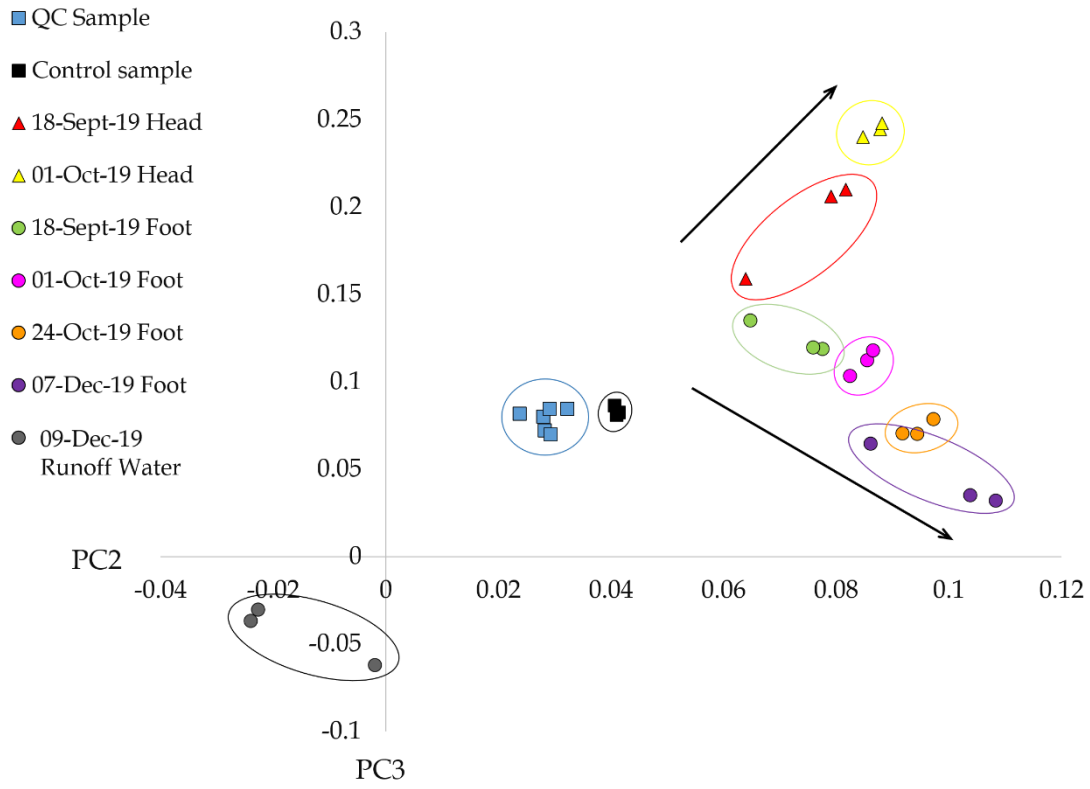

Figure 6.29: PCA score plot of PC2 (30.36%) and PC3 (14.30%) for leachate samples from the head and foot of the body using a HILIC column.

Table 6.22 shows the size of the compounds that are significantly different between each time point. The percentage of smaller compounds increase followed by a decrease, whilst larger compounds decrease, followed by an increase. This may suggest that the smaller breakdown products are not detected with a HILIC method, a similar result following analysis with a C18 column.

Table 6.22: Table showing the percentage of compounds of a specific m/z at each time point, using a HILIC column.

Area	% of m/z	Compounds showing significant differences between :		
		18 Sept – 01 Oct	01 Oct – 24 Oct	24 Oct – 7 Dec
Foot of the body	100-300	31%	60%	45%
	301-500	22%	24%	32%
	501+	47%	18%	23%
Head of the body	100-300	46%	N/A	N/A
	301-500	31%	N/A	N/A
	501+	23%	N/A	N/A

6.6.4 Statistical analysis

The total number of features detected in the leachate samples was 1380. Following the removal of all features with a CV value over 30%, 1136 remained. Statistical analysis was performed on samples from the head and foot of the body separately. Features with a *p-value* of more than 0.05 were removed, leaving 343 features from samples taken by the foot of the body, and 154 features from the head of the body. Table 6.23 looks at the compounds that show significant difference between two time points, detected from samples taken at the head of the body. Each compound in the table show significant differences between all three time points during the experiment.

Table 6.23: Summary of the top 20 markers that show significant differences between time points at the foot of the body, analysed using a HILIC column.

m/z	Retention time (minutes)	CV	p-value		
			Compounds showing significant differences between :		
			18-Sept and 01-Oct	01-Oct and 24-Oct	24-Oct and 7-Dec
107.9637	0.63	6%	p<0.05	p<0.05	p<0.05
115.9566	0.58	12%	p<0.05	p<0.05	p<0.05
126.0768	0.53	19%	p<0.05	p<0.05	p<0.05
129.9778	0.53	13%	p<0.05	p<0.05	p<0.05
132.0066	0.56	18%	p<0.05	p<0.05	p<0.05
150.0859	0.71	25%	p<0.05	p<0.05	p<0.05
159.9339	0.61	19%	p<0.05	p<0.05	p<0.05
169.0713	0.75	25%	p<0.05	p<0.05	p<0.05
175.9121	0.61	18%	p<0.05	p<0.05	p<0.05
176.8644	0.61	17%	p<0.05	p<0.05	p<0.05
184.8956	0.63	13%	p<0.05	p<0.05	p<0.05
206.9525	0.59	8%	p<0.05	p<0.05	p<0.05
210.1087	0.72	16%	p<0.05	p<0.05	p<0.05
214.9172	0.53	12%	p<0.05	p<0.05	p<0.05
236.1829	0.73	11%	p<0.05	p<0.05	p<0.05
253.1393	0.66	7%	p<0.05	p<0.05	p<0.05
272.8776	0.88	23%	p<0.05	p<0.05	p<0.05
328.8162	0.64	18%	p<0.05	p<0.05	p<0.05
378.8278	0.65	11%	p<0.05	p<0.05	p<0.05
410.9186	0.51	10%	p<0.05	p<0.05	p<0.05

Table 6.24 also displays that each marker shows a significant difference between the first two time points in samples taken at the head of the body. The compound *m/z* 167.1152 identified in samples taken at the head of the body was also a significant marker detected using a Hypercarb column. This was the only similarity between HILIC and the other column chemistries. The average CV value for the top 20 compounds detected at both head and foot of the body were 15%. This shows that the robustness of the markers produced with a HILIC column sit in between the C18 and Hypercarb columns.

Table 6.24: Summary of the top 20 markers that show significant differences between time points at the head of the body, analysed using a HILIC column.

m/z	Retention time (minutes)	CV	p-value
			Compounds showing significant differences between :
			18-Sept - 01-Oct
109.0752	0.79	13%	p<0.05
147.9779	0.58	5%	p<0.05
167.1152	0.79	15%	p<0.05
168.1178	0.79	10%	p<0.05
169.0713	0.75	25%	p<0.05
172.0982	0.73	19%	p<0.05
210.1087	0.72	16%	p<0.05
214.1358	0.71	20%	p<0.05
216.1553	0.71	8%	p<0.05
232.1536	0.70	24%	p<0.05
234.1683	0.71	17%	p<0.05
256.1511	0.71	25%	p<0.05
334.9088	0.65	4%	p<0.05
377.9007	0.54	21%	p<0.05
385.8979	0.53	18%	p<0.05
398.1057	0.68	8%	p<0.05
399.1023	0.68	17%	p<0.05
402.8959	0.68	9%	p<0.05
544.3656	0.53	20%	p<0.05
640.3604	0.53	20%	p<0.05

Using the results obtained from *XCMS Online* on the *METLIN* metabolite identification software, it was not possible to tentatively identify any of the markers found at the head or foot of the body as no clear structures could be identified from the predicted formulas. Despite this, a select few of the markers presented in the tables above were investigated further based on their significance. This allowed some insight into the patterns emerging in the chemical signature of the sample.

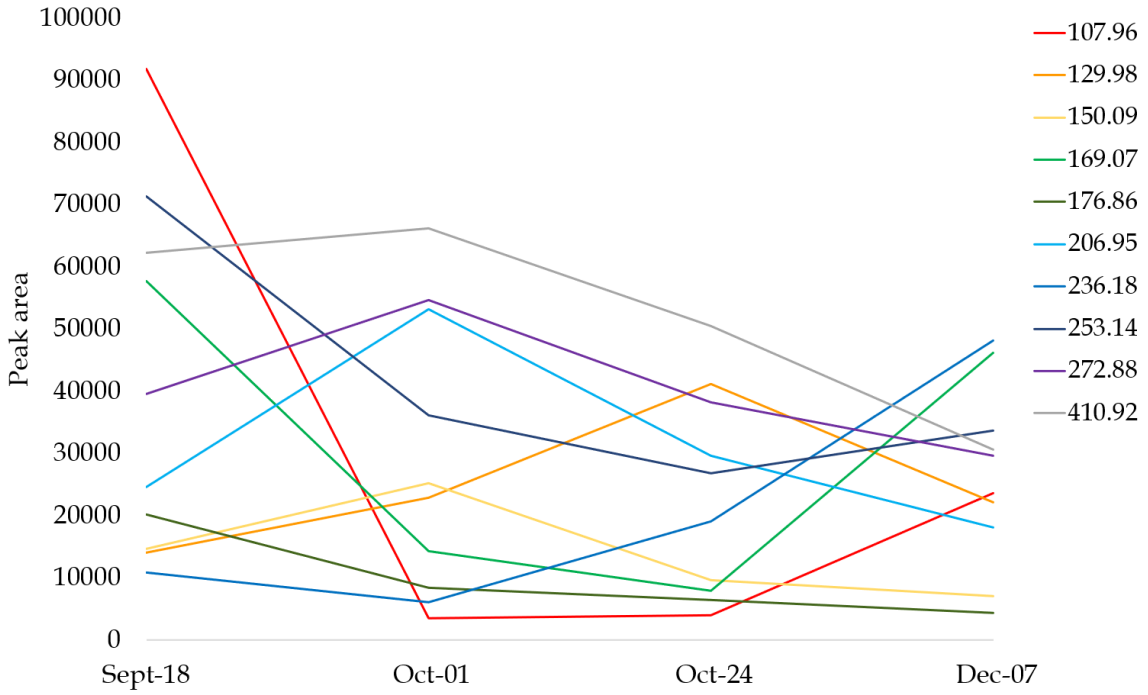

Figure 6.30: Trends of the top 10 markers identified with significant differences between time points from samples taken at the foot of the body, analysed using a HILIC column.

The graph in Figure 6.30 highlights the trends of 10 markers detected from samples taken at the foot of the body. There are two main trends observed across these markers. The first is a decrease in abundance from September to the end of October, followed by a slow increase towards December (For example, *m/z* 169.07). The majority of the markers showing this trend have a smaller *m/z*. One possible reason for this particular trend is that these compounds could be leaching out initially as small compounds already present in the body. The increase of these compounds at further time points could then be due to larger proteins/carbohydrates breaking down into the same products. The second trend shows an increase in abundance from September to the beginning of October, followed by a slow decrease through the end of October to December (For example, *m/z* 206.95). It is likely that these compounds are involved in breakdown processes happening at the earlier stages of

decomposition that have peaked at the beginning of October. The slow decrease in abundance could then reflect the remaining few still present in the soil.

The marker *m/z* 129.98 is the only one that does not follow either pattern. The abundance for this marker seems to increase and peaks at October 24th. This may suggest that this marker is a by-product of a later breakdown process occurring during decomposition. However, it is impossible to tell if this is the case without being able to identify what these compounds are.

The lack of chromatography, yet successful multivariate and statistical analysis on the data obtained when analysing the leachate samples with a HILIC column suggests the possibility of using a direct injection approach. This approach involves directly injecting the sample into the ionisation source, completely bypassing any chromatography [52]. This type of analysis has been used frequently in recent years for general analytical chemistry [53], and specifically for research focusing on the chemistry of decomposition [54]. Although it produces successful results, issues can arise with the production of ions all at once. The presence of highly abundant ions can easily mask the detection of low abundant ions (ion suppression), which can also lead to ion competition where the detector will have a capacity in terms of the number of ions it can detect at a time [55]. Overall, this can lower the sensitivity of the instrument, insinuating that if possible, chromatography should be used to ensure the maximum amount of sensitivity possible. This is especially important in non-targeted analysis, as the studies above seem to focus on targeted analysis.

6.7 Conclusion and future work

This work has shown that it is possible to use metabonomic profiling methods to identify breakdown products of decomposition from leachate samples collected near a body. An investigation using three different columns (C18, Hypercarb and HILIC) yielded positive and promising results. The C18 and Hypercarb columns showed excellent stability in both peak area and retention time throughout the analysis, showing reproducibility and reliability within the data obtained.

Investigation into the use of a HILIC column to detect compounds of interest in the leachate samples produced ambiguous results. The lack of retention on the stationary phase suggests that the compounds in the sample were not interacting with the stationary phase, as the majority of the sample eluted in the void volume. The sample retained successfully on both the C18 and Hypercarb column. The Hypercarb column produced a high number of peaks throughout the chromatogram, with good separation and good peak shape. Although the abundance of some of these peaks were low, a substantial amount of information was extracted. The C18 column also retained compounds from the sample, however, only very few peaks were produced and those were low in abundance.

Statistical analysis obtained from these analyses also yielded interesting results. While the Hypercarb and HILIC columns presented an abundance of markers showing statistical significance throughout the experiment, the analysis with a C18 column offered only a very limited selection. Regardless, many compounds were tentatively identified using both the C18 and Hypercarb column, with those markers showing relevance and interesting insight into the decomposition process.

One of the most predominant group of compounds tentatively identified in this experiment were amino acids. Amino acids are ubiquitous, known as the building blocks to create proteins, facilitate growth and repair in various parts of the body in a variety of different species, therefore cannot be attributed as human-specific markers. However, we would expect to be able to identify a variety of amino acids in the leachate samples, as protein degradation is an important factor of decomposition. The fact that these methods achieved this suggests that we are heading in the right direction. It would be a concern if the methods developed were not able to detect even the basic products of decomposition. Consequently, if these preliminary workflows prove that they can detect small known breakdown products at various time points during the experiment, it gives a high level of confidence that it has the potential to identify new human-specific markers in future research.

It is clear from the results of this experiment that a combination of a variety of techniques, data processing and identification procedures are essential in metabonomic analyses, supported by recent publications [56, 57]. Simply running the analysis on an LC-QTOF and only changing the type of column used showed the quantity of data that was produced, with each column producing valuable results with both similarities and differences.

Due to the non-targeted nature of this analysis, future work in this field would require a more in-depth development of a variety of factors within the method. This would optimise the output from the instrument, to ensure the maximum amount of information is collected from each sample. This will help get an overall picture of the chemical profile of the leachate sample, to encourage an advance in science surrounding human decomposition. This would aid the development of a system that could assist in real-life forensic investigations. For further success into identifying human-specific markers, it would be beneficial to investigate whether these methods are able to identify the larger proteins and peptides

ahead of the degradation into their respective amino acids, as these larger compounds may add a more unique chemical signature to human decomposition.

6.8 References

[1] D. Wescott, Recent advances in forensic anthropology: decomposition research, Forensic Sciences Research 3(4) (2018) 327-342.

[2] A. Ericsson, M. Crim, C. Franklin, A Brief History of Animal Modeling, Science of Medicine 110(3) (2013) 201-205.

[3] D. Hopkins, P. Wiltshire, B. Turner, Microbial characteristics of soils from graves: an investigation at the interface of soil microbiology and forensic science, Applied Soil Ecology 14 (2000) 283-288.

[4] J. Meyer, B. Anderson, D. Carter, Seasonal Variation of Carcass Decomposition and Gravesoil Chemistry in a Cold (Dfa) Climate, Journal of Forensic Sciences 58(5) (2013) 1175-1182.

[5] S. Matuszewski, M. Hall, G. Moreau, K. Schoenly, A. Tarone, M. Villet, Pigs vs people: the use of pigs as analogues for humans in forensic entomology and taphonomy research, International Journal of Legal Medicine 134 (2020) 793-810.

[6] A. Wilson, R. Janaway, A. Holland, H. Dodson, E. Baran, M. Pollard, D. Tobin, Modelling the buried human body environment in upland climes using three contrasting field sites, Forensic Science International 169 (2007) 6-18.

[7] J. Metcalf, L. Parfrey, A. Gonzalez, C. Lauber, D. Knights, G. Ackermann, G. Humphrey, M. Gebert, W. Treuren, A microbial clock provides an accurate estimate of the post mortem interval in a mouse model system, Ecology, Microbiology and Infectious Diseases (2013) 1-19.

[8] C. Lauber, J. Metcalf, K. Keepers, G. Ackermann, C. D, R. Knight, Vertebrate Decomposition Is Accelerated by Soil Microbes, Applied and Environmental Microbiology 80(16) (2014) 4920-4929.

[9] D. Carter, D. Yellowlees, M. Tibbett, Moisture can be the dominant environmental parameter governing cadaver decomposition in soil, Forensic Science International 200 (2010) 60-66.

[10] H. Reed, A Study of Dog Carcass Communities in Tennessee, with Special Reference to the Insects, American Midlands Naturalist 59(1) (1958) 213-245.

[11] H. Al-Mesbah, C. Moffat, O. El-Azazy, Q. Majeed, The decomposition of rabbit carcasses and associated necrophagous Diptera in Kuwait, Forensic Science International 217 (2012) 27-31.

[12] R. Ley, M. Hamady, C. Lozupone, P. Turnbaugh, R. Ramey, S. Bircher, M. Schlegel, T. Tucker, M. Schrenzel, R. Knight, J. Gordon, Evolution of mammals and their gut microbes, Science 320(5883) (2008) 1647-1651.

[13] S. Notter, B. Stuart, R. Rowe, N. Langlois, The Initial Changes of Fat Deposits During the Decomposition of Human and Pig Remains, Journal of Forensic Sciences 54(1) (2009) 195-201.

[14] D. Carter, D. Yellowlees, M. Tibbett, Moisture can be the dominant environmental parameter governing cadaver decomposition in soil, Forensic Science International 200 (2007) 60-66.

[15] A. Vass, R. Smith, C. Thompson, Odor Analysis of Decomposition Buried Human Remains, Journal of Forensic Sciences 53(2) (2008).

[16] J. DeBruyn, K. Hoeland, L. Taylor, J. Stevens, M. Moats, S. Bandopadhyay, S. Dearth, H. Castro, K. Hewitt, S. Campagna, A. Dautartas, G. Vidoli, A. Mundorff, D. Steadman, Comparative Decomposition of Humans and Pigs: Soil Biogeochemistry, Microbial Activity and Metabolomic Profiles, Frontiers in Microbiology 11 (2021) 1-16.

[17] A. Dautartas, M. Kenyhercz, G. Vidoli, L. Jantz, A. Mundorff, D. Steadman, Differential Decomposition Among Pig, Rabbit, and Human Remains, Journal of Forensic Sciences 63(6) (2018) 1673-1683.

[18] D. Steadman, A. Dautartas, M. Kenyhercz, L. Jantz, A. Mundorff, G. Vidoli, Differential Scavenging Among Pig, Rabbit, and Human Subjects, Journal of Forensic Sciences 63(6) (2018) 1684-1691.

[19] L. Jantz, R. Jantz, The Anthropology Research Facility: The Outdoor Laboratory of the Forensic Anthropology Center, University of Tennessee, in: M. Warren, H. Walsh-Hanley, L. Freas (Eds.), The Forensic Anthropology Laboratory, CRC Press, FL, 2008, pp. 7-19.

[20] M. Marks, Williams M. Bass and the development of forensic anthropology in Tennessee, Journal of Forensic Sciences 40(5) (1995) 741-750.

[21] W. Rodriguez, W. Bass, Insect Activity and its Relationship to Decay Rates of Human Cadavers in East Tennessee, Journal of Forensic Sciences 28(2) (1983) 423-432.

[22] W. Rodriguez, W. Bass, Decomposition of buried bodies and methods that may aid in their location, Journal of Forensic Sciences 30(3) (1985) 836-852.

[23] T. O'Brien, Human Soft-Tissue Decomposition in an Aquatic Environment and its Transformation Into Adipocere (Thesis), University of Tennessee, Knoxville, TN, 1994, p. 174.

[24] A. Vass, W. Bass, J. Wolt, J. Foss, J. Ammons, Time Since Death Determinations of Human Cadavers Using Soil Solutions, Journal of Forensic Sciences 37(5) (1992) 1236-1253.

[25] A. Vass, S. Barshick, G. Sega, J. Caton, J. Skeen, J. Love, J. Synstelien, Decomposition Chemistry of Human Remains: A New Methodology for Determining the Postmortem Interval, Journal of Forensic Sciences 47(3) (2002) 542-553.

[26] A. Vass, R. Smith, C. Thompson, Decompositional odor analysis database, Journal of Forensic Sciences 49(4) (2004) 760-769.

[27] S. Shahid, K. Schoenly, N. Haskell, R. Hall, W. Zhang, Carcass Enrichment Does Not Alter Decay Rates or Arthropod Community Structure: A Test of the Arthropod Saturation Hypothesis at the Anthropology Research Facility in Knoxville, Tennessee, Journal of Medical Entomology 40(4) (2003) 559-569.

[28] S. Forbes, Body farms, Forensic Science, Medicine and Pathology 13 (2017) 477-479.

[29] M. Iqbal, K. Nizio, M. Ueland, S. Forbes, Forensic decomposition odour profiling: A review of experimental designs and analytical techniques, Trends in Analytical Chemistry 91 (2017) 112-124.

[30] K. Nizio, S. Forbes, Preliminary Investigation of the Influence of Fire Modification on the Odour of Decomposition using GC x GC - TOFMS, Chromatography Today (2018) 32-39.

[31] R. Buis, L. Rust, K. Nizio, T. Rai, B. Stuart, S. Forbes, Investigating the Sensitivity of Cadaver-Detection Dogs to Aged, Diluted Decomposition Fluid, Journal of Forensic Identification 69(3) (2019) 367-377.

[32] W. Zhang, T. Liu, M. Ueland, S. Forbes, R. Wang, S. Su, Design of an efficient electronic nose system for odour analysis and assessment, Measurement 165 (2020) 1-9.

[33] R. Oostra, T. Gelderman, W. Groen, H. Uiterdijk, E. Cammeraat, T. Krap, L. Wilk, M. Luschen, W. Morrien, F. Wobben, W. Duijst, M. Aalders, Amsterdam Research Initiative for Sub-surface Taphonomy and Anthropology (ARISTA) - A taphonomic research facility in the Netherlands for the study of human remains, Forensic Science International 317 (2020) 1-6.

[34] R. Tautenham, G. Patti, D. Rinehart, G. Siuzdak, XCMS Online: A Web-Based Platform to Process Untargeted Metabolomic Data, Analytical Chemistry 84 (2012) 5035-5039.

[35] B. Ioan, C. Manea, B. Hanganu, L. Statescu, L. Solovastru, I. Manoilescu, The Chemistry Decomposition in Human Corpses, Revista de Chimie 68(6) (2017) 1353-1354.

[36] A. Mero, Leucine Supplementation and Intensive Training, Sports Medicine 27(347-358) (1999).

[37] K. Guo, Y. Yu, J. Hou, Y. Zhang, Chronic leucine supplementation improves glycemic control in etiologically distinct mouse models of obesity and diabetes mellitus, Nutrition and Metabolism 7(57) (2010) 1-10.

[38] J. Yang, Y. Chi, B. Burkhardt, Y. Guan, B. Wolf, Leucine metabolism in regulation of insulin secretion from pancreatic beta cells, Nutrition Reviews 68(5) (2010) 270-279.

[39] S. Forbes, Decomposition Chemistry in a Burial Enviornment, Soil Analysis in Forensic Taphonomy, CRC Press, New York, 2008, pp. 203-223.

[40] P. Molinoff, J. Axelrod, Biochemistry of Catecholamines, Annual Review of Biochemistry 40 (1971) 465-500.

[41] A. Cesura, Monoamine Oxidases, in: S. Enna, D. Bylund (Eds.), xPharm: The Comprehensive Pharmacology Reference, Elseiver, Amsterdam ; Boston, 2008, pp. 1-5.

[42] D. Goldstein, The Catecholaldehyde Hypothesis for the Pathogenesis of Catecholaminergic Neurodegeneration: What We Know and What We Do Not Know, International Journal of Molecular Sciences 22(5999) (2021).

[43] K. Shortall, A. Djeghader, E. Manger, T. Soulimane, Insights into Aldehyde Dehydrogenase Enzymes: A Structural Perspective, Frontiers in Molecular Biosciences 8 (2021) 2-15.

[44] S. Marchitti, R. Deitrich, V. Vasiliou, Neurotoxicity and Metabolism of the Catecholamine-Derived 3,4-Dihydroxyphenylacetaldehyde and 3,4-Dihydroxyphenylglycolaldehyde: The Role of Aldehyde Dehydrogenase, Pharmacological Reviews 59(2) (2007) 125-150.

[45] G. Eisenhofer, I. Kopin, D. Goldsten, Catecholamine Metabolism: A Contemporary View with Implications for Physiology and Medicine, Pharmacological Reviews 56(3) (2004) 331-349.

[46] C. Platell, S. Kong, R. McCauley, J. Hall, Branched-chain amino acids, Journal of Gastroenterology and Hepatology 15 (2000) 706-717.

[47] Y. Zhou, N. Danbolt, Glutamate as a neurotransmitter in the healthy brain, Journal of Neural Transmission 121 (2014) 799-817.

[48] O. Kambur, P. Mannisto, Catechol-O-Methyltransferase and Pain, International Review of Neurobiology 95 (2010) 227-279.

[49] T. Halbig, W. Koller, Levodopa; Metabolization, Handbook of Clinical Neurology 84 (2007) 31-72.

[50] J. Meiser, D. Weindl, K. Hiller, Complexity of dopamine metabolism, Cell Communication and Signalling 11(1) (2013) 34.

[51] D. Lunn, Y. Yun, J. Jorgenson, Retention and effective diffusion of model metabolites on porous graphitic carbon, Journal of Chromatography A 1530 (2017) 112-119.

[52] H. Kai, K. Kinoshita, H. Harada, Y. Uesawa, Establishment of a direct-injection electron ionization-mass spectrometry Metabolomics method and its application to Lichen Profiling, Analytical Chemistry 89(12) (2017) 6408-6414.

[53] H. Kai, Y. Usawa, H. Kunitake, Direct-injection electron ionization-mass spectrometry Metabolomics method for analyzing blueberry leaf metabolites that inhibit adult T-cell leukemia proliferation, Plant Medica 85(01) (2019) 81-87.

[54] L. Swann, F. Busetti, S. Lewis, Determination of amino acids and amines in mammalian decomposition fluid by direct injection liquid-chromatography-electrospray ionisation-tandem mass spectrometry, Analytical Methods 4(2) (2012) 315-582.

[55] B. Sarvin, S. Lagziel, N. Sarvin, D. Mukha, P. Kumar, E. Aizenshtein, T. Shlomi, Fast and sensitive flow-injection mass spectrometry metabolomics by analyzing sample-specific ion distributions, Nature Communications 3186 (2020) 3186.

[56] A. Cambiaghi, M. Ferrario, M. Masseroli, Analysis of metabolomic data: tools, current strategies and future challenges for omics data integration, Briefings in Bioinformatics 18(3) (2017) 498-510.

[57] A. Zhang, H. Sun, P. Wang, Y. Han, X. Wang, Modern analytical techniques in metabolomics analysis, Analyst 137 (2012) 293-300.

Chapter 7

Conclusions and future work

7.1 Conclusions

This research aimed to investigate the potential of using a non-targeted metabonomic workflow to detect the chemical signature of decomposing remains in water using liquid chromatography-mass spectrometry. Current methods mostly rely on physical observations and geoforensic techniques, however, new chemical studies could improve our understanding of decomposition, and how it can be used in the field for forensic investigations.

There were six main aims outlined for this work. The first aim was to develop an effective and robust workflow suitable for non-targeted metabonomic analysis using these particular samples. The method development work carried out in Chapter 3 explored two different sample preparation techniques, with three different column chemistries to identify the most appropriate experimental method. It was clear from an early stage that taking a sample directly from the water showed very limited results. Due to poor peak shape, lack of separation on the PCA plot and only a very small number of potential markers, it was evident that pre-concentrating the sample was necessary. Due to the non-targeted nature of this work it was difficult to decide on a solid-phase extraction (SPE) cartridge, as it was important to ensure none of the compounds in the sample were lost in the pre-concentration step. Results showed that a cartridge containing activated

charcoal was successful in pre-concentrating 1 L of sample, obtaining the maximum amount of information from each sample and improving the quality of the results. Investigating the effectiveness of three different column chemistries also ensured that the chromatography was suitable based on its interaction with the compounds present in the sample, again due to the non-targeted nature of the work. Looking at a C18, HILIC and a Hypercarb column provided an opportunity to work with a variety of chemistries and interactions with polar and non-polar phases. A C18 column combined with a pre-concentration step using SPE produced the best results in terms of reliability, quality and quantity. This was based on the experimental conditions of this particular experiment.

The second aim was to investigate whether it was possible to create a chemical profile of water that is influenced by decomposing remains. The second preliminary experiment in Chapter 3 confirmed that the developed workflow was successful. A combination of chromatography, multivariate analysis (PCA) and statistical analysis was able to create a detailed chemical profile of water that was influenced by decomposing remains. This chemical profile could be monitored over time with the use of markers. This chemical signature was not identified in the control sample, which confirmed that the results obtained were as a direct result of decomposition, not the natural chemical signature of water. The third aim was to determine if there were any metabolic differences between two species decomposing in water. The work carried out in Chapter 4 was able to successfully differentiate between rabbit and duck species decomposing in water. Multivariate analysis was a useful tool that showed increasing differences between species over time, which was also reflected in the remarkable differences in peak patterns and intensities presented in the chromatograms. The data also produced markers that showed significant differences between species at three time points, and were identified with the use of standards as cadaverine, leucine and creatinine. All three markers are

connected to familiar processes and pathways associated with decomposition, further confirming that these methods are identifying the correct group of compounds.

The fourth aim was to analyse the effects of moving and still water on the chemical signature of the water during decomposition. This would help gain deeper insight into the effects of chemical decomposition when the nature of the water is different. Overall it seemed that the chemical signature of the water was vaguely similar from decomposition in moving and still water. The most pronounced differences between their chemical profiles was seen when monitoring them over time. Whilst very similar features were detected in both experimental conditions, the time point in which they appeared and the quantity of these features were often different. The results suggested that the movement of the water not only affected the speed of the decomposition process, but also influenced the stagnation of compounds in certain areas of the box. This opened discussions on what effect this may have on the sampling technique such as depth, location and consistency.

The fifth aim was to determine the effect of temperature on chemical decomposition. Temperature is known to be the most important factor influencing the rate of decomposition. Whilst UK temperatures do not fluctuate as much as other countries around the world, it was clear from the results that temperature had a significant effect on the chemical signature of the water influenced by decomposing remains. The experiments conducted in winter in both Chapter 4 and 5 showed lower peak numbers, poor separation on the PCA scores plot, and overall a smaller number of markers showing significant differences between species, and the effect of moving and still water.

Whilst it is already established that lower temperatures hinder the decomposition process, it was important to consider the full effects of temperature on the chemical aspect of decomposition. One of the most astonishing discoveries in this study was that although

decomposition was clearly affected by lower temperatures, a remarkable amount of information could still be obtained from the samples exposed to these temperatures. Whilst differences were scarce, it was still possible to differentiate between species ever so slightly using multivariate analysis. Although not very many, there were markers showing significant differences between both species and moving and still water conditions. It was unforeseen that changes to the chemical signature of the water could still be visualised, even with temperatures of 0°C and below. This is an important milestone for the use of metabonomic profiling in this field, as it has proven that chemical decomposition does not halt at 4°C, but continues, albeit slowly.

Finally, the work aimed to incorporate the workflow developed during this preliminary work into a more realistic environment. Chapter 6 presents an initial investigation into the use of the workflow developed in the lab to analyse leachate samples collected from below human remains in soil. These samples were analysed using three different column chemistries (C18, Hypercarb and HILIC). The Hypercarb column was chosen for future analysis as it produced the most robust and reliable data, and provided results that were the most applicable to decomposition studies. The results from these analyses showed promising signs that it is possible to apply this preliminary workflow to samples taken from a realistic forensic environment using human remains.

Overall, this research has shown that a preliminary metabonomic approach was successful in identifying a chemical signature of decomposition in water influenced by a decomposing carcass. The chemical signature for this particular experimental setup could be monitored over time, and used to investigate metabolic differences between species and changes in the environment.

7.2 Future work

The experimental workflow designed for this research has been proven robust and reliable for preliminary experiments to capture the chemical signature of decomposition in water influenced by decomposing remains. Despite this, there are factors that need to be taken into consideration for any future work.

The sample size is an important factor to consider, as there were only three replicates of each species in each environmental condition. Increasing the sample size would not only increase the strength of the statistical analysis, but it can also highlight any differences in the decomposition pattern within species. Each carcass is likely to produce slightly different decomposition patterns due to factors such as weight, fur, health, amount of air in lungs etc., therefore increasing the sample size would allow an opportunity to see the true effects of these factors on the chemical signature of the water.

Improving the sampling technique is an important aspect of any future work carried out in this area. When discussing the results in Chapter 5, it was highlighted that the sampling location in the still water boxes could influence the results. Due to the stagnation of the water, the pooling of compounds would likely influence the results from different sampling locations. Additionally, it would be interesting to investigate whether different sampling locations would influence data collected from moving water boxes. Improving the frequency that samples were taken would also improve this study. Due to the availability of materials, access to the site and time constraints, a sample was taken once a week. Taking a sample 2/3 times a week would allow deeper insight to the more subtle chemical changes happening throughout decomposition. Another important area for future work is to focus on the very early stages of decomposition, and if there are any important chemical changes before any physical appearances occurs. Taking a sample

every hour from hour 0 to 12 would allow a more detailed investigation into the very initial chemical changes that occur during decomposition.

The studies carried out in Chapter 4 and 5 were limited to only rabbit and duck carcasses. Using a wider variety of animal carcasses in future experiments would be an opportunity to identify more chemical similarities and differences between different species. It is also important to consider introducing pigs as a subject. Pigs are known to show very similar decomposition characteristics to humans, and as a result are the most popular subjects used in decomposition research in the UK.

Due to circumstances beyond our control, the collaboration with The University in the Netherlands for the ARISTA project (Chapter 6) was postponed, and eventually cancelled. Future work would focus on efforts to resume communications with the University to continue with this exciting new direction of using human remains. Studying the chemistry of decomposition using human remains would be an opportunity to use the workflow designed in a lab environment in a more realistic environment, to search for human-specific markers. Assessing the ability of this workflow to detect the chemical signature of a decomposing human in water is important, as the detection of any human-specific markers associated with decomposition would revolutionise the field, and more importantly the search and rescue service for missing people.

As well as improvements to the experimental setup and procedures, additional analytical considerations could improve and increase the amount of data available. All samples were analysed in positive ionisation mode, whilst analysing the samples in negative ionisation mode would further increase the data set and the probability of finding features of importance to the decomposition process. The activated carbon solid-phase extraction cartridge was successfully capturing the compounds of interest in this study, however,

additional work to validate this technique is essential. Each cartridge was assembled by hand, therefore it is important to consider the consequence of variation between each cartridge. An investigation into the use of pre-made activated carbon cartridges such as *Thermo Fisher Dionex™ SolEx™ Carbon-Based SPE Cartridges* and whether they produce the same result would improve the validity of this study by using an official regulated product.

Leucine was one of three compounds positively identified during this study. Valine was also tentatively identified. A targeted approach looking at a range of amino acids would give greater insight into the presence of amino acids in the sample even at low levels, and whether it is possible to identify a combined behavioural pattern over time.

One of the most difficult challenges in any untargeted metabonomic research is the ability to confirm the identity of a compound. The majority of compounds showing significant differences or important patterns in the data are not accompanied by predictive formula. Additionally, the software available to provide a tentative identification based on MS data are limited and expensive. Many of these compounds are also not available to purchase as standards, therefore it is often difficult to move forward from a tentative identification. This problem would need to be addressed globally, as an approach to ensure there is access to effective tools and populated databases specifically for untargeted metabonomics.